INSULIN-LIKE GROWTH FACTOR RECEPTORS IN COLORECTAL CANCER

Gemma Victoria Brierley
B.Sc [Hons.]

CSIRO Molecular and Health Technologies and
The Preventative Health National Research Flagship

&

Discipline of Biochemistry
School of Molecular and Biomedical Science
The University of Adelaide
Adelaide, South Australia

A thesis submitted to the University of Adelaide, South Australia
in fulfilment of the requirements for the degree of
DOCTOR OF PHILOSOPHY

May 2008

Abstract

The IGF system is a crucial regulator of normal growth and development, however dysregulation of the system on multiple levels is associated with the incidence of a wide variety of malignancies including the breast, thyroid, lung, and colon, making the IGF system an important anti-cancer therapeutic target. Due to its role in mediating cellular proliferation, protection from apoptosis, and metastasis, traditional focus has been set on examining the role of the type 1 IGF receptor [IGF1R] in cancer. However there is mounting evidence to suggest the insulin receptor [IR] may also be involved in the potentiation and pathogenesis of cancers.

The observation that IGF-II is overexpressed, compared to normal tissues, by cancers suggests signaling via target receptors by this ligand has important implications on cancer pathogenesis. Indeed, both the IGF1R and IR have been demonstrated to be up-regulated in a variety of malignancies. In regards to IR isoform, the IGF-II binding IR-A is preferentially expressed by a number of cancer cell types. Together with the observation that an autocrine proliferative loop exists between IGF-II and the IR-A in malignant thyrocytes and cultured breast cancer cells, suggests signaling via the IR-A may play a role in cancer cell growth and survival. However, very few studies on the IR-A have been conducted in cells co-expressing the IGF1R. This is mainly due to the difficulties associated with discrimination between signaling arising from IGF1R homodimers, IR-A homodimers, and IGF1R/IR-A hybrid receptors.

It is not known how the IR-A interacts, and functions in conjunction with the other receptors of the IGF system to signal biologically relevant outcomes, especially in terms of anti-cancer therapeutics that aim to block and down-regulate the IGF1R. Current anti-cancer therapies targeting the IGF system have concentrated on blocking IGF signaling via the IGF1R, due mostly to the functional properties of the receptor, but also in part due to the metabolic consequences associated with blockade and inhibition of the IR. This individual targeting of the IGF1R potentially leaves a pathway by which IGF-II secreted by the tumour can circumvent current IGF1R based therapies. Consequently, this thesis investigated whether the IR-A could compensate for the targeted loss of the IGF1R and how the IR-A interacts with the IGF1R in cells co-expressing these two receptors. In addition, the individual ability of the IR isoforms to signal biological outcomes in response to IGF stimulation was assessed.

The main experimental techniques used throughout this body of work included; assessment of protein expression and activation by Western blot, siRNA mediated gene silencing, and measures of cell proliferation, survival, and migration.

The key areas of investigation included:

1. Investigation of the individual ability of the IR isoforms to signal biological outcomes in response to IGF stimulation

2. Identification of an appropriate cell line model in which to investigate the interactions between the IR-A and IGF1R

3. Optimisation of siRNA mediated knock-down of the IR-A and IGF1R in SW480 colorectal adenocarcinoma cells

4. Determination of the biological role of the IR-A in SW480 cells co-expressing the IGF1R

The key findings from this work included:

1. The IR-A could not compensate for IGF1R depletion in SW480 cells

2. Dual silencing of the IR-A and IGF1R indicated signaling via the IGF1R was dominant to signaling via the IR-A in SW480 cells

3. Signaling via IR-A/IGF1R hybrid receptors may not be as potent as signaling via IGF1R homodimers

4. IGF-I at physiological concentrations can stimulate biological responses via both isoforms of the IR.

Declaration

This thesis contains no material that has been accepted for the award of any other degree or diploma in any University. To the best of my knowledge and belief, it contains no material that has previously been published by any other person except where due reference is made.

I give consent for my thesis, when deposited in the library of the University of Adelaide to be available for loan and photocopying

Gemma Victoria Brierley

Acknowledgements

Here we are, at the end of it all. A year ago I thought I would be struggling to write a very different thesis. What now forms this thesis makes for a pleasant and welcome surprise. I'd like to start by acknowledging and thanking Prof. John Wallace [Department of Biochemistry, University of Adelaide], Dr. Leah Cosgrove [CSIRO, Molecular and Health Technologies, Adelaide], and Dr. Lance Macaulay [CSIRO, Molecular and Health Technologies, Melbourne] for their supervision. Particular thanks to Lance for his thoughtful and detailed feedback throughout the preparation of this document. I also acknowledge the input of Dr. Briony Forbes at the beginning of this project.

The majority of the work outlined in this thesis was performed in the laboratory of Dr. Leah Cosgrove, and was funded by the Preventative Health National Research Flagship. I have been financially supported by the University of Adelaide Department of Biochemistry and the Preventative Health National Research Flagship - I am grateful to both institutions for allowing me the opportunity to pursue this research. In addition, I was afforded the wonderful opportunity to conduct six months of research in the laboratory of Dr. Val Macaulay at the Weatherall Institute of Molecular Medicine, University of Oxford. My time spent in Val's laboratory was second to none. My sincere thanks to Val not only for hosting me in her lab, but also for her mentorship. I learnt so much during my visits, I will always reflect on my time in Oxford with great fondness. My thanks also go to Prof. Richard Head, Director of the P-Health Flagship for funding my travel to Oxford.

Throughout the last four years, the encouragement and support I have received from my family and friends has been unrelenting. "Thank you", doesn't quite seem adequate enough. One question I have been asked a lot over the last few weeks is "if you could go back, would you do it all again?" The answer is "yes - but I would approach it differently". My reasons for beginning a PhD in the first place have not changed, and through circumstance of location I have been extremely fortunate to forge strong friendships with several fun-loving, smart, inspirational, like-minded people. To them I am especially thankful and grateful. For the opportunity to have crossed paths with them, I would do it all again.

And finally, to one in particular, who was often my last bastion of sanity over the last two years [especially this year] - Friday nights at the pub are always something special, never underestimate the power of several pints shared in the presence of exceptional company. Thank you.

> He who learns must suffer,
> Even in our sleep, pain which cannot forget,
> Falls drop by drop upon the heart,
> Until, in our own despair,
> Against our will,
> Comes wisdom
>   - Aeschylus

Table of Contents

List of Publications

Peer reviewed publications [see appendix]
      * Denotes joint first authorship

Denley A*, Carroll JM*, **Brierley GV**, Cosgrove LJ, Wallace JC, Forbes BE, Roberts CT Jr. Differential activation of insulin receptor substrates 1 and 2 by insulin-like growth factor-activated insulin receptors. *Molecular Cell Biology* 2007 May; 27[10]: 3569 - 77

Denley A, **Brierley GV**, Carroll JM, Lindenberg A, Booker GW, Cosgrove LJ, Wallace JC, Forbes BE, Roberts CT Jr. Differential activation of insulin receptor isoforms by insulin-like growth factors is determined by the C domain. *Endocrinology* 2006 Feb; 147[2]: 1029 – 1036

Conference Proceedings

Brierley GV, Forbes BE, Macaulay L, Siddle K, Wallace JC, Cosgrove LJ. The biological role of insulin-like growth factors signalling via IR-A and IR-A/IGF1R hybrid receptors in cell survival, migration, and invasion. *The role of the IGF system in Cancer – Taormina, Sicily, Italy. November 2005*

Brierley GV, Forbes BE, Wallace JC, Cosgrove LJ. The biological role of insulin-like growth factors signalling via IR-A and IR-A/IGF1R hybrid receptors in cell survival, migration, and invasion. *Gordon Research Conference: Insulin-like growth factors in physiology and disease – Ventura, California, U.S.A. April 2005*

Abbreviations

^{o}C	degrees celcius
μg	microgram
μl	microlitre
μm	micrometre
3'	three prime
5'	five prime
95% CI	ninety five percent confidence interval
bp	base pair
Ab	antibody
ACF	aberrant crypt foci
APC	Adenomatosis Polyposis coli
ASO	anti-sense oligonucleotide
ATP	adenosine triphosphate
BMI	body mass index
BuA	butyrate
BRET	bioluminescence resonance energy transfer
BSA	bovine serum albumin
CO_2	carbon dioxide
cDNA	complementary DNA
c.f	compared with
COX-2	cyclooxygenase-2
CR	cystine-rich
CRC	colorectal cancer
CT	carboxy-terminal tail
C-terminus	Carboxyl-terminus
dATP	2`-Deoxyadenosine 5`-triphosphate
DEPC	diethyl pyrocarbonate
DEPC-MQ H_2O	dethyl pyrocarbonate milliQ water
DMEM	Dulbecco's modified eagles medium
DMSO	dimethyl sulfoxide
DNA	deoxyribonucleic acid
dL	decilitre
dATP	2'-deoxyadenosine 5'-triphosphate
dCTP	2'-deoxycytidine 5'-triphosphate
dGTP	2'-deoxyguanosine 5'-triphosphate
dTTP	2'-deoxythymidine 5'-triphosphate
dNTPs	deoxynucleotide triphosphates
DTT	dithiothreitol
EC_{50}	50% effective concentration
EDTA	ethylene diamine tetra-acetic acid
EGF	Epidermal Growth Factor
EGFR	Epidermal Growth Factor Receptor
EPIC	European Prospective Investigation into Cancer and Nutrition
Erk-1/2	extracellular signalling-related kinase – 1/2
Eu	Europium
FACS	fluorescent-activated cell sorting
FCS	foetal calf serum
FITC	fluorescein isothiocyanate
F_n	fibronectin domain
GH	growth hormone
Grb2	Growth factor receptor-bound protein 2
H_2O	water
HEPES	4-(2-hydroxyethyl)-1-piperazineethanesulfonic acid
HER-2	Human Epidermal Growth Factor-2
Hybrid-A	IGF1R/IR-A hybrid receptor
Hybrid-B	IGF1R/IR-B hybrid receptor
IB	immunoblot
IC_{50}	concentration of inhibitor which reduces binding by 50%
IGF1R	Type 1 IGF receptor
$IGF1R_{\alpha}$	Type 1 IGF receptor alpha-subunit
$IGF1R_{\beta}$	Type 1 IGF receptor beta-subunit
IGF2R	Type 2 IGF receptor
IGFBPs	Insulin-like growth factor binding proteins
IGF-I	Insulin-like growth factor I
IGF-I CII	IGF-I containing the IGF-II C domain
IGF-I DII	IGF-I containing the IGF-II D domain
IGF-I CIIDII	IGF-I containing the IGF-II C and D domains
IGF-II	Insulin-like growth factor II
IGF-II CI	IGF-II containing the IGF-I C domain
IGF-II DI	IGF-II containing the IGF-I D domain
IGF-II CIDI	IGF-II containing the IGF-I C and D domains
Ins	insert domain
IP	immunoprecipitate
IR	Insulin receptor

IR$_\alpha$	Insulin receptor alpha-subunit
IR$_\beta$	Insulin receptor beta-subunit
IR-A	A isoform of the human insulin receptor [exon 11-]
IR-B	B isoform of the human insulin receptor [exon 11+]
IRS-1	Insulin Receptor Substrate -1
IRS-2	Insulin Receptor Substrate -2
JM	juxtamembrane domain
kDa	kilodalton
L1	large domain 1
L2	large domain 2
L-chain	light chain
LHS	left-hand side
LOI	loss of imprinting
M	molar
mAb	monoclonal antibody
MALDI-TOF	matrix-assisted laser desorption/ionisation – time of flight
MAPK	Mitogen-activated protein kinase
Max.	maximum
mg	milligram
MgCl$_2$	magnesium chloride
ml	millilitre
mM	millimolar
MMP	matrix metalloprotienase
MOPS	3-(N-morpholino)propanesulfonic acid
mRNA	messenger ribonucleic acid
N/A	not applicable
NaCl	sodium chloride
NaF	sodium fluoride
Na$_4$O$_7$P$_2$	sodium orthovanidate
Na$_3$PO$_4$	sodium pyrophosphate
ng	nanogram
NH$_4$	ammonia
nm	nanometer
nM	nanomolar
n/s	not significant
NSAIDs	non-steroidal anti-inflammatory drugs
nt	nucleotide
N-terminus	amino-terminus
OD$_{260}$	optical density at 260 nm
OD$_{280}$	optical density at 280 nm
p53	protein 53
pAb	polyclonal antibody
PAGE	polyacrylamide gel electrophoresis
PBS	phosphate buffered saline
PCR	polymerase chain reaction
PFA	paraformaldehyde
PI3K	phosphoinositide kinase-3
pIRS-1	phosphorylated IRS-1
pIRS-2	phosphorylated IRS-2
PKB	protein kinase B
PMSF	phenylmethanesulphonyl fluoride
PTEN	phosphatase and tensin homologue
R$^-$	IGF1R negative NIH 3T3-like mouse fibroblasts
R$^-$IGF1R	IGF1R negative NIH 3T3-like mouse fibroblasts recombinantly expressing human IGF1R
R$^-$IRA	IGF1R negative NIH 3T3-like mouse fibroblasts recombinantly expressing human IR-A
R$^-$IRB	IGF1R negative NIH 3T3-like mouse fibroblasts recombinantly expressing human IR-B
RHS	right-hand side
RISC	RNA-inducing silencing complex
RNA	ribonucleic acid
RNAi	RNA interference
rpm	revolutions per minute
RR	relative risk
RT-PCR	reverse-transcriptase PCR
SCFA	short-chain fatty acid
SDS	sodium dodecyl sulphate
SH2	Src-homology domain
siRNA	short interfering RNA
SEM	standard error of the mean
TAE	Tris-acetate EDTA
TK	tyrosine-kinase domain
Tris-Cl	Tris (hydroxymethyl) aminomethane
Tyr	tyrosine
VEGF	vascular epidermal growth factor
vs.	versus
WB	Western blot
WCL	Whole cell lysate

Chapter 1

Introduction and Literature Review

1.1   The IGF System

1.1.1   Overview of the IGF Axis

The IGF system is vital for normal mammalian development and acts via an intricate network of peptide hormones, cell surface receptors, circulating binding proteins and proteases. The system consists of the three peptide hormones; insulin, insulin-like growth factor I and insulin-like growth factor II [IGF-II]; six high affinity IGF binding proteins [IGFBPs 1 to 6]; and a range of cell surface receptors including, the type I IGF receptor [IGF1R], the type 2 IGF receptor [IGF2R], the insulin receptors [IR], and IGF1R/IR hybrid receptors [See Figure 1.1]. IGF-I, IGF-II, and insulin bind and activate the IGF1R and IR leading to the initiation of intracellular signaling cascades that regulate a range of biological outcomes including metabolic, mitogenic, transforming, and migratory responses. Although it has been demonstrated that IGF1R/IR hybrid receptors can bind the three peptide hormones of the IGF system resulting in their activation, it has yet to be determined if signals originating from hybrid receptors are biologically relevant. In contrast to the other IGF receptors, the IGF2R binds only IGF-II, does not have signaling capabilities, and is thought to reduce circulating levels of IGF-II by mediating its internalization and degradation. The six high affinity IGFBPs and specific IGFBP proteases regulate the actions of IGF-I and IGF-II by controlling their ability to bind to the various receptors of the IGF system.

1.1.2   The Insulin-like Growth Factors

IGF-I and IGF-II are small, single-chain polypeptides that share a high degree of sequence and structural homology[1-3]. The *IGF1* gene is located on chromosome 12 and encodes a 70 amino acid mature protein[4]. The *IGF2* gene is located 1.4 kilobases downstream of the *Insulin* gene on chromosome 11, and gives rise to a 67 amino acid mature protein[4]. Both IGF-I and IGF-II are expressed as multiple transcripts due to initiation of transcription from multiple promoter sites on each of the genes and alternative splicing of the mRNA transcripts[5]. The single-chain polypeptides of IGF-I and IGF-II are folded into four domains: B, C, A, and, D [in order of N to C terminus], see

Figure 1.2. The A and B domains of these two growth factors are structurally analogous to mature insulin. The flexible C domains are similar to the C domain in pro-insulin but are not proteolytically removed[6]. The D domain is unique to the IGFs[6]. Despite their structural similarities, IGF-I and IGF-II display differential abilities to bind and activate receptors[7-11], see Tables 1.1 – 1.3. The creation of IGF chimeras by swapping the C and D domains of IGF-I and IGF-II has demonstrated that these two domains are primarily responsible for binding specificity[12, 13].

Expression of IGF-I and IGF-II is both tissue and developmentally specific. The liver is the primary site of both IGF-I and IGF-II production, however most other tissues can produce these proteins[5]. Therefore, the IGFs are widely expressed and can act as endocrine, paracrine, and autocrine growth factors[5]. IGF-I expression in the liver is principally controlled by growth hormone [GH], whereas expression from extra-hepatic sites has been shown to be independent of GH[14]. In addition, diet has been demonstrated to affect IGF-I levels[5]. In contrast to IGF-I, IGF-II production is not controlled by GH[15] but is subject to genomic imprinting[16]. IGF-II expression occurs from the paternal allele only, while the maternal allele is transcriptionally silent[16]. IGF-II expression is generally higher in the foetus than in the adult, where expression levels are maintained at a constant level[17]. In addition, expression of IGF-II is generally higher than IGF-I expression in the human foetus[18] suggesting that IGF-II is primarily a foetal development growth factor. Through mouse knockout studies[19] and the identification of two growth restricted humans with a lack of functional circulating IGF-I[20, 21], IGF-I has been demonstrated to be critical to both pre and post natal development. Via activation of the IGF receptors, the two IGFs stimulate a range of pleiotropic actions including regulation of somatic growth, cellular proliferation, differentiation, migration, and protection from apoptosis[22-24]. These actions are vital to normal growth and development, but are also commonly perturbed in cancer. The role of IGFs in cancer and normal growth will be covered in more detail in the sections pertaining to the IGF receptors.

1.1.3   IGF Binding Proteins

The six high affinity IGFBPs regulate the endocrine, paracrine, and autocrine actions of IGF-I and IGF-II by controlling their ability to bind the IGF1R or IR[25]. The affinity of the IGFBPs for IGF-I and
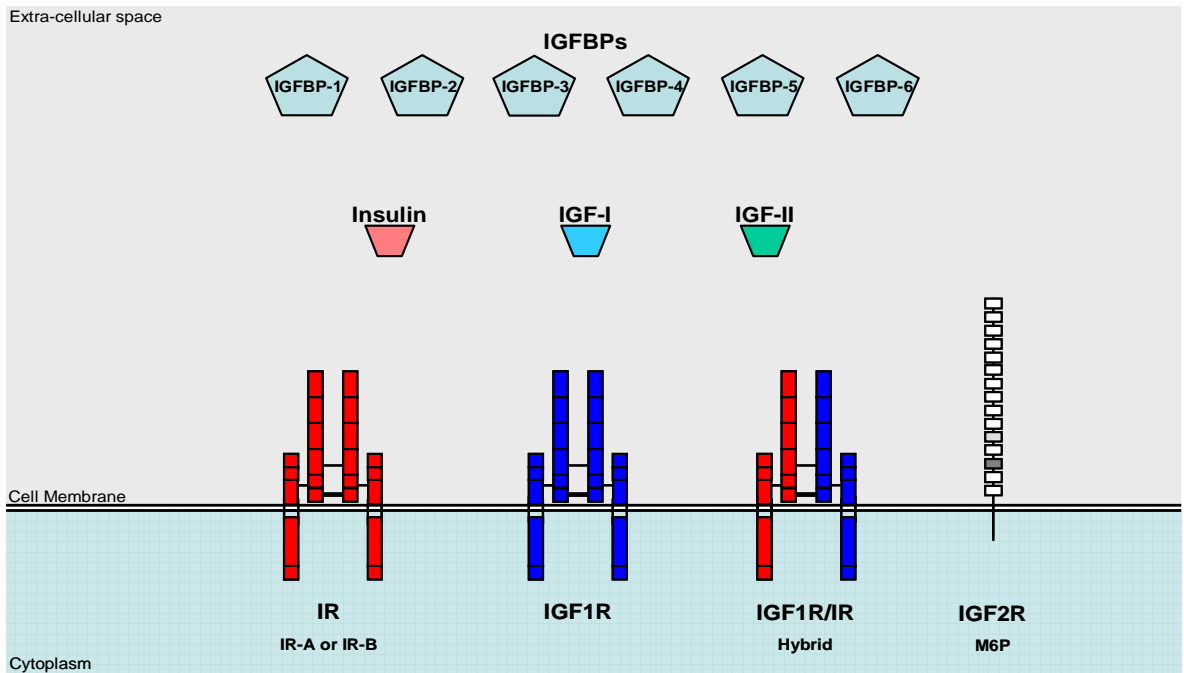
Figure 1.1 Summary of the IGF system

The IGF axis comprises of an intricate network of three peptide hormones, a range of cell surface receptors, six circulating binding proteins and related proteases. IGF-I, IGF-II, and Insulin bind and activate the IGF1R and IR leading to the initiation of intracellular signalling cascades that then regulate a range of biological responses. Although IGF1R/IR hybrid receptors are functional in terms of ligand binding, it has yet to be determined whether signalling via these receptors are biologically relevant. In contrast to the other IGF receptors, the IGF2R binds only IGF-II, does not have signalling capabilities, and is thought to reduce circulating levels of IGF-II by mediating its internalisation and degradation. The six high affinity IGFBPs and specific IGFBP proteases regulate the actions of IGF-I and IGF-II by mediating their bioavailability, and hence controlling their ability to bind the various receptors of the system.
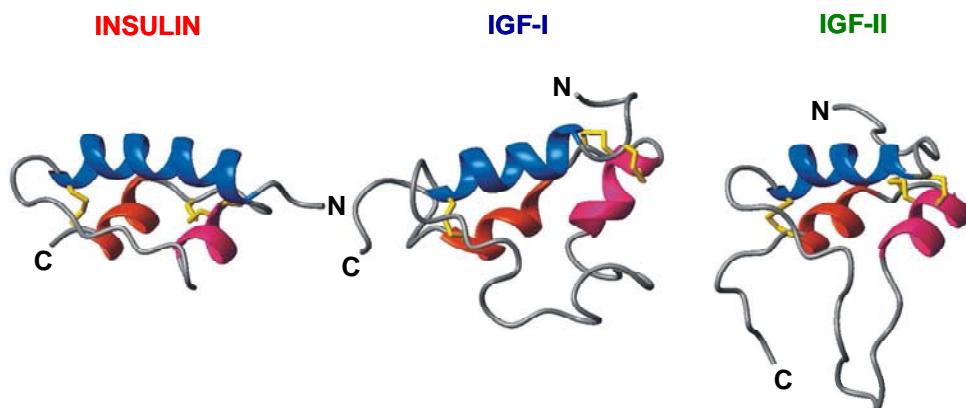
Figure 1.2 Structural comparison of Insulin, IGF-I, and IGF-II

Aligned along the B domain helix, shown in blue, are the structures of insulin, IGF-I, and IGF-II. The first and second helix of the A domain are shown in magenta and orange. Gold denotes disulphide bonds. The N and C terminus are as indicated. Figure adapted from G.Brierley, 2003 Honours Thesis and A.Denley, 2004 PhD thesis.

IGF-II is mediated by specific IGFBP proteases, which cleave the IGFBPs into forms that have little or no affinity for the IGFs thereby releasing active IGFs[25]. In terms of regulating the biological activities of the IGFs, the IGFBPs are proposed to have four major functions: 1) to act as transport proteins for the IGFs in plasma, 2) to protect the IGFs from degradation thereby controlling their metabolic clearance, 3) enable tissue and cell specific delivery and localization of the IGFs, and 4) regulate the interaction between the IGFs and the IGF1R and IR [as reviewed in[15]]. There is also evidence to suggest IGFBPs have actions that are independent of IGFs, such as interactions with transcription factors in the nucleus, and signaling via a specific putative cell surface receptor[25].

1.1.4   The Type II IGF Receptor

The IGF2R [also called the cation-independent mannose-6-phosphate receptor] is a monomeric receptor that, in terms of the IGF system, acts to modulate IGF-II bioavailability[15]. The IGF2R is structurally dissimilar from the IGF1R and IR, and consists of 15 extracellular repeating domains, a transmembrane domain, and an intracellular domain[26]. The intracellular domain of the IGF2R does not possess kinase activity, and therefore the IGF2R does not have any intrinsic capacity for signal transduction[27]. The IGF2R binds a wide range of mannose-6-phosphate containing glycoproteins including: renin, proliferin, thyroglobulin, and transforming growth factor-β [TGF-β], and they are involved in IGF-independent functions[15, 27]. Only a small portion of total cellular IGF2R is expressed at the cell surface, with the majority located on intracellular membranes. Therefore, the IGF2R primary function is in the trans-Golgi network, where it is involved in sorting newly synthesized lysosomal enzymes into endosomes[15]. In terms of the IGF axis, cell surface IGF2R binds IGF-II with high affinity, IGF-I with a 500-fold lower affinity, and does not bind insulin[28-30]. Mice with a homozygous knock-out of the IGF2R have demonstrated that the IGF2R helps regulate circulating levels of IGF-II[31, 32]. The IGF2R does this by mediating internalisation and degradation of IGF-II[33], thereby sequestering it from activating its target receptors[34]. In addition, the extracellular domain of the IGF2R is proteolytically cleaved to give rise to a soluble form of the receptor that can bind IGF-II and facilitate its degradation[35-37]. Due to its regulatory effect on circulating IGF-II levels, the IGF2R is thought to act as a tumour suppressor[38]. Indeed, mutation, loss of expression, and receptor down-regulation has been demonstrated in a wide variety of cancers and are correlated with poor prognosis[39-41].

1.1.5   The Type I IGF Receptor

1.1.5.1 IGF1R structure

The IGF1R is a heterotetrameric transmembrane tyrosine kinase that is highly homologous to the IR[42]. The *IGF1R* gene is located on chromosome 15, and the resultant transcript is not only homologous to the IR in terms of exon organization and size, but encodes a single polypeptide that shares approximately 70% amino acid homology with the IR[43]. Processing of the IGF1R polypeptide into mature receptor is also similar to the IR. Single-chain IGF1R precursor proteins en route to the cell membrane are glycosylated on the eventual extracellular regions, folded, and dimerised prior to transport to the Golgi apparatus where they are then cleaved to give rise to separate α and β subunits[42, 43]. The subunits are then assembled into the mature processed IGF1R homodimer that consists of two α and two β subunits linked together by disulphide bonds prior to transport to the cell surface[42]. Both the IGF1R and IR are distinct from other transmembrane tyrosine kinases, such as the EGFR, PDGFR, and VEGFR, in that they are expressed at the cell surface as pre-formed dimers, and therefore do not require ligand binding for dimerisation that is a common feature of the other receptors.

1.1.5.2 IGF1R signaling and role in normal biology

The IGF1R is a high affinity receptor for IGF-I but is also able to bind IGF-II and insulin with a 4- and 100- fold lower affinity than IGF-I, respectively[44], see Table 1.1 and 1.3. Binding of ligand to the extracellular α-subunit induces a conformational change in the receptor, which results in the auto-phosphorylation of tyrosine residues in the intracellular portions of the transmembrane β-subunits and activation of their tyrosine kinase domains[42, 45]. Activation of the IGF1R results in the initiation of a variety of intracellular signaling pathways, which are briefly discussed below, but are also extensively reviewed in[46-48]. Phosphorylation of tyrosine residues in the β-subunit enables recruitment of adaptor proteins including insulin-receptor substrate 1 [IRS-1] and Shc. These intermediates are in turn phosphorylated by the intrinsic kinase activity of the activated IGF1R, providing docking sites for signaling molecules containing SH2 domains such as: growth factor

Figure 1.3 Signalling pathways activated by the IGF1R [or IR]

Ligand binding to the extracellular α-subunits of the IGF1R [or IR] results in phosphorylation of the intracellular β-subunits and activation of the tyrosine kinase domain. Phosphorylation of the β-subunits enables recruitment of IRS-1 and Shc thereby providing a mechanism for activation of the MAPK and PI3K pathways. A cascade of molecular interactions results in a range of cellular events, including: change in transcription, cell proliferation, protein synthesis, protection from apoptosis, rearrangement of the cytoskeleton, and initiation of cellular migration. Figure adapted from A.Denley, 2004 PhD thesis.

receptor binding protein 2 [Grb2] and the p85 regulatory subunit of phosphatidyl-inositol 3'
phosphate kinase [PI3K][49]. Activation of the PI3K pathway has been shown to be essential for
induction of protein synthesis, cell cycle regulation, and protection from apoptosis[50]. Recruitment of
Grb2 to the IGF1R, Grb2 binding of SOS, and eventual activation of Ras, and its initiation of the
mitogen-activated protein kinase [MAPK] pathway have been demonstrated to be involved in the
regulation of gene transcription[49], cell survival[51], differentiation[52, 53]. Therefore, by activating the
IGF1R, IGF-I and IGF-II trigger a series of signal transduction cascades that result in a range of
pleiotropic actions including regulation of somatic growth, cellular proliferation, differentiation and
transformation, migration, and protection from apoptosis[22-24, 42, 54]. The IGF1R has also been
demonstrated to induce differentiation in adipocytes, neurons, osteoblasts, and haemopoietic
cells[52, 53]. Activation of the IGF1R therefore is important in normal mammalian development, as
demonstrated by mice IGF1R knockout models and *in vitro* data. Mice with a targeted disruption of
the IGF1R are 45% smaller than their wild-type litter mates and die shortly after birth[19].

1.1.5.3 IGF1R in cancer

Due to its ability to promote proliferative, migratory, transforming, and anti-apoptotic responses, the
IGF1R is thought to play an important role in the pathogenesis and progression of cancer[22, 54].
Overexpression of the IGF1R has been demonstrated to promote tumour formation in nude mice
and ligand-dependent colony formation in soft agar[55, 56]. In addition, embryonic fibroblasts derived
from IGF1R knock-out mice are unable to undergo anchorage-independent proliferation[57], and are
resistant to transformation by several oncogenes[57-60]. The finding that overexpression of the IGF1R
is associated with a more aggressive metastatic phenotype in a range of malignancies including;
breast cancer[61], pancreatic carcinoma[62], sarcoma[63], melanoma[64], and colon[65], suggests the IGF1R
is not only important in the early stages of tumour establishment but also in the progression to
metastatic disease. In addition, the IGF1R has been demonstrated to enhance hypoxia signaling
and expression of vascular endothelial growth factor [VEGF][66] thereby enabling cancer cell survival
in large tumour microenvironments[67]. Moreover, signaling via the IGF1R can promote secretion of
matrix metalloproteinases [MMPs][68], and lead to the disruption of cellular adhesions thereby
promoting cell motility[69-71]. In addition, it has been recently demonstrated that signaling via the
IGF1R can protect cancer cells from a range of chemotherapeutic drugs[67, 72-74]. Therefore, due to

its functional properties and involvement in cancer pathogenesis, the IGF1R has recently gained a lot of attention as a potential anti-cancer therapeutic target. Current therapeutic strategies aimed at targeting the IGF1R are discussed further in Section 1.4.

1.1.6   The Insulin Receptor

1.1.6.1 Structure and function in normal biology

The insulin receptor [IR] is a member of the tyrosine kinase growth factor receptor family and is highly homologous to the IGF1R[75]. The IR is synthesized as a single-chain precursor polypeptide that undergoes glycosylation, proteolytic cleavage, and dimerisation during transport to the cell surface[75]. Mature IR forms from the dimerisation of two αβ monomers linked by disulfide bonds giving rise to a β-α-α-β configuration[75, 76], see Figure 1.3. The extracellular α-subunits are approximately 130kDa in size and contain the ligand-binding domain[77]. It has been demonstrated that the IR is capable of binding two molecules of insulin, and curvilinear Scatchard plots suggest that each molecule binds with differing affinities displaying negative cooperativity[78]. This led to the proposal that high affinity binding occurred via one molecule of insulin cross-linking two separate epitopes on each α-subunit [denoted site 1 and site 2', respectively] that then allows a second molecule of insulin to bind with lower affinity to only one α-subunit[79], see Figure 1.4. The recent publication of the disulfide-linked IR ectodomain crystal structure has demonstrated that the receptor assumes a folded-over conformation such that the ligand binding regions of the α-subunits are in juxtaposition with site 1 involving the L1 domain, and site 2' involving the C-terminal surface of the first fibronectin type III domain[80].

Ligand binding to the α-subunit results in a conformational change in the receptor enables tyrosine residues in the intracellular portions of the β-subunits to undergo trans-phosphorylation thereby activating the tyrosine kinase domains contained within the β-subunits[81, 82]. This enables the recruitment and activation of adaptor proteins resulting in the initiation of intracellular signaling pathways. Docking of the insulin receptor substrates [IRS1-4] and Shc results in their phosphorylation by the IR kinase, thereby leading to the eventual activation of the PI3K and MAPK signaling cascades[83]. Activation of the PI3K pathway has been demonstrated to mediate a number

of insulin effects including stimulation of glucose transport and glycogen synthesis. It has also been implicated in mediating protein synthesis, mitogenesis, inhibition of apoptosis and transcriptional regulation[84]. MAPK signaling has been demonstrated to be involved in mediating inhibition of apoptosis and regulation of gene transcription[85]. Therefore, both the IR and IGF1R initiate similar intracellular signaling pathways that culminate in similar endpoint responses. It is yet to be determined whether signaling via the IR and IGF1R are actually distinct. The expression of receptor chimeras has revealed there may be subtle differences in signaling and resultant end-point responses[86-89]. These differences may depend on cell background and it remains unclear whether intrinsic diversities in the ability of the two receptors to activate distinct intracellular pathways or extrinsic factors such as developmental regulation, tissue expression, or relative abundance account for the differential physiological roles of the IR and IGF1R[83, 88].

The importance of the IR during normal development and metabolic homeostasis has been demonstrated by a range of knockout studies in mice. Dual IR and IGF1R knockout mice have revealed that both the IGF1R and IR are required for optimal foetal development[90]. IR null mice have demonstrated that the IR is not necessary for glucose metabolism in the embryo, however, when born they are 90% of the birth weight of their wild type littermates but die within several days of diabetic ketoacidosis[90-92]. In addition, tissue specific IR knockout models have established the IR to be key in regulation of hepatic glucose production[93], glucose metabolism in muscle and adipose tissue[94], pancreatic insulin secretion in response to glucose[95], adipogenesis[96], and are involved in neovascularisation[97].

1.1.6.2 The Insulin Receptor Isoforms

It has been demonstrated that the insulin receptor is expressed at the cell surface as two different isoforms[77, 98]. Characterisation of the primary transcripts of the IR gene has shown that the two isoforms are generated by the alternative splicing of the 36 nucleotide exon 11[99]. The alternatively spliced mRNA transcripts encode receptors that differ at the carboxyl-terminus of the α-subunits by 12 amino acids[9, 99], see Figure 1.3. Studies using minigene constructs containing exons 10 – 12 and the intervening introns of the IR have demonstrated that elements within intron 10 and exon 11 regulate the splicing process[100]. Three proteins have been shown to be involved in mediating the
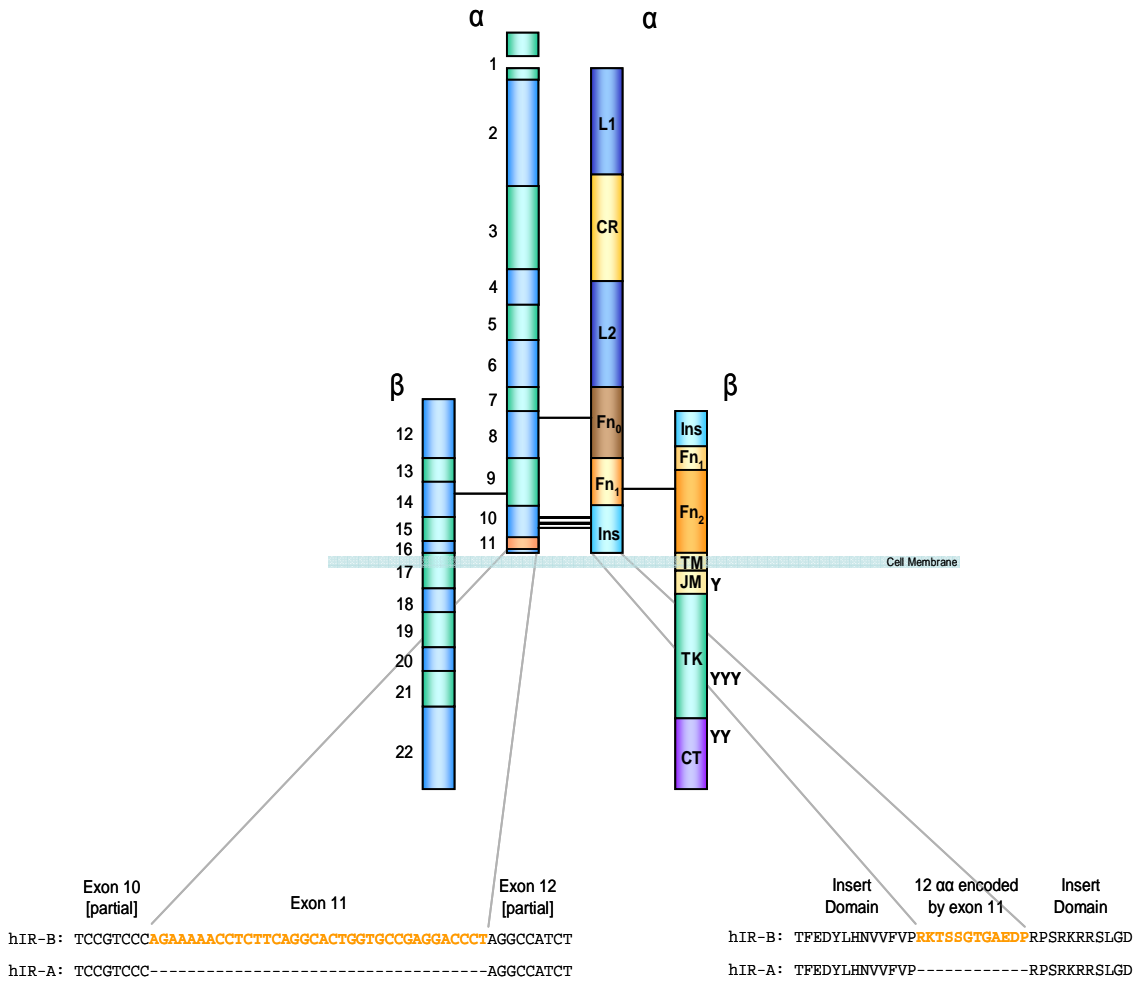
Figure 1.4 The Insulin Receptor Isoforms

The above schematic demonstrates the β-α-α-β structure of the Insulin Receptor. The two α-subunits are linked by a single disulphide bond in the Fn0 domain and three disulphide bridges in the Insert domain. A single disulphide bond forms between the Fn1 and Fn2 domains linking the α- and β-subunits. The left hand αβ monomer indicates the boundaries of the 22 exons of the insulin receptor gene, with the magnified section detailing the 36 nucleotides that comprise exon 11. The right hand αβ monomer indicates the domain organization of the encoded polypeptide, with the magnified section detailing the 12 amino acids encoded by exon 11. 'Y' denotes intracellular tyrosine residues that become phosphorylated upon ligand binding[82]. L1 and L2, large domains 1 and 2 (leucine-rich repeats); CR, cystine-rich domain; Fn0, Fn1, Fn2, fibronectin type III domains; Ins, insert domain; TM, transmembrane domain; JM, juxtamembrane domain; TK, tyrosine-kinase domain; CT, carboxy-terminal tail. Figure adapted from De Meyts & Whittaker 2002 Nature[79], and Denley et al 2003 Horm Metab Res[101]

inclusion or exclusion of exon 11 from IR mRNA transcripts. CELF-6 and Muscleblind 1 are putative IR mRNA splicing proteins, with CELF-6 demonstrated to promote exon 11 exclusion[102], while Muscleblind 1 appears to promote exon 11 inclusion[103]. In addition, overexpression of the CUG-binding protein, an RNA processing factor, in NIH 3T3 fibroblasts has been demonstrated to bind a sequence within intron 10 resulting in decreased inclusion of exon 11 in resultant IR mRNA transcripts[104]. However, the exact factors involved and mechanisms by which alternate splicing occurs to date is unknown, although differential tissue expression of the two isoforms suggests that the alternate splicing of exon 11 is regulated in both a developmentally and tissue specific manner[7, 9, 99].

Studies conducted on isolated receptors have established that the presence [IR-B or IR exon 11+] or absence [IR-A or IR exon 11-] of the 12 amino acids encoded by exon 11 alters the functional properties of the insulin receptor. The inclusion of the 12 amino acids at the C-terminus of the α-subunits appears to have negative effects on the binding of IGFs to the IR[8]. As a consequence, the IR-B binds insulin with high affinity but binds IGFs poorly[8, 10, 11]. Conversely, the IR-A binds both insulin and IGF-II with high affinity[8, 10, 11]. Both receptor isoforms have relatively poor affinities for IGF-I, see Tables 1.1 and 1.3[8, 10, 11]. Interestingly, the affinity of the IR-A for insulin is reported to be 2-fold greater than the IR-B, suggesting that the additional 12 amino acids present in the IR-B confers a slightly different conformation on the ligand binding site of the receptor resulting in a small decrease in affinity for insulin[8, 10, 11]. In contrast to ligand binding, the IR-B has been demonstrated to possess greater autophosphorylation than the IR-A, and a 2.5-fold higher tyrosine kinase activity[105]. Moreover, a study examining the internalization kinetics of the two isoforms suggests that the structure of the α-subunit also has an impact on the intracellular navigation of internalized receptors, due to the IR-A, but not IR-B, being recycled following internalisation[106]. The two isoforms appear to be similar in some regards to insulin signaling in that both the IR-A and IR-B stimulate glucose uptake and thymidine incorporation upon insulin activation[8, 11]. However, in pancreatic β cells it appears insulin can preferentially activate different classes of PI3K pathways via the two IR isoforms resulting in differential activation of insulin and glucokinase transcription[107, 108]. This differential ability of insulin to activate the different PI3K class pathways was demonstrated to be dependent on the differential localization of the IR isoforms in noncaveolae lipid rafts[108]. From this observation it was concluded that the IR-A and IR-B localized to different regions of the plasma membrane, with the 12 amino acids encoded by exon 11 acting as a targeting signal, and IR-A/IR-

B heterodimers could therefore not form[108]. This observation is interesting considering receptor dimerisation occurs at the endoplasmic reticulum as an immediate post-translational event[109]. However, it has been recently established that IR-A/IR-B heterodimers can form, and it was suggested in that study that if segregation of the IR isoforms occurred to prevent heterodimerisation, this event would most likely be specific for certain cell types[110]. The biological relevance of IR-A/IR-B hybrids is unknown. However it has been demonstrated that they bind insulin with a similar affinity to IR isoform homodimers[110].

The two insulin receptor isoforms are thought to have unique biological functions due to their relative expression being controlled in a developmental, tissue specific, and pathophysiological manner. In normal pathology, the IR-B is the predominant isoform in adult insulin responsive tissues such as the liver, skeletal muscle, adipose tissue, and is therefore implicated in mediating the metabolic effects of insulin[99, 101]. In addition, it has been shown that high glucose and insulin concentrations can both induce IR-B expression in insulin-responsive cell lines and tissues suggesting IR-B actions are more metabolic[111-114]. Moreover, it has also been demonstrated that inducing differentiation of HepG2 cells by treatment with dexamethasone induces a shift from IR-A expression to IR-B expression, suggesting that the IR-B is associated with a more adult phenotype[112]. However, in the adult, some tissues, such as the brain, spleen, and peripheral blood cells, do not express the IR-B, but almost exclusively express the IR-A[9, 99]. In general the IR-A has been suggested to be the major isoform involved in the regulation of growth and development since it is the predominant isoform in foetal tissues such as the kidney, muscle, liver, and also in fibroblasts[7]. Furthermore the IR appears to mediate embryonic growth in response to IGF-II[90].

1.1.6.3 The Insulin Receptor and cancer

Epidemiological studies have demonstrated an association between obesity, insulin resistance, hyperinsulinemia and increased risk for developing malignancies of the breast, prostate, kidney, and colon[5, 17]. In addition, exogenous administration of insulin to diabetic rodents has revealed insulin to be involved in the growth of MCF-7 human breast cancer cell xenografts[115, 116]. Together these studies suggested a possible role of the IR in cancer progression, which led to the investigation of IR expression and function in common human malignancies. Early studies in breast

cancer specimens, revealed higher levels of IR expression in 80% of tumours than in normal breast tissue[117]. Interestingly, multivariate analysis of breast cancer specimens has indicated IR expression is an independent prognostic marker for disease-free survival [DFS][118]. Immunohistochemical analysis of IR expression in node-negative breast carcinomas, demonstrate patients with undetectable IR had a lower 5-year DFS than those with detectable IR expression[118]. However, DFS was decreased in patients with carcinomas with very high IR content[118]. A separate study, found high IR expression to correlate with favorable prognostic markers in early stage breast cancer[119]. Investigation of other malignancies revealed that overexpression of the IR was not specific to breast cancer, but common to a range of cancers including those of the colon, lung, ovary, and thyroid[7, 117, 120-124]. The observation that many cancers overexpress IGF-II, together with the discovery of the ability of the IR-A to bind IGF-II with high affinity, led to the investigation of the differential expression of the IR isoforms in cancer tissues compared to normal tissues. Predominant expression of the IR-A over the IR-B has been found to occur in cancers of the breast[7, 125], thyroid[123], lung[7], colon[7], ovaries[126], and smooth and striated muscle[127].

Multiple mechanisms that affect gene transcription are thought to be primarily responsible for the overexpression of the IR in cancer[121]. When primary breast carcinomas were analysed by Southern blot and Fluorescence in situ hybridization [FISH] only 8% of the 96 primary tissue samples tested demonstrated increased IR gene copy number, suggesting that amplification of the IR gene itself may be a relatively uncommon event in cancer cells[122]. Oncogenes such as Wnt, Neu, and Ret have been demonstrated in transgenic mice to result in the upregulation of the IR[128]. This suggests that increased transcription and the resulting overexpression of the IR may be due to mutations in oncogenes and anti-oncogenes that are common in cancer[129]. Giving particular support to this theory are studies with mutated p53. Mutations resulting in the inactivation of p53 are common in multiple malignancies where overexpression of the IR and IGF1R are also common[130]. Wild-type p53 has been demonstrated to suppress transcriptional activation of the IR promoter by binding specific sequences in the promoter region. In addition, wild-type p53 has also been shown to suppress IGF1R transcription, however in contrast to the IR, this has been shown to be by sequestering the activator protein Sp1[131]. Moreover, the archetypal nuclear transcription factor HMGA1 has been demonstrated to interact with sequences in the IR promoter region and, via formation of a complex with Sp1 and C/EBP, is required for activation of transcription[132]. Dysregulation of expression of HMGA1 has been demonstrated in malignant cells and correlates

with transformed phenotypes[133, 134], suggesting other mechanisms of IR overexpression may exist in cells that express functional p53[129]. What mechanisms are involved that lead to the predominance of the IR-A isoform over the IR-B are as yet unknown. However, since expression of the IR-A is associated with dedifferentiated cells[7, 112], the predominance of the IR-A in cancer is generally thought to be reflective of the dedifferentiation of cancer cells back to a more foetal phenotype.

The finding that the IR-A is a second physiological receptor for IGF-II and is overexpressed in a variety of cancers prompted the investigation of whether this receptor could signal biological responses important to cancer biology. Utilising 3T3-like fibroblasts derived from IGF1R null mice transfected to express the IR-A, Morrione *et al* 1997 demonstrated that the IR-A could indeed signal proliferative responses to IGF-II[135]. Inhibitory antibodies against the IR established the presence of autocrine proliferative loops existing between IGF-II and the IR-A in breast cancer cell lines[125]. In addition, in SKUT-I leiomyosarcoma cells devoid of the IGF1R, activation of the IR-A by IGF-II has been shown to protect these cells from apoptosis[127]. This same study, also demonstrated IGF-II to be more effective than insulin at stimulating SKUT-I cell migration and invasion[127]. Furthermore, signaling via the IR-A confers resistance to the EGFR inhibitor gefitnib in LoVo colorectal cancer cells that lack functional IGF1R and express predominantly IR-A over IR-B[136]. Together, these studies indicate the IR-A may be important in mediating the biological outcomes of IGF-II. However, most studies investigating the biological function of the IR-A were conducted in cell lines devoid of the IGF1R and over-expressing the IR-A. Therefore, very few studies on the IR-A have been conducted in cells co-expressing the IGF1R and IR-A. It is not known how the IR-A interacts, and functions in conjunction with the other receptors of the IGF system to signal biologically relevant outcomes. Work outlined in this thesis aims to address this issue.

1.1.7 IGF1R/IR hybrid receptors

1.1.7.1 Structure and formation

Functional hybrid receptors can form between the IGF1R and IR due to the high degree of sequence and structural homology between these two receptor types[137-139]. Both the IR and IGF1R

homodimers exist at the cell surface as pre-formed dimers, and dimerisation occurs as a post-translational event at the endoplasmic reticulum prior to the generation of the α and β subunits by cleavage of the pro-receptors[109]. It is at this dimerisation stage in cells co-expressing both the IR and IGF1R that pro-receptors can heterodimerise to give rise to IGF1R/IR hybrid receptors[137-139]. Hybrid receptors therefore consist of one αβ monomer of the IGF1R and one αβ monomer of the IR, and are widely expressed in normal mammalian tissues[137-140]. Heterodimerisation has been demonstrated to occur in a random fashion with a similar efficiency to homodimerisation, such that the proportion of hybrid receptors expressed by a cell is directly related to the molar fractions of the individual IR or IGF1R[140, 141]. Therefore in cells expressing equal levels of IR and IGF1R, the ratio of IGF1R homodimers: IGF1R/IR hybrids: IR homodimers is found to be 1:2:1, such that hybrid receptors are the most abundant receptor type expressed[142, 143]. Moreover, if one receptor type [IR or IGF1R] is expressed at a higher level than the other, the less abundant receptor is present predominantly in hybrids rather than homodimers[140, 141].

1.1.7.2 Functional properties of IGF1R/IR hybrid receptors

There has been some contention in the literature regarding the ability of hybrid receptors to bind ligands. An early report suggested that hybrid receptors could bind both insulin and IGF-I with high affinity *in vitro*[139]. This finding was supported by transfected cell studies that also showed hybrids could bind both insulin and IGF-I with high affinity. However in these studies each ligand had a differential ability to compete off the reciprocal ligand[138]. IGF-I was observed to prevent subsequent binding of insulin. In contrast, insulin bound to hybrid receptors did not appear to affect the affinity of hybrid receptors for IGF-I[138]. Further *in vitro* studies by this group using immunopurified hybrid receptors showed hybrids bound IGF-I with high affinity similar to that of homodimer IGF1R, and bound insulin with approximately 10-fold lower affinity than homodimer IR, leading to the suggestion that hybrid receptors functioned more like IGF1R homodimers[137]. Studies that investigated other functional properties such as receptor internalization and autophosphorylation further substantiated the proposal that hybrid receptors functioned more like IGF1R homodimers than IR homodimers. Studies utilising truncated receptors demonstrated that *trans* but not *cis* signal transduction is the major mechanism mediating hybrid receptor autophosphorylation and endocytosis[144-146]. Due to the difference in intracellular itinerary of the IGF1R and IR upon

Table 1.1 Binding affinities of the IGF receptors for ligand

Binding affinities determined by antibody capture binding assays, competing ligand as indicated.

Receptor	IC50 [nM]			Competing Ligand	Reference
	IGF-I	IGF-II	Insulin		
IGF1R	0.8	4.4	>100	Eu Labelled IGF-I	Denley et al 2004 [13]
	0.2	0.6	>30	125-I- IGF-I	Pandini et al 2002 [148]
	0.5	-	>1µM	125-I- IGF-I	Benyoucef et al 2007 [110]
IR-A	120	18.2	2.8	Eu Labelled Insulin	Denley et al 2004 [13]
	>30	0.9	0.2	125-I- IGF-I	Pandini et al 2002 [148]
	9	2.2	0.3	125-I- Insulin	Benyoucef et al 2007 [110]
IR-B	366	68	1.4	Eu Labelled Insulin	Denley et al 2004 [13]
	>30	11	0.3	125-I- IGF-I	Pandini et al 2002 [148]
	90	10	0.5	125-I- Insulin	Benyoucef et al 2007 [110]
IGF1R/IR-A	0.3	0.6	3.7	125-I- IGF-I	Pandini et al 2002 [148]
[Hybrid-A]	0.5	0.7	70	125-I- IGF-I	Benyoucef et al 2007 [Ref no#]
IGF1R/IR-B	2.5	15	>100	125-I- IGF-I	Pandini et al 2002 [148]
[Hybrid-B]	0.3	0.3	76	125-I- IGF-I	Benyoucef et al 2007 [110]

Table 1.2 Binding affinities of Hybrid receptors from Slaaby et al 2006[147]

Ab Capture denotes antibody capture binding assays. PEG denotes Polyethylene glycol precipitation binding assay. Competing ligand as indicated.

	EC50 [nM]		Assay Type
	IGF-I Competitor	Insulin Competitor	
IGF1R/IR-A	0.017	2.6	Ab Capture
[Hybrid-A]	0.018	4.6	PEG
IGF1R/IR-B	0.012	2.8	Ab Capture
[Hybrid-B]	0.017	5.1	PEG

internalization, Seely *et al* 1995 demonstrated that hybrid receptors functioned more like IGF1R homodimers than IR homodimers with respect to internalization and ligand degradation[146].

However, these early studies did not consider the IR isoform involved in hybrid formation. Pandini *et al* 2002 analyzed hybrid receptors in context of the IR isoform involved, and observed the two IR isoforms gave rise to hybrid receptors with differential functional properties[148]. IGF1R/IR-A [Hybrid-A] receptors were bound and activated by IGF-I and IGF-II with high affinity similar to that of IGF1R binding, and were also found to have higher affinity for IGF-I and IGF-II than IGF1R/IR-B [Hybrid-B] receptors[148]. Hybrid-A receptors were also bound and activated by insulin, however at a 20-fold lower affinity than homodimer IR-A[148]. In contrast to this, hybrids containing the IR-B were not bound by insulin, but were bound by IGF-I with high affinity and IGF-II with low affinity[148] [see Table 1.1]. In addition, the IR isoform involved in the hybrid receptor was reported to determine differential signaling outcomes as demonstrated by insulin's ability to activate the IGF1R specific substrate CrkII via Hybrid-A but not Hybrid-B[148]. Overall, the Pandini *et al* 2002 study suggested a further mechanism by which differential expression of the IR isoforms could affect the IGF system. However, a more recent study by Slaaby *et al* 2006 contrast these findings. In this study utilising both semi-purified [like the Pandini study] and purified hybrid receptors, irrespective of the IR isoform involved in hybrid formation, hybrid receptors had high affinity for IGF-I but low affinity for insulin [see Table 1.2][147]. In addition, both Hybrid-A and Hybrid-B were observed to have similar affinities for IGF-II[147], again suggesting that hybrid receptors function more like homodimer IGF1R.

Perhaps fuelling the ambiguous nature of the published literature is the difficulty in studying hybrid receptors in isolation without interference from either IR or IGF1R homodimers. Two separate research groups have since addressed this quandary utilising bioluminescence resonance energy transfer, or BRET, to specifically study hybrid receptors. Blanquart *et al* 2006, utilised BRET to specifically monitor the activation state of Hybrid-A receptors both in vitro and in intact living cells[149]. This study essentially established proof of concept, based on the premise that Hybrid-A receptors could be important in cancer biology, they set up high-throughput BRET based assays to specifically study the activation state of Hybrid-A receptors by ligand[149]. Benyoucef *et al* 2007, utilised BRET in conjunction with RLIC [radioligand immunocapture assays utilised by both the Pandini 2002 and Slaaby 2006 studies] and autophosphorylation studies to further delineate the effect of IR isoform expression on hybrid receptor functional characteristics. They found that the IR
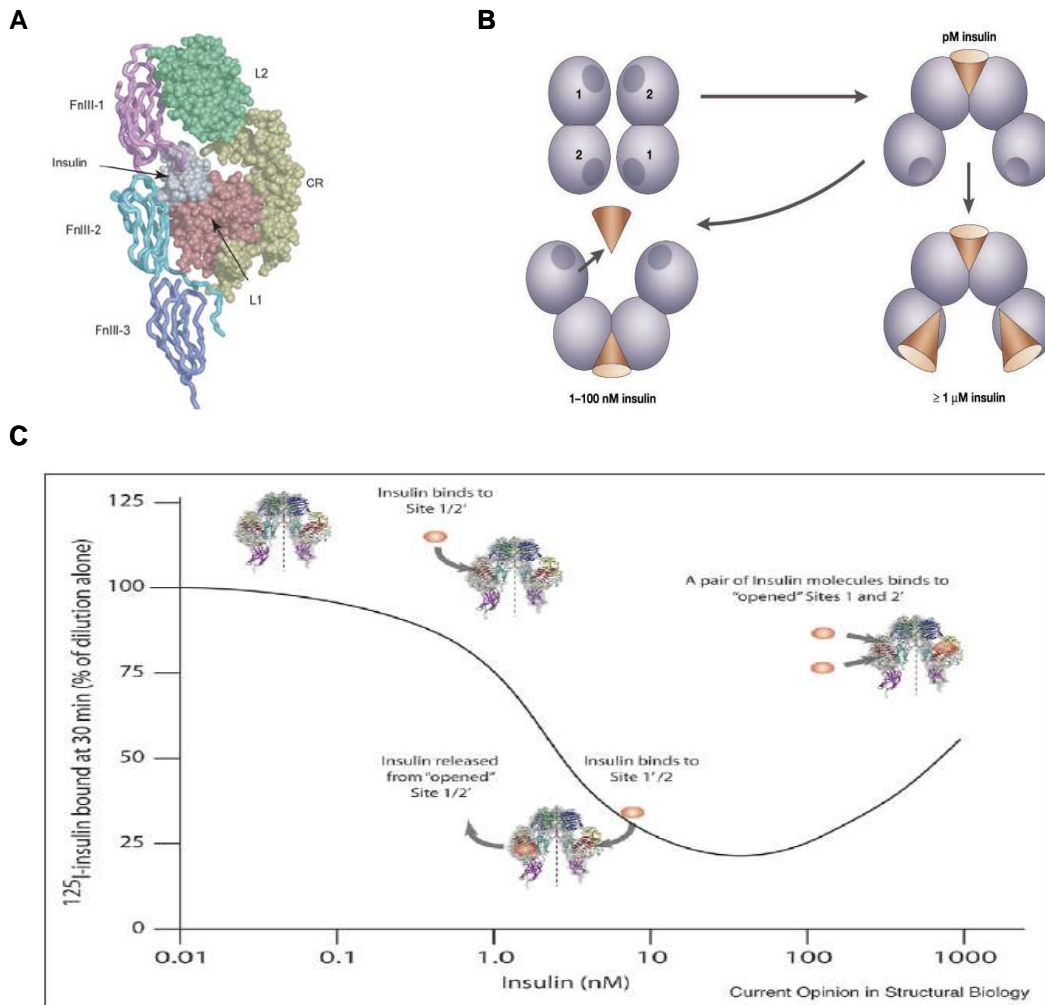
Figure 1.5 Model of Insulin binding to the Insulin Receptor

[**A**], insulin bridging two monomers in the IRΔβ homodimer. Atomic spheres representation of the L1, CR, and L2 domains are from one monomer of the IR homodimer. Tube representation of FnIII domains are from the other monomer. Insulin is represented as grey atomic spheres. Figure reproduced from McKern et al 2006[80]. [**B**], model of the insulin binding mechanism. The orange cone represents one molecule of insulin. The first insulin molecule cross-links sites 1 and 2 and binds with high affinity. Partial dissociation of the first insulin molecule enables a second insulin molecule to cross-link the remaining sites 1 and 2. This causes complete dissociation of the first insulin molecule. Monovalent binding of two extra insulin molecules occurs at high concentrations of insulin and saturates the left over sites 1 and 2. Figure reproduced from DeMeyts and Whittaker 2002[79]. [**C**], proposed basis of negative co-operatively of insulin binding to the IR. Overlaid on a stylized representation of the dose response of the dissociation of ^{125}I-labelled insulin from IR are the structural events proposed to underlie the negative cooperatively of ligand binding. These events follow the ligand binding model proposed by DeMeyts and Whittaker 2002[79] and are as outlined in [**B**]. Figure reproduced from Lawrence et al 2007[150].
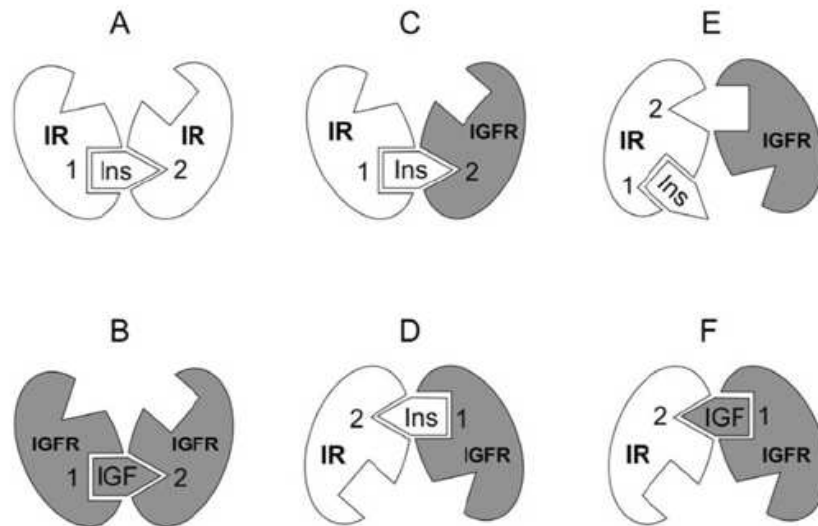
Figure 1.6 Model of ligand binding to hybrid receptors

Follows the model of ligand binding to the insulin receptor outlined in Figure 1.4. This model assumes only one molecule of ligand can bind with high affinity by cross-linking sites 1 and 2 on the α-subunits. Site 1 contributes the greater fraction of binding energy. [A] and [B] demonstrate high affinity ligand binding to IR and IGF1R homodimers respectively. [C] and [D] represent two potential models of ligand binding to hybrid receptors. In these models site 1 is contributed by either the IR [C] or IGF1R monomer [D]. [E] and [F] represent the binding modes of labelled insulin and IGF-I, respectively. These models account for the differential ability of unlabelled insulin to compete for bound labelled insulin or IGF-I. Figure reproduced from Benyoucef et al 2007[110]

isoform did not affect the functional properties of hybrids in any of the three assays, and showed hybrid receptors had high affinity for IGF-I and low affinity for insulin irrespective of the IR isoform involved [see Table 1.1][110]. Hybrids containing either IR isoform were found to have affinity for IGF-I and IGF-II similar to that of IGF1R homodimers, and substantially lower affinity for insulin than IR homodimers[110]. Therefore the results of the Benyoucef *et al* 2007 study are consistent with those of the Slaaby *et al* 2006 study. There appears to be no technical reason behind the discordant results in the Pandini *et al* 2002 study. Benyoucef *et al* 2007 suggest that since both IR-A and IR-B homodimers bind insulin with similar affinities, there would be no specific reason to expect that IR isoform involvement would affect the affinity of hybrid receptors for insulin[110]. Furthermore, through IR-A/IR-B heterodimers they demonstrated that any asymmetry in IR/IGF1R hybrids due to the amino acids encoded by exon 11 of the IR is not inhibitory to ligand binding, as IR-A/IR-B heterodimers bound insulin with a similar affinity to IR isoform homodimers[110]. The recent crystal structure of the disulfide-linked ectodomain of the IR[80], confirming the insulin binding models proposed by DeMeyts and Whittaker[79], suggest a possible reason for hybrid IGF1R/IR receptors having low affinity for insulin. The models suggest that high affinity binding of insulin to homodimer IR requires the interaction of insulin with site 1 of one α-subunit and site 2' of the other α-subunit[79] [see Figure 1.5]. In the case of IGF1R/IR hybrid receptors, site 2' provided by the reciprocal IR α-subunit would be missing and replaced by the α-subunit of the IGF1R. A study utilising chimeric receptors has suggested that cross-linking of the L2/Fn domains in the IR α-subunits is required for high affinity insulin binding[110]. In this study hybrid receptors formed by wild-type IR-A and chimeric IGF1R where the L2/Fn domain had been swapped for the reciprocal portion of the IR, increased affinity of the chimeric hybrids for insulin 20-fold compared to wild-type IGF1R/IR-A hybrid receptors[110]. This suggests that in the context of hybrid receptors there is asymmetry that enables high affinity IGF-I binding, but not high affinity insulin binding[110]. However, further research is required to further delineate the binding epitopes for ligands in the context of both homodimers and hybrid receptors.

1.1.7.3 Potential role of hybrid receptors in cancer

Elevated expression of IGF1R/IR hybrid receptors has been demonstrated in thyroid[142] and breast[143] cancers. Up-regulation of hybrid receptors was concomitant with over expression of the

IGF1R and/or IR, and was found to follow the random dimerisation model of assembly[142, 143]. In breast cancer cells with elevated hybrid receptor content, IGF-I stimulated phosphorylation of hybrid receptors exceeded that of IGF1R homodimers suggesting the majority of signaling in response to IGF-I occurred via hybrid receptors[143]. Consistent with this, in both studies, IGF-I stimulated cell growth was inhibited by blocking antibody to either hybrid receptors or IGF1R homodimers, and demonstrated that the mitogenic effects of IGF-I were mediated by the more abundant receptor type, be that hybrid or homodimer, in both breast cancer[143] and thyroid cancer cell lines[142]. One caveat to note with these observations, is the recent publication by another group demonstrating that the antibodies utilised in the aforementioned studies do not distinguish between hybrid receptors and IR homodimers[151]. Since hybrid receptors can bind IGF-I and IGF-II with high affinity resulting in their autophosphorylation, and are up-regulated in cancer, this suggests these receptors could play a role in cancer biology. The biological relevance of signaling via hybrid receptors is yet to be determined, again hampered by the inability to study these receptors in isolation without interference from homodimers.

1.2   Colorectal Cancer

Colorectal cancer [CRC] is the second highest cause of cancer death in the westernized world[152]. The increasing incidence worldwide has prompted many investigators to focus on the possible mechanisms behind the etiology of this cancer. Patients with a high familial risk of developing the disease comprise approximately 20 percent of all reported colorectal cancer cases[153, 154]. Only 5 - 10 percent of cases are known to be inherited in an autosomal dominant manner, although the precise genetic basis of this form of hereditary colorectal cancer is unknown[153, 154]. Therefore, the two major forms of hereditary colorectal cancer encompass only 25 – 30 percent of all reported cases[153, 154]. Variations in the incidence rates of colorectal cancer in different world regions, as well as migrant studies, suggest that some aspects of a Western lifestyle could play and important role in colorectal carcinogenesis[152]. Environmental and lifestyle factors, such as diet, obesity, and physical activity, are therefore thought to be largely responsible for the potentiation of this disease.

The clinical and histopathological stages of colorectal cancer are quite distinct [see Figure 1.6] and range from a lesion resulting from a single colonic crypt, giving rise to adenomatous polyps [small

benign tumors], and eventually resulting in malignant carcinomas[155]. Several genetic changes are required for the initiation and progression of colorectal cancer, and are termed either the 'gatekeeper' or 'caretaker' pathways[156]. The gatekeeper pathway accounts for 85% of sporadic colorectal cancer and is associated with mutations in genes involved in growth regulation such as the tumor-suppressors APC, p53, DPC4/Smad4, and oncogenes such as K-ras and c-myc, to name a few[156]. The caretaker pathway accounts for 15% of sporadic colorectal cancer and is associated with mutations in genes that maintain genetic stability[156]. However, it is noted in the review by Weitz *et al* 2005 that the two pathways may not be distinct as some gene products can maintain genetic stability while being involved in growth regulation, for example APC[156].

Early detection and screening are effective in reducing colorectal cancer mortality rates and since lifestyle factors are primarily implicated in the potentiation of the disease, the most important preventative measure for reducing colorectal cancer risk is lifestyle change[156]. The primary therapeutic strategy is surgery, and recent developments in techniques have had important implications on local recurrences, perioperative morbidity, and improved quality of life[156]. Depending on the staging of the cancer, post-operative follow-up treatment can involve radiotherapy, radiochemotherapy, chemotherapy, or palliative chemotherapy. Discussion of such treatment strategies are beyond the scope of this literature review, however, the Weitz *et al* 2005 review on colorectal cancer provides excellent discussion on differential treatment strategies[156]. This introductory literature review, in Section 1.4, will cover novel therapeutic strategies aimed at targeting the IGF system.

1.2.1 Environmental risk factors that contribute to colorectal carcinogenesis

1.2.1.1 Diet

Epidemiological evidence suggests that components of a more westernized diet, namely high consumption of red meat, processed meats, saturated fats, and highly processed carbohydrates are not only associated with increased risk but also contribute to colorectal carcinogenesis[157].
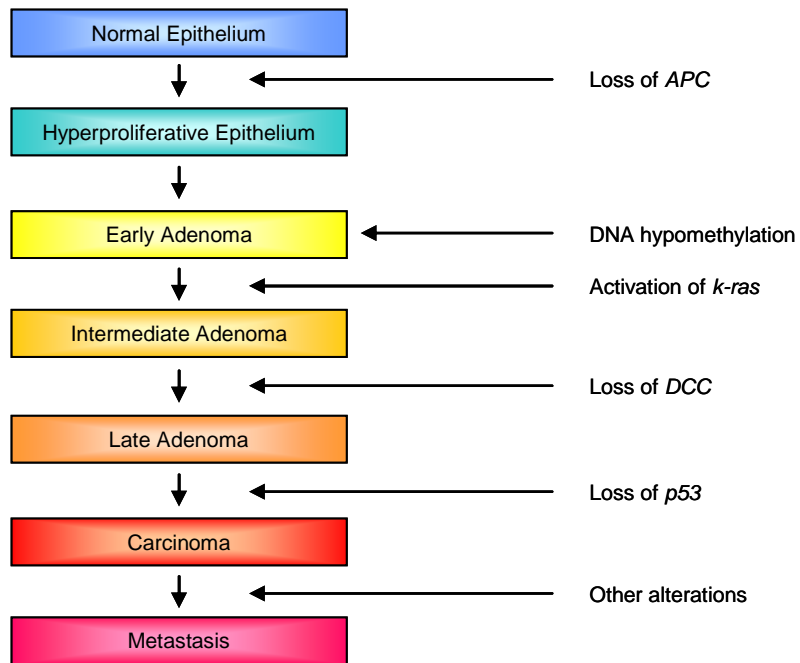
Figure 1.7 A genetic model for colorectal tumorigenesis

Figure reproduced with alteration from Vogelstein 1993[158] and Kinzler & Vogelstein 1996[159]. Demonstration of the distinct histopathological stages associated with colorectal cancer progression along with the common genetic mutations required for the initiation and progression of the disease.

Metabolic by-products of red meat digestion are thought to promote DNA damage in the colonic epithelium[160] and a considerable amount of research has been devoted to elucidating the mechanisms behind this, but are beyond the scope of this thesis. Therefore, in terms of dietary risk factors this literature review focuses upon those that influence the IGF axis. Studies in rodents have demonstrated the effect of different diets on colon cancer and insulin resistance[161, 162]. The impact insulin resistance has on colorectal cancer risk will be discussed further in the upcoming sections. Rats fed diets high in sucrose have larger more dysplastic carcinogen induced aberrant crypt foci [ACF] than rats fed a starch diet[161]. ACF are preneoplastic lesions that indicate early stage colon cancer in the rat, and are therefore used as an experimental model to measure tumour promotion[161, 162]. Rats fed diets high in fat and energy content displayed insulin resistance and increased ACF growth[162]. Therefore, these studies correlate with epidemiological evidence suggesting that highly processed carbohydrates and saturated fats contribute to colorectal carcinogenesis. Moreover, a study examining the effect of dietary fat intake on colonic IGF1R and IGF2R expression in rats demonstrated increased IGF1R expression in the proximal and middle colon, while increased fat intake had differential effects on IGF2R expression in differing regions of the rat colon[163]. Nevertheless, the study indicated that IGF receptor expression can be modified by dietary intake of fats, and together with the finding that rats fed high corn oil diets exhibited increased colonocyte proliferation[164], suggests that dietary fat intake can potentially influence IGF regulated colonocyte mitogenesis.

In contrast to the adverse effects of saturated fat and processed carbohydrate, some dietary components have been demonstrated to be protective. Indeed, consumption of dietary fibre has been shown to be protective against colorectal cancer in a dose-dependent manner[165]. Dietary fibre consists primarily of non-starch polysaccharides and resistant starch that can escape enzymatic digestion and absorption in the small intestine that then undergo complete or partial fermentation in the large intestine by anaerobic microflora. This bacterial fermentation of carbohydrates results in the production of short-chain fatty acids [SCFAs], of which acetate, propionate, and butyrate are the three major SCFAs produced[166]. SCFAs have been shown to improve visceral function, namely by raising blood flow and increasing mineral and water absorption[167, 168], increasing the acidity of the luminal environment thereby resulting in diminished degradation of primary bile acids to carcinogens[169]. In addition, increased luminal acidity facilitates uptake of SCFAs by colonocytes where they are utilised as an energy source[170]. Butyrate is

gaining particular attention for its trophic effects on colonocytes *in vivo* and *in vitro*. Butyrate is the primary metabolic substrate of colonocytes[171], and a modulator of the epithelial cell cycle[172] and mucosal immune response[173]. Therefore, *in vivo* butyrate plays a vital role in the homeostasis of the colonic epithelium. However, in contrast to this, *in vitro* butyrate induces differentiation, inhibits cellular proliferation and stimulates apoptosis in cultured colorectal cancer cells[174-176]. Therefore, there appears to be a switch between butyrate being used as a fuel source by normal colonocytes, and butyrate inducing apoptosis in colorectal cancer cells. Deficiencies in the availability of butyrate could therefore be involved in colorectal carcinogenesis[177]. In addition *in vitro*, butyrate has also been demonstrated to be a potent inhibitor of histone deacetylase, resulting in the hyper-acetylation of histones[178]. Via its action as a histone deacetylase, butyrate has been demonstrated to alter the secretion of IGFBPs in the Caco-2 colorectal cancer cell line[179], thereby suggesting another potential mechanism whereby butyrate can modulate cellular proliferation, by altering the bioavailability of IGF-I and IGF-II[179]. However, to date, it is unknown what role butyrate-induced apoptosis plays in preventing colorectal carcinogenesis *in vivo*.

1.2.1.2 Physical Activity and Obesity

Exercise has been associated with diminished risk of developing colorectal cancer[180, 181]. One study reported physical activity to result in a 50 percent reduction in colorectal cancer risk[182]. Several suggestions have been made to explain why physical activity may be so beneficial in reducing colorectal cancer risk. These include enhancement of the immune system, stimulation of colon peristalsis thereby decreasing the time dietary carcinogens are present in the colon, and control of body weight[180, 182, 183]. Another mechanism by which physical activity may be beneficial is that it increases insulin sensitivity and lowers circulating insulin[184]. Indeed, several large cohort studies, the largest being the European Prospective Investigation into Cancer and Nutrition [EPIC], utilizing body mass index [BMI = kg/m^2] as an indicator of obesity, have found a positive correlation between obesity and the risk of developing colorectal cancer[185-188]. This correlation appears to be stronger and more linear in men, than in women[185]. The weakness of the correlation between BMI and colorectal cancer risk in women may be accounted for by menopausal state[187]. An investigation into menopausal state, observed a BMI of 30 was associated with a 2-fold increased risk of developing colorectal caner among pre-menopausal women[187]. However, no association
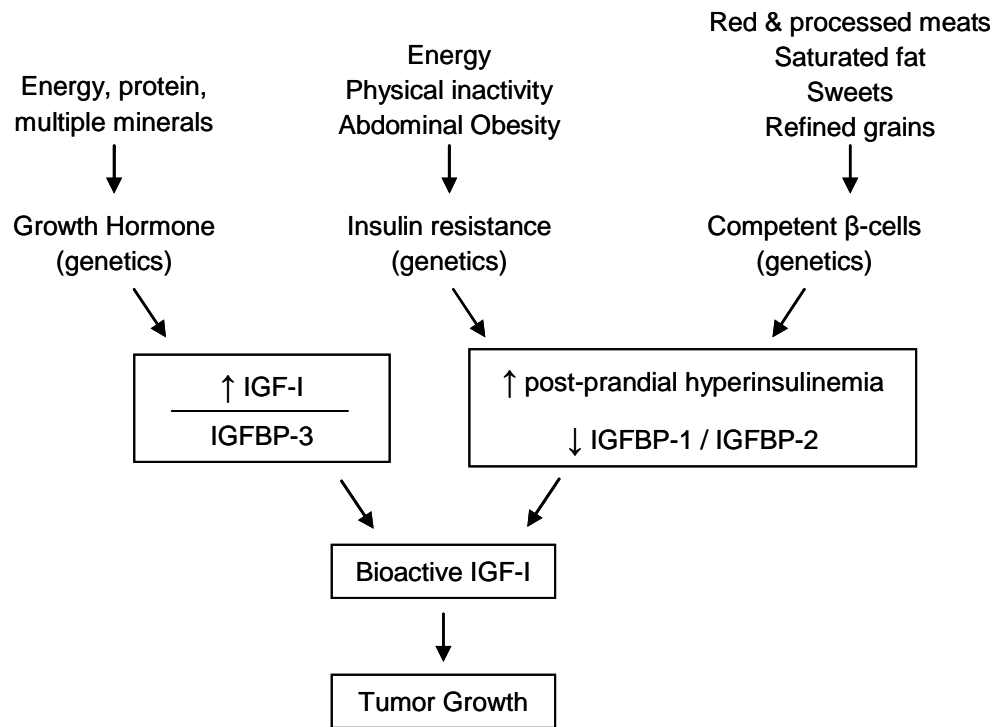
Figure 1.8 A model whereby nutritional factors may affect colon cancer risk by influencing the IGF axis

Figure reproduced from Giovannucci & Michaud 2007[189], and demonstrates a model whereby dietary factors could alter the bioavailable levels of IGF-I resulting in the stimulation of tumor growth. Alterations in GH secretion, insulin resistance, and insulin secretion by pancreatic β-cells caused by energy balance and dietary factors then perturb IGF-I levels. Alterations in IGF-I levels could occur via increases in insulin that then decreases IGFBP-1 and IGFBP-2 levels, or increases in the IGF-I/IGFBP-3 ratio or IGF-I itself.

was found in post-menopausal women[187]. It was suggested that in post-menopausal women, the deleterious effects of obesity on IGF-I and insulin levels may be negated by the conversion of androgens to oestrogens by adipose tissue[187]. Several studies, of which the aforementioned EPIC study is the largest, have found waist-to-hip ratio to be a more consistent indicator of colorectal cancer risk than BMI and that higher waist-to-hip ratio is associated with increased risk for both men and women[186, 190-192].

1.2.1.3 Type 2 diabetes and hyperinsulinemia

It is well known that diets high in fat and energy, together with a lack of physical activity result in weight gain and obesity. In addition, the association between obesity and type 2 diabetes is also well recognised[193]. The correlation between obesity and type 2 diabetes is thought to arise from the effect of obesity to confer insulin resistance[193, 194]. Insulin resistance results in the overproduction of insulin by pancreatic β cells and is a fundamental aspect of type 2 diabetes[194]. Hyperinsulinemia, is a compensatory response that maintains glucose homeostasis in insulin resistant individuals[195]. Hyperinsulinemia underlies the association between diet, physical inactivity, obesity, type 2 diabetes and colorectal cancer[195, 196]. When pancreatic β cells can no longer compensate for increasing insulin requirements to maintain glucose homeostasis, hyperglycemia results[195]. Individuals with high [116 - 448 mg/dL] fasting blood glucose levels have 80 percent increased risk of developing colorectal cancer compared to individuals with low [61 – 96 mg/dL] fasting blood glucose levels[197]. In addition, two independent studies have shown that individuals with high glucose and insulin levels after glucose challenge have a 2-fold increased risk for developing colorectal cancer[197, 198]. Moreover, prospective cohort studies have demonstrated that type 2 diabetes is associated with an increased relative risk of 1.16 to 1.55 in developing colorectal cancer[182, 199, 200].

The molecular mechanisms underpinning the association between insulin levels and colorectal cancer risk are largely unknown. However, two reviews Sandhu *et al* 2002, and more recently, Giovannucci and Michaud 2007, have proposed several possible mechanisms by which increased insulin levels may play a role in the pathology of colorectal cancer[189, 195] [see Figure 1.7]. The first model suggests that insulin may have direct effects on promoting cellular proliferation via activating

the IR, IGF1R, or hybrid IR/IGF1R[189, 195]. The second, suggests that insulin resistance gives rise to increased circulating levels of insulin, triglycerides, and non-esterified fatty acids which then might in turn promote colorectal carcinogenesis by stimulating proliferation of colonic epithelial cells[195]. Thirdly, increased insulin levels may increase the bioavailability of IGFs by altering IGFBP concentrations thereby promoting the proliferation of colonic epithelial cells[189, 195, 196].

1.2.1.4 Circulating IGF levels

Insulin has been demonstrated to have a large influence on the IGF axis by reducing levels of IGFBP-I and IGFBP–II, thereby resulting in an increase of free circulating IGF-I[201]. Along with other human and animal studies and hyperinsulinemia being an important determinant in the etiology of colorectal cancer, there is strong evidence to suggest that the IGF axis could play an important role in colorectal carcinogenesis. Prospective colonoscopic examination has revealed a significantly higher prevalence of tubulovillous adenomas in patients with acromegaly[202]. Acromegalics have abnormally high circulating levels of IGF-I, due to increased GH secretion, and have a higher risk of developing colorectal cancer [RR = 1.2 – 4.9][202-204]. Mice with a liver specific disruption of the IGF-I gene [LID mice] have a 75% reduction in circulating IGF-I, and when compared to normal mice, have significantly reduced tumour growth and hepatic metastasis following transplantation of murine colorectal adenocarcinoma tissue[205]. In addition, administration of recombinant human IGF-I to these mice resulted in a significant increase in tumour growth and metastasis, further suggesting that circulating IGF-I level affects the rate of colonic tumour growth and metastasis[205]. Moreover, a prospective biomarker study that examined plasma levels of IGF-I found men in the highest quartile for IGF-I levels had an increased risk [RR = 2.51] of developing colorectal cancer than men in the lowest quartile for IGF-I levels[183]. This study additionally demonstrated that men with higher circulating levels of IGFBP-3 had a significantly lower relative risk [RR = 0.28] of developing colorectal cancer than men with low levels of IGFBP-3[183]. However, utilizing circulating IGF-I and IGFBP-3 levels as a biomarker for colorectal cancer risk is an area of contention[196]. A systematic review and meta-regression analysis of case controlled studies has suggested there to be a modest association between IGF-I levels and colorectal cancer risk, and indicates individual assay characteristics, study design, and study populations may underlie the differences seen between different prospective studies[206]. Despite the differences in the prospective studies, they

support the suggestion that colorectal cancer is a multi-step process, and that increased bioavailability of IGFs may promote cell survival. The increased proliferative rates of colonic epithelial cells may therefore lead to the accumulation of the molecular modifications that are required to the development of colorectal adenocarcinomas[205, 207].

1.3   The molecular role of the IGF system and colorectal cancer

Several excellent reviews[22, 208, 209] have recently focused on the molecular aspects concerning the role of the IGF system in colorectal cancer and the clinical and experimental evidence linking the IGF axis to the pathogenesis of colorectal cancer. The main findings pertaining to expression of the IGFs and their receptors will be outlined in the following section.

1.3.1   IGF-I and IGF-II expression

In the mid eighties, northern blot analysis of colorectal cancer specimens demonstrated increased mRNA expression of both IGF-I and IGF-II transcripts compared to normal colonic epithelium[210]. Serial analysis of gene expression, SAGE, showed IGF-II to be the most abundant over-expressed RNA in primary colorectal cancer tissue and cell lines[211]. However, oligonucleotide gene array chips failed to confirm this observation, but did identify alterations in IGFBP expression[212]. Increased expression of IGF-II may be associated with a loss of imprinting [LOI] of the IGF-II gene. LOI has been demonstrated to occur in 30% of patients with colorectal cancer[213] and is not restricted to the tumour but can also occur in the surrounding normal colonic mucosa and in the peripheral blood mono-nuclear cells[214-216]. This could provide a plausible explanation for why gene chips failed to confirm results of SAGE analysis. Indeed, gene chips only identified a relatively few genes that were over-expressed in colorectal adenoma and carcinoma tissues compared to normal colonic tissue[212].

It is well established that mRNA levels do not necessarily reflect protein expression. Several studies have therefore determined IGF-II protein expression in colorectal cancer specimens[213, 217]. In one study, immunohistochemical staining of IGF-II expression demonstrated 74% of colorectal cancer specimens to be positive for IGF-II expression compared to 11% of normal colonic

samples[213]. A positive association was also found between IGF-II expression and size and depth of tumour invasion[213]. Patients with tumours negative for IGF-II expression were found to have a statistically significant increased chance of survival[213]. A similar study with a ten-year patient follow-up period also revealed a correlation between IGF-II expression and poor clinical prognosis[218]. Similar findings have also been reported in APC mice models genetically crossed with IGF-II paternal allele knock-out mice[212]. These mice were shown to have a reduced IGF-II supply and this was correlated with reduced adenoma size and frequency[212]. In adenomas that did form, IGF-II expression was detected, indicating LOI of the maternal allele occurred in these adenomas[212].

The liver is the most frequent site of secondary metastasis in colorectal cancer, which may reflect the liver being a primary site of IGF production[219]. Indeed, analysis of liver metastases has suggested a possible role for hepatocyte derived IGF-II in paracrine stimulation of colorectal cancer cell growth and metastasis[220]. These findings have also been observed in liver specific IGF-II knockout [LID] mice models, where the frequency of hepatic metastases is significantly lower than in control mice[205]. However, despite these associations, systemic IGF-II expression does not appear to be predictive for susceptibility to colorectal cancer[221, 222]. It is possible that increases in IGF-II expression at the tumour may not be detectable systemically, or may be functionally redundant if there is up-regulation of the IGFBPs or the IGF2R[209]. One way by which compensatory IGFBP secretion is counteracted by the tumour is the degradation of IGFBPs by specific proteases secreted by colorectal cancer cells[223]. IGF-II expression has been clearly demonstrated in a range of colorectal cancer cell lines[224, 225], and has been established to be involved in the autocrine stimulation of proliferation in these cells[224]. Alteration in IGF expression has been reported in stromal and tumour cells suggesting that local changes in IGF expression at the tumour site could involve autocrine and paracrine stimulation[209]. This finding along with the liver being the primary site of metastasis, suggests distribution, rather than total level of IGF expression may play a role in the transition from adenoma to invasive carcinoma[209].

1.3.2   IGF Receptor Expression

The pleiotropic actions of IGF-I and IGF-II that are relevant to cancer biology, namely cellular proliferation, differentiation, migration, and protection from apoptosis occur via their ability to bind

and activate the IGF receptors. In terms of gut physiology, IGF1R is expressed in the intestine in both the muscular and musosal layers, and in crypt enterocytes is mainly expressed on the basolateral region[226]. Colorectal cancer cells have been demonstrated to overexpress the IGF1R[65, 223, 227], and higher expression of IGF1R is associated with a more metastatic phenotype[24, 65]. In experimentally induced colonic tumours in rats, elevated levels of IR protein expression have been observed in tumour tissue compared to the normal-appearing mucosae[228]. However, the study did not observe any significant alterations in IR mRNA levels between tumour and normal mucosal tissue, suggesting the upregulation of IR protein expression in the tumours was due to altered post-transcriptional regulation of the IR[228]. This correlates with data suggesting the IR is over-expressed in human colorectal cancer, with the IR-A the predominant isoform expressed[7].

Colorectal cancer cells secrete IGF-I and IGF-II. They also secrete proteases that target the IGFBPs thus potentially increasing localized bioavailability of the IGFs[223, 224, 229]. Increased bioavailability of the IGFs together with the overexpression of the IGF1R and IR-A would lead to the establishment of autocrine proliferative loops. Inhibition of IGF-II interacting with the IGF1R by treatment with soluble IGF1R inhibits growth of colorectal cancer xenografts *in vivo*[230]. Moreover, inhibition of IRS-1, the major substrate for activated IR and IGF1R, results in decreased colorectal cancer cell growth[231]. Interestingly, a micro RNA, miR145 that targets IRS-1 has been found to be down-regulated in colorectal adenocarcinomas compared to matched normal colonic epithelia and reported treatment with miR145 causes growth arrest of human colon cancer cells[232].

Overexpression of IGF1R and IR-A may have other implications apart from mediating proliferation of tumour cells, such as conferring resistance to treatment strategies. Cross-talk between the IR-A and EGFR has been demonstrated to confer resistance of LoVo colorectal cancer cells to treatment with the EGFR inhibitor gefitnib[136]. IGF-II has also enables LIM2405 colorectal cancer cells to escape butyrate induced apoptosis[233], suggesting a mechanism by which colorectal cancer cells may escape the beneficial effects of butyrate. In addition, IGF-II acting via the IGF1R has been demonstrated to up-regulate COX-2 expression in colorectal cancer cells[234, 235]. COX-2 may play an important role in colorectal carcinogenesis and is overexpressed in 80 – 90% of colorectal cancers[236, 237]. Mice with a targeted inactivation of the COX-2 gene show decreased intestinal tumourigenesis[238]. Moreover, the chemopreventative effects of nonsteroidal anti-inflammatory drugs [NSAIDs] on colorectal carcinogenesis is thought to be due to their ability to inhibit COX-2

activity, thereby resulting in reduced prostaglandin biosynthesis[236, 237]. Therefore, inhibition of the IGF1R may increase the effectiveness of NSAIDs in treating colorectal cancer[235]. Altered expression of the IGF system components along with their potential role in mediating multiple aspects of cancer biology has thus made the IGF system an attractive therapeutic target not only in the treatment of colorectal cancer, but also a wide range of cancer types. The section to follow outlines the various novel anti-cancer therapeutic strategies that target the IGF system.

1.4 Current anti-cancer therapeutic strategies aimed at targeting the IGF system

Recent attempts to block the IGF system, as a cancer therapeutic, have focused on targeting either the expression or function of the IGF1R. Early strategies aimed at reducing circulating IGF-I levels were largely unsuccessful in preventing tumour growth, possibly because circulating levels of IGFs may not necessarily reflect their bioavailability at the tumour site[239]. However, GH releasing hormone antagonists have been shown to decrease serum IGF-I levels and described to have anti-tumor activity[240], although, these strategies do not effect IGF-II levels[241]. IGFBP-1 conjugated to polyethylene glycol to prolong its serum half-life has been demonstrated to reduce tumour growth in athymic mice[242]. Neutralizing antibodies against either IGF-I or IGF-II have been shown to have antimetastatic effects in mice with intrasplenic injections of human colorectal cancer cell lines[243]. In addition, this study also demonstrated dual inhibition of both IGF-I and IGF-II to be moderately more effective at inhibiting liver metastasis than single targeting of each IGF and prolonged survival[243].These studies suggest that inhibiting IGF bioavailability may be a potentially effective anti-cancer therapeutic strategy.

Potential problems facing the more recent approaches to target the IGF1R include treatment localization due to the ubiquitous expression of the IGF1R causing toxicity in normal tissues. This is of particular concern in rapidly proliferating tissues such as bone marrow and the epithelial lining of the gastrointestinal tract[239]. In addition, constitutive activation of downstream signaling molecules or compensatory signaling via other receptor tyrosine kinases [including the IR-A] could render IGF1R targeting ineffective[244] [discussed further in Section 1.4.2.2]. Furthermore, cross-reactivity of IGF1R based therapeutics with the IR could have detrimental consequences on metabolism [and are discussed further in the following sections]. However, given the potential role of IR-A mediating

32

IGF-II signaling, cancer cell inhibition of the IR may be therapeutically advantageous. While the potential benefits of inhibiting the IGF system are clear, whether this translates to relevant clinical outcomes has yet to be fully established. Several excellent reviews have recently addressed the multiple methods to disrupt IGF1R signaling and have provided discussion on the careful balance that needs to be struck between clinically relevant anti-cancer outcomes and detrimental toxicity to normal tissues[239, 241, 244-246]. For the purpose of this introductory literature review, the following sections will briefly discuss the main strategies for targeting the IGF1R, their efficacy and how they may impact upon or avoid the IR.

1.4.1   Strategies aimed at inhibiting IGF1R protein function

1.4.1.1 Inhibitory antibodies

Several antibodies that inhibit IGF1R receptor function have been developed[247-253]. These antibodies inhibit growth of cancer cell lines *in vitro* and inhibit xenograft tumor growth *in vivo*[247-253]. Indeed, some anti-IGF1R monoclonal antibodies are now in the early stages of clinical trials[253-255]. These antibodies appear to prevent ligand binding to the IGF1R and trigger receptor internalization[253-255]. IGF1R bound by antibody has been demonstrated to go through endosomal degradation, therefore resulting in down-regulation of the IGF1R at the cell surface[253, 256]. Interestingly, an agonistic anti-IGF1R antibody has been demonstrated to have anti-tumour properties[251, 256]. Since the anti-tumour properties of the antibody are thought to be due to the ability of the antibody to down-regulate the IGF1R, these data suggest that this mechanism of action may be more effective than an antibody inhibition of ligand binding to the receptor[241, 251, 256]. Indeed, it is via this mechanism of antibody-induced IGF1R downregulation that specific antibodies directed against the IGF1R can also affect the IR, by co-downregulation of IR involved in IGF1R/IR hybrid receptors or via the endocytosis of IR homodimers in close proximity to IGF1R in lipid rafts of the cell membrane[257]. In terms of an anti-cancer therapeutic, dual inhibition of both receptors could be beneficial. Dual treatment of cancer cells with antibodies against both the IR and IGF1R have been demonstrated to be more effective at inhibiting cancer cell growth *in vitro* than treatment with either antibody alone[123]. What effect this might have on insulin and glucose homeostasis is as yet unknown. However, Sachdev *et al* 2006 reported [but did not publish the data] that two anti-

IGF1R antibodies did not down-regulate the IR in HepG2 cells, suggesting that these antibodies may not disrupt insulin action in the liver[257]. Why anti-IGF1R antibodies are able to co-downregulate the IR in some cell types that co-express both receptors and not others is not clear. Another potential downfall of antibody-based therapeutics is efficacy in solid tumors, due to the large size of antibodies restricting their access to central regions of the tumour[258]. Antibodies can be cleaved by proteases to separate the Fc region and antigen-binding Fab regions. These smaller antibody fragments [Fab's] are currently being examined to improve access and uptake in solid tumours compared to whole antibodies[251, 256, 259]. However, it should be noted that the use of Fab's potentially bypasses any potential beneficial effect of the Fc region being involved in the mediation of the immune response.

1.4.1.2 Dominant-negative Receptors

Dominant-negative proteins sequester and inhibit the functions of their wild-type counterparts. Dominant-negative IGF1R have been engineered to function as inhibitors of the IGF system in a variety of ways, resulting in reduced tumour growth. IGF1R dominant-negative receptors with a truncation in the β-subunit form heterodimers with their wild-type counterparts preventing them from activating intracellular signaling pathways upon ligand binding[260]. Another dominant-negative IGF1R lacks the transmembrane domain. It is secreted from the cell, and competes for IGF-I and IGF-II preventing them from binding to, and activating, wild-type IGF1R[261]. Both strategies, along with different plasmid-based or adenoviral delivery systems, have been demonstrated to promote chemosensitisation and decrease growth in several tumour models[260-265]. However, adenoviral vectors have been demonstrated to be more efficient and practical than plasmid-based systems[230, 263, 265]. Theoretically, these dominant-negative receptors would be able to form hybrids with the IR-A and inhibit its function, although this has not been reported on to date.

1.4.1.3 Small Molecule Inhibitors

Small molecule inhibitors are generally identified by high throughput screening of libraries of 400 – 600 molecular weight compounds. Lead candidate molecules are generally chosen for their specificity for their target, favorable pharmacokinetic properties, and ability to be administered

orally with high bioavailablity[239]. Small molecules have been designed to inhibit the tyrosine kinase activity of the IGF1R by either targeting the ATP binding cleft or active site of the tyrosine kinase. Inhibitor design for IGF1R or IR specificity is complicated since the kinase domains of both receptors share 85% homology, and the ATP binding cleft is 100% conserved between the two receptors[43]. However, crystal structures of the phosphorylated forms of the IGF1R and IR tyrosine kinase domains have revealed differences in conformation that have been exploited in the hope of designing a specific IGF1R inhibitor[79].

Several small molecule inhibitors of the IGF1R have been shown to be active against a wide range of cancers *in vitro*[266], and have been demonstrated to enhance tumour cell chemosensitivity and inhibit tumour growth *in vivo*[266]. Other inhibitors have been designed to block IGF1R function by preventing substrate phosphorylation. Picropodophyllin [PPP] inhibits IGF1R autophosphorylation at the substrate level and is effective in inhibiting metastasis and inducing tumour regression in a range of cancer models[267]. One caveat facing small molecule inhibitors is while specificity for the IGF1R may benefit glucose metabolism, they may not provide complete inhibition of signaling in the tumour[241]. Another IGF1R inhibiting compound nordihydroguaiaretic acid [NDGA] has been demonstrated to also inhibit human epidermal growth factor-2 [HER-2] signaling which may be desirable in treating HER-2 positive breast cancers[268]. In addition, the dual IGF1R/IR inhibitor BMS-554417 has been ascertained to have anti-proliferative and pro-apoptotic activity *in vitro* and *in vivo*[269]. However, the most effective dose of this compound caused transient hyperglycemia and hyperinsulinemia when administered to mice suggesting it has adverse metabolic consequences[269]. Indeed, effects of all these compounds on glucose metabolism are of concern. Even if compounds are designed that show complete specificity for the IGF1R without affecting the IR, they may still have adverse metabolic consequences as disruption of the IGF1R affects survival of pancreatic beta cells[270]. While it is noted that temporary hyperinsulinemia or hyperglycemia may be tolerated by patients, long term insulin resistance or induction of type I or type II diabetes would be detrimental[241]. Co-administration of metformin has been established to reduce hyperglycemia in *in vivo* models and may indicate that joint management of side effects of these small molecule inhibitors may be necessary[266].

1.4.2 Strategies aimed at targeting the expression of IGF1R

Strategies aimed at silencing the expression of the IGF1R are advantageous as targeting to the gene of interest requires sequence specific base-pairing to the complementary strand of mRNA[239], therefore these strategies would not directly affect the IR. Antisense oligonucleotides [ASOs] and short-interfering RNAs [siRNAs] are effective at silencing the IGF1R and have potential clinical applications[239]. In addition, siRNAs have been an important research tool in the establishment of molecular determinants that may render IGF1R inhibition ineffective.

1.4.2.1 Antisense Oligonucleotides

Blockage of translation or RNase H-mediated mRNA cleavage via the introduction of antisense oligonucleotides is an effective mechanism to inhibit specific gene expression[271, 272]. ASOs have an advantage over siRNA in terms of design as there aren't any sequence specific restrictions. However, secondary structure of the target mRNA heavily influences the effectiveness of an ASO[273]. ASOs targeting the IGF1R have been found to be effective at decreasing IGF1R expression, inhibiting proliferation, and inducing apoptosis in a wide range of cell lines[73, 74, 274-279] and have been shown to stimulate tumour regression in *in vivo* animal studies[73, 74]. In addition, ASOs targeting the IGF1R also inhibit metastasis[280, 281]. Stabilizing chemical modifications to create mixed backbone oligonucleotides has enabled problems such as susceptibility to nuclease attack to be overcome[272, 282]. However, limited cellular uptake and non-specific toxicity has hampered systemic efficacy of ASOs[283]. In the clinical setting, surgically removed malignant astrocytoma cells treated *ex vivo* with anti-IGF1R ASOs and reimplanted into end-stage patients has been shown to elicit a host response that protects against unmodified tumour cells resulting in clinical improvement[284].

1.4.2.2 RNA interference [RNAi]

RNA interference [RNAi] was first recognized in *Caenorhabditis elegans* where contaminating double-stranded RNAs [dsRNAs] induced potent gene silencing[285, 286]. In this process, long dsRNAs are cleaved by Dicer, a member of the RNase III family of dsRNA-specific ribonucleases,

into short 21-23 nucleotide fragments with two nucleotide single-stranded 3' overhangs[285]. These short interfering RNAs [siRNAs] are then incorporated into the RISC complex, a multi-protein RNA-inducing silencing complex. The anti-sense strand of the unwound siRNA then acts as a targeting sequence resulting in the cleavage of complementary mRNA resulting in gene silencing[285]. This process was also found to occur in mammalian cells, but, introduction of long dsRNA can result in activation of dsRNA-dependent protein kinase and stimulation of interferon expression, ultimately resulting in the induction of apoptosis[287, 288]. Later, it was established that direct introduction of the 21-23 nucleotide siRNAs into cultured mammalian cells circumvented this problem enabling the RNAi mechanism of gene silencing to become a significant research tool[289] [see Figure 5.1].

Several important factors dictate the efficacy of siRNAs including secondary structure and primary sequence requirements, which will be discussed in further detail in Chapter 7. One of the early studies demonstrating the importance of transcript accessibility in siRNA efficacy resulted in the generation of a series of sequence-specific siRNAs that induced potent knockdown of the IGF1R without affecting the IR[290]. These siRNAs inhibited IGF1R expression, blocked IGF signaling, and inhibited the survival of several human and murine tumour cell lines[290-292]. Since targeting the IGF1R could be rendered ineffective by compensatory signaling from other receptor tyrosine kinases or constitutive activation of downstream signaling pathways[244], the majority of research concentrating on siRNA mediated knockdown of the IGF1R has focused on identifying potential mechanisms of resistance to IGF1R silencing.

Many intracellular signaling components downstream of the IGF1R are commonly mutated in cancers, and therefore inactivation of these tumour suppressors or activation of oncogenes may render IGF1R inhibition ineffective in cancers harboring these mutations. For example, the tumour suppressor *PTEN* is commonly mutated in prostate cancer leading to dysregulation of the PI3K-AKT pathway[293]. The anti-apoptotic functions of the IGF1R primarily occur via activation of the PI3K pathway resulting in the inhibitory phosphorylation of the proapoptotic Bad[294]. PTEN acts as a tumour suppressor by antagonizing PI3K, therefore functional loss of PTEN leads to apoptosis protection[295]. In addition to enhancing sensitivity to DNA-damaging agents, siRNA mediated silencing of the IGF1R was able to inhibit cell survival in prostate cancer cells expressing both wild-type and mutated PTEN[291]. Furthermore, activation of components of the RAS/RAF/MAPK pathway have also been established to be sensitive to inhibition of the IGF1R[292]. Human myeloma

cell lines expressing either wild-type or mutant BRAF exhibited inhibited cell survival and enhanced apoptosis when IGF1R was targeted by siRNA[292]. Therefore these two studies suggest that activating mutations of downstream signaling pathways of IGF1R may not be sufficient to render IGF1R targeting strategies ineffective in cancers harboring these mutations. These findings therefore have positive implications on the range of cancer types that could be potentially treated by anti-IGF1R strategies[244].

Compensatory signaling from other receptor tyrosine kinases are another mechanism by which IGF1R targeting could be rendered ineffective. The establishment that there is cross-talk between the IGF and EGF systems and IGF1R can mediate resistance to anti-EGFR theraputics[296] prompted the investigation of whether the EGFR could likewise compensate for loss of IGF1R and mediate resistance to anti-IGF1R theraputics[297]. Although siRNA mediated knockdown of the IGF1R did not effect EGFR expression it did result in prolonged EGF-stimulated phosphorylation of the EGFR along with several downstream signaling molecules of the EGFR[297]. However despite this, IGF1R knockdown still resulted in enhanced apoptosis and inhibition of cell survival[297]. In addition, dual knockdown of the EGFR and IGF1R did not induce any greater inhibition of cell survival than IGF1R knockdown alone[297]. Therefore, these results suggest that at least *in vitro,* the EGFR cannot compensate for loss of the IGF1R[297]. It has yet to be established whether signaling via the IR-A can compensate for targeted loss of the IGF1R, and experiments described in the later parts of this PhD thesis aim to investigate this possibility.

1.5 Scope and Aims of this Thesis

The IR-A is over-expressed in a wide range of human malignancies, including colorectal cancer. This receptor binds IGF-II with high affinity resulting in a range of outcomes relevant to cancer biology. Due to this, interest has recently focused on the potential role of the IR-A in mediating proliferation, migration, and survival responses to IGF-II in the development of cancer[7, 123, 124, 126, 127]. However, the majority of research conducted on the IR-A has been performed in cells devoid of the IGF1R. It is not known how the IR-A interacts and functions in conjunction with the other IGF receptors, namely IGF1R and hybrid receptors, to signal biologically relevant outcomes.

Investigation into the biological role of the IR-A within context of the IGF1R and hybrid receptors forms the major focus of this thesis.

Determining how the IR-A functions in cells co-expressing the IGF1R is of particular relevance when considering novel anti-cancer therapeutics that target the IGF1R. Compensatory signaling from the IR-A is one possible mechanism by which IGF1R targeting could be rendered ineffective. The establishment that IR-A signaling confers resistance of LoVo cells to the EGFR inhibitor gefitnib, suggests the IR-A is capable of providing a growth advantage in cells where other receptor tyrosine kinases have been inhibited[136]. Therefore, ***the major aim of this thesis was to determine whether signaling via the IR-A could compensate for the targeted loss of the IGF1R***. An siRNA based approach was successfully utilised to address this possibility and results suggested the IR-A could not compensate for IGF1R down-regulation. Furthermore, dual silencing of the IR-A and IGF1R did not confer any additional inhibition of IGF stimulated SW480 cell survival and proliferation than IGF1R silencing alone. Moreover, these experiments demonstrated how IR-A co-expression can influence and affect the function of the IGF1R.

In the broader context of investigating the biological role of the IR, a secondary, but related aim, *was to investigate the ability of a range of IGF chimeras to signal biological responses through the IR-A and IR-B*. These experiments, conducted in cells devoid of the IGF1R, provided insights into the biological response elicited by IGF ligand-receptor interactions, and identified a novel pathway for IGF activation through the IR. IGF-I was demonstrated to act through both isoforms of the IR to preferentially activate IRS-2, resulting in downstream biological outcomes relevant to cancer biology.

By addressing the two aims of this thesis, the biological outcomes of cross-talk between multiple components of the IGF system were investigated. Results suggested the implications of IR expression on the efficacy of anti-cancer therapeutics aimed at targeting the IGF1R may not be as considerable as first anticipated. Moreover, results inferred signaling via IGF1R/IR-A hybrid receptors may not be as potent as signals arising from IGF1R homodimers, thereby providing some insight into the functionality of hybrid receptors.

Chapter 2

Materials and Methods

2.1 Materials

2.1.1 Mammalian Cell Culture: Materials, Chemicals, and Reagents

Listed below are the materials, chemicals, and reagents used throughout this study in the mammalian cell culture techniques. All chemicals and reagents were of analytical grade or of the highest purity available. Tables 2.1 and 2.2 list the mammalian cell lines that were used. All cell lines were routinely assessed in house for Mycoplasma by PCR and found to be negative for contamination. Table 2.3 lists the growth media used for general maintenance of each cell line. Sequences of the siRNAs used for gene silencing are listed in Tables 2.4 and 2.5.

100mM Sodium Pyruvate Solution	Invitrogen
10mM Non-Essential Amino Acids Solution	Invitrogen
12µm pore polycarbonate filter membranes	NeuroProbe
AC96 NeuroProbe A Series 96 Well Chamber	NeuroProbe
Actrapid Human Insulin [pyr]	Novo Nordisk
Bovine Serum Albumin	Bovogen Biologicals
Calcein-AM	Molecular Probes
Crystal Violet	Sigma
Dulbecco's Modified Eagle Medium	Invitrogen
F-12 HAM Nutrient Mixture	Invitrogen
Foetal Calf Serum, Certified, Heat-Inactivated	Invitrogen
G418 [Geneticin 50mg/ml]	Invitrogen
Glacial Acetic Acid	BDH
HiPerFect	Qiagen
IGF-I [Receptor Grade]	GroPep
IGF-II [Receptor Grade]	GroPep
IGF Chimeras	Dr. Adam Denley [Uni.Adelaide]
INTERFERin^{TM}	Polyplus-Transfection
Lipofectamine 2000^{TM}	Invitrogen
Lipofectamine RNAiMAX^{TM}	Invitrogen
Methanol	BDH
Ministart 0.2µm Syringe Filter	Sartorius
Nuncleon Delta White Microwell Plate	Nunc
Nuncleon Delta Black Microwell Plate	Nunc
Oligofectamine^{TM}	Invitrogen
Opti-MEM I Reduced Serum Media	Invitrogen
PBS tablets	Amresco
RPMI Medium 1640	Invitrogen
Sodium Butyrate	Sigma
TerriWipes	Kimberly-Clark
Tissue culture flasks, dishes and plates	Falcon
Trypan Blue Cell Stain	Sigma
Trypsin/EDTA	Gibco/Invitrogen
Type I Collagen	Sigma

Table 2.1 Cell lines of human origin

ATCC refers to the Global Bioresource Centre. All cell lines were purchased from the ATCC.

Cell Line	Cell Type	ATCC No#	Information
Caco-2	Epithelial	HTB-37	colorectal adenocarcinoma
HCT-116	Epithelial	CCL-247	colorectal adenocarcinoma
HT-29	Epithelial	HTB-38	colorectal adenocarcinoma
MDA-MB-231	Epithelial	HTB-26	breast adenocarcinoma
SW480	Epithelial	CCL-228	colorectal adenocarcinoma

Table 2.2 Cell lines of murine origin

R^- cells were obtained from Professor Renato Baserga, Thomas Jefferson University. R^-IRA, R^-IRB, R^-IGF1R generated by Dr. Eric Bonython, School of Molecular and Biomedical Sciences, University of Adelaide

Cell Line	Cell Type	Information
R^-	Fibroblast	IGF1R negative 3T3-like embryonic fibroblasts isolated from a mouse with a targeted disruption of the IGF1R gene
R^-IRA	Fibroblast	R^- cells stably transfected with cDNA encoding the human IR-A. Express ~75,000 receptors/cell
R^-IRB	Fibroblast	R^- cells stably transfected with cDNA encoding the human IR-B. Express ~75,000 receptors/cell
R^-IGF1R	Fibroblast	R^- cells stably transfected with cDNA encoding the human IGF1R. Express ~75,000 receptors/cell

Table 2.3 Growth media for cell lines

Cell lines were routinely maintained in the growth media listed below. In the case of serum-free treatments cells were treated in the same media with the exception that the FCS was removed.

Cell Line	Growth Media
Caco-2	DMEM, 20% FCS, 1% 100mM sodium pyruvate, 1% MEM non-essential amino acids
HCT-116	McCoy's 5A, 10% FCS
HT-29	47.5% DMEM, 47.5% F-12 Nutrient Mixture [HAM], 5% FCS
MDA-MB-231	RPMI 1640, 10% FCS
R^-	DMEM, 10% FCS
R^-IRA	DMEM, 10% FCS, 0.5% G418
R^-IRB	DMEM, 10% FCS, 0.5% G418
R^-IGF1R	DMEM, 10% FCS, 0.5% G418
SW480	RPMI 1640, 10% FCS

Table 2.4 siRNA sequences used for gene silencing

All sequences presented 5' to 3'. With the exception of IR29 and IR31, all siRNAs were HPP synthesised, purified by IE-HPLC and sequence confirmed by MALDI-TOF spectrometric analysis by Qiagen. See Figure 5. 3 for location of IR siRNAs.

siRNA	Sense	Antisense
R4 [IGF1R]	CAAUGAGUACAACUACCGCTT	GCGGUAGUUGUACUCAUUGTT
ScrR4	GUCACACCGAUAAGUCACATT	UGUGACUUAUCGGUGUGACTT
IRboth	CUAGUCCUGCAGAGGAUUU	AAAUCCUCUGCAGGACUAG
A10+10	UCGUCCCCAGGCCAUCUCGG	CCGAGAUGGCCUGGGGACGA
A5+16	CCCAGGCCAUCUCGGAAACGC	GCGUUUCCGAGAUGGCCUGGG
AB10	ACGUGGUUUUCGUCCCCAG	CUGGGGACGAAAACCACGU
AB12	GCCAUCUCGGAAACGCAGG	CCUGCGUUUCCGAGAUGGC
IR29	GGAACUCGGCCUCUACAAC	GUUGUAGAGGCCGAGUUCC
IR31	GGUGUUGAAAUUUGUCAUG	CAUGACAAAUUUCAACACC
Control	UUCUCCGAACGUGUCACGU	ACGUGACACGUUCGGAGAA

Table 2.5 Commercially purchased siRNAs used for gene silencing

Information regarding siRNAs purchased from commercial retailers. For sequences of specific siRNAs see Table 2.4

siRNA	Company	Cat #	Available Information
Control	Qiagen	1022076	Target sequence does not have homology with any known mammalian transcripts
IR29	Ambion	siRNA ID#: 29	*Silencer*® Validated siRNA: INSR. *Targeted exon(s): NM_000208: Exon 2*
IR31	Ambion	siRNA ID#: 31	*Silencer*® Validated siRNA: INSR. Targeted exon(s): NM_000208: Exon 21

Table 2.6 Oligonucleotide primers for PCR

Sequences of oligonucleotide primer pairs used for PCR amplification of the IR, IGF1R, and β-tubulin. Expected product size of amplification by each primer pair is given in base pairs [bp].

Name	Sequence 5' - 3'	Expected product size
hIR-fwd	CTGGGAGAGGCAGGCATATGACAGTGAGCTGTTCG	IR-A: 473; IR-B: 509
hIR-rev	CCTGGTTGCAAGCCTGCAGATCGATGCGATAGCCC	
hIGF1R-fwd	ACTTCTGCGCCAACATCCTCA	572
hIGF1R-rev	CCCTTTAGTCCCCGTCACTTCC	
β-actin-fwd	CTGGCACCACACCTTCTAC	242
β-actin-rev	GGGCACAGTGTGGGTGAC	

2.1.2   Molecular Biology: Materials, Chemicals, and Reagents

Listed below are the materials, chemicals, and reagents used in the molecular biology techniques, along with the manufacturer they were purchased from. Oligonucleotides were synthesized by Geneworks [South Australia] and the sequences are listed in Table 2.6.

2-Log DNA Ladder	New England Biolabs
Agarose Powder	Promega
BioTaq Taq Polymerase	Bioline
Bromophenol Blue	Sigma
dNTPs [100mM dATP, dGTP, dCTP, dTTP]	Invitrogen
DEPC	Sigma
Ethanol	BDH
GelGreen	Biotium
Glycerol	Univar
Isopropanol	Sigma
Random Hexamer Primers	Invitrogen
RNAse-Free DNAseI	Qiagen
SuperIN RNase Inhibitor	Ambion
Superscript II RNase H⁻ Reverse Transcriptase	Invitrogen
Xylene Cyanole	Sigma

2.1.3   Protein Chemistry: Materials, Chemicals, and Reagents

Listed below are the materials, chemicals, and reagents used in the protein chemistry techniques, along with the manufacturer they were purchased from. All chemicals were of analytical grade or the highest purity available.

β-mercapto-ethanol	Sigma
Amersham ECL Plus Western Blotting Detection System	Amersham
Bromophenol Blue	Sigma
Complete Mini Protease Inhibitor Tables	Roche
EDTA	Amresco
HEPES	BDH
iBlot™ Dry Transfer System	Invitrogen
iBlot™ Gel Transfer Stacks: Nitrocellulose	Invitrogen
Glycerol	Univar
Kodak Biomax Light Film	Kodak
NuPAGE® 4-12% Bis-Tris Gels	Invitrogen
NuPAGE® MOPS SDS Running Buffer	Invitrogen
Paraformaldehyde	Sigma
PBS tablets	Amresco
PMSF	Sigma
Protein A-Agarose	Sigma
Protein G-Agarose	Sigma
SeeBlue Plus 2 Pre-stained Standard	Invitrogen
Skim Milk Powder	Diploma
Sodium Azide	Sigma
Sodium Chloride	Amresco
Sodium Dodecyl Sulfate	Amresco
Sodium Fluoride	Sigma
Sodium Orthovanadate	Sigma
Sodium Pyrophosphate	Sigma
Triton X-100	Amresco
Tween-20	Amresco

2.1.4   *Solutions and Buffers*

The solutions listed below were prepared as indicated using water purified by the Milli-Q Ultra Pure water system [Millipore]. If necessary, solutions were sterilized by autoclaving.

1x PBS
    50mM NaHPO$_4$, 150mM NaCl, pH 7.4

1x PBST
    0.05% Tween-20 in 1xPBS

1x TAE
    40mM Tris-acetate [pH 8.0], 1mM EDTA

3x Sample Amplification Buffer [SAB] pH 6.8
    30% glycerol, 15% βME, 9% (w/v) SDS, 0.03% (w/v) bromophenol blue, 150mM Tris-Cl

5x RNA/DNA loading buffer
    50% glycerol, 0.125% (w/v) bromophenol blue, 0.125% (w/v) xylene cyanol, 0.1% TAE

Blotto
    5% skim milk powder in 1xPBST

FACS wash solution
    1% FCS, 0.01% sodium azide, in 1xPBS

Freeze media
    95% FCS, 5% DMSO

Lysis buffer
    50mM HEPES, 100mM NaCl, 10mM EDTA, 4mM Na$_4$O$_7$P$_2$, 2mM Na$_3$PO$_4$, 10mM NaF,
    1mM PMSF, 1% Triton X-100, 1 tablet complete protease inhibitors [Roche]

2.1.5   *Antibodies*

Table 2.7 lists the various antibodies utilised throughout this study. Table 2.8 lists the final concentration of the antibodies in a particular application.

2.1.6   *Commercial Kits*

Listed below are the commercial kits used in this study. Manufacturers and catalogue numbers are as indicated. All kits were used as per manufacturers' instructions unless otherwise noted in Section 2.2.

Apo-ONE Homogenous Caspase-3/7 Assay [G7791]	Promega
Bicinchoninic Acid Kit for Protein Determination [BCA1-1KT]	Sigma
CellTiter-Glo^{TM} Luminescent Cell Viability Assay [G7571]	Promega
CellTiter-Blue^{TM} Cell Viability Assay [G8080]	Promega
RNeasy Mini Spin Columns [74104]	Qiagen
Superscript II Reverse Transcriptase [18064-014]	Invitrogen
VenorGEM Mycoplasma Detection Kit [11-1050]	Minerva Biolabs

Table 2.7 Antibodies used throughout this study
*FACS, fluorescent-activated cell sorting. IP, immunoprecipitation. WB, Western blot. N/A, not applicable. ** Antibody clones 24-60, 83-7, and 83-14 kindly provided by Professor Ken Siddle, University of Cambridge*

Antibody	Company	Cat#:	Source	Target	Application
P-Tyr-100	Cell Signalling	9411	Mouse/IgG1/mAb	phosphorylated tyrosine residues	IP
Phospho-IGF1R/IR [19H7]	Cell Signalling	3024	Rabbit/IgG/mAb	Tyr1135/1136 IGF1Rβ and Tyr1150/1151 IRβ	WB
IGF1Rβ	Cell Signalling	3027	Rabbit/pAb	β-subunit human IGF1R	WB
24-60	**	N/A	Mouse/mAb	α-subunit human IGF1R	FACS, IP
IRβ [C-19]	Santa Cruz	sc-711	Rabbit/pAb	β-subunit human IR	WB
83-7	**	N/A	Mouse/mAb	α-subunit human IR	FACS
83-14	**	N/A	Mouse/mAb	α-subunit human IR	IP
anti-β-tubulin	Sigma	T4026	Mouse/IgG1/mAb	β-tubulin	WB
Negative control IgG1	Chemicon	MABC002	Mouse/IgG1/mAb	non-specific mouse monoclonal Ab	FACS
anti-Mouse Immunoglobulins-HRP	Dako	P0447	Goat/pAb	HRP conjugated goat anti-mouse secondary	WB
anti-Rabbit Immunoglobulins-HRP	Dako	P0448	Goat/pAb	HRP conjugated goat anti-rabbit secondary	WB
anti-Mouse Ig -FITC	Chemicon	AP326F	Sheep/pAb	FITC conjugated sheep anti-mouse secondary	FACS

Table 2.8 Final concentrations and dilutions of antibodies used in various applications
FACS, fluorescent-activated cell sorting. IP, immunoprecipitation. WB, Western blot. For composition of diluents see Section 2.1.4.

Antibody	Application	Final Conc./Dilution	Diluent
P-Tyr-100	IP	20µg	Lysis buffer
Phospho-IGF1R/IR [19H7]	WB	1:400	Blotto
IGF1Rβ	WB	1:400	Blotto
24-60	FACS, IP	FACS: 25µg/ml, IP: 20µg	FACS wash solution / Lysis buffer
IRβ [C-19]	WB	1:100	Blotto
83-7	FACS	25µg/ml	FACS wash solution
83-14	IP	20µg	Lysis buffer
anti-β-tubulin	WB	1:2000	Blotto
Negative control IgG1	FACS	25µg/ml	FACS wash solution
anti-Mouse Immunoglobulins-HRP	WB	1:10,000	Blotto
anti-Rabbit Immunoglobulins-HRP	WB	1:5,000	Blotto
anti-Mouse Ig -FITC	FACS	25µg/ml	FACS wash solution

2.1.7   Electronic Resources

Listed below are the various electronic resources utilised in this study along with their web addresses [current at the time of preparation of this thesis].

NCBI Blast	http://www.ncbi.nlm.nih.gov/blast/Blast.cgi
PubMed	http://www.ncbi.nlm.nih.gov/sites/entrez/
Qiagen siRNA design algorithm [BIOPREDsi]	http://www.biopredsi.org/start.html
Ambion siRNA resources	http://ambion.com/techlib/resources/RNAi/index.html
Qiagen siRNA resources	http://www1.qiagen.com/Literature/LiteratureToc.aspx

2.1.8   Computer Software

CellQuest Pro	Becton Dickinson
ImageQuant TL	GE Health Care
Prism v4.0	Graph Pad
Wallac 1420 Workstation Manager	Perkin Elmer

2.2   Methods

2.2.1   Methods: Mammalian Cell Culture

2.2.1.1 General Cell Culture

2.2.1.1.1   Maintenance of mammalian cell lines

All cell lines were maintained utilising standard tissue culture techniques. All cell culture work was conducted in a BH 2000 Series Biosafety Cabinet Type II [Clyde Apac]. Working stocks of each cell line were maintained in the appropriate growth media as indicated by Table 2.3. All cells were incubated in sterile tissue-culture grade flasks [Falcon] at $37^{o}C$ in the presence of 5% [v/v] CO_2 in a Sanyo CO_2 Incubator [Sanyo MCO-18AIC]. Cell density was closely monitored and cells were routinely passaged upon reaching 80% confluence. Working cell stocks were passaged a maximum of 10 times before returning to a new cryostock. All cell lines were routinely screened for Mycoplasma [Venor®GeM, Minerva Biolabs] and found to be negative for contamination.

2.2.1.1.2   Recovery of mammalian cell line cryostocks

Cells stored in liquid nitrogen were thawed by the addition of 1ml of the appropriate growth media warmed to 37°C. The cells were then washed to remove the DMSO present in the freeze medium by dilution in 10 ml of appropriate growth media followed by centrifugation at 1,000 rpm [Eppendorf Centrifuge 5702] for 5 minutes. Upon resuspension in fresh media the cells were transferred to the appropriate sized tissue culture flask containing appropriate growth media and allowed to grow to 80% confluence before passage. All thawed cell lines were passaged at least once prior to being utilised in any assay.

2.2.1.1.3   Sub-culture of mammalian cell lines

Upon reaching 80% confluence, adherent cell monolayers were washed once with sterile 1x PBS and treated with 1 – 2 ml of 0.05% trypsin-EDTA for 5 minutes at 37°C/5% CO_2 to ensure a single cell suspension. Detached cells were washed with 10 ml of the appropriate growth media followed by centrifugation at 1,000 rpm [Eppendorf Centrifuge 5702] for 5 minutes to pellet the cells. Upon resuspension in fresh growth media, depending on the cell type, dilutions between 1:4 and 1:80 were made and transferred to new tissue culture flasks containing appropriate fresh growth media.

2.2.1.1.4   Generation of mammalian cell line cryostocks

To generate cell line stocks to be stored in liquid nitrogen, cells at approximately 70% confluence were trypsinised into a single cell suspension and washed with 10ml of appropriate growth media. The cells were then pelleted by centrifugation at 1,000 rpm [Eppendorf Centrifuge 5702] for 5 minutes and the growth media aspirated. Freeze medium consisting of 95% [v/v] FCS, 5% [v/v] DMSO was used to resuspend the cell pellet. The resuspended cells were then aliquoted into Cyro-tubes [Nunc] which were stored at -80°C for two days, upon which the cells were then transferred to liquid nitrogen for long term storage.

2.2.1.1.5   Determination and numeration of viable cells

Prior to use in assays, cell viability was determined after adherent cell monolayers had been trypsinised to single cell suspensions and washed to remove any residual trypsin. After a 1:2 dilution in 0.4% Trypan Blue Solution [Sigma], viable cells were identified as those that excluded the stain and counted using a haemocytometer.

2.2.1.2 Biological Endpoint Assays

2.2.1.2.1   Cell Migration Assays

Boyden Chamber migration assays were employed to assess the ability of IGF-I, IGF-II, and Insulin to stimulate cell chemotaxis. The lower wells of an AC96 NeuroProbe A Series 96 well chamber were loaded with serum-free media containing 0.5% [w/v] BSA and different concentrations of either IGF-I, IGF-II, or Insulin. Framed polycarbonate filters with 12 μm pores [NeuroProbe] were treated overnight at 4°C in 25 μg/ml type 1 collagen in 10 mM acetic acid prior to use in the assays. The filters were then rinsed in 1x PBS and either allowed to dry and be stored at room temperature for future assays, or slotted against the rubber gasket of the top plate of the chamber. The top plate of the chamber was then gently lowered onto the lower wells of the chamber containing the chemoattractants and fastened with screws. Cells from approximately 80% confluent monolayers were trypsinised and washed two times in serum-free media containing 0.5% [w/v] BSA prior to performing viable cell counts to determine cell concentration. Cells were then diluted to the appropriate concentration as indicated by Table 2.9 in serum-free media containing 0.5% BSA. Calcein-AM [Molecular Probes] was then added to a final concentration of 1 mg/ml. To allow uptake of the Calcein dye, the cells were incubated at 37°C/5% CO_2 for 30 minutes. To remove any residual dye, cells were washed twice in serum-free media containing 0.5% BSA prior to being resuspended to the appropriate density. The top wells of the chamber were loaded with the appropriate amount of cells and cells were allowed to migrate for five and a half hours at 37°C/5% CO_2. Following the incubation, the chamber was carefully disassembled and any cells that had not migrated and remained on the upper surface of the polycarbonate filters were wiped away using a Terriwipe [Kimberly] moistened with 1x PBS. The filters were then allowed to dry and the resultant

fluorescent signal from the Calcein-labelled migrated cells on the underside of the filters was quantified using a Wallac Victor^{3}V 1420 Multilabel Counter plate reader [Perkin Elmer] utilising 535 nm emission and 485 nm excitation filters.

2.2.1.2.2 CellTiter-Glo^{TM} Luminescent Cell Viability Assay

To assess the ability of IGF-I, IGF-II, and Insulin to rescue cells from butyrate-induced apoptosis cells were plated in their appropriate growth media at various densities, depending on the cell type [see Table 2.9], into Nucleon Delta White 96 microwell plates [Nunc] and incubated at 37°C/5% CO_2 for 48 hours. The medium was then carefully aspirated from the wells and the cells washed twice with serum-free media to remove any remaining growth factors from the FCS. The cells were then serum-starved for five hours in serum-free media at 37oC/5% CO2 to allow recycling of any ligand bound receptors to the cell surface. Following the serum starvation the medium was again carefully aspirated from the wells and the cells treated with serum-free media containing 0.1% (w/v) BSA, 5 mM butyrate, and different concentrations of either IGF-I, IGF-II, or Insulin. The cells were incubated for a further 48 hours at 37oC/5% CO2. CellTiter-Glo^{TM} reagent was prepared as per manufacturers' instructions, and following a 30 minute incubation at room temperature, an equal volume of CellTiter-Glo^{TM} reagent to cell culture medium containing treatments was added to each well. The plates were then shaken at 920 rpm on a Wallac 1296-003 Delfia Plateshaker [Perkin Elmer] for 2 minutes to induce cell lysis. Following a 10 minute incubation at room temperature to allow stabilisation of the resultant luminescent signal corresponding to the number of viable cells, luminescence at 535 nm was recorded using a Wallac Victor3V 1420 Multilabel Counter plate reader [Perkin Elmer].

2.2.1.2.3 CellTiter-Blue^{TM} Cell Viability Assay

During the course of this study, the laboratory switched from using CellTiter-Glo^{TM} to CellTiter-Blue^{TM}. Two reasons were behind this decision. Firstly, CellTiter-Blue^{TM} is vastly cheaper than CellTiter-Glo^{TM} but just as reliable. Secondly, CellTiter-Blue^{TM} could be multiplexed with the Apo-One^{TM} assay. Cell viability studies were conducted as outlined above in 2.2.1.2.2 with the following modification. Following the 48 hour treatment with butyrate and IGFs, 20µl/well CellTiter-Blue^{TM}

reagent was added and the cells incubated for a further 2 hours at 37°C/5% CO_2. The resultant fluorescent signal, indicative of viable cells, was measured using a Wallac Victor^{3}V 1420 Multilabel Counter plate reader [Perkin Elmer] utilising 550 nm excitation and 615 nm emission filters.

2.2.1.2.4 *CellTiter-Blue^{TM} Cell Viability Assay: Post-siRNA transfection – Final Protocol*

Cells were trypsinised and re-plated into black Nucleon Delta White 96 microwell plates [Nunc] 48 hours post-transfection and incubated at 37°C/5% CO_2 for 24 hours. The cells were then serum-starved for five hours in serum-free media at 37°C/5% CO_2 to allow recycling of any ligand bound receptors to the cell surface. Following the serum starvation the medium was again carefully aspirated from the wells and the cells treated with serum-free media containing 0.1% [w/v] BSA, 5 mM butyrate, and different concentrations of either IGF-I, IGF-II, or Insulin. The cells were incubated for a further 48 hours at 37°C/5% CO_2. Following the 48 hour treatment with butyrate and IGFs, 20µl/well CellTiter-Blue^{TM} reagent was added and the cells incubated for a further 2 hours at 37°C/5% CO_2. The resultant fluorescent signal, indicative of viable cells, was measured using a Wallac Victor^{3}V 1420 Multilabel Counter plate reader [Perkin Elmer] utilising 550 nm excitation and 615 nm emission filters.

2.2.1.2.5 *Apo-One^{TM} Homogenous Caspase 3/7 Assay*

Following trypsinisation, cells were plated at the appropriate density [Table 2.9] in black 96 well plates and incubated for 48 hours at 37°C/5% CO_2. Growth media was then removed and the cells washed twice with serum-free media before a 5 hour serum-starvation at 37°C/5%CO_2. Cells were then treated for 46 hours at 37°C/5% CO_2 in appropriate media containing 5mM butyrate. Following treatment, 20µl/well CellTiter-Blue^{TM} reagent was added and incubated for 2 hours at 37°C/5% CO_2. Cell viability was assessed by reading the plate on a Wallac Victor^{3}V 1420 Multilabel Counter plate reader [Perkin Elmer] utilising 550 nm excitation and 615 nm emission filters. Following the assessment of cell viability, 100µl/well Apo-One^{TM} reagent was added and the plates incubated for a further 2 hours at room temperature, in the dark, on a plate shaker. Apoptosis was assessed by

recording the resultant signal in a Wallac Victor^{3}V 1420 Multilabel Counter plate reader at 485nm excitation, 535nm emission.

2.2.1.2.6 *Clonogenic Assay*

To assess anchorage-dependent clonogenic survival, 48 hours after transfection cells were trypsinised and replated at a density of 2,000 cells/10cm dish in growth medium, in triplicate and allowed to adhere overnight. The following day, cells were washed twice with serum-free medium before treatments were added. Treatments consisted of growth medium, or 24 or 48 hour treatment with serum-free medium containing 5mM butyrate. After the appropriate period, treatments were removed and the cells washed twice with serum-free medium. Cells were then grown in fresh growth medium for a further 3 days. Following this incubation, growth medium was removed and the cells washed once with 1x PBS to remove any cell debris. Cell colonies were then fixed by 1 hour incubation at room temperature with methanol:acetic acid [3:1] prior to being stained with 400µg/ml Crystal Violet for 2 hours at room temperature. Excess stain was removed by washing the dishes in slowly running RO water. Dishes were allowed to air dry prior to being scanned at 1200dpi using a flat bed scanner [Hewlet Packard]. Colonies were then enumerated using ImageQuant TL colony counting software [GE].

2.2.1.2.7 *Stimulation of cells with ligand for receptor phosphorylation assessment*

Thirty six hours after transfection, medium containing transfection complexes was removed and cell monolayers were washed twice with serum-free medium to remove any residual FCS. Following an overnight serum-starvation cells were stimulated with serum-free medium containing 0.1% BSA and 10nM of either IGF-I, IGF-II, or insulin for 10 minutes at 37°C/5% CO_2. After stimulation, cells were immediately washed with ice-cold 1xPBS and lysed according to 2.2.3.1. Receptor phosphorylation was determined by immunoprecipitation of proteins containing phosphorylated tyrosine residues [see 2.2.3.3.1] and detecting specific receptors by Western blot [see 2.2.3.4].

2.2.1.3 Transfection of mammalian cells with siRNA

2.2.1.3.1 Preparation of lyophilised siRNA for use in transfection

siRNAs were synthesized, HPLC purified, and sequence confirmed by MALDI-TOF spectrometric analysis at Qiagen. All siRNA samples were handled under strict RNAse-free conditions. Resuspension of lyophilized siRNA was performed as per manufacturer's instructions. This process maximizes the siRNA silencing potential of a given siRNA by disrupting higher aggregates that may have formed during the lyophilisation process.

2.2.1.3.2 Oligofectamine[TM]

Oligofectamine[TM] was initially used as a transfection reagent for SW480 cells as it had been routinely used by our collaborators[290-292, 297, 298]. Transfections were performed as per manufacturer's instructions, and are briefly outlined below. Initial optimisation experiments revealed Oligofectamine[TM] to be toxic to SW480 cells, therefore a suitable replacement transfection reagent for use in this cell line was sought.

2.2.1.3.2.1 Forward Transfection: Oligofectamine[TM]

Forward transfection refers to the traditional method of transfecting cells with siRNAs. In this method, cells are pre-plated the day before transfection and allowed to attach and recover prior to transfection. For forward transfection of mammalian cells with siRNA, cells were plated in growth medium in 6cm tissue culture dishes the day before transfection and incubated at $37^{o}C/5\%$ CO_2. Cells were plated such that they would be 50% confluent at the time of transfection. The appropriate amount of siRNA and Oligofectamine[TM] were diluted using Opti-MEM I and incubated separately for 10 minutes at room temperature. The diluted siRNA and Oligofectamine[TM] were then combined and allowed to form complexes prior to transfection by incubation at room temperature for 25 minutes. While transfection complexes were allowed to form, growth medium was removed from the cells and the cells washed twice with 2.5ml Opti-MEM I. After the final wash, 285μl Opti-MEM I was added to the cells. The transfection complexes were gently mixed then added to the

cells in a drop-wise fashion such that all cells were covered. Cells were incubated in this state for 4 hours at $37^{o}C/5\%$ CO_2 before being 'topped-up' with complete growth medium containing extra FCS to take into account the volume of the transfection mixture such that the final FCS concentration would be 10%. Cells were incubated for a further 44 hours prior to use in cell viability studies or analysis for gene expression by Western blot. For experiments where the effect of incubation time on toxicity was assessed, after the initial 4 hour incubation with transfection reagent, medium containing transfection reagent were removed and replaced with fresh growth medium.

2.2.1.3.2.2   *Reverse Transfection: Oligofectamine^{TM}*

The reverse transfection method combines plating and transfection, such that the cells are still in suspension when the transfection reagent and siRNA are added. For reverse mock transfections, the appropriate amount of Oligofectamine^{TM} was diluted in Opti-MEM I and incubated at room temperature for 10 minutes. During this time, a stock culture of SW480 cells was trypsinised and viable cells enumerated. Cells were resuspended to a concentration of $1x10^5$ cells/ml in Opti-MEM I. To 4ml of cells at this concentration, the diluted Oligofectamine^{TM} was added and gently mixed with the cells. The cells were immediately transferred to a 6cm tissue culture dish and incubated for 48 hours at $37^{o}C/5\%$ CO_2. Gene expression was assessed 48 hours post-transfection. For experiments where the effect of incubation time on toxicity was assessed, after the initial 4 hour incubation with transfection reagent, medium containing transfection reagent were removed and replaced with fresh growth medium.

2.2.1.3.3   *INTERFERin^{TM}*

INTERFERin^{TM} was assessed for its suitability for use as a transfection reagent for SW480 cells in both forward and reverse mock transfections. Mock transfections do not contain siRNA and are an indication of the toxicity of a given transfection reagent in a particular cell line. Transfections were performed as per manufacturers' instructions, and are outlined below.

2.2.1.3.3.1 Forward Transfection: INTERFERin^{TM}

For mock forward transfection of SW480 cells, cells were plated in growth medium in 6cm tissue culture dishes the day before transfection and incubated at 37°C/5% CO_2. Cells were plated such that they would be 50% confluent at the time of transfection. The appropriate amount of INTERFERin^{TM} was diluted in Opti-MEM I and incubated at room temperature for 10 minutes. Growth medium were removed from the cells and replaced with 4ml of fresh growth medium. The diluted INTERFERin^{TM} was added to the cells and homogenized by gently swirling the plate. Cells were incubated for 48 hours at 37°C/5% CO_2. Gene expression was assessed 48 hours post-transfection. For experiments where the effect of incubation time on toxicity was assessed, after the initial 4 hour incubation with transfection reagent, medium containing transfection reagent was removed and replaced with fresh growth medium.

2.2.1.3.3.2 Reverse Transfection: INTERFERin^{TM}

In a 6cm tissue culture dish, the appropriate amount of INTERFERin^{TM} was diluted with Opti-MEM I and incubated at room temperature for 10 minutes. During this time, a stock culture of SW480 cells was trypsinised and viable cells enumerated. Cells were resuspended to a concentration of $1x10^5$ cells/ml in growth medium. To the 6cm dish containing diluted transfection reagent, 4ml of SW480 cells at $1x10^5$ cells/ml were added and gently swirled to ensure uniform distribution within the plate. The cells were then incubated for 48 hours at 37°C/5% CO_2 before assessment of gene expression by Western blot. For experiments where the effect of incubation time on toxicity was assessed, after the initial 4 hour incubation with transfection reagent, medium containing transfection reagent was removed and replaced with fresh growth medium.

2.2.1.3.4 Lipofectamine 2000^{TM} and Lipofectamine RNAiMAX^{TM}

Both Lipofectamine 2000^{TM} and Lipofectamine RNAiMAX^{TM} were assessed for their suitability for use as transfection reagents for SW480 cells in both forward and reverse mock transfections. Transfections were performed as per manufacturers' instructions, and are outlined below.

2.2.1.3.4.1 Forward Transfection: Lipofectamine 2000^{TM} and Lipofectamine RNAiMAX^{TM}

For mock forward transfection of SW480 cells, cells were plated in growth medium in 6cm tissue culture dishes the day before transfection and incubated at 37^oC/5% CO_2. Cells were plated such that they would be 50% confluent at the time of transfection. The appropriate amount of transfection reagent was diluted in Opti-MEM I and incubated at room temperature for 10 minutes. Growth medium was removed from the cells and replaced with 4ml of fresh growth medium. The diluted transfection reagent was added to the cells and homogenized by gently swirling the plate. Cells were incubated for 48 hours at 37^oC/5% CO_2. Gene expression was assessed 48 hours post-transfection. For experiments where the effect of incubation time on toxicity was assessed, after the initial 4 hour incubation with transfection reagent, medium containing transfection reagent was removed and replaced with fresh growth medium.

2.2.1.3.4.2 Reverse Transfection: Lipofectamine 2000^{TM} and Lipofectamine RNAiMAX^{TM}

In a 6cm tissue culture dish, the appropriate amount of transfection reagent was diluted with Opti-MEM I and incubated at room temperature for 10 minutes. During this time, a stock culture of SW480 cells was trypsinised and viable cells enumerated. Cells were resuspended to a concentration of $1x10^5$ cells/ml in growth medium. To the 6cm dish containing diluted transfection reagent, 4ml of SW480 cells at $1x10^5$ cells/ml were added and gently swirled to ensure uniform distribution within the plate. The cells were then incubated for 48 hours at 37^oC/5% CO_2 before assessment of gene expression by Western blot. For experiments where the effect of incubation time on toxicity was assessed [Figure 5.6b], after the initial 4 hour incubation with transfection reagent, medium containing transfection reagent was removed and replaced with fresh growth medium.

2.2.1.3.5 HiPerFect

HiPerFect was initially assessed for its suitability for use as a transfection reagent for SW480 cells in both forward and reverse mock transfections. Transfections were performed as per

manufacturers' instructions. Initial experiments revealed forward transfections with HiPerFect to be potentially suitable for use in SW480 cells. The transfection protocol was optimised further and the final protocol is outlined below in Section 2.2.1.3.5.4.

2.2.1.3.5.1   Reverse Transfection: HiPerFect

In a 6cm tissue culture dish, the appropriate amount of HiPerFect was diluted with Opti-MEM I and incubated at room temperature for 10 minutes. During this time, a stock culture of SW480 cells was trypsinised and viable cells enumerated. Cells were resuspended to a concentration of $1x10^5$ cells/ml in growth medium. To the 6cm dish containing diluted HiPerFect, 4ml of SW480 cells at $1x10^5$ cells/ml were added and gently swirled to ensure uniform distribution within the plate. The cells were then incubated for 48 hours at 37^oC/5% CO_2 before assessment of gene expression by Western blot. For experiments where the effect of incubation time on toxicity was assessed [Figure 5.6b], after the initial 4 hour incubation with transfection reagent, medium containing transfection reagent was removed and replaced with fresh growth medium.

2.2.1.3.5.2   Forward Transfection: HiPerFect – Manufacturers' Instructions

For forward transfection of SW480 cells according to manufacturer's instructions, cells were plated at $4x10^5$ cells/6cm dish in growth medium the day before transfection and incubated at 37^oC/5% CO_2. Cells were plated such that they would be approximately 50 – 70 % confluent at the time of transfection. The following day, the appropriate amount of siRNA was diluted in 100 μl Opti-MEM I. To the diluted siRNA, 20 μl HiPerFect was added and briefly vortexed to mix. The diluted siRNA/transfection reagent mix was incubated at room temperature for 10 minutes to allow complexes to form. During this time, medium in which the cells were plated the previous day was removed and replaced with 4ml fresh growth medium. The transfection complexes were then added to the dish in a drop-wise fashion and the dish gently swirled to ensure uniform distribution. The cells were then incubated for 48 hours at 37^oC/5% CO_2. Assessment of gene silencing was performed 48 hours post-transfection.

Table 2.9 Cell plating densities

The table outlines the densities various cells lines were plated at in the assays used in this study. N/A, denotes not applicable.

Cell Line	Assay	Plating Density	
		Cells/Well	**Cells/ml**
	Apoptosis	12,000	120,000
	Cell Viability	12,000	120,000
SW480	Clonogenic	2,000	N/A
	Migration	$2x10^5$	$4x10^6$
	siRNA transfection	$4x10^5$	N/A
R-IRA / R-IRB / R-IGF1R	Cell Viability	2,500	25,000
	Migration	$2x10^5$	4x106
HT-29	Cell Viability	12,000	120,000
HCT-116	Cell Viability	10,000	100,000
Caco-2	Cell Viability	12,000	120,000

Table 2.10 Conversions between tissue culture dishes for up-scaling

Dish	Growth Area [cm^2]	Relative to Input
96 well plate	0.3	0.02
24 well plate	0.8	0.09
6 well plate	9.6	0.45
60 mm dish	21.3	1
100 mm dish	58.1	2.73

Table 2.11 Alterations made to the 10cm dish HiPerFect transfection protocol

Labels correspond to those in Figure 5.8c and denote the various changes made to the transfection protocol with the aim of improving efficacy of 10cm dish HiPerFect siRNA transfections

Label	Volume HiPerFect [µl]	Final siRNA conc.	Volume Growth Media
1a	40	100nM	7 ml
1b	54.6	100nM	7 ml
2a	40	100nM	15 ml
2b	87.15	100nM	15 ml
2c	54.6	100nM	15 ml

2.2.1.3.5.3   Forward Transfection: HiPerFect – 10cm dish optimization

Transfection of SW480 cells in 10cm dishes was performed essentially as outlined above in Section 2.2.1.3.5.2 with variation. Variations included: proportional up-scaling of reagents according to Table 2.10 to suit 10cm dishes; the volume of growth medium cells were treated in; and variation of the transfection reagent to siRNA ratio. In accordance with the labeling of results in Figure 5.8c, Table 2.11 outlines the various changes that were made to the HiPerFect transfection protocol with the aim of optimizing 10cm dish transfections.

2.2.1.3.5.4   Forward Transfection: HiPerFect – Final Protocol

SW480 cells were plated at 4×10^5 cells/6cm dish in growth medium the day before transfection and incubated at $37^oC/5\%$ CO_2. Cells were plated such that they would be approximately 50 – 70 % confluent at the time of transfection. The following day, the appropriate amount of siRNA was diluted in 100 µl Opti-MEM I. To the diluted siRNA, 20 µl HiPerFect was added and vortexed for 20 seconds to mix. The diluted siRNA/transfection reagent mix was incubated at room temperature for 10 minutes to allow complexes to form. The medium in which the cells were plated the previous day was removed and the transfection complexes added directly onto the cells in a drop-wise fashion. In a drop-wise fashion, 4ml of growth medium was gently added to the dish. The cells were then incubated for 48 hours at $37^oC/5\%$ CO_2. For dual receptor silencing, 24 hours after the initial transfection with 10nM IGF1R siRNA, cells were transfected with 10nM IR siRNA by following the same procedure outlined above. Cells were then incubated for a further 24 hours at $37^oC/5\%$ CO_2 prior to use in further experiments.

2.2.1.3.6   siRNA mediated knock-down of IRS-2 in R⁻IRB cells

siRNA mediated knock-down of IRS-2 in R⁻IRB cells was performed by Julie M Carroll, Oregon Health and Science University, Portland, Oregon, USA. ON-TARGETplus Smartpool small interfering RNA [containing a mixture of four siRNAs] for human IRS-2, ON-TARGETplus TARGETplus siCONTROL non-targeting pool [negative control], and DharmaFECT 3 transfection reagent were purchased from Dharmacon, Inc. [Lafayette, CO].

2.2.2   Methods: Molecular Biology

2.2.2.1 Isolation of total cellular RNA

Following appropriate culture conditions cell monolayers were washed twice with 1xPBS to remove any residual FCS. Cells were lysed directly by the addition of buffer RLT [Qiagen] and scraped well before transferring the lysates to RNase-free microcentrifuge tubes. Samples were then homogenized by passing though a 25 gauge needle at least 5 times. Total cellular RNA was then isolated using Qiagen RNeasy Mini spin columns, including an on-column DNAse I treatment, according to manufacturers' instructions. Following isolation, RNA was stored at -80°C.

2.2.2.2 Quantification of RNA

After isolation, total cellular RNA was quantified using a Nanodrop-1000 [Nanodrop Technologies]. Absorbance was recorded at 260nm and 280nm. Concentration of RNA samples was determined by the Nanodrop-1000 software programme according to the formula: OD_{260} x dilution factor x 0.04 = RNA concentration in μg/μl. In addition, RNA quality was assessed by calculating OD_{260}/OD_{280}. RNA with values ≥ 1.8 were accepted as being of high quality.

2.2.2.3 Synthesis of cDNA

cDNA was synthesised from 5 μg of purified RNA using SuperScript II RNase H⁻ Reverse Transcriptase [Invitrogen]. Reactions [12 μl] were assembled containing 5 μg purified RNA, 100 ng random hexamer primers, and 0.5 mM dNTPs, and incubated at 65°C for 5 minutes. Following a quick chill on ice, the contents of the reaction tube was collected by brief centrifugation. After the addition of 21% 5X First-Strand buffer, 100 mM DTT and 40 units SuperIn RNase Inhibitor the contents of the tube was gently mixed and incubated at 42°C for 2 minutes. SuperScript II RNase H⁻ Reverse Transcriptase [200 units] was added and the reaction vessel incubated at 42°C for 50 minutes to allow synthesis of first strand cDNA. The reaction was inactivated by heating at 70°C for 15 minutes and the samples were stored at -20°C until use.

2.2.2.4 Polymerase Chain Reaction

2.2.2.4.1 PCR amplification of β-actin

To confirm the integrity of the DNase treated RNA samples, cell line cDNA synthesised from purified RNA samples was used as a template in the PCR amplification of β-actin. Reactions [25 µl] were assembled containing 1 unit of BioTaq polymerase, 10% NH_4 buffer [Bioline], 1.5mM $MgCl_2$, 100 ng each of appropriate oligonucleotide, 0.5 mM dNTPs, and 1 µl of cDNA. All PCR reactions for amplification of β-actin were performed under the following conditions: denature at $92^{o}C$ for 5 minutes; 40 cycles of denaturation at $92^{o}C$ for 30 seconds, annealing at $60^{o}C$ for 30 seconds and extension at $72^{o}C$ for 30 seconds. A final extension at $72^{o}C$ was performed for 10 minutes. The reactions were stored at $-20^{0}C$ until analysed by agarose gel electrophoresis.

2.2.2.4.2 PCR amplification of IGF1R and IR

Polymerase chain reactions [PCR] were used to amplify specific segments of DNA between two oligonucleotide primers. Primers were chosen such that specific amplification of the IGF1R, or IR isoforms would ensue. It should be noted, all primers used in the PCR experiments spanned at least one intron/exon junction therefore would not amplify genomic DNA should any remain after DNAse digestion. Given that the two IR isoforms are generated by the alternate splicing of the 36 nucleotide exon 11, specific primers flanking exon 11 were employed in the PCR analysis of IR gene expression. The forward primer was homologous to a sequence within exon 10 and the reverse primer was homologous to a sequence within exon 12 of the IR, such that PCR amplification across the exons would generate a smaller product if splicing of exon 11 had occurred. PCR products amplified from transcripts of the IR-A were therefore expected to be 36bp shorter [473bp] than those generated from transcripts of the IR-B [509bp]. Reactions were assembled as above [Section 2.2.2.4.1]. All PCR reactions for amplification of IGF1R and IR isoforms were performed under the following conditions: denature at $92^{o}C$ for 5 minutes; 40 cycles of denaturation at $92^{o}C$ for 30 seconds, annealing at $60^{o}C$ for 30 seconds and extension at $72^{o}C$ for 30 seconds. A final extension at $72^{o}C$ was performed for 10 minutes. The reactions were stored at $-20^{0}C$ until analysed by agarose gel electrophoresis.

2.2.2.5 Agarose gel electrophoresis of RNA/DNA samples

To check the integrity of the purified RNA samples, 1µl of purified RNA was diluted in RNase-free molecular grade water and 5x RNA/DNA loading buffer. In the case of PCR amplification products, 10µl of DNA was diluted in molecular grade water and 5xRNA/DNA loading buffer. Diluted RNA/DNA samples were electrophoresed through 1.5% [w/v] agarose gels containing a 1:10,000 dilution of GelGreen. Separated RNA/DNA bands were visualized on a Dark Reader and digitally photographed.

2.2.3   Methods: Protein Chemistry

2.2.3.1 Lysis of mammalian cells

Following transfection or ligand stimulation, cells were washed with ice-cold 1xPBS and any excess PBS removed by blotting the edge of the tissue culture dish with 3M paper. Cells were then lysed directly by the addition of ice-cold lysis buffer and scraping prior to transfer to microcentrifuge tubes. For the lysis of cells remaining from plating bioassays, cells were pelleted by centrifugation at 1,000 rpm for 5 minutes [Eppendorf Centrifuge 5417R] at room temperature and washed twice in ice-cold 1xPBS prior to being transferred to microcentrifuge tubes on ice. The cells were then lysed by the addition of ice-cold lysis buffer. In both cases, lysates were incubated on ice for a further 30 minutes before the removal of insoluble debris by centrifugation at 13,000 rpm [Eppendorf Centrifuge 5417R] at 4°C for 15 minutes. Lysates were kept on ice until immediate use in other applications. For storage, lysates were kept at -80°C.

2.2.3.2 Determination of protein concentration

Protein concentration was determined by the bicinchoninic acid [BCA] protein assay. BSA standards [0 – 2mg/ml] and sample [neat or diluted] were added to a 96-well plate with 200µl BCA assay reagent. Following 30 minute incubation at 37°C, the OD_{562}nm was measured on a Wallac Victor^{3}V 1420 Multilabel Counter plate reader. A standard curve was calculated and used to determine the sample concentration.

2.2.3.3 Immunoprecipitation of proteins expressed in mammalian cells

2.2.3.3.1 Immunoprecipitation of phosphorylated proteins: IGF1R$_\beta$ and IR$_\beta$

Following stimulation and lysis, lysates [1000µg] were pre-cleared with 40µl of a 50:50 mix of protein A-agarose and protein G-agarose beads for 30 minutes at 4°C on a rotating wheel. The beads were then pelleted by centrifugation at 13,000 rpm [Eppendorf Centrifuge 5417R] for 1 minute at 4°C. Pre-cleared lysates were then transferred to fresh microcentrifuge tubes and incubated overnight at 4°C on a rotating wheel with 20µg anti-phosphotyrosine antibody P-Tyr-100. Immunoreactive proteins were collected by the addition of 60ul of a 50:50 mix of protein A-agarose and protein G-agarose and incubation at 4°C on a rotating wheel for 2 hours. Immunoprecipitates were collected by centrifugation at 13,000 rpm [Eppendorf Centrifuge 5417R] for 1 minute at 4°C, and washed three times in 1 ml ice-cold lysis buffer. After the final wash, immunoprecipitates were resuspended in 40µl 3x SAB and boiled at 95°C for 5 minutes. Prior to Western blot analysis, beads were pelleted by centrifugation at 13,000 rpm [Eppendorf Centrifuge 5417R] for 3 minutes at room temperature.

2.2.3.3.2 Co-immunoprecipitation of hybrid receptors

Following lysis, lysates [1000µg] were pre-cleared with 40µl of a 50:50 mix of protein A-agarose and protein G-agarose beads for 30 minutes at 4°C on a rotating wheel. The beads were then pelleted by centrifugation at 13,000 rpm [Eppendorf Centrifuge 5417R] for 1 minute at 4°C. Pre-cleared lysates were then transferred to fresh microcentrifuge tubes and incubated overnight at 4°C on a rotating wheel with 20µg of either anti-IR or anti-IGF1R antibody. Immunoreactive proteins were collected by the addition of 60ul of a 50:50 mix of protein A-agarose and protein G-agarose and incubation at 4°C on a rotating wheel for 2 hours. Immunoprecipitates were collected by centrifugation at 13,000 rpm [Eppendorf Centrifuge 5417R] for 1 minute at 4°C, supernatants were kept for analysis of immunodepletion by Western blot. Immunoprecipitates were then washed three times in 1 ml ice-cold lysis buffer. After the final wash, immunoprecipitates were resuspended in 40µl 3x SAB and boiled at 95°C for 5 minutes. Prior to Western blot analysis, beads were pelleted by centrifugation at 13,000 rpm [Eppendorf Centrifuge 5417R] for 3 minutes at room temperature.

2.2.3.4 Western blot analysis

Immunoprecipitates or whole-cell lysates [25 - 50µg] were subjected to reducing SDS-polyacrylamide gel electrophoresis on 4-12% Bis-Tris NuPAGE® gels using MOPS running buffer. After separation, the electrophoresed proteins were transferred to nitrocellulose membranes using the iBlot dry transfer system [Invitrogen]. Following transfer, nitrocellulose membranes were blocked in Blotto for at least one hour at room temperature with rocking. Nitrocellulose membranes were probed with appropriate primary antibody by overnight rocking at 4°C. Primary antibodies were probed by incubation with appropriate HRP-conjugated secondary antibody for one hour at room temperature with rocking. Immunoreactive bands were detected using enhanced chemiluminescence [ECL] Plus and exposure to X-ray film [Kodak].

2.2.3.5 Labeling of cell surface proteins with antibodies for detection by flow cytometry

Cell monolayers were disaggregated by trypsinisation to a single cell suspension. Trypsinisation did not affect the ability of the antibodies to recognize the IR and IGF1R [data not shown]. Cells were then resuspended in media containing FCS to stop the action of trypsin. Cells were then washed twice in 10ml 1xPBS, centrifuging at 1,000 rpm [Eppendorf Centrifuge 5702] for 5 minutes to pellet cells between washes. The cells were then resuspended to 3 ml in 1xPBS before being aliquoted equally into 1.5ml microcentrifuge tubes. Cells were pelleted by centrifugation at 1,000 rpm [Eppendorf Centrifuge 5417R] for 5 minutes and supernatant removed, prior to resuspension in 50µl of 25µg/ml primary antibody and incubation on ice for 40 minutes. Excess primary antibody was removed by washing the cells twice in 1 ml ice-cold FACS wash solution and centrifuging at 1,000 rpm [Eppendorf Centrifuge 5417R] for 5 minutes to pellet cells between washes. Following the final wash, cells were resuspended in 50µl of 25µg/ml FITC conjugated anti-mouse IgG secondary antibody. After a further incubation for 40 minutes on ice, cells were again washed twice in 1 ml ice-cold FACS wash solution. Finally, the cells were fixed in 1 ml 1xPBS/1%paraformaldehyde and stored in the dark at 4oC until analysed the following day in a FACScan Flow Cytometer using CellQuest Pro software [Becton Dickinson].

2.2.3.6 IR-A and IR-B phosphorylation and activation of intracellular signaling molecules in response to insulin, IGF-I, IGF-II, and IGF chimeras

Analysis of IR-A and IR-B phosphorylation and activation of intracellular signalling molecules in response to insulin, IGF-I, IGF-II, and IGF chimeras [Chapter 3] was performed by Dr. Adam Denley, University of Adelaide, Australia, as outlined below.

2.2.3.6.1 Materials

The following antibodies were purchased: IRS-1, phospho-Erk 1/2, Erk 1/2, Akt from Cell Signalling Technology [Beverly, MA, U.S.A.]. Phospho-Akt [pS^{473}], Phospho-IR/IGF-1R [$pYpYpY^{1158/1162/1163}$], phospho IR [pY^{972}] from the Biosource International [Camarillo, CA, U.S.A]. Rat carboxy-terminal IRS-1 and IRS-2 purchased from Upstate Biotechnology [Lake Placid, N.Y, U.S.A]. Pepstatin and sodium orthovanadate was obtained from Sigma Chemical Co., [MO, U.S.A.]. The Criterion gels 12 % Tris-tricine gels were purchased from Biorad [Hercules, CA, U.S.A.].

2.2.3.6.2 Methods

2.2.3.6.2.1 Cell stimulation and preparation of whole cell lysates

R⁻IR-A or R⁻IR-B cells were grown to 80 % confluency and serum-starved overnight at 37°C, 5 % CO_2. The cells were then treated with 10 nM ligand for either 5 minutes or a time course of 2, 5, 10 and 60 minutes. Stimulation was terminated by two washes with ice-cold PBS [pH 7.4] and addition of lysis buffer [50 mM Tris [pH 6.8], 1% [w/v] SDS and 10 % [v/v] glycerol]. After scraping the cells, the lysates were boiled immediately to inhibit protease and phosphatase action and centrifuged at 13,200 rpm for 1 minute. The protein concentration was determined with a DC protein assay kit [Bio-Rad, Hercules, CA].

2.2.3.6.2.2   IRS-1 immunoprecipitation

Cells were stimulated as above, but were lysed in a different lysis buffer [150 mM NaCl, 10 % [v/v] glycerol, 20 mM Tris [pH8], 1 mM EDTA, 0.2 % SDS, 1 tablet complete protease inhibitors, 2 mM sodium orthovanadate and 1μg/ml pepstatin]. Lysates [500 μg] were pre-cleared with protein A-agarose beads for 30 min rocking at 4°C, before addition of 5 μg of anti-IRS-1 antibody and incubation overnight at 4°C rocking. Protein A-agarose beads were added for 3 hours at 4°C and then the immunoprecipitates were eluted and subjected to SDS polyacrylamide gel electrophoresis.

2.2.3.6.2.3   Western blot analysis

Immunoprecipitates or whole-cell lysates [20 μg] were subjected to reducing SDS-polyacrylamide gel electrophoresis on 10 % Bis-tris acrylamide Criterion™ gels [for IR, PKB/Akt, and Erk1/2] or 7 % tris-acetate acrylamide gel Criterion™ gels [IRS-1]. After separation, the electrophoresed proteins were transferred to nitrocellulose membranes and immunoblotted with phospho-specific antibodies or, in the case of IRS-1, immunoprecipitates were probed with the antiphosphotyrosine antibody PY20. In all cases, after probing with the phospho-specific antibody, the nitrocellulose was stripped [100 mM Tris-HCl [pH 6.8], 10 % SDS and 100 mM β-mercaptoethanol for 30 minutes at 60°C] and re-probed with a pan-specific antibody. Immunoreactive bands were detected using enhanced chemiluminescence [ECL] Western blotting protocol [Amersham]. Densitometry was performed to quantitate the ECL visualized bands. Statistical analysis to determine significance was by Students t-test.

2.2.3.6.3   Binding analysis of IGF chimeras to insulin receptor isoforms

Binding analysis of IGF chimeras to the insulin receptor isoforms was performed by Dr. Adam Denley, University of Adelaide, Australia, as outlined below.

Receptor binding affinities were measured using an assay similar to that measuring EGF binding to the EGF receptor[299]. R⁻IR-A and R⁻IR-B were used as sources of IR-A and IR-B respectively. Cells were lysed with lysis buffer [20 mM HEPES, 150 mM NaCl, 1.5 mM $MgCl_2$, 10% [v/v] glycerol, 1%

[v/v] Triton X-100, 1 mM EGTA pH 7.5] for 1 hour at 4°C. Lysates were centrifuged for 10 minutes at 3500 rpm and then 100 μl was added per well to a white Greiner Lumitrac 600 plate previously coated with anti-insulin receptor antibody 83-7. Europium-labelled receptor grade human insulin were prepared as instructed by the manufacturer [DELFIA® Eu-labelling kit, Perkin Elmer, Turku, Finland]. Briefly, 0.43 mM peptide was incubated with 2 mM labelling reagent in a 30μl reaction [0.1 M Na_2CO_3 pH 8.5], 4°C for 2 days. The reaction was terminated with 0.05 M Tris-HCl, 0.15 M NaCl, pH 7.5 and unbound europium was removed by size exclusion chromatography in the termination buffer [Superdex 75, Pharmacia, Sweden]. Approximately 100,000 fluorescent counts of europium-labelled insulin were added to each well along with various amounts of unlabelled competitor and incubated for 16 hours at 4°C. Wells were washed with 1x TBST and DELFIA® enhancement solution [100 μl/well] was added. Time-resolved fluorescence was measured using 340 nm excitation and 612 nm emission filters with a BMG Lab Technologies Polarstar™ Fluorimeter. IC_{50} values were calculated, using Prism 3.03, by curve-fitting with a one-site competition model. The baseline used to calculate all IC_{50} values was set at the % bound/total value of the highest competing insulin concentration.

Chapter 3

Physiological concentrations of IGF-I can stimulate biological responses via the IR

3.1   Introduction

IGF-I and IGF-II share a high degree of sequence and structural homology[1-3]. The single-chain polypeptides are folded into four domains: B, C, A, and D [in order of N to C terminus] to form mature IGF-I and IGF-II. Despite their structural similarities, IGF-I and IGF-II display differential abilities to bind and activate receptors[7-11]. The pleiotropic actions of IGF-I and IGF-II are thought to be primarily due to their activation of the IGF1R, while insulin functions via activation of the IR[300]. However, mechanisms exist that enable cross-talk between the IGF and insulin ligands and their respective receptors. At supra-physiological levels, IGFs can activate the IR, and conversely, insulin can activate the IGF1R. These observations are not thought to be indicative of a general biological occurrence, especially in the case of insulin activation of the IGF1R where the concentrations required for activation vastly exceed those observed in vivo[301, 302]. In contrast to the aberrant activation of the IGF1R by insulin, two distinct molecular mechanisms exist that enable IGF cross-talk with the IR, namely IGF1R/IR hybrid receptors and the alternative splicing of the IR.

Hybrid receptors form via the random dimerisation of one αβ monomer of the IR and one αβ monomer of the IGF1R in cells that co-express both receptors[303]. Hybrid receptors containing either IR isoform have similar affinities for IGF-I and IGF-II to that of IGF1R homodimers, and substantially lower affinity for insulin than IR homodimers[110, 147]. Hybrid receptors therefore allow IGF ligands to simultaneously activate IGF1R and IR β-subunits, although, the overall biological relevance of hybrid receptor signaling is as yet unclear.

Alternative splicing of exon 11 provides a second mechanism for IGF activation of the IR. The 12 amino acid sequence at the carboxyl terminus of the IR α-subunit encoded by exon 11 confers differential ability of the two IR isoforms to bind ligands[7, 9, 13]. The IR-A, lacking these 12 amino acids, displays high affinity for insulin, intermediate affinity for IGF-II, and low affinity for IGF-I[7, 13]. The IR-B, containing these 12 amino acids, displays high affinity for insulin and only low affinities

for IGF-II and IGF-I[13]. The two IR isoforms are thought to have unique biological functions because their relative expression is controlled in a developmental, tissue specific, and pathophysiological manner. The IR-A is preferentially expressed in foetal and tumour tissues[7, 90], whereas the IR-B is preferentially expressed in differentiated tissues, especially insulin target tissues[99]. Signaling via the IR-A tends to result in more proliferative than metabolic downstream effects[7, 90]. Signaling via the IR-B is implicated in mediating the metabolic effects of insulin[99].

In this chapter, a third novel pathway for IGF activation through the IR is described. The results presented in this chapter have been published[13, 304, 305] [see Appendix] and were produced in collaboration with Dr. Adam Denley, University of Adelaide, and Julie M. Carroll, Oregon Health and Science University in the laboratory of Prof. Charles T. Roberts Jr. Dr. Denley's studies identified the binding requirements and signaling processes involved. My studies provide the essential biological characterization. Because these studies integrate closely with each other, Denley's findings are described in detail in the remainder of this introduction [Section 3.1] followed by my studies in the Results section [3.2]. Results demonstrated that the differential ability of the IGFs to stimulate biological responses via the IR isoforms was due the IGF C domains. However, these results also identified that physiological concentrations of IGF-I could stimulate biological outcomes via the IR-A and IR-B. Subsequent validation of the R⁻IRA and R⁻IRB cell lines utilised in the study and analysis of IRS activation identified IGF-I can act through both IR isoforms to preferentially activate IRS-2 resulting in downstream biological effects.

3.1.1   IGF Chimeras

Six chimeric IGFs were produced by Dr. Denley in order to determine the effect of the C and D domains on the differential ability of the IGFs to bind and activate the IR-A. These chimeras of IGF-I and IGF-II were generated by swapping the C and D domains either singly [IGF-I CII, IGF-I DI, IGF-II CI, IGF-II DI] or together [IGF-I CIIDII and IGF-II CIDI] [Figure 3.1]. BIAcore analysis of IGFBP-3 binding of each of the chimeras revealed swapping the domains did not result in any global structural change[306], data not shown.

A

```
B domain              1                              29
                  GP-ETLCGAELVDA LQFVCGDRGFY FNKPT          IGF-I
                  AYRPSETLCGGELVDT LQFVCGDRGFY FSRPA        IGF-II
                    FVNQHLCG SHLVEA LYLVCGERGFF YTPKT       Insulin
                  B1                             B30

C domain              30            41
                  GYGSSSRRAPQT                              IGF-I
                  SR__VSRRS_R_                              IGF-II
                                                            Insulin

A domain              42                      62
                  GIVDECCFRS CDLRRL EMYCA                   IGF-I
                  GIVEECCFRS CDLALL ETYCA                   IGF-II
                  GIVEQCCTSI CSLYQL ENYCN                   Insulin

D domain              63        70
                  PLKPAKSA                                  IGF-I
                    TPAKSE                                  IGF-II
                                                            Insulin
```

B

NOTE: This figure is included on page 69 of the print copy of the thesis held in the University of Adelaide Library.

Figure 3.1 Sequence relationship of IGF-I, IGF-II, and Insulin

[A], Sequence alignment of human IGF-I, IGF-II, and insulin using Clustal W. Numbering of amino acids is indicated above for IGF-I and below for insulin. [B], diagrammatic representation of the domain exchanged chimeras. Amino acid numbers and molecular weights are given. Each linear representation is divided into the domain structure: B, C, A, D with all IGF-I domains in blue and all IGF-II domains in green. Figure reproduced from Denley et al 2004 Mol Endo[13.] IGF chimeras generated by Dr. Adam Denley.

Figure 3.2 Competition binding curves of Eu-Insulin binding to immunopurified IR-A or IR-B

Immunocaptured IR-A or IR-B were incubated with Eu-Insulin in the presence or absence of increasing concentrations of insulin, IGF-I, IGF-II, or IGF chimeras. The graphs presented are a representative of three experiments. [A] and [C] competition for binding to the IR-A. [B] and [D] competition for binding to the IR-B. Results are expressed as a percentage Eu-Insulin bound in the absence of competing ligand, and the data points are means ± SEM of triplicate samples. Errors are shown when greater than the size of the symbols. In [A] and [B] the ligands are as follows: Insulin [▼]; IGF-II [▲]; IGF-I [Δ]; IGF-I CII [○]; IGF-I DII [◊]; IGF-II CI [●]; and IGF-II DI [♦]. In [C] and [D] the ligands are as follows: Insulin [▼]; IGF-II [▲]; IGF-I [Δ]; IGF-I CIIDII [□]; and IGF-II CIDI [■]. Binding assays performed by Dr. Adam Denley and figure reproduced from Denley et al 2004 Mol. Endo[13].

3.1.2 Binding specificity of the IGFs to the IR-A and IR-B is regulated by their C and D domains

Cells expressing IR-A [R⁻IRA] or IR-B [R⁻IRB] in an IGF1R null background were generated by Dr. Eric Bonython in our laboratory. The differential binding affinities for insulin, IGFs, or IGF chimeras to immunocaptured receptors were assessed in competition binding curves and results are presented in Figure 3.3 and Table 3.1. Insulin was found to bind to the IR-A with 6.5-fold higher affinity than IGF-II. IGF-I bound with a 6.5-fold lower affinity than that of IGF-II [Figure 3.2 A and C and Table 3.1]. The difference in the ability of IGF-II and IGF-I to bind the IR-A were due to the C, and to a lesser extent, the D domain. IGF-I chimeras containing either IGF-II C or D domains [IGF-I CII and IGF-I DII] had increased affinity for the IR-A and were more IGF-II like. The contributions of the C and D domains were additive, with IGF-I CIIDII able to bind the IR-A with a similar affinity as IGF-II. Conversely, IGF-II chimeras containing either IGF-I C or D domains [IGF-II CI and IGF-II DI] had decreased affinity for the IR-A and were more IGF-I like. Again, the effects of a double domain swap were additive with IGF-II CIDI possessing the same affinity for the IR-A as IGF-I.

Insulin bound with a 48-fold higher affinity than IGF-II to the IR-B, while IGF-I bound with a 5.4-fold lower affinity than that of IGF-II [Figure 3.2 B and D and Table 3.1]. Like the results observed with the IR-A, the differential ability of the IGFs to bind the IR-B was due to the C and D domains. IGF-I chimeras containing IGF-II C and D domains bound with affinities more like that of IGF-II. Conversely, IGF-II chimeras containing IGF-I C and D domains bound the IR-B with affinities more like that of IGF-I. The IR-B had a 2-fold higher affinity for insulin than the IR-A, while IGF-II, IGF-I, and IGF chimeras had higher affinities for the IR-A than the IR-B [Table 3.1].

3.1.3 Induction of IR-A and IR-B tyrosine autophosphorylation by insulin, IGF-II, IGF-I, and IGF chimeras

After ligand binding to the IR, phosphorylation of tyrosine residues Y1158, Y1162, and Y1163 [Y1170, Y1174, and Y1175 in the IR-B] in the activation loop occurs. This allows access of ATP

Table 3.1 Inhibition of Eu-Insulin binding to the IR-A and IR-B by Insulin, IGF-I, IGF-II, and IGF Chimeras.

Values are the mean ± SEM from three independent experiments. Table reproduced from Denley et al 2004 Mol Endo[13].

NOTE: This figure is included on page 72 of the print copy of the thesis held in the University of Adelaide Library.
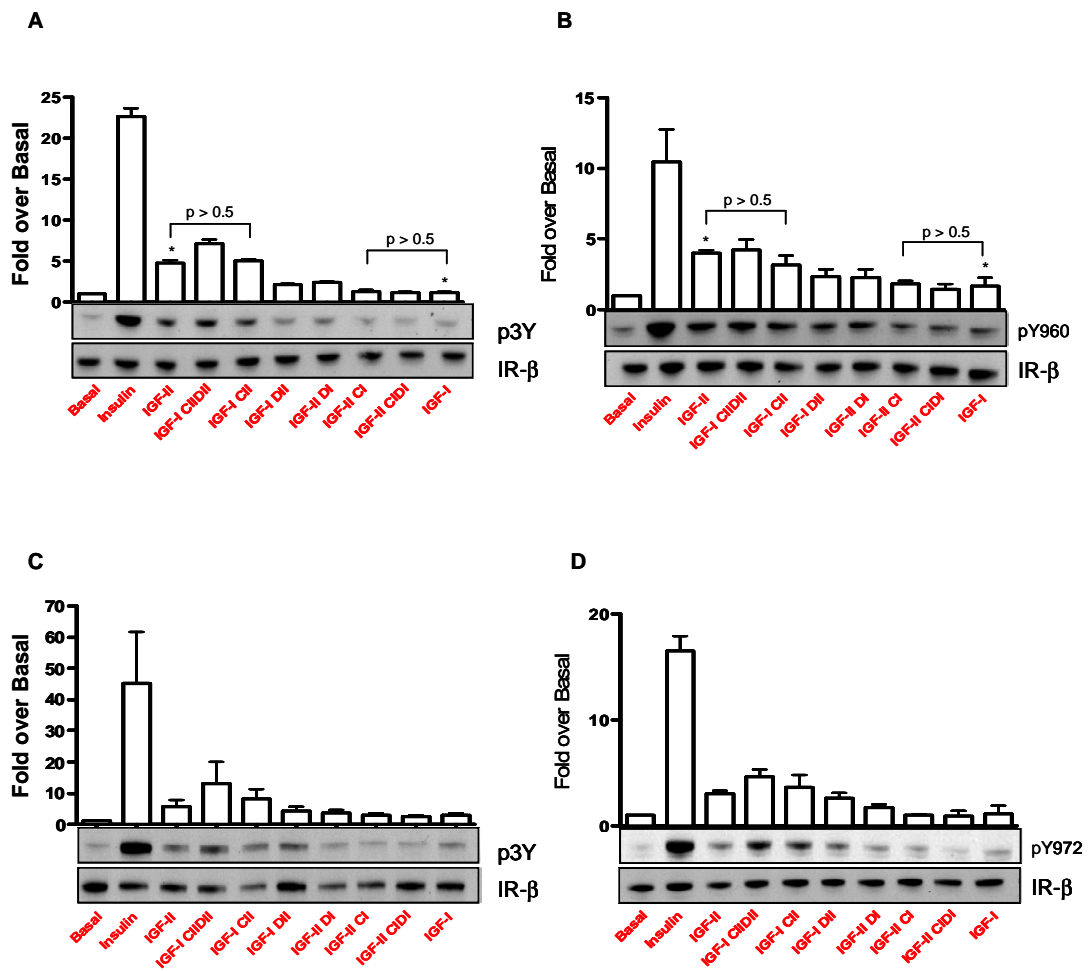
Figure 3.3 Induction of IR-A Y1158, Y1162, and Y1163 [p3Y] or Y960 autophosphorylation and IR-B Y1170, Y1174, and Y1175 [p3Y] or Y972 autophosphorylation by Insulin, IGF-II, IGF-I, and IGF chimeras.

Serum-starved R⁻IRA [**A**] and [**B**] or R⁻IRB [**C**] and [**D**] cells were treated with 10nM ligand for 5 minutes. Whole-cell lysates were prepared and subjected to SDS-PAGE and then immunoblotted and assayed for phosphorylated Y1158, Y1162, and Y1163 [p3Y] [**A** and **C**] or phosphorylated Y960 [**B** and **D**]. In each panel, densitometry of three independent experiments ± SEM [p3Y/total IRβ subunit] are shown as a column graph. Upper blots, p3Y or Y960 Western blot showing a representative result of three independent experiments. Lower blots, re-blotting with anti-IR β-subunit antibody. [**A**] * IGF-II vs. IGF-I p < 0.01. [**B**] * IGF-II vs. IGF-I p < 0.05. Induction of IR-A and IR-B phosphorylation experiments performed by Dr. Adam Denley.

and peptide substrates to the kinase active site[82]. The ability of 10nM insulin, IGF-II, IGF-I, and IGF chimeras to induce phosphorylation of these residues in the IR-A and the IR-B, abbreviated to 3Y, was therefore examined by Dr. Adam Denley.

Insulin stimulated a 22-fold increase in 3Y phosphorylation of the IR-A. IGF-II stimulated a 5-fold increase in 3Y phosphorylation [Figure 3.3 A]. IGF-I only activated 3Y phosphorylation slightly above basal levels [IGF-II vs. IGF-I, p <0.01]. IGF-I chimeras IGF-I CIIDII and IGF-I CII were equally as effective as IGF-II at stimulating 3Y phosphorylation of the IR-A [IGF-II vs. IGF-I CII, p > 0.5]. Single D domain swap, IGF-I DII, was only slightly better than IGF-I at inducing 3Y phosphorylation. IGF-II chimeras IGF-II CIDI and IGF-II CI did not differ in their ability to stimulate 3Y phosphorylation compared to IGF-I [IGF-I vs. IGF-II CI, p > 0.5]. Finally, IGF-II DI had decreased ability to stimulate 3Y phosphorylation compared to IGF-II [IGF-II vs. IGF-II DI, p < 0.05]. These results suggest that both insulin and IGF-II induce strong 3Y phosphorylation, while IGF-I is a poor activator of IR-A 3Y phosphorylation. In addition, the differential ability of IGF-I and IGF-II to induce 3Y phosphorylation is due to the C domain.

Insulin stimulation caused a 45-fold increase in 3Y phosphorylation of the IR-B [Figure 3.3 C], which was a 2-fold greater than the 3Y phosphorylation stimulated by insulin in the IR-A. This observation correlates with previous reports that insulin-activated IR-B had greater auto-phosphorylation activity than the IR-A[307]. Relative to insulin, IGF-II stimulated 8-fold lower 3Y phosphorylation, but 1.9-fold higher 3Y phosphorylation relative to IGF-I. Exchange of the IGF-I and IGF-II C and D domains had the same relative effect on 3Y phosphorylation in the IR-B as on the IR-A, however 3Y phosphorylation stimulated by each ligand did not differ statistically [p > 0.5].

3.1.4   Induction of Y960 [IR-A] and Y972 [IR-B] phosphorylation by insulin, IGF-II, IGF-I, and IGF chimeras

Autophosphorylation of the activation loop and subsequent activation of the kinase active site enables both the receptor itself and signaling molecules to become phosphorylated. Phosphorylation of Y960 in the juxtamembrane domain of the IR-A [Y972 in the IR-B] provides a docking site for binding of adaptor molecules such as, Shc, IRS-1, and IRS-2[308]. Therefore, the

ability of insulin, IGF-II, IGF-I, and IGF chimeras to induce phosphorylation of this tyrosine residue in the IR-A and the IR-B was examined. Y960 and Y972 phosphorylation experiments were conducted by Dr. Adam Denley, University of Adelaide.

In the IR-A, insulin stimulated Y960 phosphorylation 10-fold over basal, IGF-II induced 4-fold Y960 phosphorylation over basal, while IGF-I only increased Y960 phosphorylation 1.6-fold over basal levels [Figure 3.3 B]. IGF-I chimeras IGF-I CIIDII and IGF-I CII stimulated Y960 phosphorylation to the same extent as IGF-II [IGF-II vs. IGF-I CII, $p > 0.5$], while IGF-II chimeras IGF-II CIDI and IGF-II CI were as poor as IGF-I at inducing Y960 phosphorylation [IGF-I vs. IGF-II CI, $p > 0.5$]. Single exchange of the D domains had only a small effect on the ability of the IGF chimeras to stimulate Y960 phosphorylation compared to their relative wild-type ligand.

In the IR-B, insulin stimulated Y972 phosphorylation 16-fold over basal, IGF-II induced a 3-fold increase in phosphorylation, while IGF-I did not significantly increase Y972 phosphorylation over basal levels [Figure 3.3 D]. IGF-I CII induced Y972 phosphorylation to the same extent as IGF-II [IGF-II vs. IGF-I CII, $p > 0.5$]. Exchange of the IGF-II C domain for that of the IGF-I [IGF-II CI] reduced the ability of IGF-II to stimulate Y972 phosphorylation to that of IGF-I. Together these results suggest the differential ability of IGF-I and IGF-II to induce Y960 and Y972 phosphorylation is due to the C domain.

3.1.5 Insulin, IGF-II, IGF-I, and IGF C domain chimera induced phosphorylation of IRS-1 and IRS-2 via the IR-A and IR-B

Phosphorylation of Y960 in the IR-A and Y972 in the IR-B provides a docking site for IRS-1 and IRS-2 via their SH2 domains, although it should be noted IRS-2 can bind the IR via a non-SH2 mediated mechanism[309]. Recruitment of IRS-1 and IRS-2 allows these two molecules to be phosphorylated by the IR kinase domain. The ability of insulin, IGF-II, IGF-I, and IGF C-domain chimeras to induce IRS-1 and IRS-2 phosphorylation via the IR-A and the IR-B was assessed [Figure 3.4]. IRS-1 and IRS-2 phosphorylation experiments were conducted by Dr. Adam Denley in conjunction with Julie M. Carroll, Oregon Health and Science University.
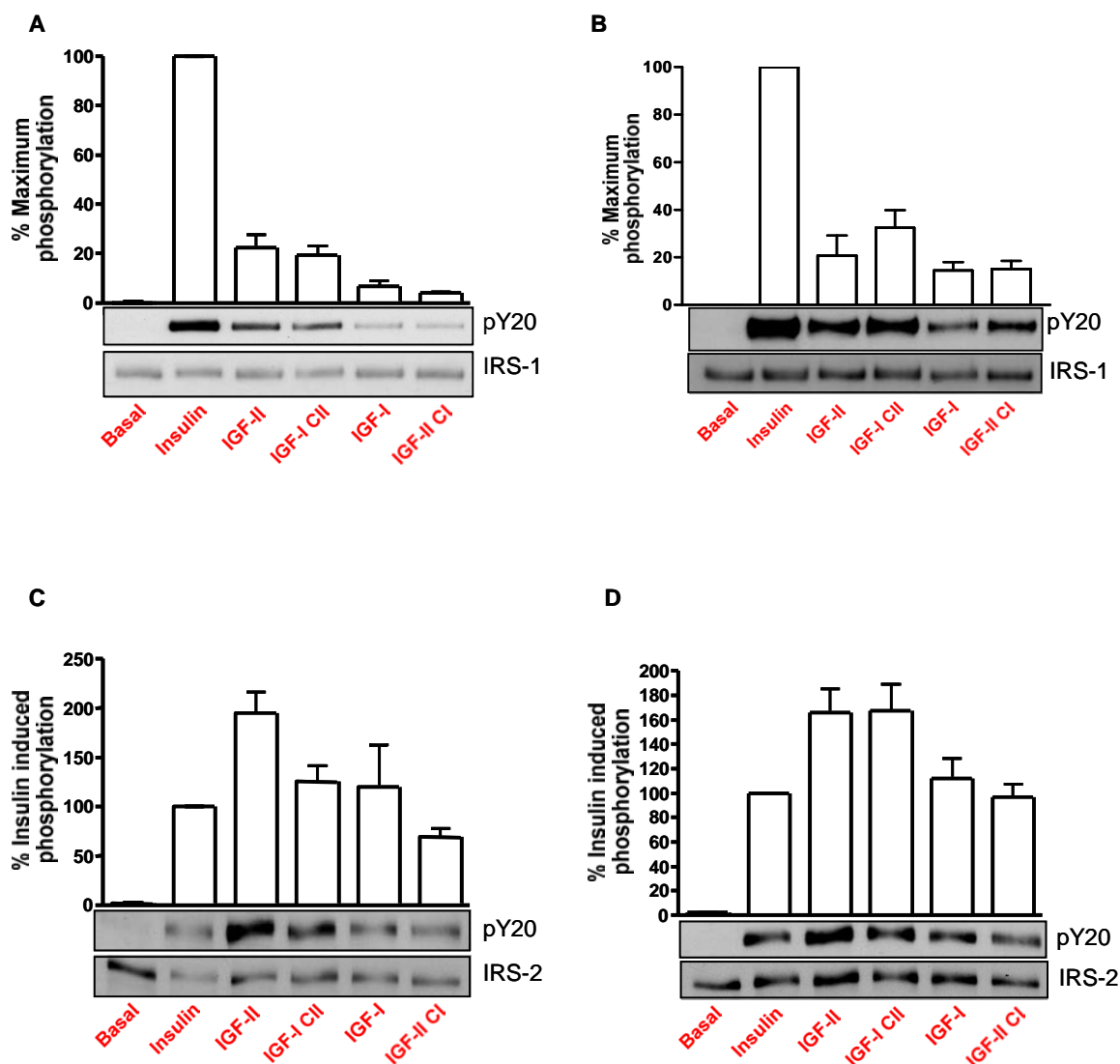
Figure 3.4 IRS-1 and IRS-2 phosphorylation in R⁻IRA and R⁻IRB cells

*Serum-starved R⁻IRA [**A** and **C**] or R⁻IRB [**B** and **D**] were treated with 10nM ligand for 5 minutes. Whole-cell lysates were prepared and immunoprecipitated with either an anti-IRS-1 antibody [**A** and **B**] or an anti-IRS-2 antibody [**C** and **D**]. Graphs represent normalized densitometry results from three independent experiments ± SEM. Upper blots are representative results of three independent experiments where IRS-1 or IRS-2 IPs were probed with anti-phosphotyrosine antibody PY20. Lower blots, demonstrate re-blotting with either anti-IRS-1 [**A** and **B**] or anti-IRS-2 antibodies [**C** and **D**]. IR-A: IGF-II vs. IGF-I, p < 0.05. IRS-1 and IRS-2 phosphorylation experiments conducted by Dr. Adam Denley.*
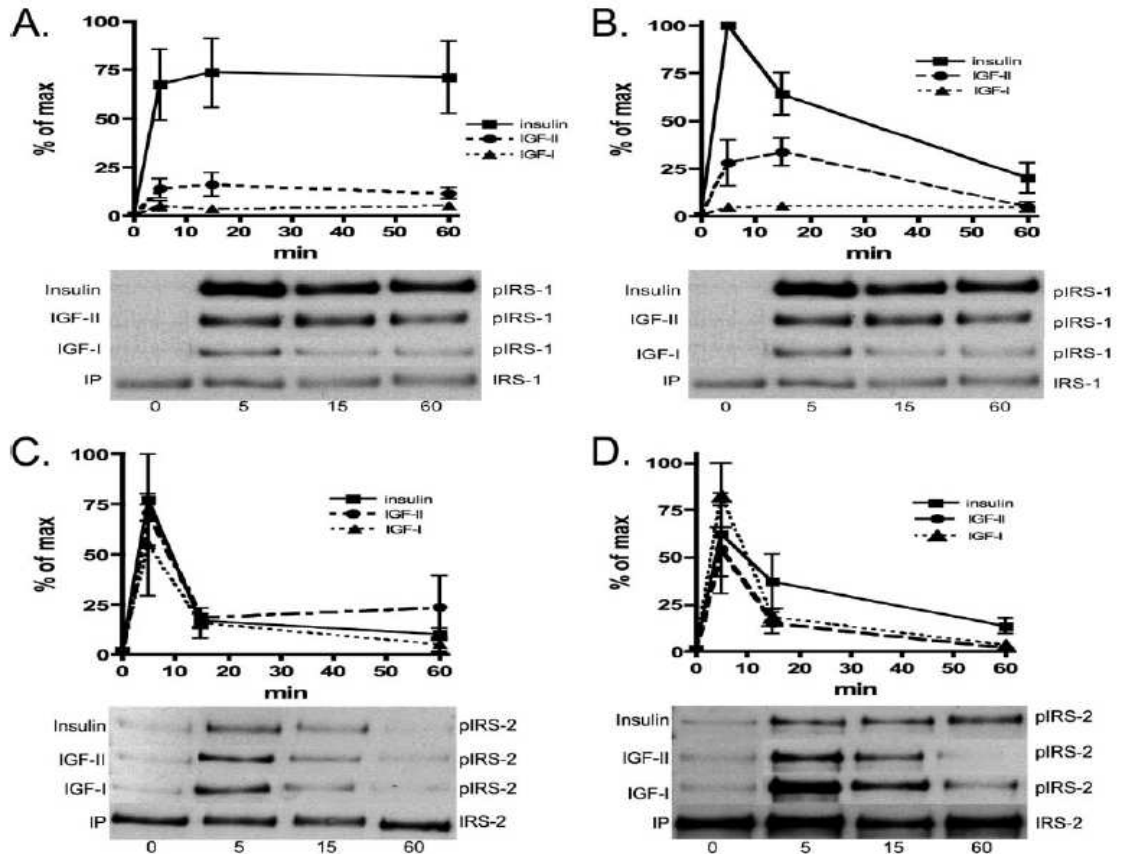
Figure 3.5 Time-course of IRS-1 and IRS-2 activation by Insulin, IGF-II, and IGF-I.

Cells were serum-starved overnight and treated with 10nM ligand for the indicated time periods. Lysates were immunoprecipitated with anti-IRS-1 and anti-IRS-2 antibodies, followed by Western immunoblotting with anti-IRS and PY20 antibodies. [A] IRS-1 activation in R⁻IRA cells; [B] IRS-1 activation in R⁻IRB cells; [C] IRS-2 activation in R⁻IRA cells; [D] IRS-2 activation in R⁻IRB cells. Representative blots are shown below each graph. In each case, the PY20 signal was normalized for IRS-1 or IRS-2 levels as determined by blotting with the respective antibody separately for each sample. Error bars represent SEM of three independent experiments. The bottom portion of the gel image in each case corresponds to a single representative IRS-1 or IRS-2 control blot. Max, maximum; pIRS-1, phosphorylated IRS-1; pIRS-2, phosphorylated IRS-2. IRS-1 and IRS-2 time course experiments conducted by Julie M. Carroll.

In R⁻IRA cells, IRS-1 was strongly phosphorylated following five minute stimulation with insulin [Figure 3.4 A]. Relative to insulin, IGF-II stimulated a 4-fold lower level of IRS-1 phosphorylation. Compared to IGF-II, IGF-I stimulated a 3.5-fold lower level of IRS-1 phosphorylation. Exchange of the IGF C-domains accounted for the differential ability of IGF-I and IGF-II to stimulate IRS-1 phosphorylation via the IR-A [IGF-II vs. IGF-I CII, $p > 0.5$; IGF-I vs. IGF-II CI, $p > 0.5$]. In R⁻IRB cells, IRS-1 was strongly phosphorylated by insulin [Figure 3.4 B]. Relative to insulin, IGF-II stimulated a 4-fold lower level of IRS-1 phosphorylation in R⁻IRB cells. Compared to IGF-II, IGF-I stimulated only a 1.4-fold lower level of IRS-1 phosphorylation. Again, exchange of the IGF C-domains accounted for the differential ability of IGF-I and IGF-II to stimulate IRS-1 phosphorylation. These results are interesting, as despite the difference in IR-A and IR-B binding affinities for IGF-II, relative IGF-II stimulation of IRS-1 in R⁻IRB cells was similar to that observed in R⁻IRA cells. Moreover, relative IGF-I stimulated IRS-1 phosphorylation was greater in R⁻IRB cells than in R⁻IRA cells. The differential ability of IGF-I and IGF-II to induce IRS-1 phosphorylation was less in R⁻IRB cells than in R⁻IRA cells, and was in keeping with the relative binding affinities of these ligands for the IR-A and IR-B [Table 3.1]. Similar relative IRS-1 phosphorylation was induced by insulin, IGF-II, and IGF-I over a time course of 60 minutes [Figure 3.5 A and B]

Five minute stimulation of R⁻IRA cells with insulin induced strong phosphorylation of IRS-2, however, relative to insulin, IGF-II was 2-fold more effective at inducing IRS-2 phosphorylation [Figure 3.4 C]. The ability of IGF-II to induce IRS-2 phosphorylation relative to insulin is contrary to the relative abilities of these two ligands to stimulate 3Y, Y960, and IRS-1 phosphorylation via the IR-A. In addition, IGF-I stimulated the same level of IRS-2 phosphorylation as insulin, despite its poor ability to activate the IR-A. IGF-I CII did not exhibit the same ability as IGF-II to induce IRS-2 phosphorylation, while IGF-II CI did not differ significantly from IGF-I in its ability to induce IRS-2 phosphorylation via the IR-A [IGF-I vs. IGF-II CI, $p > 0.5$]. In R⁻IRB cells [Figure 3.4 D], the ability of ligands to stimulate IRS-2 phosphorylation were similar to the trends observed in R⁻IRA cells. IGF-II was more effective than insulin at inducing IRS-2 phosphorylation, while IGF-I stimulated the same level of IRS-2 phosphorylation as insulin. In R⁻IRB cells, exchange of the IGF C-domains accounted for the differential ability of IGF-I and IGF-II to induce IRS-2 phosphorylation. Similar relative IRS-2 phosphorylation was induced by insulin, IGF-II, and IGF-I over a time course of 60 minutes [Figure 3.5 C and D].

### 3.1.6 Ligand stimulated activation of Akt/PKB via the IR-A and IR-B

Activation of IRS-1 and IRS-2 provides a link between the IR and the PI3K pathway. This pathway mediates insulin's ability to stimulate glucose uptake[310], cell-cycle progression, regulation of transcription, and protection from apoptosis[311, 312]. Akt/PKB are major effector proteins of the PI3K pathway. Therefore, the ability of insulin, IGF-II, IGF-I, and IGF chimeras to stimulate Akt/PKB phosphorylation via the IR-A and IR-B was assessed by Dr. Adam Denley and Julie M. Carroll.

In R⁻IRA cells, insulin stimulated strong phosphorylation of Akt/PKB [Figure 3.6 A]. IGF-II and IGF-I were 30% and 11% as effective as insulin at stimulating Akt/PKB phosphorylation, respectively. IGF chimeras containing IGF-II C-domains were as effective as IGF-II at stimulating Akt/PKB phosphorylation via the IR-A. Moreover, IGF chimeras containing IGF-I C-domains stimulated Akt/PKB phosphorylation to a level comparable to that of IGF-I.

In R⁻IRB cells, insulin again stimulated strong phosphorylation of Akt/PKB [Figure 3.6 B]. IGF-II and IGF-I were 30% and 15% as effective as insulin at stimulating Akt/PKB phosphorylation, respectively. IGF chimeras containing IGF-II C-domains induced slightly higher levels of Akt/PKB phosphorylation compared to IGF-II, whereas IGF chimeras containing IGF-I C-domains stimulated Akt/PKB phosphorylation to the same level as IGF-I. A time course experiment was performed in order to ascertain whether IGF-I activated PI3K/Akt pathway at other time points [Figure 3.6 C]. IGF-I could activate the PI3K/Akt pathway, however to a lesser extent than insulin. A significant increase in Akt phosphorylation over basal by IGF-I was only observed at 60 minutes.

3.1.7 Ligand stimulated phosphorylation of Erk-1/2 via the IR-A and IR-B

Activation of IRS-1 and Shc provides a link between the IR and the MAPK pathway[313]. MAPK signaling has been demonstrated to be involved in mediating inhibition of apoptosis and regulation of gene transcription[85], therefore the ability of ligand to stimulate Erk-1/2 phosphorylation via the IR-A and IR-B was investigated by Dr. Adam Denley.
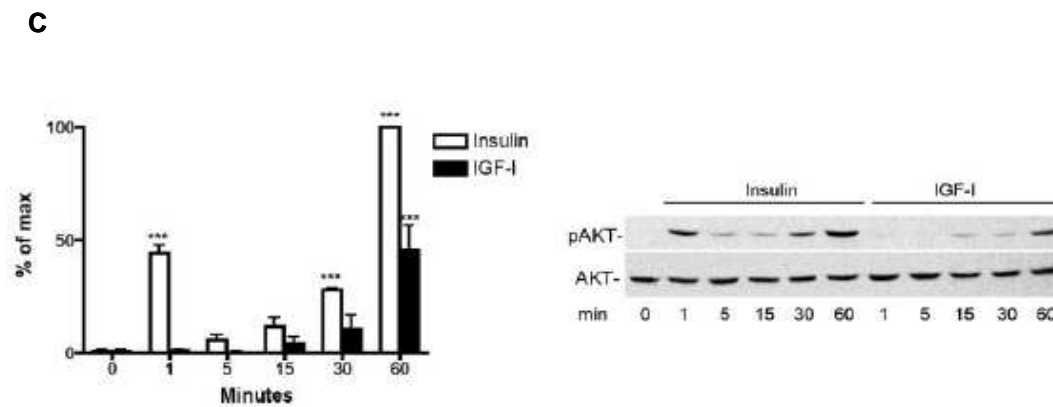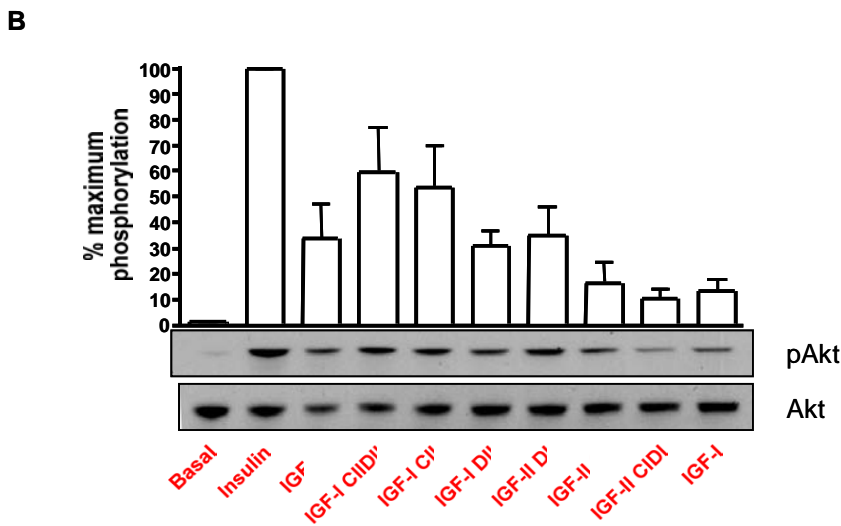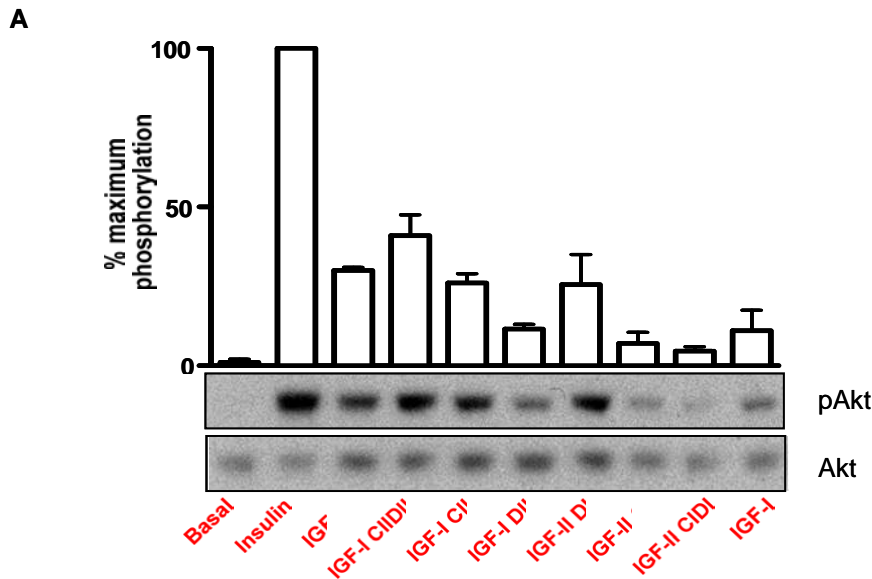
Figure 3.6 Akt/PKB phosphorylation in R⁻IRA and R⁻IRB cells stimulated with Insulin, IGF-II, IGF-I, or IGF chimeras.

*Serum-starved R⁻IRA or R⁻IRB cells were stimulated with 10nM ligand for 5 minutes. Whole-cell lysates were prepared and subjected to SDS-PAGE and then immunoblotted and assayed for phosphorylated Akt/PKB [Ser473] in R⁻IRA [**A**] and R⁻IRB [**B**] cells. In each panel, densitometry results of the three independent experiments ± SEM [phospho-Akt/total Akt] are shown. Upper blot, representative Western blot with anti-phospho-Akt/PKB [Ser473] antibody. Lower blot, re-blotting with anti-Akt/PKB antibody. Akt/PKB phosphorylation experiments conducted by Dr. Adam Denley. [**C**] Time course of Akt activation by 10nM IGF-I and insulin. Time course experiment performed by Julie M. Carroll.*
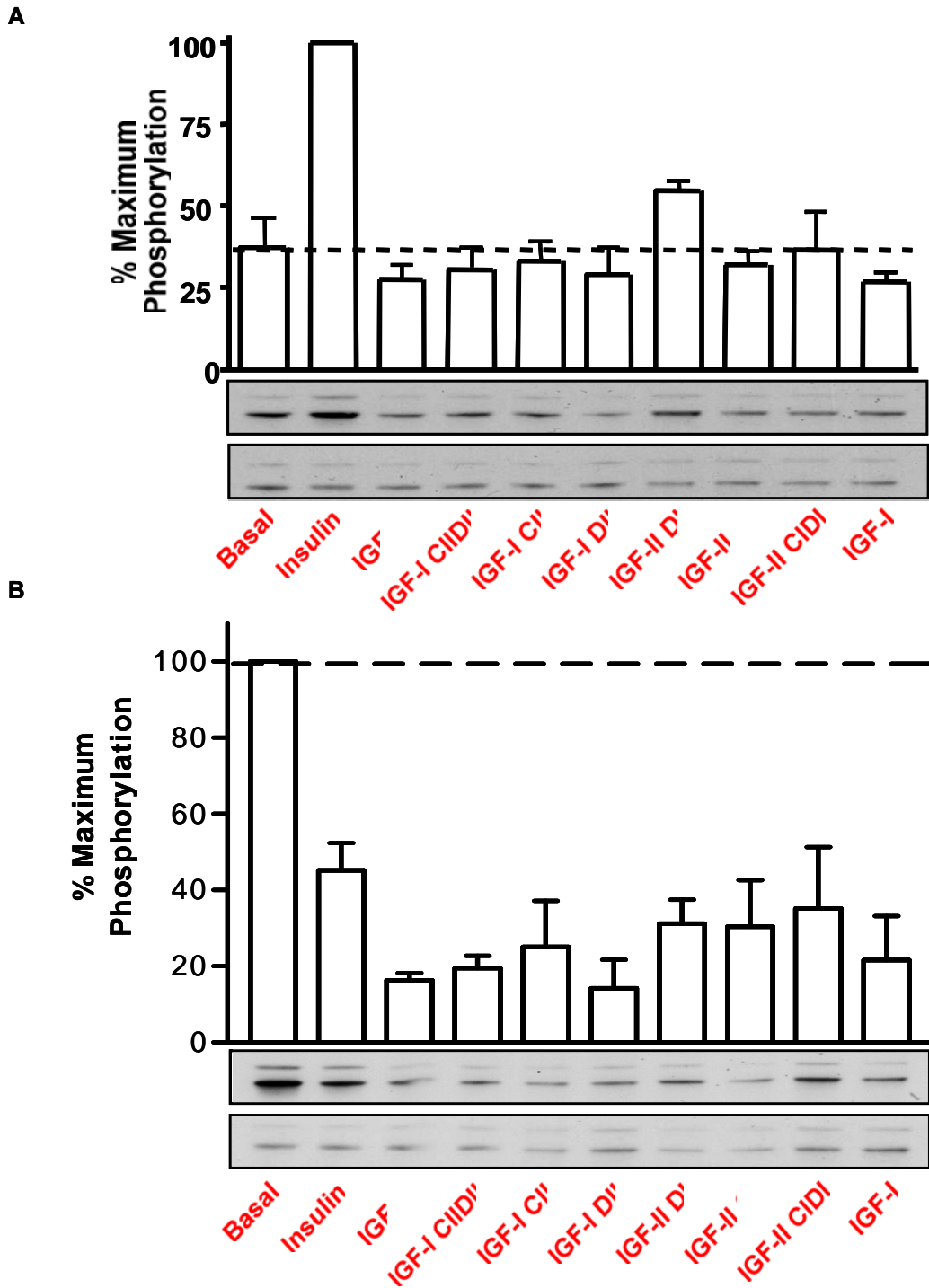
Figure 3.7 Insulin, IGF-II, IGF-I, and IGF chimera stimulated Erk-1/2 phosphorylation in R⁻IRA and R⁻IRB cells

*Serum-starved R⁻IRA [**A**] or R⁻IRB [**B**] cells were treated with 10nM ligand for 5 minutes. Whole-cell lysates were prepared and subjected to SDS-PAGE prior to being immunoblotted for phosphorylated Erk-1/2. In each panel normalized densitometry results of three independent experiments ± SEM are graphed. Upper blots demonstrate anti-phosphorylated Erk-1/2 antibody blots representative of results obtained from three independent experiments. Lower blots demonstrate re-blotting for total Erk-1/2 with an anti-Erk-1/2 antibody. Erk-1/2 phosphorylation experiments conducted by Dr. Adam Denley.*

In R⁻IRA cells, only insulin stimulated a significant increase in Erk-1/2 phosphorylation over basal levels [Figure 3.7 A]. Interestingly, in R⁻IRB cells all ligands failed to produce Erk-1/2 phosphorylation above that of basal [Figure 3.7 B]. Indeed, treatment of R⁻IRB cells with ligand resulted in decreased phosphorylation of Erk-1/2 below that of basal levels. Furthermore, IGF-I did not induce Erk-1/2 phosphorylation over a 60 minute time course, data not shown.

These studies thus established the ability of insulin, IGF-II, IGF-I, and IGF chimeras to stimulate phosphorylation of the IR and initiate major downstream signalling molecules. It was therefore important to assess whether these signals were translated into biological responses.

3.2   Results

3.2.1   Validation of R⁻IRA and R⁻IRB cells

The R⁻IRA and R⁻IRB cell lines provided an IGF1R null background in which the signaling and resultant biological response to ligand via the IR-A or IR-B could be investigated without interference from either IGF1R or IGF1R/IR hybrid receptors. However, to confirm the signaling and biological responses elicited by the R-IRA and R-IRB cells were due to the presence of the IR-A or IR-B the two cell lines were validated by RT-PCR and cell surface analysis of receptor expression [Figure 3.8]. Confirmation of IR isoform expression was performed by RT-PCR, and results demonstrated R⁻IRA cells only expressed the A isoform of the IR [Figure 3.8 A]. While the R⁻IRB cells only expressed the B isoform [Figure 3.8 B]. Absence of IGF1R expression was confirmed in both cell lines at both the transcript level and at the cell surface.

3.2.2   Ability of ligand to rescue R⁻IRA and R⁻IRB cells from butyrate-induced apoptosis

Both the PI3K and MAPK pathways have been implemented in mediating cell survival and inhibition of apoptosis[84, 85], therefore the ability of insulin, IGF-II, IGF-I, and IGF C-domain chimeras to stimulate R⁻IRA and R⁻IRB survival from butyrate induced apoptosis was investigated. Despite
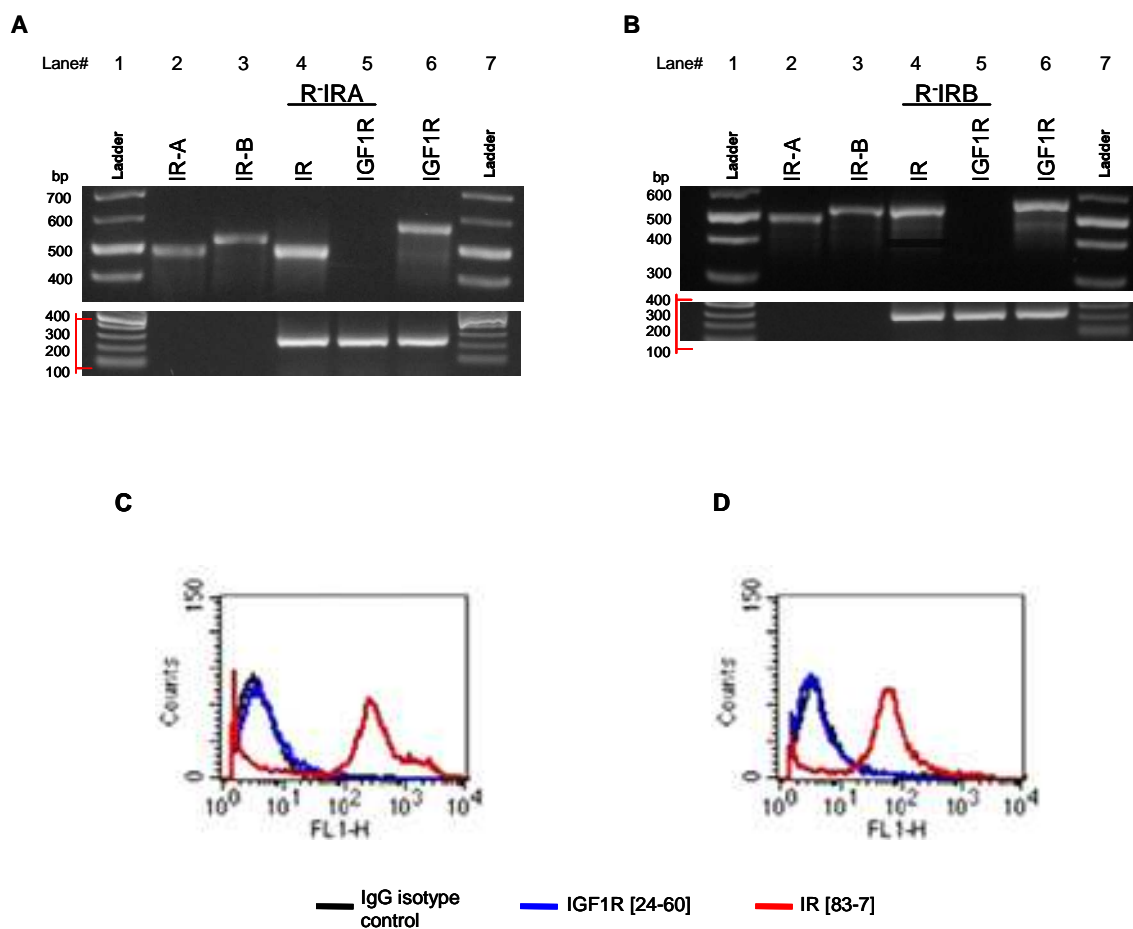
Figure 3.8 Characterisation of R⁻IRA and R⁻IRB receptor expression

*Confirmation of IR isoform expression in R⁻IRA [**A**, lane 4] and R⁻IRB [**B**, lane 4] cells by RT-PCR. PCR primers that flank exon 11 were used to distinguish between to the two IR isoforms. Amplification of the IR-A [exon 11-] would result in a 473bp product, while amplification of the IR-B [exon 11+] would result in a 509bp product. Absence of IGF1R expression was confirmed in both cell lines at the transcript level [lane 5, **A** and **B**]. Amplification of plasmids containing cDNA encoding either IR transcript along with β-actin [242bp] served as a positive control [lanes 2 and 3, **A** and **B**]. In addition, amplification of cDNA derived from R-IGF1R cells resulting in a 572bp product served as a positive control for IGF1R [lane 6, **A** and **B**]. Cell surface expression of IR receptors in R⁻IRA [**C**] and R⁻IRB [**D**] cells was confirmed by flow cytometry. Absence of hIGF1R expression in both R⁻IRA and R⁻IRB was confirmed at the cell surface by flow cytometry further authenticating the two cell lines.*

A
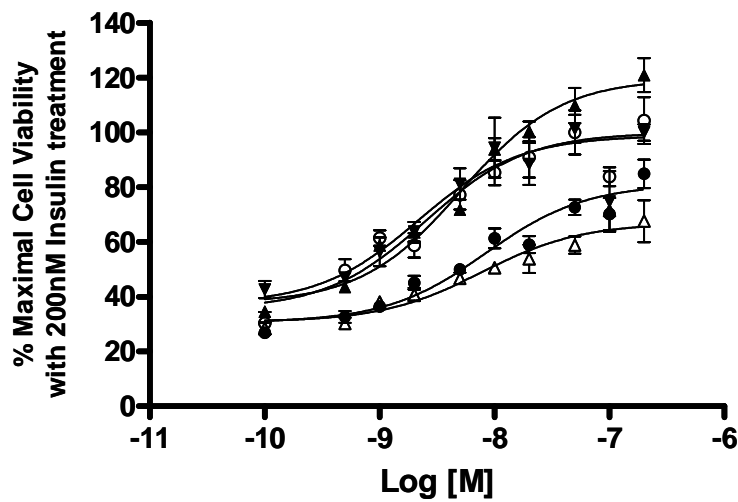
B
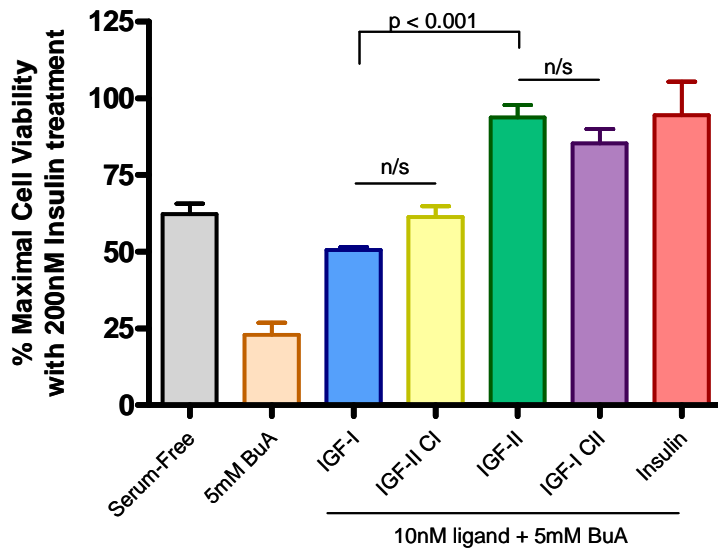
Figure 3.9 Effect of IGF-I, IGF-II, Insulin, and IGF C-domain chimeras on butyrate treated R⁻IRA cell viability

*[**A**], butyrate-treated [5mM] R⁻IRA cells were incubated in the presence or absence of increasing concentrations of insulin [▼], IGF-II, [▲], IGF-I [Δ], IGF-I CII [○], and IGF-II CI [●]. Results are expressed as a percentage of maximal cell viability compared with 200nM insulin treatment. Data points are the mean ± SEM of duplicate samples from three independent experiments conducted on separate occasions. Errors are shown when greater than the size of the symbols. [**B**], stimulation of R⁻IRA cell viability by 10nM ligand relative to serum-free media and 5mM butyrate [BuA] controls. All ligands vs. 5mM butyrate p < 0.001. IGF-I vs. IGF-II p < 0.001. Statistical significance determined by ANOVA with Bonferroni's multiple comparison test. n/s denotes not significant, p > 0.05.*

A

B
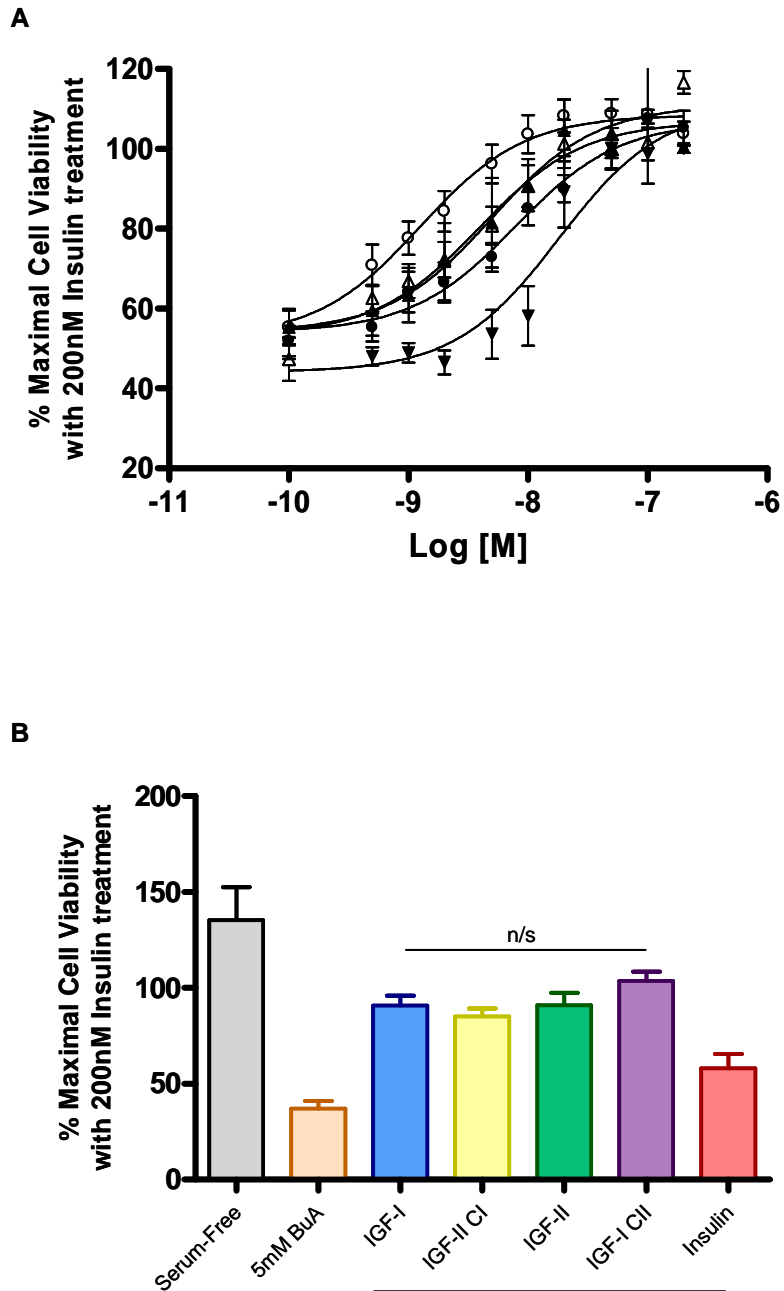
Figure 3.10 Effect of IGF-I, IGF-II, Insulin, and IGF C-domain chimeras on butyrate treated R⁻IRB cell viability

*[**A**], butyrate-treated [5mM] R⁻IRB cells were incubated in the presence or absence of increasing concentrations of insulin [▼], IGF-II, [▲], IGF-I [Δ], IGF-I CII [○], and IGF-II CI [●]. Results are expressed as a percentage of maximal cell viability compared with 200nM insulin treatment. Data points are the mean ± SEM of duplicate samples from three independent experiments conducted on separate occasions. Errors are shown when greater than the size of the symbols. [**B**], stimulation of R⁻IRB cell viability by 10nM ligand relative to serum-free media and 5mM butyrate [BuA] controls. All ligands, except Insulin, vs. 5mM butyrate p < 0.001. Insulin vs. 5mM butyrate p > 0.05. n/s denotes no statistical significance between the response elicited by the four indicated ligands. Statistical significance determined by ANOVA with Bonferroni's multiple comparison test.*

the decreased ability of IGF-II to stimulate downstream signaling via the IR-A compared to insulin, IGF-II was as effective as insulin at stimulating R-IRA cell survival [Figures 3.9 B and 3.11 A]. At supra-physiological levels, IGF-II stimulated R⁻IRA cell survival surpassed that stimulated by insulin [Figure 3.9 A]. As expected from receptor binding and signaling molecule activation experiments, IGF-II stimulated R⁻IRA cell survival to a significantly greater extent than IGF-I. IGF-II CI was as effective as IGF-I at stimulating R⁻IRA cell survival [IGF-I vs. IGF-II CI, $p > 0.5$]. Likewise, IGF-I CII was as effective as IGF-II at stimulating R⁻IRA cell survival [IGF-II vs. IGF-I CII, $p > 0.5$]. These results suggest that the C-domain of the IGFs not only account for the differential ability of IGF-I and IGF-II to recruit and activate downstream signaling molecules, but also accounts for their differential ability to promote cell survival via the IR-A. Interestingly, despite the poor ability of IGF-I to bind and activate the IR-A, physiological concentrations of IGF-I were able to stimulate significant R⁻IRA cell survival from butyrate induced apoptosis [Figure 3.11 A].

Despite the differential ability of IGF-I and IGF-II to bind and activate the IR-B both ligands stimulated equipotent survival of R⁻IRB cells [Figures 3.10 and 3.11 B]. Interestingly, both IGF-I and IGF-II were able to stimulate R⁻IRB cell survival to a greater extent than insulin. IGF-II CI was as effective as IGF-I at stimulating R⁻IRB cell survival. Likewise, IGF-I CII was as effective as IGF-II at stimulating R⁻IRB cell survival.

3.2.3 Insulin, IGF-II, IGF-I, and IGF C-domain chimera stimulated R⁻IRA chemotaxis

Migration of cancer cells to secondary sites in the body is another important biological event in the progression of cancer. Therefore, the ability of insulin, IGF-II, IGF-I, and IGF C-domain chimeras to stimulate R⁻IRA cell migration was assessed by Boyden chamber assay. Insulin stimulated the greatest amount of R⁻IRA chemotaxis, while IGF-II stimulated chemotaxis to a greater extent than IGF-I [Figure 3.12]. The data from IGF chimeras containing C-domain exchanges demonstrated the C domain accounted for the differential ability of IGF-I and IGF-II to stimulate R⁻IRA cell chemotaxis.
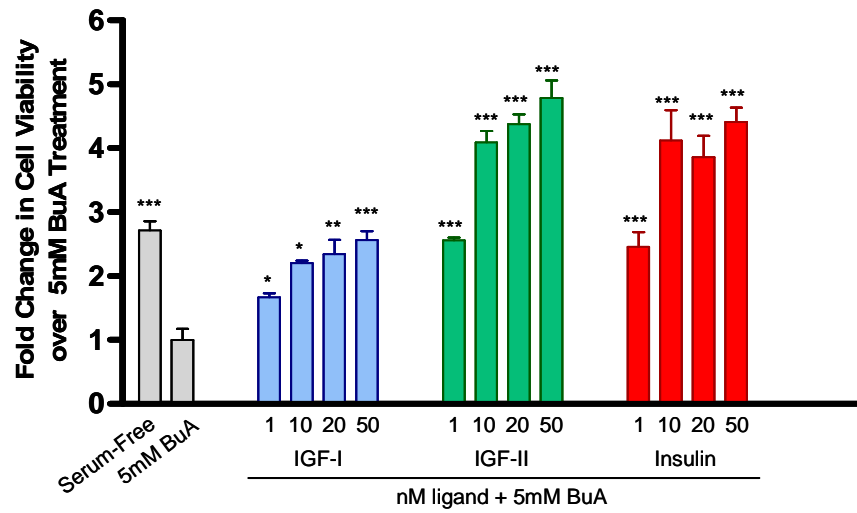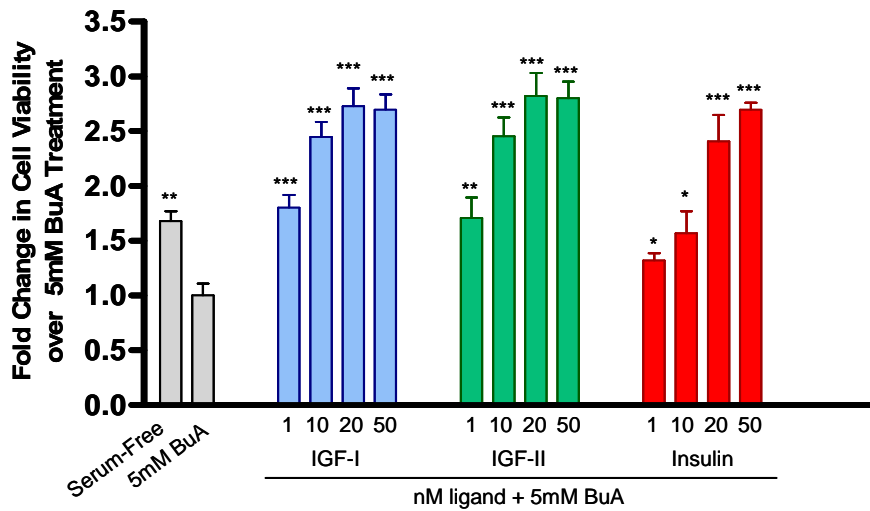
Figure 3.11 Comparison of the ability of IGF-I, IGF-II and insulin to rescue R⁻IRA [A] and R⁻IRB [B] cells from butyrate-induced apoptosis

Butyrate-treated [5mM] cells were incubated in the presence or absence of increasing concentrations of IGF-I, IGF-II, or insulin. Results are expressed as the fold change in cell viability over treatment with 5mM butyrate [BuA]. Data points are the mean ± SEM of duplicate samples from three independent experiments conducted on separate occasions. Statistically significant increase in cell viability above that of 5mM BuA treated cells was determined by ANOVA with Bonferroni's multiple comparisons test. * p < 0.5, **p < 0.01, ***p < 0.001.
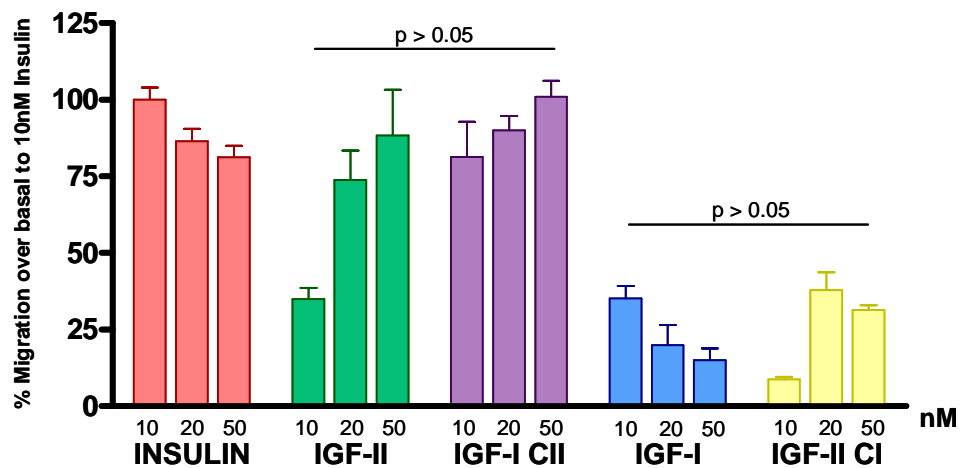
Figure 3.12 IGF-I, IGF-II, Insulin, and IGF C-domain chimera stimulated chemotaxis of R⁻IRA cells.

R⁻IRA cell chemotaxis in the presence of increasing concentrations of insulin, IGF-I, IGF-II, and IGF C-domain chimeras. Results are expressed as the percentage of maximal migration in response to 10nM insulin. The data points are mean ± SEM of triplicate samples from three independent experiments conducted on separate occasions. One-way ANOVA with Bonferroni's multiple comparison test was used to determine the overall statistical significance between the migratory responses elicited by the ligands. IGF-II vs. IGF-I CII $p > 0.05$. IGF-I vs. IGF-II CI $p > 0.05$. IGF-I CII vs. IGF-II CI $p < 0.01$. IGF-I vs. IGF-I CII $p < 0.01$.
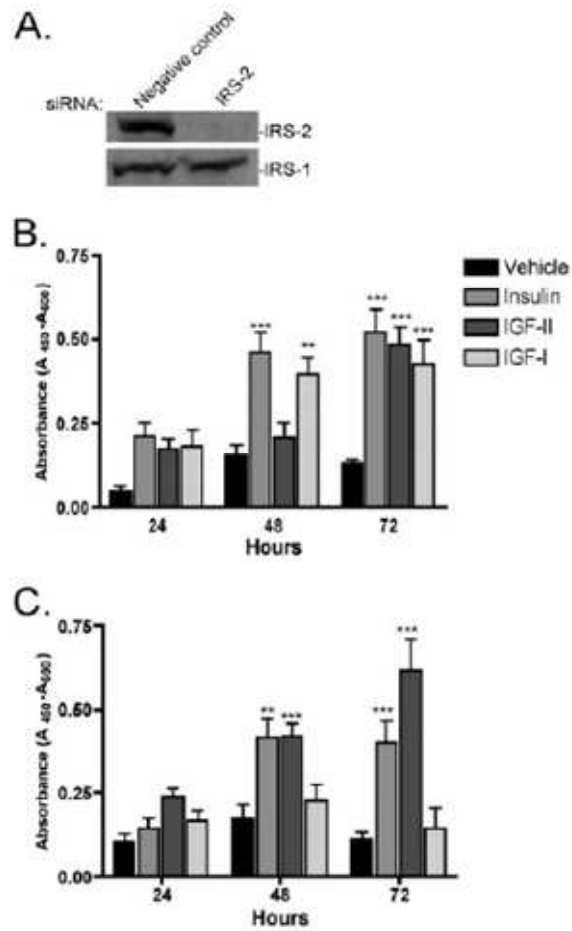
Figure 3.13 Proliferation/viability of R⁻IRB cells after IRS-2 knock-down with siRNA.

[**A**] Western immunoblot of IRS-2 and IRS-1 expression in R⁻IRB cells 48 hours after transfection with negative-control and IRS-2 siRNAs. Effect of 10nM Insulin, IGF-II, and IGF-I on R-IRB cell proliferation/viability as determined by WST assay after transfection with negative-control siRNA [**B**] or IRS-2 siRNA [**C**]. Error bars represent SEM of three independent experiments. Statistical significance is shown in relation to vehicle control at each time point. P values are represented as follows: ** $p < 0.01$; *** $p < 0.001$. IRS-2 knock-down experiments conducted by Julie M. Carroll.

3.2.4   The role of IRS-2 in IGF-I mediated effects through the IR

An siRNA mediated knock-down strategy was employed to ascertain the requirement for IRS-2 activation in the biological effects elicited by IGF-I by Julie M. Carroll. Transfection of R⁻IRB cells with an IRS-2 siRNA pool eliminated IRS-2 protein expression but had no effect on IRS-1 expression [Figure 3.13 A]. IRS-2 knock-down effectively inhibited IGF-I stimulated cell viability but had no effect on either insulin or IGF-II stimulated cell viability [Figure 3.13 C]. Transfection of R⁻IRB cells with negative-control siRNA did not affect IRS-1 or IRS-2 expression [Figure 3.13 A], nor ligand stimulated cell viability [Figure 3.13 B].

3.3   Discussion

Work presented in this chapter investigated signalling and biological outcomes in cells devoid of the IGF1R expressing either the IR-A or IR-B following activation by insulin, IGF-II, IGF-I, or IGF chimeras. Competition binding studies had previously revealed the C domain, and to a lesser extent, the D domain of the IGFs accounted for the differential abilities of the IGFs to bind the IR isoforms [Figure 3.2 and Table 3.1][13]. Analysis of tyrosine phosphorylation in the activation loop of the kinase domain [Figure 3.3 A and C], Y960 and Y972 in the IR-A and IR-B respectively [Figure 3.3 B and D], demonstrated the relative abilities of ligand to induce autophosphorylation was proportional to their relative receptor binding affinities [Table 3.1].

Activation of the kinase active site and subsequent phosphorylation of Y960 [IR-A] and Y972 [IR-B] provides a docking site for binding of adaptor molecules enabling their recruitment and activation. Docking and activation of such adaptor molecules is crucial for the recruitment and activation of downstream signalling molecules[83]. Phosphorylation of Y960/Y972 enables recruitment of IRS-1 and IRS-2, which when phosphorylated by the IR provides docking sites for SH2-domain containing proteins. Analysis of IRS-1 phosphorylation data revealed insulin strongly phosphorylated IRS-1 via both the IR-A and IR-B [Figure 3.4 A and B]. In R-IRA cells, IGF-II stimulated IRS-1 phosphorylation to a lesser extent than did insulin, but was substantially better than IGF-I. Data from IGF chimeras demonstrated the C domain mediated the differential ability of the IGFs to stimulate IRS-1 phosphorylation. In R-IRB cells, IGF-I and IGF-II stimulated similar levels of IRS-1

phosphorylation. Differences between the ligand sensitivity of IRS-1 activation in R⁻IRA and R⁻IRB cells were observed during the 60 minute time course. Activation of IRS-1 by ligand via the IR-A was rapid and sustained over the 60 minutes, while activation of IRS-1 via the IR-B was transient [Figure 3.5]. Moreover, the relative ability of IGF-II, compared to insulin, to induce IRS-1 phosphorylation via the IR-A was less than the relative ability of these ligands to activate the IR-A. Activation of IRS-1 by IGF-II via the IR-B was far greater than expected, considering the relative ability of insulin and IGF-II to bind and phosphorylate the IR-B. These results suggest that the 12 amino acids encoded by exon 11 may modulate both the time course of IRS-1 phosphorylation and the relationship between IGF-II binding affinity, IR activation and phosphorylation of IRS-1.

In contrast to IRS-1, IRS-2 can interact with the IR in two separate ways. Firstly, by the interaction of the SH2-domain of IRS-2 with tyrosine 960/972 on the IR[314], and secondly, by a non-SH2 mediated interaction between residues 591-786 of IRS-2 and the IR[309]. Despite the significantly lower affinity of IGF-I for the IR and lack of appreciable IGF-I stimulated phosphorylation of Y960/972 in either IR isoform, the level of IRS-2 phosphorylation stimulated by IGF-I was similar to that elicited by insulin and IGF-II. These results suggest that although binding of IGF-I to the IR may not stimulate high levels of Y960/972 phosphorylation, it may induce a conformational change that does recruit IRS-2 via the non-SH2 mediated interaction allowing it to be phosphorylated. Indeed, in a separate study where Y960 was mutated to alanine, ligand mediated phosphorylation of IRS-2 was not affected, suggesting this non-SH2 mediated interaction may be more critical for the interaction of IRS-2 with the IR[315]. Comparison of IRS-1 and IRS-2 phosphorylation revealed differential abilities of ligands to active these two adaptor molecules. Insulin and IGF-II activated both IRS-1 and IRS-2 while IGF-I activation was more prominent for IRS-2. The observation that IGF-II and Insulin activation of IRS-1 and IRS-2 did not reflect their relative abilities to bind and phosphorylate either IR isoform further suggests that the non-SH2 mechanism of IRS-2 recruitment to the IR may mediate these effects. Indeed, given the relative binding affinity and receptor activation of IGF-II for the IR isoforms compared to that of insulin, IGF-II activation of IRS-2 was far greater than expected.

Phosphorylation of IRS-1 and IRS-2 provides docking sites for a number of SH2-domain containing proteins, and through recruitment and activation of a number of intermediate signalling molecules, link the IR to the PI3K and MAPK pathways. Akt/PKB are the major effector proteins of the PI3K

pathway. Akt was found to be strongly phosphorylated by insulin, IGF-II, and IGF-II C domain containing chimeras acting through both IR isoforms [Figure 3.6]. Compared to IGF-II and insulin, IGF-I did not appreciably induce phosphorylation of Akt after 5 minute stimulation [Figure 3.6 A and B]. Interestingly, when Erk-1/2 activation was assessed, insulin was the only ligand able to stimulate phosphorylation of Erk-1/2 above basal, and this was observed in R-IRA but not R-IRB cells [Figure 3.7]. This was interesting since both insulin and IGF-II can induce IR, IRS-1, and IRS-2 phosphorylation in both cell lines. Studies by other groups have demonstrated IGF-II, but not IGF-I, phosphorylation of Erk above basal acting thorough the IR-A[7, 148]. However, in those studies the IR-A was overexpressed in cells to a vastly greater extent [500,000 receptors/cell] than the cells used in the present study [75,000 receptors/cell], and could possibly explain the differential results observed between the two studies.

Together the results obtained from ligand binding, receptor activation, and phosphorylation of downstream signalling molecules provide insights into the distinction between ligand binding and receptor signalling. Binding studies revealed that exchange of both the IGF C and D domains was required for total conversion of the IGFs binding specificity for the IR-A and IR-B. However, analysis of events downstream of receptor binding indicated that substitution of the C domain alone was sufficient to allow the IGF chimera to activate the IR, IRS-1, IRS-2, and Akt/PKB to the same extent as its wild-type counterpart. Therefore a discrepancy between the requirements for ligand binding and receptor activation was observed. One possible explanation for this may be the conformational change in the IR induced by the C domain. Although the IGF C domain alone may not completely account for the difference in free energy in binding of the IR by the IGFs, it may induce a conformational change in the IR that is sufficient to elicit receptor activation to the same extent as wild-type IGF.

To ascertain whether the signals elicited by receptor activation were translated into biological outcomes, the ability of IGFs to influence biological processes important to cancer progression, namely cellular proliferation, migration, and survival from apoptosis was assessed. All ligands were observed to stimulate migration of R⁻IRA cells above that of the basal rate. Insulin stimulated the greatest rate of migration, followed by IGF-II then IGF-I [Figure 3.12]. The observation that insulin can stimulate chemotaxis via the IR-A is particularly relevant as previous studies have suggested that insulin-stimulated cell migration is due to activation of the IGF1R[148]. Similar to the results

observed in cell survival, exchange of the IGF C domains accounted for the differential ability of the IGFs to induce R⁻IRA cell chemotaxis.

Butyrate is a potent pro-apoptotic compound, and results presented here demonstrate for the first time that IGF signalling via both isoforms of the IR can protect cells from butyrate-induced apoptosis [Figures 3.9 - 3.11]. The ability of butyrate to induce apoptosis is thought to reflect its ability to inhibit histone deacetylase activity, however this mechanism is yet to be fully delineated[316]. It is particularly notable that IGFs signalling via the IR-B were also able to protect cells from butyrate-induced apoptosis, as the IR-B is generally considered to be specific for insulin action. In R⁻IRB cells, IGF-II and IGF-I were not only equipotent at inhibiting butyrate-induced apoptosis, but at lower concentrations were more effective than insulin [Figure 3.10 and 3.11 B]. However, in R⁻IRA cells, IGF-II was able to inhibit butyrate-induced apoptosis to a significantly greater extent than IGF-I [Figure 3.9 and 3.11 A]. Exchange of the IGF C domains accounted for the differential ability of the IGFs to inhibit butyrate-induced apoptosis via the IR-A. A previous study in LIM 2405 human colon cancer cells demonstrated that IGF-II rendered these cells resistant to butyrate-induced apoptosis, but failed to examine IGF1R and IR receptor expression[233]. Another study in SKUT-1 cells, which do not express the IGF1R and express >95% IR-A, demonstrated that IGF-II protected them from staurosporine-induced apoptosis[127]. Staurosporine is a protein kinase inhibitor and induces apoptosis by both caspase-dependent and independent mechanisms[317]. Therefore the SKUT-1 study, together with the results presented here, suggest that IGF-II signalling via the IR-A can protect cells from apoptotic agents with differential modes of action. Results presented here indicated that IGF-II was as effective as insulin at protecting R⁻IRA cells from butyrate-induced apoptosis and even surpassed insulin at supra-physiological concentrations [Figure 3.9 A]. Similar results were observed in the SKUT-1 study, where both IGF-II and insulin were equipotent at protecting these cells from staurosporine-induced apoptosis[127]. This was interesting considering IGF-II has a lower affinity for the IR-A compared to insulin and was significantly poorer than insulin at inducing phosphorylation of IRS-1 and Akt/PKB. However, although insulin was more potent than IGF-II at inducing IRS-1 activation, IGF-II was more potent than insulin at inducing IRS-2 activation, suggesting that activation of IRS-2 may play a role in potentiating these responses. These results therefore emphasize the significance of delineating the signalling pathways elicited by IGF-II and insulin activation of the IR-A.

Perhaps of most interest, despite the low affinity of IGF-I for the IR, was the observation that physiological concentrations of IGF-I was capable of stimulating biological responses via both IR isoforms. Validation of the R⁻IRA and R⁻IRB cell lines utilised in the study confirmed their integrity [Figure 3.8], indicating these results were due to the presence of the IR and not contaminating IGF1R. IGF-I acted via both IR isoforms to significantly activate IRS-2 [Figure 3.4 and 3.5] suggesting that the biological responses elicited by IGF-I were mediated by IRS-2. IGF-I induced similar levels of IRS-2 phosphorylation as did both IGF-II and insulin, but did not significantly activate IRS-1. Interestingly, other groups have demonstrated IRS-2 activation to be important for cell migration[318] and cell survival[319-321]. Further support for this conclusion was provided by the effect of IRS-2 silencing in R⁻IRB cells [Figure 3.13]. siRNA mediated knock-down of IRS-2 inhibited the ability of IGF-I to stimulate R⁻IRB cell viability [Figure 3.13 C], thereby demonstrating the requirement of IRS-2 activation for the biological effects of IGF-I through the IR-B in R⁻IRB cells. The effect of IGF-I on biological outcomes was observed in the absence of Erk-1/2 activation, but was associated with a modestly delayed activation of the Akt/PKB pathway [Figure 3.6 C]. This suggests that the delayed activation of the Akt/PKB pathway may underlie these observations. However, it is conceivable that other signalling cascades are recruited by IRS-2 downstream of the IGF-I activated IR that could mediate these effects. The ability of IGF-I to activate the IR may explain results obtained by other studies where IGF-I was observed to mimic insulin action and to increase insulin sensitivity[322, 323].

The ability of the IR to mediate cellular migration and survival from apoptosis in response to insulin, IGF-II, and IGF-I stimulation may have important ramifications on the use of IGF1R inhibitors as a potential anti-cancer therapy. The IR-A is overexpressed in a wide range of tumours[7, 123, 125-127] suggesting that targeting of the IGF1R alone in tumour cells also expressing the IR-A potentially provides a mechanism by which IGFs secreted by the tumour can still mediate cell survival and migration in the presence of IGF1R inhibitors. To date, the majority of research conducted on the IR-A has been performed in cells devoid of the IGF1R[7, 127, 135, 136] or in cells where the IR-A is expressed in vast excess of the IGF1R[123]. Therefore it is not known whether the IR-A can provide an avenue by which cells can remain viable in the presence of IGF1R inhibitors. Work outlined in the remainder of this thesis aims to address this.

3.4   Conclusions

In this chapter the ability of insulin, IGF-II, IGF-I, and IGF chimeras to activate and signal biological outcomes via the IR-A or IR-B was investigated in cells devoid of the IGF1R. Results revealed that exchange of the IGF C domain alone accounted for the differential ability of the IGF-I and IGF-II to activate and signal biological responses, namely cell survival and migration, via the two IR isoforms. Insulin was observed to stimulate chemotaxis directly via the IR-A, a particularly relevant observation as previous studies have suggested that insulin-stimulated cell migration was due to spill-over and activation of the IGF1R. Moreover, for the first time it was demonstrated that IGFs and insulin signalling via the two IR isoforms could protect cells from butyrate-induced apoptosis. These results also identified that IGF-I, at physiological concentrations, could stimulate biological outcomes via the IR-A and IR-B. Subsequent analysis of IRS activation identified that IGF-I can act through both IR isoforms to preferentially activate IRS-2 resulting in biologically relevant outcomes, thereby identifying a third novel pathway by which IGF activation can occur through the IR.

Chapter 4

Identification and characterisation of a cell line model for the investigation of the biological role of the IR-A in cells co-expressing the IGF1R

4.1   Introduction

The actions of IGF-I and IGF-II relevant to cancer biology, namely cellular proliferation, differentiation, migration, and protection from apoptosis occur via their ability to bind and activate the IGF receptors. Chapter 3 identified a novel pathway by which IGF-I can act through both IR isoforms to preferentially activate IRS-2 resulting in downstream biological effects. In addition to this, two other molecular mechanisms exist that enable IGF cross-talk with the IR, namely alternative splicing of the IR and IGF1R/IR hybrid receptors. Alternative splicing of the IR transcript generates two IR isoforms that differ in their functional properties, as discussed in both Chapters 1 and 3. The IR, along with the IGF1R[61-65], is overexpressed in a wide range of malignancies[117, 118], with the IR-A expressed in preference to the IR-B[7, 123, 125-127]. Activation of the IR-A by IGF-II has been demonstrated to protect cells from apoptosis[12, 127,Chapter 3], confer resistance to the EGFR inhibitor gefitnib[324], and result in proliferative[135, 324] and migratory outcomes[12, 127,Chapter3]. Together these results suggest the IR-A may play an important role in the potentiation and progression of cancer.

As indicated in the Introduction [Chapter 1] and Chapter 3, the majority of studies examining the biological role of the IR-A have been conducted in cells either devoid of the IGF1R[12, 127, 135, 136, 305], where the IGF1R expression was not reported, or in cells where the IR-A is expressed in vast excess to the IGF1R[125]. Therefore it is not known how the IR-A interacts, and functions in conjunction with the other receptors of the IGF system to signal biologically relevant outcomes. It is possible that in cells co-expressing the IR-A and IGF1R, the IR-A could provide an avenue by which cells could remain viable in the presence of IGF1R inhibitors. Such a finding would have important implications for the vast array of novel anti-cancer therapeutics designed to specifically target the IGF1R. In light of this, work presented in this chapter aimed to identify a colorectal cancer cell line that could be used to investigate how the IR-A functions in conjunction with the

IGF1R to signal biologically relevant outcomes. An appropriate cell line model would express relatively equal levels of the IR-A and IGF1R and preferably be suitable for use in multiple biological endpoint assays. Experiments outlined in this chapter identified SW480 colorectal adenocarcinoma cells to be an adequate cell line model. SW480 cells were identified to express similar levels of IR-A and IGF1R at the cell surface. SW480 cells did not express the IR-B. Moreover, these cells were found to be suitable for range of biological endpoint assays representative of cellular processes relevant to colorectal cancer pathology, namely cellular migration, cell viability, and survival from butyrate-induced apoptosis.

4.2 Results

4.2.1 Characterisation of colorectal adenocarcinoma cell IGF1R and IR gene expression by RT-PCR

Reverse-transcriptase polymerase chain reaction [RT-PCR] experiments were conducted in order to assess the expression of both the IGF1R and IR at the transcript level in a panel of four common colorectal adenocarcinoma cell lines. Total cellular RNA was extracted from cultured colorectal cancer cell monolayers and contaminating genomic DNA removed by digestion with RNAse-free DNase I. All primers used in the PCR experiments spanned at least one intron/exon junction and would thus not amplify genomic DNA should any remain after digestion. RNA integrity was confirmed by PCR amplification of β-actin from cDNA reverse-transcribed from each RNA sample. Successful use of the DNase I-treated RNA as a template in RT-PCR was indicated by a 242bp β-actin product [Figure 4.1 C].

PCR primers homologous to sequences within the IGF1R were employed to specifically amplify IGF1R transcripts. cDNA derived from R⁻IGF1R cells was employed as a positive control and gave rise to a single product of expected size, 572bp. Amplification of cDNA derived from the four colorectal adenocarcinoma cell lines generated a single product of approximately 572bp in size, similar to that of the positive control, indicating that all four cell lines were positive for IGF1R transcript expression [Figure 4.1 C]. Given that the two IR isoforms are generated by the alternate splicing of the 36 nucleotide exon 11, specific primers flanking exon 11 were employed in the PCR
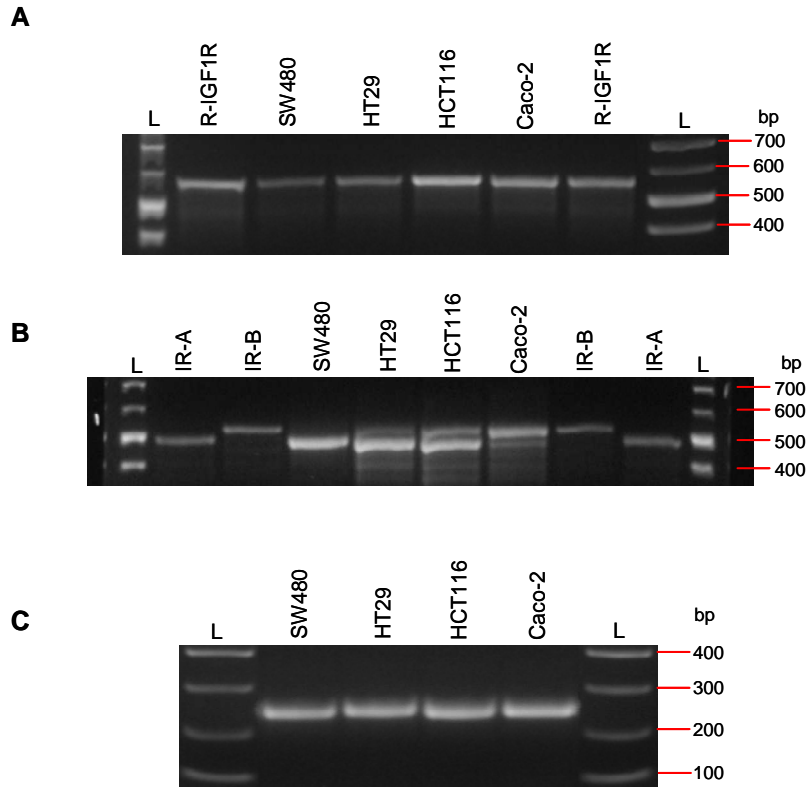
Figure 4.1 Expression of IGF1R, IR-A, and IR-B mRNA transcripts in colorectal adenocarcinoma cell lines

Identification of IGF1R [A] and IR isoform [B] expression by RT-PCR. Amplification of IGF1R transcripts result in a 572bp product, and amplification of cDNA derived from R⁻IGF1R cells served as a positive control for IGF1R. PCR primers that flank exon 11 were used to distinguish between the two IR isoforms. Amplification of the IR-A [exon 11-] would result in a 473bp product, while amplification of the IR-B [exon 11+] would result in a 509bp product. Amplification of plasmids containing cDNA encoding either IR transcript served as positive controls. [C] Amplification of β-actin [242bp] served as a control for the integrity of the RNA used to generate the cDNA used in the PCR reactions. PCR products were separated by electrophoresis on 1.5 and 2% agarose gels and visualized using GelGreen staining.

analysis of IR gene expression. The forward primer was homologous to a sequence within exon 10 and the reverse primer was homologous to a sequence within exon 12 of the IR, such that PCR amplification across the exons would generate a smaller product if splicing of exon 11 had occurred. PCR products amplified from transcripts of the IR-A were therefore expected to be 36bp shorter [473bp] than those generated from transcripts of the IR-B [509bp]. In addition, the plasmids used to transfect the R⁻IRA and R⁻IRB cells containing either the human IR-A or IR-B cDNA sequence were amplified as positive controls. All four colorectal cancer cell lines analysed were positive for IR transcript expression with the IR-A being the overall predominant isoform expressed in all cell lines, except Caco-2 cells where the IR-B was more abundant [Figure 4.1 B]. HT29, HCT116, and Caco-2 cells were observed to express both IR isoforms. In HT29 and HCT116 cells the IR-A was the most predominant transcript. In contrast to this, the IR-B transcript was more abundant in Caco-2 cells than the IR-A transcript. SW480 cells were observed to only express the IR-A.

4.2.2 Identification of IGF1R, IR, and IGF1R/IR hybrid receptor protein expression in colorectal adenocarcinoma cells

Transcript expression does not necessarily equate to protein expression. Therefore IGF1R and IR protein expression was assessed by Western blot. Whole cell lysates [25µg] from all four colorectal adenocarcinoma cell lines were resolved by SDS-PAGE prior to Western transfer and immunodetection by anti-IGFIR$_β$ and anti-IR$_β$ antibodies [Figure 4.2]. All four colorectal adenocarcinoma cell lines expressed both the IGF1R and IR at the protein level, which correlated with RT-PCR results.

Hybrid receptor expression was also analysed [Figure 4.2]. Hybrid receptors form via the random dimerisation of one αβ monomer of the IGF1R and one αβ monomer of the IR and are therefore expressed in cells that co-express the IGF1R and IR [136-139-intro]. Pre-cleared whole cell lysates [1mg protein] from each of the four colorectal adenocarcinoma cell lines were immunoprecipitated with either anti-IGF1R$_α$ or anti-IR$_α$ antibodies overnight prior to SDS-PAGE. Hybrid receptors were detected by immunoblotting [IB] with an antibody directed towards the β-subunit of the reciprocal receptor targeted in the immunoprecipitation [IP]. Hybrid receptor expression was detected in all four colorectal adenocarcinoma cell lines.
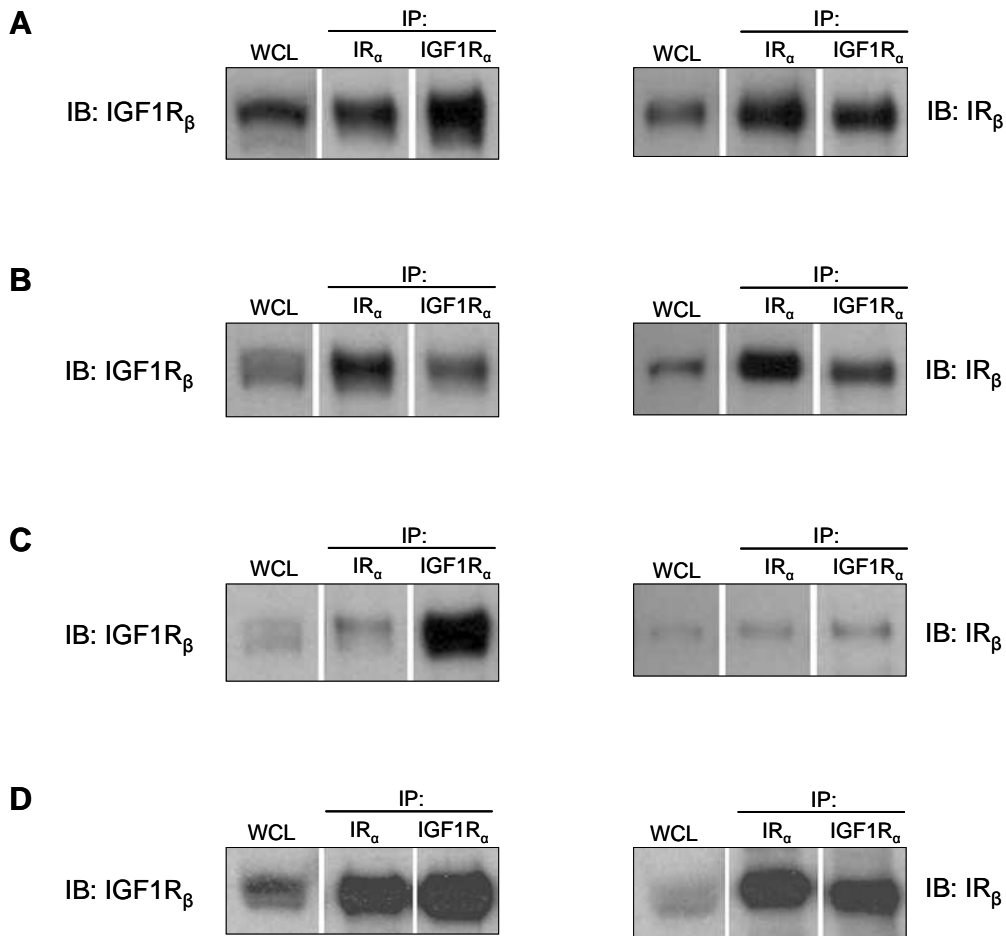
Figure 4.2 Colorectal adenocarcinoma cell expression of IGF1R, IR, and IGF1R/IR hybrid receptors

Colorectal adenocarcinoma cell monolayers were lysed and 1mg whole cell lysate [WCL] immunoprecipitated [IP] overnight with antibodies directed towards either the IGF1Rα [24-60] or IRα [83-14]. WCL and immunoprecipitates were subjected to SDS-PAGE prior to transfer to nitrocellulose membranes. Immunoblotting [IB] occurred using antibodies directed against either the IGF1Rβ or IRβ as indicated. [A] Caco-2; [B] HCT116; [C] HT29; [D] SW480.

4.2.3   Colorectal adenocarcinoma cell surface expression of IGF1R and IR

It was important to confirm receptor expression at the cell surface, to complement the results of the Western blot experiments. Indirect-immunofluroescence flow cytometry was employed to observe the cell surface expression profiles of IGF1R and IR in the four colorectal adenocarcinoma cell lines. Total cell surface IR expression was examined due to the lack of an antibody that can discriminate between the two IR isoforms. A monoclonal IgG1 negative control antibody was used to assess any non-specific binding of antibody by surface Fc receptors and cellular auto-fluorescence.

The relative cell surface expression of IGF1R and IR receptors on colorectal adenocarcinoma cells are displayed in Figure 4.3. Broad, single, peaks were recorded for Caco-2 cells [Figure 4.3 A] labeled with either anti-IGF1R$_\alpha$ [24-60] or anti-IR$_\alpha$ [83-7] antibodies, suggesting a single population of cells expressing various levels of IGF1R and IR expression. Whereas single sharp peaks were recorded for HT29, HCT116, and SW480 cells [Figure 4.3 B, C, and D respectively] labeled with antibodies targeting either receptor, suggesting single populations of cells expressing a similar level of either IGF1R or IR expression. Caco-2 and SW480 cells expressed similar levels of IGF1R and IR at the cell surface [assuming similar avidity of each of the antibodies for their respective targets], with IGF1R in slight excess of the IR [Figure 4.3 A and D, respectively]. HT29 cells were observed to express significantly less IR than IGF1R at the cell surface [Figure 4.3 B]. In contrast, HCT116 cells expressed the IR in significant excess to the IGF1R [Figure 4.3 C]. Overall, results complemented those obtained by Western blotting, and confirmed expression of both the IGF1R and IR at the surface of all four colorectal adenocarcinoma cell lines.

4.2.4   Effect of IGF-I, IGF-II, and insulin on butyrate-treated colorectal adenocarcinoma cell viability

In Chapter 3 it was demonstrated that IGF-I, IGF-II, and insulin stimulation could rescue R⁻IRA and R⁻IRB cells from the effects of butyrate[12, 305]. Similar results were observed in R⁻IGF1R cells [data not shown], suggesting that ligand stimulation mediated via both the IR and IGF1R can rescue cells from the effects of butyrate. Indeed, previous studies have demonstrated IGF-II to rescue LIM2405
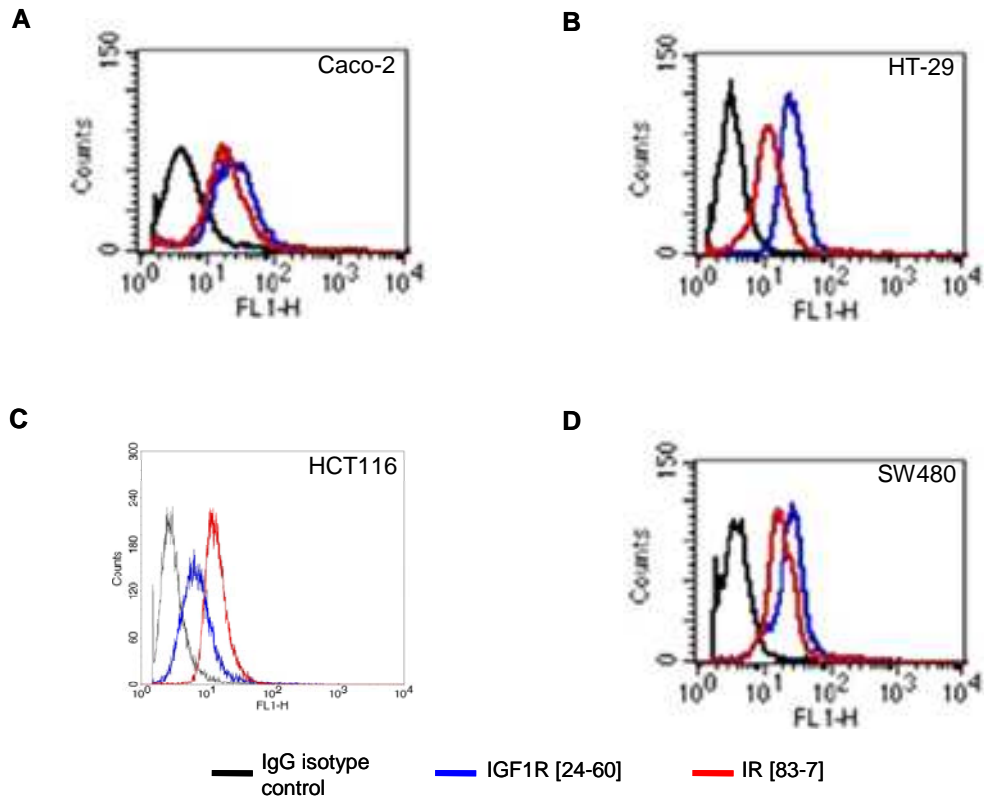
Figure 4.3 Colorectal adenocarcinoma cell surface expression of IGF1R and IR

Cell surface expression of IGF1R and IR was analysed by indirect-immunofluorescence flow cytometry utilising specific antibodies 24-60 [blue] and 83-7 [red] directed against the IGF1Rα and IRα, respectively as described in the Methods [Chapter 2]. A monoclonal IgG1 isotype control antibody that does not have specificity with any human cell surface components was used as a negative control [black]. [A] Caco-2; [B] HT29; [C] HCT116; [D] SW480.

cells from butyrate-induced apoptosis, but IR and IGF1R receptor expression was not examined[233]. Together these results suggest cells expressing the IGF1R and IR may possess a mechanism of resistance to the effects of butyrate. Such mechanisms of resistance could provide a possible explanation for the butyrate paradox observed *in vivo*. Therefore, the ability of IGF-I, IGF-II, and insulin to rescue the four colorectal adenocarcinoma cell lines from the effects of butyrate was assessed.

Each of the four colorectal adenocarcinoma cell lines tested responded differently to butyrate treatment [Figures 4.4 and 4.5]. HT29 and SW480 cells [Figure 4.5 A and B, respectively] were more sensitive to 5mM butyrate treatment than Caco-2 or HCT116 cells [Figure 4.4 A and B, respectively]. Butyrate treatment [5mM] caused a 6 fold decrease in HT29 and SW480 cell viability, but only a 2 fold decrease in Caco-2 and HCT116 cell viability. In addition, each of the cell lines responded differently to ligand stimulation, which may be indicative of a different cell surface receptor profile for each cell line [Figure 4.3]. Caco-2 cells responded to ligand stimulation in a different way to the other cell lines tested. None of the three ligands stimulated an increase in Caco-2 cell viability in a dose-dependent manner [Figure 4.4 A]. All concentrations of IGF-II stimulated statistically significant increases in Caco-2 cell viability, with 10nM IGF-II inducing the greatest increase in cell viability. Treatment with 0.5 and 100nM IGF-I, and 5, 10, and 100nM insulin also stimulated statistically significant increases in Caco-2 cell viability.

HCT116 cells responded to all ligands in a dose-dependent manner. Each concentration of ligand tested [0.5 – 200nM] stimulated a significant increase in HCT116 cell viability [Figure 4.4 B]. HCT116 cells, out of the cell lines tested, demonstrated the maximal response to insulin at the lowest concentration tested [0.5nM]. This cell line expressed the greatest level of IR expression at the cell surface. Maximal HT29 response to IGF-I was reached with the lowest concentration tested, 0.5nM [Figure 4.5 A]. HT29 cells reached maximal response to IGF-II at 2nM and then plateaued. HT29 response to insulin followed a strong dose-dependent response, and at supra-physiological levels could stimulate a similar response as IGF-I and IGF-II. SW480 cells displayed a dose-dependent response to all three ligands [Figure 4.5 B]. IGF-I stimulated the greatest response, followed by IGF-II, then insulin.
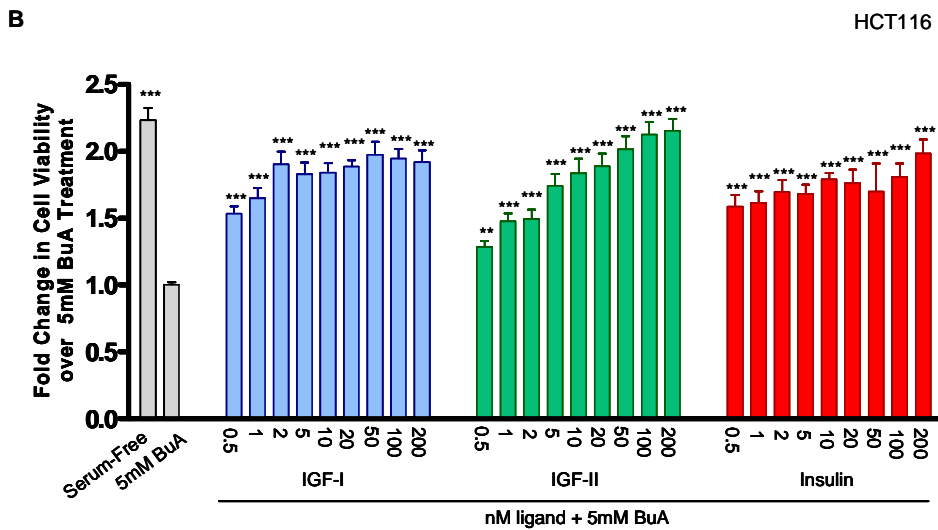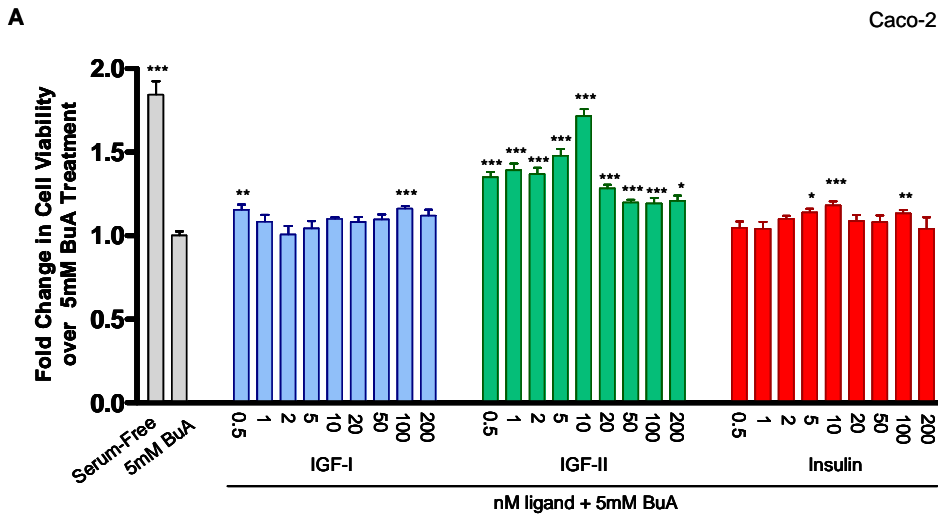
Figure 4.4 Effect of IGF-I, IGF-II, and Insulin on butyrate-treated colorectal adenocarcinoma cell viability.

Butyrate-treated [5mM] Caco-2 [**A**] and HCT116 [**B**] cells were incubated in the presence or absence of increasing concentrations of IGF-I [ ], IGF-II [ ], or Insulin [ ]. Results are expressed as fold change in viability over 5mM butyrate [BuA] treatment. Data points are the mean ± SEM of triplicate samples from three independent experiments conducted on separate occasions. Statistically significant increase in cell viability above that of 5mM BuA treated cells was determined by ANOVA with Bonferroni's multiple comparisons test. * $p < 0.05$, **$p < 0.01$, ***$p < 0.001$.

A HT-29
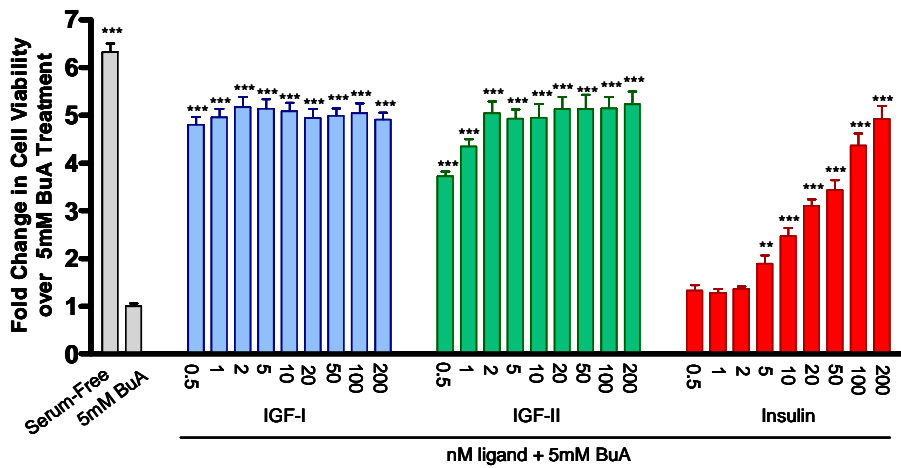
B SW480
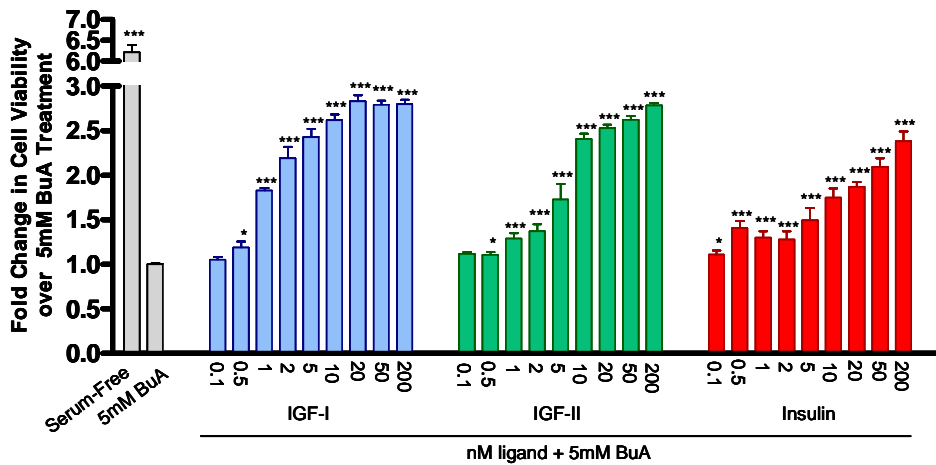
Figure 4.5 Effect of IGF-I, IGF-II, and Insulin on butyrate-treated colorectal adenocarcinoma cell viability.

Butyrate-treated [5mM] HT29 [**A**] and SW480 [**B**] cells were incubated in the presence or absence of increasing concentrations of IGF-I [   ], IGF-II [   ], or Insulin [   ]. Results are expressed as fold change in viability over 5mM butyrate [BuA] treatment. Data points are the mean ± SEM of triplicate samples from three independent experiments conducted on separate occasions. Statistically significant increase in cell viability above that of 5mM BuA treated cells was determined by ANOVA with Bonferroni's multiple comparisons test. * $p < 0.05$, **$p < 0.01$, ***$p < 0.001$.

4.2.5 Butyrate induces apoptosis in SW480 cells with concomitant decrease in cell viability

Butyrate treatment *in vitro* induces multiple effects on colorectal cancer cells. These include inhibition of proliferation and induction of differentiation and apoptosis[174-176]. To give an indication if the decrease in SW480 cell viability observed with butyrate treatment occurred in conjunction with an increase in caspase-dependent apoptosis, the CellTiter-Blue[TM] indicator of cell viability assay was multiplexed with the ApoOne[TM] apoptosis assay [Figure 4.6]. Treatment of SW480 cells with 5mM butyrate stimulated a 6 fold increase in caspase-3/7 activity [10% FCS vs. 5mM BuA; $p < 0.001$] [Figure 4.6 A]. Treatment with 5mM butyrate in the presence of 10% FCS induced a smaller 2.5 fold increase [10% FCS vs. 5mM BuA + 10% FCS; $p < 0.001$]. The increase in caspase-mediated apoptosis with butyrate treatment was observed with concomitant decrease in cell viability. Treatment with 5mM butyrate stimulated a 90% decrease in SW480 cell viability [10% FCS vs. 5mM BuA; $p < 0.001$], while treatment with butyrate in the presence of 10% FCS stimulated an 80% decrease in SW480 cell viability [10% FCS vs. 5mM BuA + 10% FCS; $p < 0.001$] [Figure 4.6 B]. Treatment of SW480 cells with 5mM butyrate in the presence of 10% FCS did not significantly alter SW480 cell viability compared to cells treated with butyrate alone [5mM BuA vs. 5mM BuA + 10% FCS; $p > 0.05$]. These results suggest growth factors present in the FCS provided some protection against butyrate-induced apoptosis but did not statistically improve SW480 cell viability upon butyrate treatment.

4.2.6 IGF-I, IGF-II, and insulin stimulates SW480 cell chemotaxis

Both, IGF-I and IGF-II have been implicated in the metastasis of colorectal cells to the liver, the most frequent site of secondary metastasis in colorectal cancer[205, 219, 220]. This suggests IGF-I and IGF-II stimulated cell migration may be an important determinant in the progression of colorectal cancer. Determination of which IGF receptors mediate this response could have important implications for the effectiveness of IGF1R based therapeutics. Therefore, SW480 cells were assessed for use as an *in vitro* model of IGF stimulated colorectal cancer cell migration.

A

B
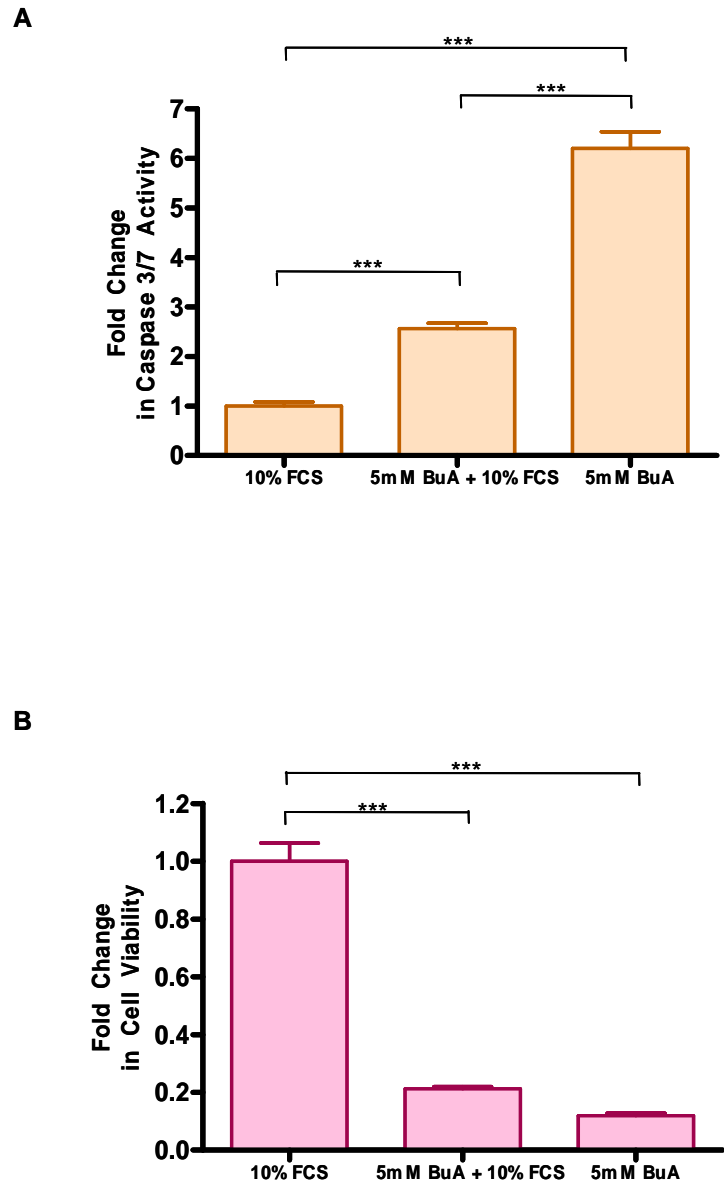
Figure 4.6 Butyrate-treatment induces apoptosis and decreases viability of SW480 cells

*SW480 cells were treated with 5mM butyrate [BuA] in the presence or absence of 10% FCS for 48 hours prior to assessment of apoptosis [**A**] and cell viability [**B**]. Results are expressed as the fold change in Caspase 3/7 activity [**A**] or fold change in cell viability [**B**]. Data points are the mean ± SEM of triplicate samples from three independent experiments conducted on separate occasions. Statistical significance was determined by ANOVA and Bonferroni's multiple comparison test. *** denotes p < 0.001.*
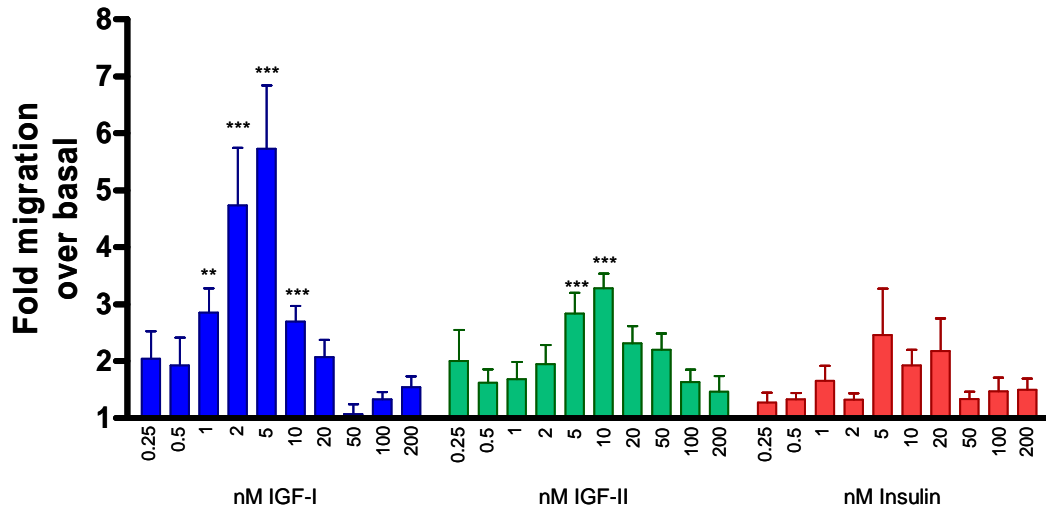
Figure 4.7 IGF-I, IGF-II, and insulin stimulated SW480 cell chemotaxis

Fold migration over basal

nM IGF-I   nM IGF-II   nM Insulin

*SW480 cell chemotaxis in the presence of increasing concentrations of IGF-I, IGF-II, and insulin. Results are expressed as the fold increase in migration over basal. The data points are mean ± SEM of triplicate samples from three independent experiments conducted on separate occasions. Statistically significant increase in cell migration above that of basal levels was determined by ANOVA with Bonferroni's multiple comparisons test. * $p < 0.05$, **$p < 0.01$, ***$p < 0.001$.*

Serum-free — 10nM ligand (IGF-I, IGF-II, Insulin)

A — 95 kDa — pIGF1R/pIR
55 kDa — β-tubulin

B — 95 kDa — IB: IR

C — 95 kDa — IB: IGF1R

IP: pTYR
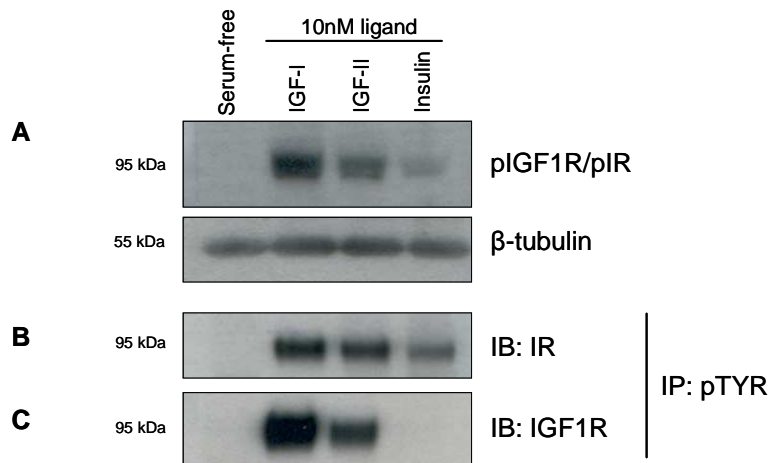
Figure 4.8 Activation of IGF1R and IR-A by 10nM IGF-I, IGF-II, and insulin in SW480 cells

SW480 cells were washed and serum-starved overnight prior to stimulation with either 10nM IGF-I, IGF-II, or insulin for 10 minutes and lysed. [A] Overall IGF1R and IR phosphorylation was assessed by probing 25µg whole cell lysate with an antibody that recognizes phosphorylated IGF1R and IR β-subunits [pIGF1R/pIR]. Detection of β-tubulin served as a load control. [B and C] Analysis of individual IGF1R and IR activation by 10nM ligand. Pre-cleared whole cell lysates [1mg protein] were immunoprecipitated overnight with an anti-phosphotyrosine antibody [pTYR-100]. Immunoprecipitates were then washed and analysed following SDS-PAGE by Western blotting. Phosphorylated IGF1R and IR β-subunits were individually detected by immunoblotting [IB] using antibodies specific for either the IGF1Rβ or IRβ as indicated. Results presented here are representative of results obtained from three individual experiments conducted on separate occasions.

The ability of IGF-I, IGF-II, and insulin to stimulate SW480 cell migration was assessed by Boyden chamber assay [Figure 4.7]. While all three ligands were able to stimulate SW480 chemotaxis to some degree, only IGF-I and IGF-II induced statistically significant migration over that of basal levels. The maximal migratory response to IGF-I was observed at 1 – 10nM and maximal response to IGF-II was observed at 5 and 10nM, indicating that both ligands can induce SW480 migration at physiologically relevant concentrations. Migratory response over the ligand concentration range resembled a bell-shaped curve. This response was typical of Boyden chamber migration assays as at higher ligand concentrations the concentration gradient between the upper and lower chambers decreases and the cells are not stimulated to migrate across the membrane.

4.2.7   *Activation of IR and IGF1R by ligand in SW480 cells*

The effect of ligand on IGF1R and IR-A phosphorylation was assessed [Figure 4.8]. SW480 cells were serum starved overnight prior to treatment with 10nM IGF-I, IGF-II, or insulin. Ligand stimulated IGF1R and IR-A phosphorylation was assessed in both whole cell lysates [Figure 4.8 A] and immunoprecipitates [Figure 4.8 B and C]. Western blotting results suggested that overall receptor phosphorylation [as determined by an antibody that recognizes phosphorylated tyrosines 1135/1136 on the $IGF1R_\beta$ and phosphorylated tyrosines 1150/1151 on the IR_β] reflected the biological response observed with ligand stimulation [Figure 4.8 A]. IGF-I stimulated the greatest level of overall phosphorylation, followed by IGF-II. Insulin stimulated the lowest level of phosphorylation. Analysis of IGF1R and IR β-subunits revealed $IGF1R_\beta$ to be strongly phosphorylated by IGF-I, then IGF-II, but were not phosphorylated by insulin. In contrast, IR_β was phosphorylated by all three ligands. Interestingly, IGF-I and IGF-II was observed to stimulate IR_β phosphorylation equally and to a greater extent than the same concentration of insulin. Previous studies have suggested that hybrid receptors undergo *trans* and a small amount of *cis*-phosphorylation[81, 146], therefore suggesting that both β-subunits involved in an activated hybrid receptor would be phosphorylated. Indeed, a recent study by Benyoucef et al 2007 suggested insulin bound poorly to hybrid receptors and did not induce hybrid receptor phosphorylation[110]. Together this therefore suggests that since insulin stimulated phosphorylation of IR_β but not $IGF1R_\beta$ in SW480 cells, activation of IR_β was indicative of IR homodimers and not hybrid receptors. Moreover, phosphorylation of IR_β by IGF-I and IGF-II in SW480 cells was greater than that

stimulated by insulin. Since the phosphorylated signal represents activation of β-subunits involved in both homodimers and hybrid receptors, these observations could be due to the trans-phosphorylation of IR$_\beta$ involved in hybrid receptors. This therefore suggests the effects of IGF-I and IGF-II stimulation were mediated by hybrid receptors as well as IGF1R and IR-A homodimers.

In addition, receptor phosphorylation was not detected under serum-free conditions. A previous study reported the IGF1R to be constitutively active in SW480 cells[325]. Constitutive activation of either the IGF1R or IR-A would render this cell line unsuitable for use in future experiments. There was no evidence of constitutive receptor phosphorylation in the SW480 cells utilised in these experiments.

4.3   *Discussion*

Work presented in this chapter identified a cell line that could be used to investigate how the IR-A functions in conjunction with the IGF1R to signal biologically relevant outcomes. Previous studies examining the biological functions of the IR-A have been conducted in cells that either do not express the IGF1R[12, 127, 135, 136, 305], or where the IR-A was expressed in vast excess to the IGF1R[125]. An appropriate cell line model in which to study the interactions between the IR-A and IGF1R would express similar levels of IR-A and IGF1R, and not express the IR-B. This cell line would also preferably be able to be used in a range of biological endpoint assays. SW480 colorectal adenocarcinoma cells were identified to satisfy these criteria.

Previous studies established that primary colorectal cancer tissue samples, in comparison to normal colorectal tissue, overexpress the IR, with the IR-A the predominant IR isoform[7]. Results from RT-PCR demonstrated the IR-A is the predominant transcript in three out of the four common colorectal adenocarcinoma cell lines [Figure 4.1 B]. IR protein expression was confirmed in both whole cell lysates [Figure 4.2] and at the cell surface [Figure 4.3] in all four cell lines. In addition, all four cell lines demonstrated IGF1R expression at both the transcript [Figure 4.1 A] and protein level [Figures 4.2 and 4.3] correlating with the observation that the IGF1R is also commonly expressed in colorectal cancer tissue samples[24, 65, 223, 227]. Detection of appropriate sized bands in Western blots and identification of both receptors at the cell surface suggested that both the IR and IGF1R

in all four cell lines were processed appropriately and transported to the cell surface after translation. The response to ligand stimulation [Figures 4.4 and 4.5] also suggested that both the IR and IGF1R were functional in each cell line.

SW480 cells were shown to express similar levels of both the IGF1R and the IR-A, but not express the IR-B. As expected in cells that co-express the IGF1R and IR, hybrid receptors were identified in SW480 cells. One initial concern with this particular cell line were reports from a previous study that suggested the IGF1R was constitutively active in SW480 cells[325]. However, analysis of serum-starved cells revealed neither the IGF1R nor the IR-A to be constitutively active in the SW480 cells [Figure 4.8]. The reasons for the discrepancy between the present study and the previous report are unclear, but may reflect clonal variation. In addition to analyzing IGF1R and IR-A for constitutive activity, the ability of these receptors to be activated by ligand was also assessed. Overall receptor activation by ligand [Figure 4.8 A] reflected the ability of each ligand to stimulate either survival from butyrate [Figure 4.5 B] or cell migration [Figure 4.7]. Analysis of individual receptor β-subunits [Figure 4.8 B and C] suggested the effects of insulin were mediated solely via IR-A homodimers, while the effects of IGF-I and IGF-II were mediated via both IR-A and IGF1R homodimers and IGF1R/IR-A hybrid receptors.

The ability of IGFs and insulin to stimulate survival from the effects of butyrate via both the IR and IGF1R may have important implications on the paradoxical effect observed with butyrate *in vivo* and *in vitro*. Butyrate plays an important physiological role in the normal colonic epithelium, in the maintenance of colonic mucosal health, where it is the primary metabolic substrate of colonocytes[171], and modulates epithelial cell cycle and mucosal immune response. However, *in vitro*, butyrate induces differentiation, inhibits cellular proliferation, and stimulates apoptosis of cultured colorectal cancer cells[174-176]. Therefore, there appears to be a switch between butyrate being used as a fuel source by normal colonocytes, and butyrate inducing apoptosis in colorectal cancer cells. The paradoxical effect of butyrate is observed with the occurrence of colorectal cancers themselves. *In vitro*, physiologically relevant concentrations are sufficient to result in the death of almost all cells treated[233], however colorectal cancers still develop *in vivo*. This therefore suggests that cancer cells develop mechanisms by which they can escape the anti-tumorigenic effects of butyrate. The finding that IGFs are overexpressed in colon cancer tissues[210, 213], along with overexpression of the IR[7, 228] and IGF1R[24, 65, 223, 227], together with the results of Leng *et al*

2001[233] and those presented here in chapters 3 and 4, suggests IGF and insulin signalling via these two receptors may provide one such mechanism by which cancer cells could evade the potent anti-tumorigenic effects of butyrate in the colonic lumen. This, along with other mechanisms of butyrate resistance, may account for the modest anti-tumorigenic effects of butyrate in *in vivo* studies[326, 327]. In addition, for the first time it has been demonstrated that insulin can have direct effects on colorectal cancer cells resulting in physiologically relevant outcomes to cancer biology, namely survival from the effects of butyrate [Figures 4.4 and 4.5]. It has previously been speculated that several direct and indirect mechanisms may underlie the association between circulating insulin levels and colorectal cancer risk[189, 195]. Results presented here provide some evidence for a direct effect of insulin on colorectal cancer cells thereby promoting their survival from the effects of butyrate.

4.4   *Conclusions*

Work presented in this chapter identified SW480 colorectal adenocarcinoma cells to be an adequate cell line model which could be used to investigate how the IR-A functions in conjunction with the IGF1R to signal biologically relevant outcomes. These cells were found to express similar levels of IR-A and IGF1R at the cell surface, and did not express the IR-B. SW480 cells did not display constitutive activation of either the IR-A or IGF1R, and both receptors were activated by ligand. Moreover, these cells could be used in a range of biological endpoint assays representative of cellular processes relevant to colorectal cancer pathology, namely cellular migration, cell viability, and survival from butyrate-induced apoptosis.

Chapter 5

Optimisation of siRNA mediated knock-down of the IGF1R and IR-A in SW480 cells

5.1   Introduction

In Chapter 4, IGF receptor expression was determined in SW480 human colorectal cancer cells. These cells expressed both the IGF1R and IR-A, but did not express the IR-B. SW480 cells were therefore established to be an appropriate model to investigate the biological role of the IR-A in cells co-expressing the IGF1R. To facilitate this investigation, the work presented in this chapter describes an siRNA transfection approach that resulted in effective, specific and reliable knock-down of the IR-A and IGF1R in SW480 cells.

Several lines of reasoning formed the basis of the decision to use an siRNA based approach. Firstly, targeting the gene of interest requires sequence specific base-pairing to the complementary strand of mRNA. Unlike antibody or small molecule inhibitor approaches, siRNA enables either the IGF1R or IR to be targeted individually without directly affecting the other. Secondly, an siRNA based approach had been successfully utilised by our collaborators to investigate interactions between the IGF1R and EGFR[297]. Therefore, it was likely that this approach would also enable the interactions between the IR-A and IGF1R to be investigated. Indeed, while the present study was in progress, Zhang *et al* 2007 described the use of siRNA targeting the IGF1R to demonstrate increased sensitivity of breast cancer cells to insulin via the IR[151]. Finally, siRNA targeting the IGF1R is gaining attention as a potential anti-cancer therapeutic strategy. Identification and circumnavigation of potential mechanisms by which IGF1R silencing could be rendered ineffective, such as compensatory signaling via other receptor tyrosine kinases like the IR-A, would be an important determinant in the likely success of these therapeutic strategies.

The mechanism of siRNA mediated gene silencing capitalises on the normal cellular process of RNAi[289] [see Figure 5.1]. Exogenous siRNAs introduced into cells by transfection act to mimic the cleavage products of long dsRNA produced by the dsRNA-specific ribonuclease Dicer [Step 1][285, 289]. The siRNAs are then incorporated into the RISC complex where they are unwound and the

Figure 5.1 The mechanism of RNA interference [RNAi]

In C.elegans initiation of RNAi involves delivery of long dsRNA to Dicer by the Rde family of proteins. Dicer cleaves the dsRNA into siRNAs which are then loaded into the RISC complex. The antisense strand of the unwound siRNA then targets complementary sequences within mRNA thereby mediating cleavage of the target mRNA by nucleases contained within the RISC. Exogenous siRNAs introduced into cells by transfection mimic the cleavage products of long dsRNA and are incorporated into the RNAi process, resulting in gene silencing. Figure reproduced with variation from Bohula et al 2003239.

NOTE: This figure is included on page 114 of the print copy of the thesis held in the University of Adelaide Library.

anti-sense strand of the siRNA acts to target complementary sequences within mRNA [Step 2][285, 289]. The endonuclease activity within the RISC complex cleaves the target mRNA resulting in gene silencing[285, 289]. Although a powerful research tool, siRNA based approaches to gene silencing do pose inherent difficulties. These challenges include: optimal siRNA design, effective delivery into the cell, non-specific toxicity of chemical transfection reagents, and off-target effects of the siRNAs themselves. Therefore, effective and specific silencing of the gene of interest requires several stages of optimisation. This chapter outlines the experiments utilised to optimise siRNA mediated knock-down of the IGF1R and IR-A in SW480 cells, therefore the discussion is incorporated in with the results.

5.2 Results and Discussion

5.2.1 Initial validation of siRNAs targeting the IGF1R and IR

5.2.1.1 An siRNA targeting the IGF1R results in specific silencing of the IGF1R in SW480 cells

The first step of the optimisation process was to validate, and if necessary design, siRNAs that individually target and down-regulate the IGF1R and IR-A. Our collaborators had designed a specific and effective siRNA that down-regulates the IGF1R through screening of the secondary structure of the IGF1R mRNA to determine areas of the transcript accessible to hybridisation by siRNAs[290]. This siRNA has been demonstrated to be effective at silencing IGF1R expression in a range of cell lines[290-292, 297, 298], and was therefore used as a positive control in initial transfection experiments in SW480 cells. Transfection of SW480 cells with the IGF1R siRNA duplex resulted in considerable and specific knock-down of the IGF1R [Figure 5.2], and was therefore determined to be an adequate siRNA for use in this cell line. Apparent off-target effects of the scrambled sequence control are discussed in section 5.2.2.

A

B

Figure 5.2 Commercially available siRNAs targeting the IR are ineffective at knocking-down IR expression in two separate human cell lines.

*Immunodetection of IR and IGF1R expression by SW480 [**A**] and MDA-MB-231 [**B**] cells 48 hours post-transfection with 200nM siRNA utilising Oligofectamine^{TM} [Invitrogen] as a transfection reagent. 50µg of whole cell lysate from each of the indicated conditions were separated on 4-12% Bis-tris NuPAGE$^{®}$ gels transferred to nitrocellulose by iBlot^{TM} dry transfer. IGF1R and IR β-subunits were detected utilising appropriate antibodies. Detection of β-tubulin served as a load control. IGF1R denotes a siRNA targeting the IGF1R. Scr denotes a scrambled sequence control siRNA of the IGF1R siRNA. IR29 and IR31 denote two siRNAs targeting the IR commercially available from Ambion. Results are representative of two independent experiments conducted on separate occasions.*

5.2.1.2 Commercially available siRNAs were ineffective at knocking-down IR expression in both SW480 and MDA-MB-231 human cell lines

siRNA is considered a key technical tool for understanding gene function[328]. As a result, many commercial companies offer a wide range of pre-designed and 'validated' siRNAs. With regard to the IR, SW480 cells only express the IR-A isoform, and so an siRNA targeting the IR for use in this

cell line does not need to be isoform specific. Therefore, two 'pre-validated' siRNAs targeting differing regions the IR transcript was purchased from Ambion [see Table 2.5]. Both pre-validated IR siRNAs were reported to cause approximately 70% reduction of the IR mRNA transcript in HeLa cells[329]. However, one downfall of commercially available siRNAs is 'pre-validation' is performed by via high-throughput screening in a standard cell line utilising established transfection protocols. The two IR siRNAs were therefore tested for their ability to knock-down IR protein expression in both SW480 colorectal adenocarcinoma and MDA-MB-231 breast cancer cells [Figure 5.2]. MDA-MB-231 cells were used as a transfection control for Oligofectamine[TM] mediated transfection of siRNA, as our collaborators had previously identified these cells to be susceptible to transfection by siRNA with Oligofectamine[TM297]. The two IR siRNAs failed to produce adequate knock-down of the IR in either cell line. They were more effective in MDA-MB-231 cells than SW480 cells, however at best they only produced approximately 50% reduction in expression compared to the control siRNA. The level of knock-down in the SW480 cells was not sufficient for use in further experiments, therefore alternate siRNAs targeting the IR were sought.

5.2.1.3 Design and initial validation of siRNAs targeting the IR

Additional siRNA candidate sequences needed to be identified since commercially available siRNAs targeting the IR failed to produce adequate knock-down of the IR in SW480 cells. Lead siRNA target sequences were identified by subjecting the entire IR transcript to the Qiagen siRNA design algorithm [see section 2.1.5]. This algorithm selects siRNA candidate sequences based on the rational design parameters outlined in Table 5.1. The highest scoring sequences for potential effectiveness as siRNAs were subjected to BLAST sequence homology searches [NCBI] for IR specificity. Only one sequence from the initial lead candidates was identified to be sequence

A

IR-A Specific

Name: A10 + 10
Target: 5'- **TTTCGTCCCCA**GGCCATCTCGG -3'

Name: A5 + 16
Target: 5'- **TCCCCAG**GCCATCTCGGAAACGC -3'

Non - IR Isoform Specific

Name: IR both
Target: 5'- **AACTAGTCCTGCAGAGGATTT** -3'
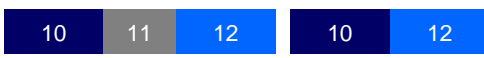
Name: AB10
Target: 5'- **CAACGTGGTTTTCGTCCCCAG** -3'
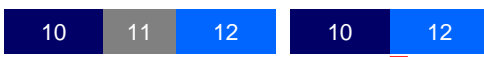
Name: AB12
Target: 5'- **AGGCCATCTCGGAAACGCAGG** -3'
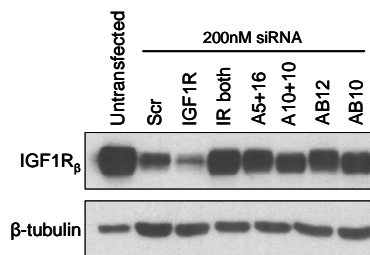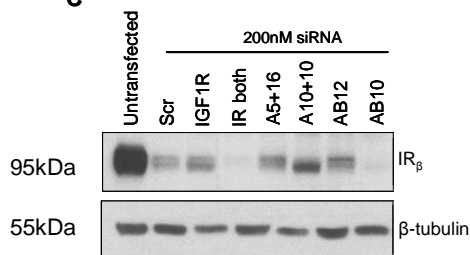
Figure 5.3 Design and initial validation of siRNAs targeting the IR

*Diagrammatical representation of the rational design of siRNAs targeting the IR [**A**]. The left-hand side represents the exon arrangement of the two IR isoforms. The red bars indicate the location of the sequence [right-hand side] targeted by the siRNAs. Target sequences are colour coded to demonstrate their position in the exons. For sequence of the sense and anti-sense strands of the siRNAs see Table 2.4. Immunodetection of IGF1R [**B**] and IR-A [**C**] expression by SW480 cells 48 hours post-transfection with 200nM siRNA utilising Oligofectamine as a transfection reagent. SW480 cells express the IR-A and not the IR-B and therefore would only enable validation of the ability of the siRNAs to knockdown the IR-A. Receptor expression for each transfection condition was assessed in 50µg whole cell lysate separated on 4-12% Bis-tris NuPAGE® gels transferred to nitrocellulose by iBlot^{TM} dry transfer.*

specific for the IR. This siRNA, denoted *IR both*, was used to transfect SW480 cells and resulted in significant and specific knock-down of the IR-A [Figure 5.3]. This siRNA was therefore an adequate candidate to take through the transfection optimisation process.

An additional, but minor goal of the design process was to design and produce an siRNA that specifically targets and down-regulates IR-A expression without affecting the IR-B. Should the IR-A be determined to be a worthwhile anti-cancer therapeutic target, among the problems facing therapeutic strategies are the metabolic consequences of inhibiting the IR. Since there is preferential expression of the IR-A over the IR-B in tumours[7, 123, 126, 127], one way to potentially minimize these effects would be to specifically target the IR-A at the site of the tumour. This would leave the IR-B in insulin-responsive tissues to function normally, thereby potentially minimizing detrimental metabolic consequences of targeting the IR-A. An siRNA based approach offers a unique way to potentially target the IR-A without affecting the IR-B since siRNAs can theoretically, be designed to target anywhere within a mRNA sequence[328]. Design of an IR-A specific siRNA is limited to the sequence spanning the exon 10/12 junction. In addition, it should be noted, although siRNAs can target anywhere within a mRNA strand, several sequence specific characteristics have been identified to govern an siRNAs effectiveness[330, 331] [Table 5.1]. These sequence specific characteristics form the basis of a set of rational design rules that should be considered when designing an siRNA[330, 331], see Table 5.1. Unfortunately, less than optimal sequences had to be chosen for potential IR-A specific siRNA candidates as the exon 10/12 junction is G/C rich and contains stretches of four or more bases, such as 'CCCC' [Figure 5.3 A]. However, two target sequences were chosen; one equally spanned the exon 10/12 junction by targeting 10 nucleotides from each exon, the second targeted 5 nucleotides from the 3' end of exon 10 and 16 nucleotides from the 5' end of exon 12. Both siRNA sequences [A10+10 and A5+16] were sequence specific for the IR-A. As previously mentioned, secondary structure of the target mRNA also determines the efficacy of a given siRNA. To address this, two additional siRNAs were designed to examine the accessibility of the area around the exon 10/12 junction to siRNA hybridisation [Figure 5.3 A]. These siRNAs would not be isoform specific as they target either the last 21 nucleotides of the 3' end of exon 10 [AB10] or the first 21 nucleotides of the 5' end of exon 12 [AB12] which are present in the mature transcript of both IR isoforms. One caveat to note with this approach, is moving the target site of a siRNA by as little as 3 nucleotides can dramatically change accessibility[290].

Table 5.1 siRNA rational design rules
Sequence characteristics of functional siRNAs[330, 331]

Moderate to low [30 - 50%] G/C content
At least three A/Us at positions 15 -19 in the sense strand
Absence of inverted repeats
Avoidance of stretches of four or more bases
An 'A' base at position 19 of the sense strand
An 'A' base at position 3 of the sense strand
A 'U' base at position 10 of the sense strand
A base other than 'G' or 'C' at position 19 of the sense strand
A base other than 'G' at position 13 of the sense strand

A
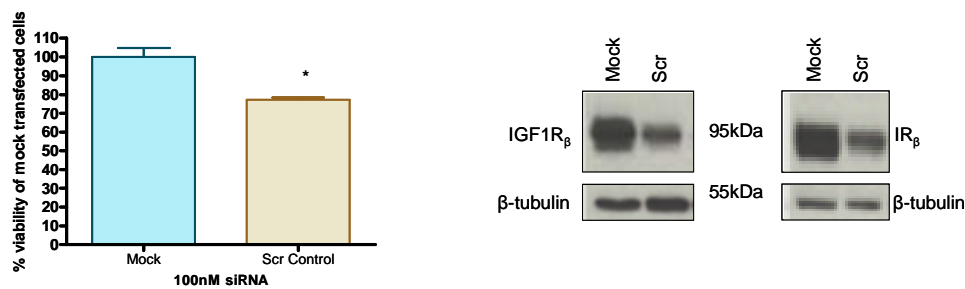
B
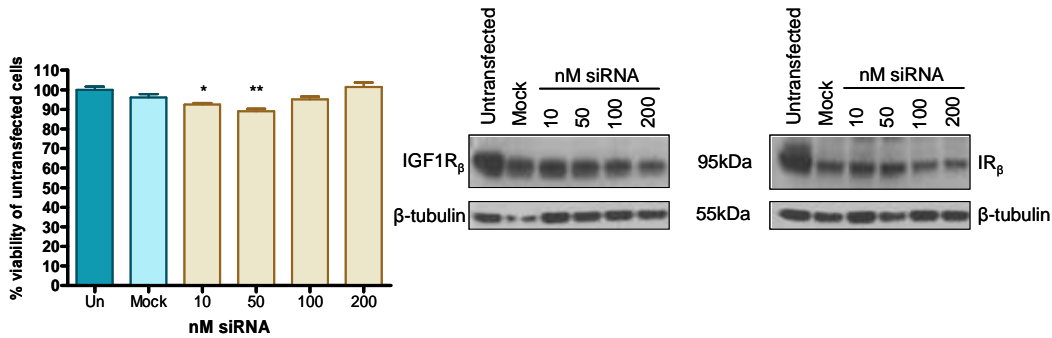
Figure 5.4 The effect of two different negative control siRNA duplexes on SW480 cell viability and receptor expression.

*[**A**], Scr denotes a scrambled sequence control of the IGF1R targeting siRNA that was utilised in conjunction with Oligofectamine[TM] to transfect SW480 cells. [**B**], a commercially available universal negative control that does not have homology with any known mammalian transcripts was used in conjunction with Oligofectamine[TM] to transfect SW480 cells. In both cases, 24 hours post-transfection cells were trypsinised and replated into 96 well tissue culture plates and cultured for a further 48 hours in 10% FCS for assessment of cell viability [left-hand side]. Cells remaining from replating were lysed and assessed for IGF1R and IR protein expression by Western blot [right-hand side]. Statistical significance, compared to untransfected control, was determined by ANOVA using Bonferroni's multiple comparison test. P values represented as follows: * $p < 0.05$; ** $p < 0.001$. Results are the mean of triplicate samples from a single experiment expressed as a percentage of untransfected cell viability ± SEM. Un, Untransfected.*

Both A5+16 and A10+10 IR-A sequence-specific siRNAs failed to produce knock-down of the IR-A in SW480 cells beyond that of the control duplex. This could be due to either the use of non-ideal target sequences, or inaccessibility of the region to hybridisation. Interestingly, AB10, despite being a less than optimal target sequence, did produce significant knock-down of the IR-A. This suggests the last 21 nucleotides of exon 10 are accessible to siRNA hybridization, and an IR-A specific siRNA may be achievable. One way to determine this would be to produce a range of siRNAs that scan along the exon10/12 junction by moving the starting point of the siRNA by a few nucleotides each time. These siRNAs could then be tested for efficacy of knock-down, and specificity for the IR-A over the IR-B. However, this was not pursued due to the cost and time involved in assessing a wide range of siRNAs. Furthermore, producing a specific IR-A siRNA was a relatively minor aim of this work and not necessary for use in the SW480 model. Importantly, this design process identified a siRNA [IRboth] that effectively and specifically targets the IR in SW480 cells that could be taken through the rest of the optimization process.

5.2.2 Optimisation of non-silencing control siRNAs and transfection reagent used for delivery of siRNAs into SW480 cells

5.2.2.1 Validation of non-silencing control siRNA duplexes

Initial SW480 cell transfections revealed the scrambled sequence control siRNA duplex to have significant effects on both IGF1R and IR-A expression [Figures 5.2 and 5.3]. Further investigation demonstrated large off-target effects, evidenced by both decreased receptor protein expression and decreased SW480 cell viability compared to mock transfected cells [Figure 5.4 A]. Therefore, a commercially available universal negative control duplex that does not have homology to any known mammalian transcripts was validated in conjunction with mock Oligofectamine[TM] transfections [Figure 5.4 B]. Increasing concentrations of control duplex did not appreciably affect either receptor protein expression or cell viability compared to the mock control. However, mock transfections containing only Oligofectamine[TM] caused significant decrease of both IGF1R and IR-A expression in SW480 cells, and suggested the reagent was toxic to this cell line.
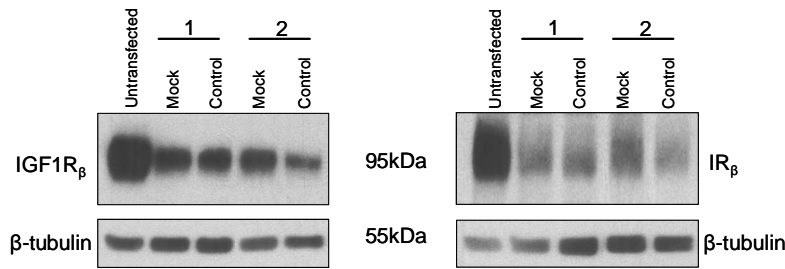
Figure 5.5 Non-specific toxicity of Oligofectamine™ on SW480 cells

Immunodetection of IGF1R and IR-A expression by SW480 cells by Western blot 48 hours post-transfection with Oligofectamine™ transfection reagent. Mock denotes transfections that did not contain any siRNA, control denotes transfections that contained 100nM non-silencing control siRNA. 1, indicates transfections carried out with the recommended concentration of Oligofectamine™. 2, indicates transfections carried out with half the recommended concentration of Oligofectamine™. Immunodetection of β-tubulin serves as a load control. Receptor expression for each transfection condition was assessed in 50µg whole cell lysate separated on 4-12% Bis-tris NuPAGE® gels transferred to nitrocellulose by iBlot™ dry transfer.
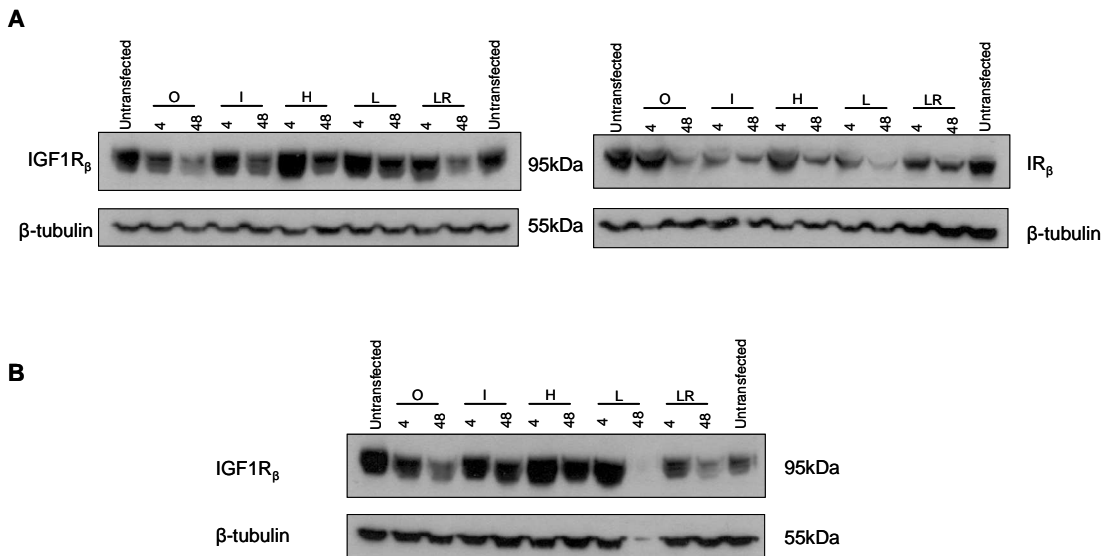
Figure 5.6 Assessment of transfection reagent toxicity

Five different transfection reagents were assessed in mock forward [A] and reverse [B] transfections for their ability to cause non-specific effects on IGF1R and IR-A expression in SW480 cells. Numbers above the lanes indicate the length of time, in hours, the cells were incubated with media containing transfection reagent. In all cases, cells were lysed 48 hours post-transfection. Receptor expression for each transfection condition was assessed in 20µg whole cell lysate separated on 4-12% Bis-tris NuPAGE® gels transferred to nitrocellulose by iBlot™ dry transfer. O, Oligofectamine™; I, INTERFERin™; H, HiPerFect; L, Lipofectamine 2000™; LR, Lipofectamine RNAiMAX™.

5.2.2.2 Optimisation of transfection reagent used for delivery of siRNAs into SW480 cells

Most commercially available transfection reagents are proprietary formulations of cationic, anionic, and neutral lipids. These formulations of charged lipids form complexes with siRNAs and are used not only to facilitate the movement of siRNAs into cells but to also mediate their release from the complex upon entry into the cell. The cationic charged lipids react spontaneously with the negatively charged siRNAs to form a cationic liposome/lipid-nucleic acid complex, or lipoplex[332]. The positive charge on the lipoplex surface enables it to bind negatively charged cellular membranes[333], thereby facilitating the entry of siRNAs into the cell via endocytosis[334]. Several factors can influence the cytotoxicity of a transfection factor. These include the amount of reagent used in the transfection, the length of time cells are treated with media containing transfection reagent, and composition of the reagent itself as charge ratios and certain structural components of these lipids can mediate toxicity[335]. Toxic effects include cell shrinking, reduced number of mitoses, inhibition of protein kinase C [PKC][336], down-regulation of total cellular protein expression[332], and vacuolisation of the cytoplasm[337]. Toxicity of a given transfection reagent is cell-specific[335].

Transfection reagent cytotoxicity can be attenuated by altering the amount of reagent used in the transfection[338]. Mock and control siRNA duplex transfections were therefore carried out in SW480 cells using half the recommended volume of Oligofectamine[TM] [Figure 5.5]. Reducing the amount of Oligofectamine[TM] did not alter its toxic effects on either IGF1R or IR-A expression, therefore an alternate transfection reagent was sought. Four different commercially available transfection reagents were assessed for their ability to alter IGF1R and IR-A expression in 4 and 48 hour mock forward and reverse transfections [Figure 5.6 and refer to section 2.2.1.3]. Oligofectamine[TM] was included in the experiments to act as an indicator of toxicity. The reverse transfection method combines plating and transfection, such that the cells are still in suspension when the transfection reagent and siRNA are added. SW480 cells did not grow sufficiently over the 48 hour reverse transfection period to give enough protein to run blots for both the IGF1R and IR [Figure 5.6 B]. In addition, increased amounts of floating cells were observed in all cultures following reverse transfection, suggesting this method of transfection was too harsh for SW480 cells and resulted in cell death. Forward transfection refers to the traditional method of transfecting cells with siRNAs. In this method, cells are pre-plated the day before transfection and allowed to attach and recover prior

to transfection. Forward transfections were more successful in terms of minimal cell death, as evidenced by few floating cells. In addition, cells appeared healthy under microscope without any identifiable morphological changes [data not shown]. Each transfection reagent was observed to differentially affect IGF1R and IR expression [Figure 5.6 A]. Across the range of transfection reagents, treatment for four hours had little effect on IGF1R expression. Forty-eight hour treatment had various affects on IGF1R expression depending on the transfection reagent. Mock transfection with all transfection reagents was observed to affect IR-A expression to a greater extent than IGF1R expression. Transfection affected IR expression in all cases at 48 hours, and in some cases, also at 4 hours. Of the transfection reagents tested, HiPerFect had the least effect on receptor expression and was therefore chosen as the lead candidate for use with SW480 cells.

5.2.3 Optimisation of HiPerFect transfection conditions

5.2.3.1 Initial optimisation of HiPerFect transfection conditions for SW480 cells

Initial results from mock transfections [Figure 5.6 A] suggested that 4 hour treatment with HiPerFect did not alter either IGF1R or IR-A expression in SW480 cells. However, 48 hour treatment did affect receptor expression. This suggested that an optimal treatment period existed within this timeframe. Optimal treatment conditions would be a treatment period that was not toxic to SW480 cells but allowed sufficient uptake of siRNA into cells for effective silencing of the target genes of interest. Initial results from 4 and 48 hour transfections on the ability of 100nM siRNA to knock-down expression of the IGF1R and IR-A expression were not encouraging [Figure 5.7]. Although 4 hour mock transfections did not affect receptor expression, transfection with siRNA also had no effect on receptor expression. In addition, although 48 hour transfection with siRNA resulted in some knock-down of both receptors, this was not significant compared to transfection with negative control siRNA. Furthermore, there was little difference between the level of receptor knock-down between 4 and 48 hour transfections of 100nM IGF1R or IR siRNA. This suggested insufficient uptake of the siRNA by the cells, as it had already been established that the two siRNA duplexes could silence the two target receptors in this cell line [Figures 5.2 and 5.3].
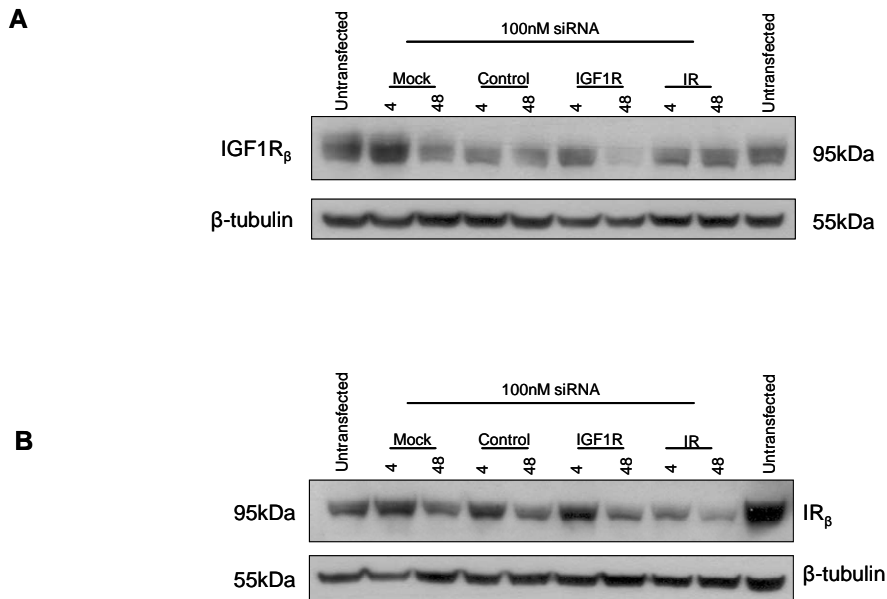
Figure 5.7 Initial optimisation of HiPerFect transfection of SW480 cells

*Length of incubation with siRNA effects the knock-down of IGF1R [**A**] and IR-A [**B**] expression in SW480 cells. Numbers above the lanes indicate the length of time, in hours, the cells were incubated with media containing HiPerFect and 100nM siRNA. In all cases, cells were lysed 48 hours post-transfection. Receptor expression for each transfection condition was assessed in 50µg whole cell lysate separated on 4-12% Bis-tris NuPAGE® gels transferred to nitrocellulose by iBlot^TM dry transfer. Mock, denotes transfections that did not contain any siRNA. Control, denotes transfections that contained 100nM non-silencing control siRNA. IGF1R and IR, denotes transfections that contained 100nM siRNA targeting the IGF1R and IR respectively.*

Transfection reagent manufacturers recommend three major changes to transfection protocols to improve transfection efficacy. These recommendations include: 1) increasing the concentration of siRNA used in the transfection, 2) increasing the length of time cells are incubated with the transfection complexes, and 3) optimising the transfection reagent to siRNA ratio. HiPerFect is formulated for transfection of cells with low siRNA concentrations[339]. The lack of transfection efficacy observed in Figure 5.7 was unlikely to be caused by suboptimal concentration of siRNA, as 100nM siRNA is considered a high concentration to transfect cells with. Since increasing the length of treatment with transfection complexes from 4 to 48 hours did not affect receptor knockdown, these data suggested the lack of transfection efficacy could be due to poor formation of the transfection complex prior to transfection. Two minor changes were therefore made to the transfection protocol with the aim of increasing lipoplex formation. These changes were; 1) increasing the length of time the siRNA and HiPerFect were vortexed from a brief vortex to a 20 second vortex, and 2) changing the order in which growth media and transfection complexes were added to the cells [for more information refer to sections 2.2.1.3.5.2 and 2.2.1.3.5.4]. These two small changes to the transfection protocol had a large and positive effect on the outcome of transfection [Figure 5.8 A]. Non-specific toxicity of mock and negative control siRNA transfections was abolished, and significant knock-down of the IGF1R was achieved with both 10nM and 100nM transfections of IGF1R siRNA. These two changes were therefore adapted into the transfection protocol [refer to section 2.2.1.3.5.4].

In order to save on reagents during the optimisation process, all experiments utilising HiPerFect as a transfection reagent presented thus far had been performed in 6cm tissue culture dishes. However, this dish size did not provide enough cells for use in subsequent bioassays, therefore up-scaling transfections to 10cm dishes was required. A comparison of transfections carried out in 6cm and 10cm dishes are presented in Figures 5.8 A and B, respectively. The transfection protocol for 6cm dishes was proportionally up-scaled to transfect 10cm dishes. However transfections conducted in 10cm dishes failed to produce knock-down of the target receptor [Figure 5.8 B]. In attempt to optimise 10cm dish transfections, the HiPerFect to siRNA ratio was altered along with the final volume the transfections were conducted in [Figure 5.8 C], refer to section 2.2.1.3.5iii and Tables 2.10 and 2.11 for more information. Although IGF1R knock-down was achieved in 10cm dishes, knock-down was not as effective as transfections conducted in 6cm dishes [Figure 5.8 A]. In addition, no alteration to the 10cm dish transfection protocol had a significant effect on the
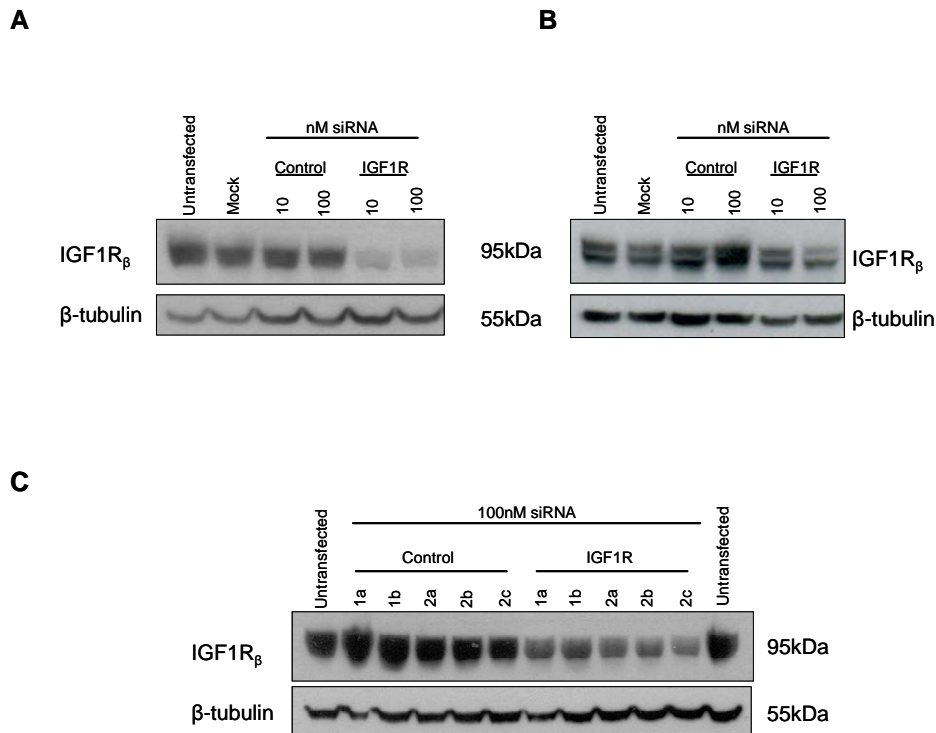
Figure 5.8 Effect of up-scaling HiPerFect transfections on the efficacy of IGF1R knock-down

*All prior HiPerFect transfections in this chapter had been performed in 6cm tissue culture dishes. A single 6cm dish did not provide enough cells to be used in subsequent bioassays, therefore up-scaling to 10cm dishes was required. [**A**] and [**B**] provide a comparison of HiPerFect transfections carried out at the same time in 6 and 10 cm dishes respectively. Numbers above the lane indicate the nM concentration of indicated siRNA used in the transfection. [**C**], demonstrates that alteration of the HiPerFect to siRNA ratio did not increase the efficacy of IGF1R knock-down in 10cm dish transfections. Lanes with a prefix of 1 denotes transfections carried out in a final volume of 7ml/dish. Lanes with a prefix of 2 denotes transfections carried out in a final volume of 15ml/dish. Explanation for the lower case letters following the numbers are as follows: a, protocol for large-scale transfection of adherent cells with siRNA in 100mm dishes from the HiPerFect Transfection Reagent Handbook[339] [Qiagen] altered for cells to be plated the day before transfection. b, proportional upscale of amount of reagents used in 6cm dish transfections to suit transfection of 10cm dishes. c, proportional upscale of the amount of reagents used in the Traditional Protocol from the HiPerFect Transfection Reagent Handbook[339] [Qiagen] to suit transfection of 10cm dishes. In all cases, transfections were carried out for a total of 48 hours. Receptor expression for each transfection condition was assessed in 50µg whole cell lysate separated on 4-12% Bis-tris NuPAGE® gels transferred to nitrocellulose by iBlot^TM dry transfer. For further information see section 2.2.1.3.5.3 and Table 2.11.*

efficacy of IGF1R knock-down. Several other modifications to the protocol could have been made, for example: modifying cell plating density and monitoring transfection efficacy with a fluorescently labeled siRNA. However, cells were approximately 70% confluent upon transfection, thus cell plating density of the 10cm dishes was on a par with that of 6 cm dishes. Since 6cm dish transfections resulted in effective and specific knock-down of the intended targets, it was decided rather than invest more time in the attempt to optimise 10cm dish transfections, multiple 6cm dish transfections would be conducted for each transfection condition. It should be noted that a doublet was observed in IGF1R blots in Figure 5.8. Due to the type of PAGE gel used, the transfection media containing 10% FCS, and the difference in size shift suggests the higher band to be most likely representative of phosphorylated IGF1R β-subunits.

5.2.3.2 Optimisation of siRNA duplex concentration used in HiPerFect transfection of SW480 cells

High siRNA concentrations cause non-specific changes in gene expression and off-target effects[340, 341], therefore it was necessary to titrate the concentration of siRNA used in transfection [Figure 5.9]. Optimal siRNA concentration was the lowest concentration of siRNA that provided effective knock-down of each receptor without affecting cell viability. It is well established that silencing of the IGF1R results in decreased cell proliferation, survival, and increased apoptosis[290-292]. Therefore, effective IGF1R knock-down was expected to result in decreased SW480 cell viability. Prior to the present study, the effect of siRNA mediated knock-down of the IR-A on cell viability was not known. Transfection of SW480 cells with increasing amounts of siRNA targeting the IGF1R and IR-A resulted in a dose-dependent decrease in expression of their respective receptors [Figure 5.9 C and D]. Knock-down of the IGF1R resulted in an expected maximal 35% decrease in cell viability [Figure 5.9 A], whereas knock-down of the IR-A did not affect cell viability beyond that of the negative control [Figure 5.9 B]. Ten nanomolar siRNA transfections were eventually chosen for future experiments, and several reasons governed this decision. Firstly, no appreciable difference in cell viability was observed between 100nM and 10nM transfections of either IGF1R or IR siRNA [Figure 5.9 A and B]. Secondly, 100nM IR siRNA transfection did not result in significant increase in IR knock-down compared to 10nM transfection [Figure 5.9 D]. Thirdly, 100nM siRNA concentrations can result in non-specific changes in gene expression[340, 341].
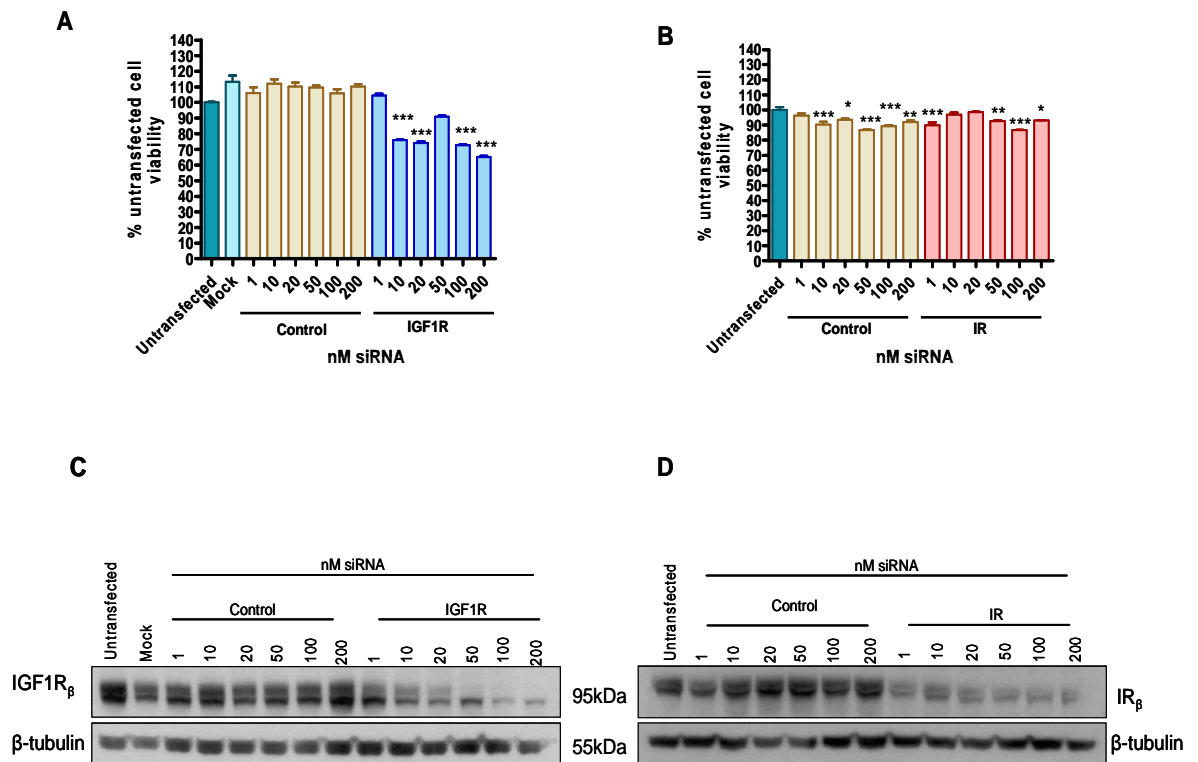
Figure 5.9 Optimisation of siRNA duplex concentration used in HiPerFect transfection of SW480 cells

*To assess the effect of increasing siRNA concentrations on SW480 cell viability, 24 hours post-transfection cells were trypsinised and replated into duplicate 96 well tissue culture plates. Cells were cultured for a further 48 hours in the presence of 10% FCS before cell viability was determined utilising CellTitreBlue cell viability assay [A and B]. Cells remaining from replating were lysed and assessed for IGF1R and IR protein expression by Western blot [C and D, respectively]. Optimal siRNA concentration was determined as the lowest concentration that caused effective knock-down of the receptor. Results are the mean of triplicate samples from a single experiment expressed as a percentage of untransfected cell viability ± SEM. For simplicity, only statistically significant decreases in cell viability are shown. Statistical significance, compared to untransfected control, was determined by ANOVA using Bonferroni's multiple comparison test. P values represented as follows: * p < 0.05; ** p < 0.01; *** p < 0.001.*
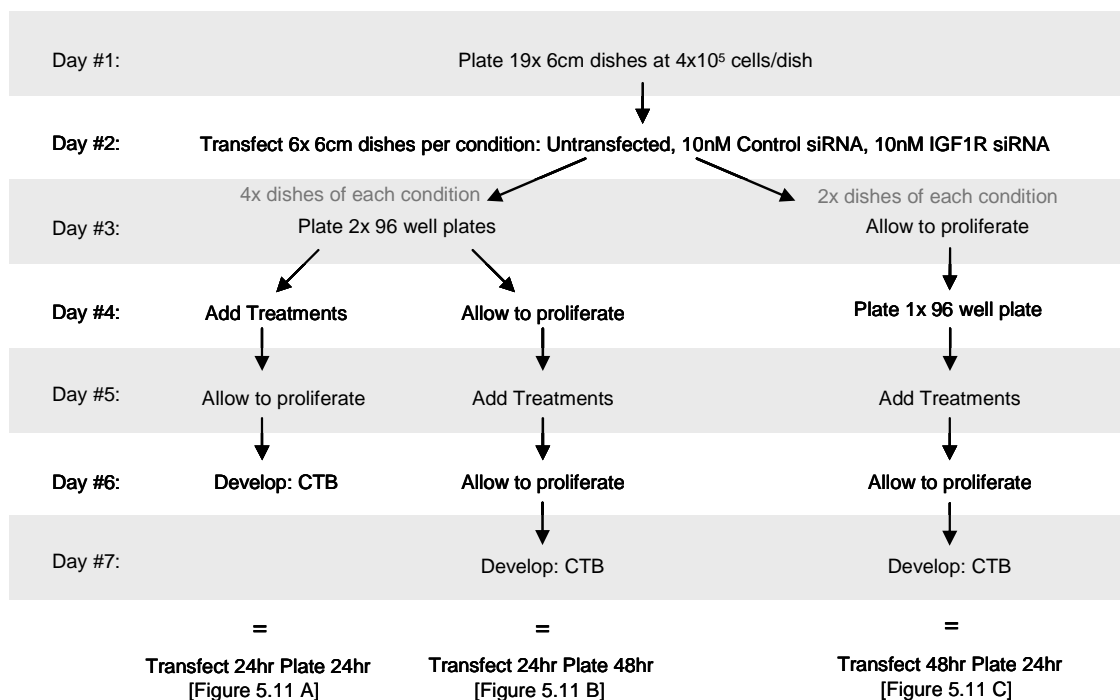
Figure 5.10 Optimisation of post-transfection survival assays: experimental set-up

Flow chart representation of the strategy to optimise post-transfection cell survival assays. Multiple 6cm dishes were transfected with the appropriate siRNA. Either 24 or 48 hours post-transfection, cells were trypsinised, pooled and plated in 96 well plates. Cells were allowed to proliferate for either 24 or 48 hours prior to a 5 hour serum-starvation. Cells were incubated with treatments consisting of 5mM butyrate and a range of IGF-I concentrations for 48 hours. Each assay was developed utilising the CellTitreBlue^{TM} [CTB] cell viability assay at the indicated time point [Promega]. The naming scheme indicates the length of transfection followed by how long the cells were plated in 96 well plates for prior to the addition of treatments.
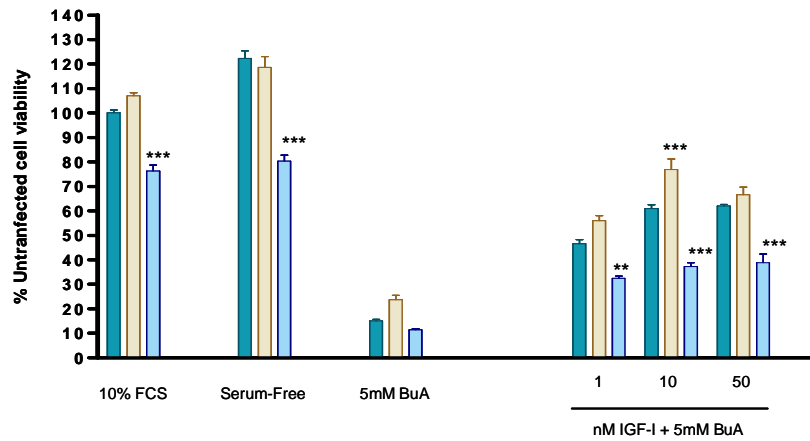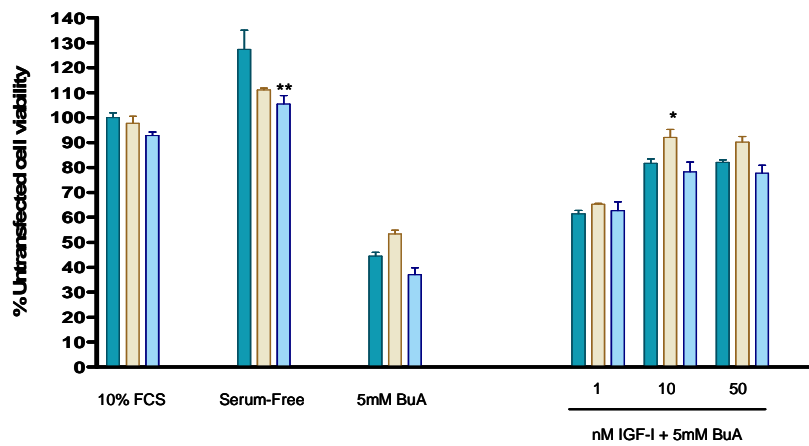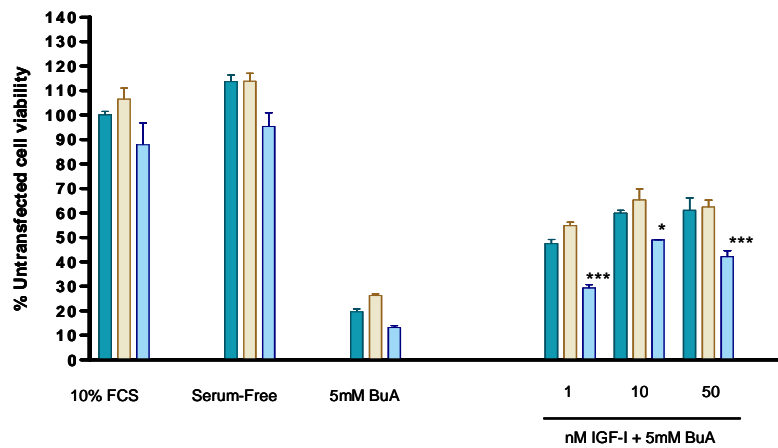
Figure 5.11 Optimisation of post-transfection cell survival assays

*Effect of different transfection and plating time points on SW480 cell survival. Following the scheme outlined in Figure 5.10, [**A**], represents transfect 24hr plate 24hr; [**B**], represents transfect 24hr plate 48hr; [**C**], represents transfect 48hr plate 24hr. Results are the mean from triplicate wells from two individual experiments conducted on separate occasions plotted as the percentage maximal cell viability of untransfected cells treated with 10% FCS, ± SEM. Coloured bars are representative of the following transfection conditions: untransfected [■], 10nM control siRNA transfected [☐], and 10nM IGF1R siRNA transfected [☐]. Statistical significance, compared to untransfected control, was determined by ANOVA using Bonferroni's multiple comparison test. P values represented as follows: * p < 0.05; ** p < 0.01; *** p < 0.001. BuA, butyrate.*

A

B

C

Day#:	1	2	3	4	5	6	7
	Plate	Transfect #1	Transfect #2	Re-Plate			Develop
A		20nM Control 10nM IGF1R + 10nM IR					
B		10nM Control 10nM IGF1R	10nM Control 10nM IR				
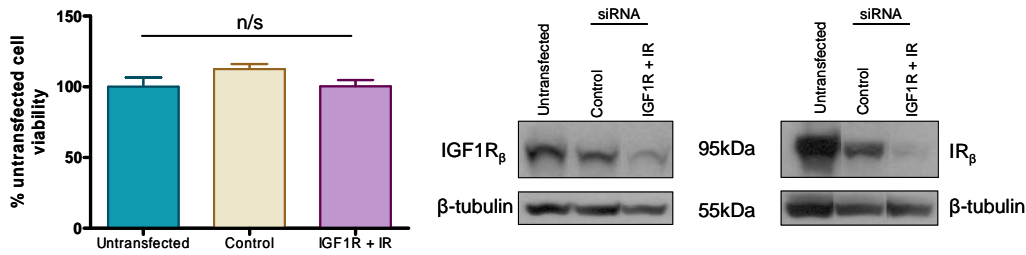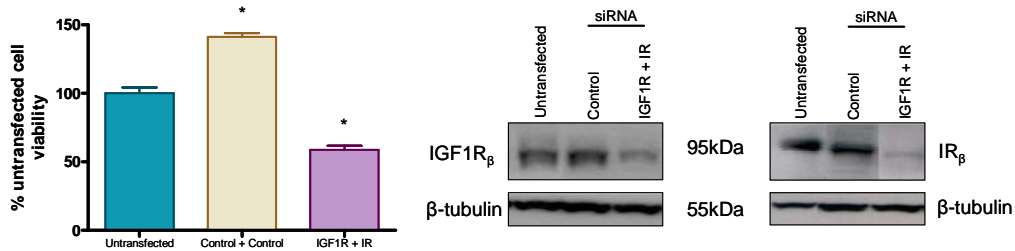
Figure 5.12 Optimisation of dual IGF1R and IR knockdown

*Demonstrates the effect of transfecting SW480 cells with siRNA targeting the IGF1R and IR on the same day [**A**] vs. transfecting SW480 cells with siRNA targeting the IGF1R followed by siRNA targeting the IR the following day [**B**]. In both cases, cells were transfected for a total of 48 hours before being trypsinised and replated into 96 well tissue culture plates. SW480 cells were cultured for a further 48 hours in 10% FCS prior to the assessment of cell viability by the addition of CellTitreBlue[TM] [left-hand side]. Results are the mean of triplicate samples from single experiments expressed as a percentage of untransfected cell viability ± SEM. Statistical significance, compared to untransfected control, was determined by ANOVA using Bonferroni's multiple comparison test. P values represented as follows: * $p < 0.05$; ** $p < 0.01$. Cells remaining from re-plating on day #4 were lysed and assessed for IGF1R and IR-A expression by Western blot [right-hand side]. [**C**], flow chart representation of transfection and replating scheme.*

Finally, further experiments [see Chapter 6] revealed 10nM transfections to be more effective at silencing both the IGF1R and IR-A than initially suggested by the data presented in Figure 5.9.

5.2.4   Optimisation of post-transfection survival assays

Cell survival assays post-butyrate challenge is a long established protocol in our laboratory. Generally, cells are plated 48 hours prior to butyrate challenge with cell viability assessed a further 48 hours post-butyrate challenge [see section 2.2.1.2.3]. However, this assay had not been optimised for use in conjunction with siRNA transfection. Therefore, a set of optimisation experiments were devised to determine the most appropriate transfection, re-plate, and challenge protocol for SW480 cells [Figure 5.10]. These experiments were conducted with IGF1R siRNA transfected cells, as knock-down of the IGF1R should decrease the ability of IGF-I to rescue SW480 cells from butyrate induced apoptosis [Figure 5.11]. Results demonstrated the length of time transfected cells were re-plated prior to butyrate challenge affected the ability of IGF-I to rescue cells from butyrate-induced apoptosis. Interestingly, the transfection period did not appear to affect the outcome of the assays, suggesting both 24 and 48 hour transfections resulted in similar levels of receptor knock-down. In light of the results discussed in the upcoming section pertaining to dual receptor knock-down, 48 hour transfection followed by 24 hour re-plating prior to treatment was eventually chosen.

5.2.5   Optimisation of dual silencing of the IGF1R and IR-A

As previously mentioned, our collaborators utilised siRNA mediated gene silencing to investigate interactions between the IGF1R and EGFR[297]. They found that simultaneous receptor gene silencing saturated the RNAi machinery[297]. Indeed, saturation of the RNAi machinery has been identified by other studies to occur with transfection of high concentrations of siRNA[342]. This was unlikely to be a concern in the present study, since only low concentrations of 10nM siRNA were utilised to knock-down IGF1R and IR-A expression. Nevertheless, dual receptor knock-down by simultaneous transfection was compared to dual knock-down achieved by sequential transfection

[see Figure 5.12 C for transfection scheme]. Both strategies resulted in decreased protein expression of both the IGF1R and the IR-A [Figure 5.12 A and B] suggesting that dual targeting was just as effective as single transfections at knocking-down each receptor. However, only sequential transfection resulted in decreased transfected cell viability when grown in 10% FCS. Since IGF1R knock-down alone results in decreased cell viability [Figures 5.9 and 5.11] it was expected dual knock-down of both the IGF1R and IR-A would result in a similar or further decrease in cell viability. Decreased cell viability was only observed in sequentially transfected cells, therefore this transfection scheme was utilised in further experiments.

5.3   Conclusions

Work presented in this chapter describes the multiple optimisation steps that were investigated to identify a protocol that enabled effective and specific siRNA mediated knock-down of the IGF1R and IR-A in SW480 cells. This optimisation process was vital as reproducible, reliable, and specific siRNA mediated gene silencing outcomes rely on protocols specifically tailored to the cell line of interest. Along with identifying a novel siRNA target sequence that resulted in effective and specific silencing of the IR-A in SW480 cells, initial validation experiments demonstrated off-target effects of scrambled control sequence siRNA and transfection reagents in SW480 cells. These off-target effects were reduced by optimisation of siRNA transfection. These control data support results observed in future experiments that were due to the effect of silencing the IR-A or IGF1R and not due to non-specific effects of the transfection process itself. Protocols were also established that enabled the effect of single or dual targeting of the IGF1R and IR-A on the ability of SW480 cells to respond to ligand stimulated cell survival from butyrate induced apoptosis.

Chapter 6

Assessment of the biological role of the IR-A in cells co-expressing the IGF1R

6.1 Introduction

The IGF system is a crucial regulator of normal growth and development[19], however dysregulation of the system on multiple levels is associated with the incidence of a wide variety of malignancies including the breast, thyroid, lung, and colon[22, 24, 124, 343, 344], making the IGF system an important anti-cancer therapeutic target. The traditional focus of research examining the role of the IGF system in cancer has been centered on the IGF1R, due to its role in mediating cellular proliferation, protection from apoptosis, and metastasis [extensively reviewed in 239]. However, recently there is mounting evidence to suggest the IR may also be involved in the potentiation and pathogenesis of cancers. The observation that IGF-II is overexpressed, compared to normal tissues, by several cancers [reviewed in 22, 24, 343], including colorectal cancer[220, 345, 346], suggests signaling via target receptors, including the IR-A, by this ligand has important implications for cancer pathogenesis. Indeed, both the IGF1R, and IR have been demonstrated to be up-regulated in a variety of malignancies[7]. With regard to IR isoform, the IGF-II binding IR-A is preferentially expressed by a number of cancer cell types [123, 125 and reviewed in 101]. Activation of the IR-A by IGF-II has been demonstrated to result in mitogenic effects on cells[7]. This observation, together with the demonstration that an autocrine proliferative loop exists between IGF-II and the IR-A in malignant thyrocytes[123] and cultured breast cancer cells[125], suggests signaling via the IR-A may play a role in cancer cell growth and survival. However, very few studies on the IR-A have been conducted in cells co-expressing the IGF1R and IR-A. This is mainly due to difficulties associated with discrimination between signaling arising from IGF1R homodimers, IR-A homodimers, and IGF1R/IR-A hybrid receptors. However, now the general functional properties of the receptor have been elucidated, it is important to turn attention to how this receptor interacts, and functions in conjunction with the other receptors of the IGF system to signal biologically relevant outcomes. This is especially important in terms of anti-cancer therapeutics that aim to block and downregulate the IGF1R. Currently, anti-cancer therapies targeting the IGF system have concentrated on blocking IGF signaling via the IGF1R[209, 239, 244], due mostly to the functional properties of the IGF1R, but also in part due to the metabolic consequences associated with blockade and inhibition of the IR[269]. This individual targeting of the

IGF1R potentially leaves a pathway by which IGF-II secreted by the tumour can circumvent current IGF1R based therapies. This chapter aimed to address this possibility and therefore examined the role of the IR-A in cells co-expressing the IGF1R. An siRNA based approach was successfully utilised to investigate this. The results suggest the IR-A could not compensate for IGF1R down-regulation. Moreover, dual silencing of the IR-A and IGF1R did not confer any additional inhibition of IGF-stimulated SW480 cell survival and proliferation than IGF1R silencing alone. Together these results suggest the implications of IR-A expression on the efficacy of anti-cancer therapeutics aimed at targeting the IGF1R may not be as considerable as first anticipated. Furthermore, these experiments demonstrate how IR-A co-expression can influence and affect the function of the IGF1R. Finally, the inference from these results suggests signaling via IGF1R/IR-A hybrid receptors may not be as potent as signals arising from IGF1R homodimers, thereby providing some insight into the functionality of hybrid receptors.

6.2   Results

6.2.1   The effect of transient siRNA transfection on SW480 cell surface expression of IGF1R and IR-A

Although Chapter 5 identified effective IGF1R and IR-A silencing at the protein level by siRNA transfection, it was important to confirm receptor down-regulation at the cell surface. Cell surface expression of IGF1R and IR-A in siRNA transfected SW480 cells was assessed by indirect-immunofluorescence flow cytometry according to section 2.2.3.5 [Figure 6.2 and 6.3]. Untransfected SW480 cells [Figure 6.1 A] were observed to have similar levels of IGF1R and IR-A, indicated by the sharp narrow peaks returned by cells labeled with either antibody. Transfection with control siRNA [Figures 6.1 B and C] caused the resultant IR-A and IGF1R peaks to broaden in comparison to the untransfected cells, indicating under transfection conditions the population of cells became more heterogeneous in the level of receptor expression. Despite the control siRNA duplex being non-specific for any known mammalian mRNA transcripts, transfection with this duplex did have a slight effect on cell surface expression of the IR-A and IGF1R. Control siRNA reduced IR-A cell surface expression to a slightly greater extent than IGF1R expression, and this

effect was observed to be more pronounced in sequentially transfected cells [Figure 6.1 C]. The effect of control siRNA transfection on IGF1R and IR-A expression was more apparent at the cell surface [Figure 6.1 and 6.2] than in whole cell lysates [Figure 6.3 A]. Flow cytometry measures cell surface expression only, whereas Western blotting measures both cell surface and internalised receptors. The difference observed between results of these two methods may reflect the mechanism of action of the transfection reagent used to facilitate siRNA delivery into the cells. The liposome/siRNA transfection complex is assumed to enter cells via endocytosis[334]. If parts of the cell membrane containing IR-A and IGF1R are involved in this process, it is conceivable that both IR-A and IGF1R will be removed from the cell surface as part of the cell membrane now involved in forming the membrane bound intracellular vesicle. If the internalized receptors do not become recycled to the cell surface, or cannot escape the endosomal degradation pathway this would be seen as an overall decrease in receptor expression. However, despite these permutations in receptor expression levels, single transfection with control siRNA did not affect the ability of SW480 cells to respond to biological stimuli [Figures 6.4 – 6.6].

Transfection of SW480 cells with 10nM IGF1R siRNA [Figure 6.1 D and Figure 6.2 A LHS] resulted in decreased cell surface expression of IGF1R compared to untransfected and control duplex transfected cells. In these cells IR-A receptor expression was unaltered compared to control duplex transfected cells [Figure 6.2 A RHS]. Transfection of SW480 cells with 10nM IR siRNA [Figure 6.1 E and 6.2 B] resulted in a dramatic decrease in cell surface expression of the IR-A compared to untransfected and control transfected cells. Knock-down of IR-A receptor expression was so effective it was not detected at the cell surface. Treatment of cells with IR siRNA did not alter IGF1R expression compared to control duplex transfected cells [Figure 6.2 B LHS]. Dual receptor knock-down by sequential transfection of 10nM IGF1R siRNA followed 24hrs later by 10nM IR siRNA [Figures 6.1 F and 6.2 C] resulted in decreased cell surface expression of both receptors compared to both untransfected and cells sequentially transfected with control duplex. The resultant decrease in each receptor was comparable to when each receptor was targeted individually. In cells transfected with both IR and IGF1R siRNA, although expression of both receptors was decreased, the overall receptor profile was one where IGF1R was expressed to a greater extent than the IR, due to the IR siRNA duplex being more efficient at knocking down the IR-A than the IGF1R siRNA duplex was at knocking down the IGF1R [Figure 6.1 F].

A
Untransfected

B
10nM Control siRNA

C
10nM + 10nM
Control siRNA

D
10nM IGF1R siRNA

E
10nM IR siRNA

F
10nM IGF1R + 10nM IR
siRNA

Legend:

— Control IgG

— IGF1R [24-60]

— IR [83-7]
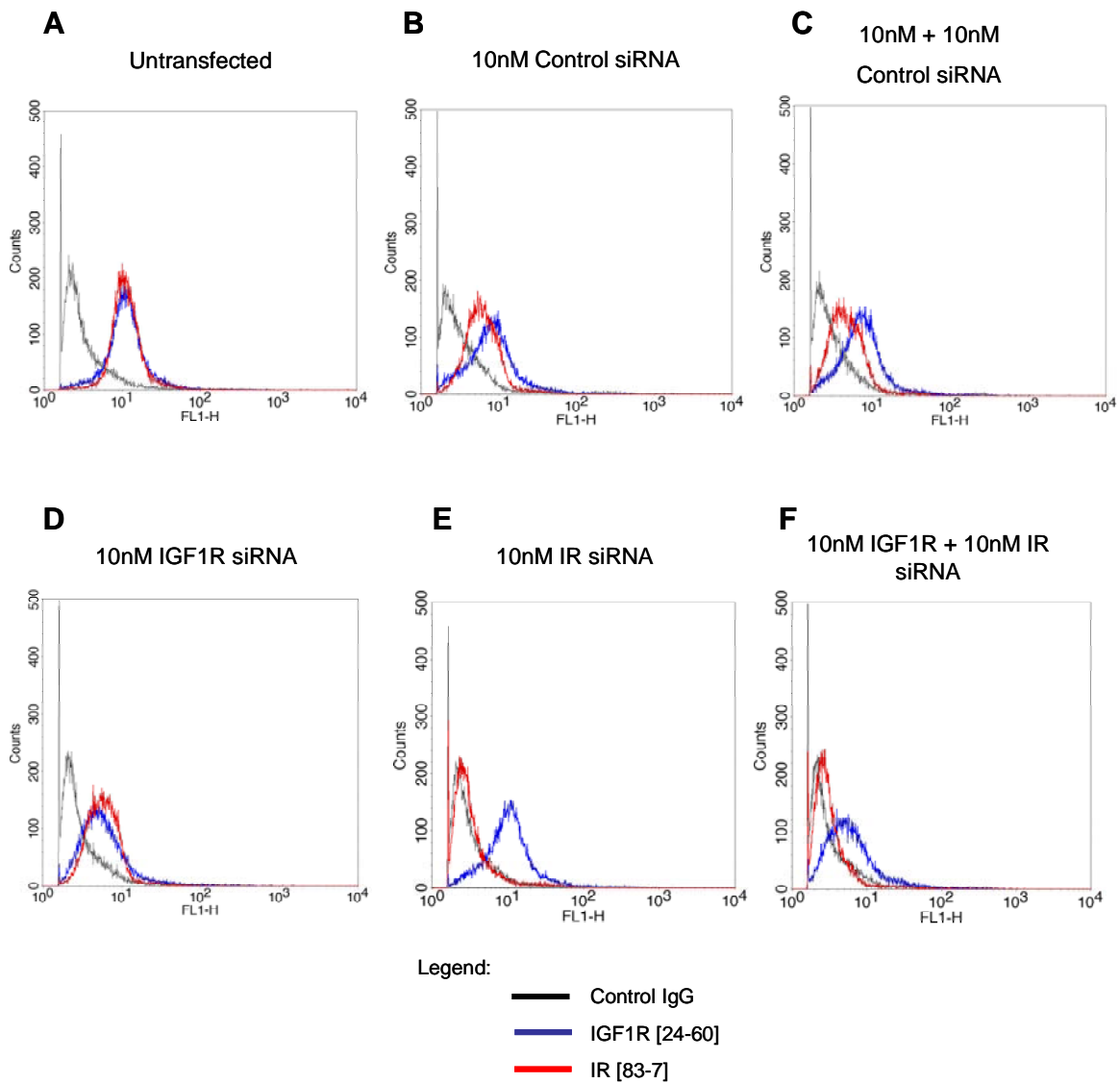
Figure 6.1 Cell surface expression of IGF1R and IR-A in siRNA transfected SW480 cells

Cell surface expression of IGF1R and IR-A was analysed by indirect-immunofluorescence flow cytometry utilising specific antibodies 24-60 [blue] and 83-7 [red] directed against the IGF1R and IR, respectively. A monoclonal IgG1 antibody that does not have specificity for any human cell surface components was used as a negative control [black]. Cell surface expression was determined 48 hours post-transfection as described in section 2.2.3.5. Transfection conditions are as indicated above each histogram. In all cases, results are representative of three independent experiments conducted on separate occasions, and demonstrates the overall receptor profile of IGF1R vs. IR-A across all transfection conditions utilised in subsequent experiments.
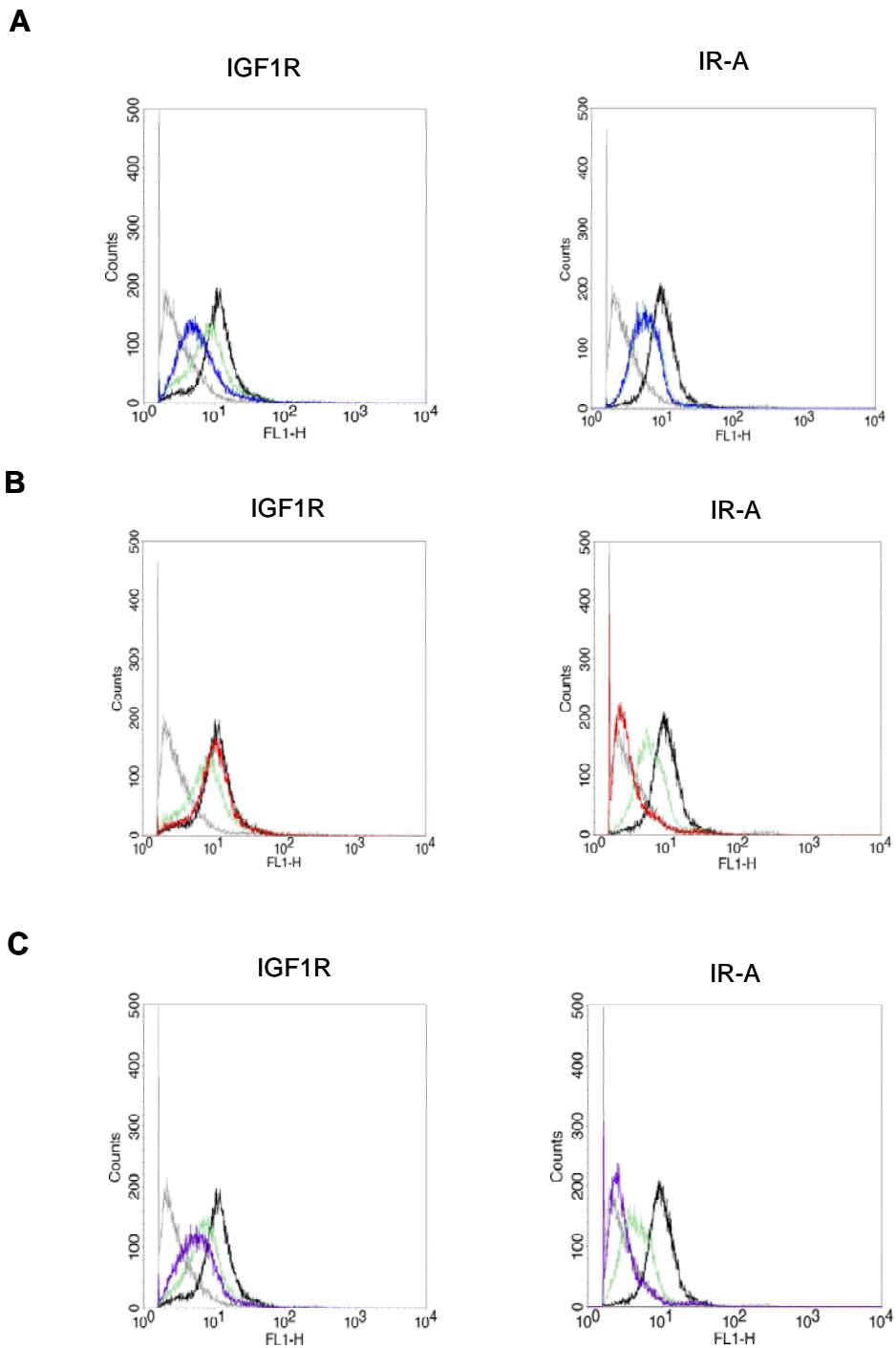
Figure 6.2 Surface receptor expression profiles of siRNA transfected SW480 cells

*Cell surface expression of IGF1R [left hand side] and IR-A [right hand side] was assessed by indirect-immunofluorescent flow cytometry, as previously described [Figure 6.1]. [**A**], Effect of 10nM control [green] and 10nM IGF1R siRNA [blue] transfection on IGF1R and IR-A expression compared to untransfected [black] cells. [**B**], Effect of 10nM control [green] and 10nM IR siRNA [red] transfection on IGF1R and IR-A expression compared to untransfected [black] cells. [**C**], Effect of sequential transfection of 10nM IGF1R siRNA followed the next day by 10nM IR siRNA [purple] on cell surface expression of IGF1R and IR compared to sequentially control siRNA transfected [green] and untransfected [black] cells. In all histograms light grey represents cells labeled with negative control IgG antibody demonstrating any cellular auto-fluorescence. Results are representative of three independent experiments conducted on separate occasions.*

6.2.2   The effect of IGF1R and IR-A knock-down on clonogenic survival and sensitivity to butyrate

Clonogenic survival assays determine the ability of cells to proliferate and give rise to colonies[347]. These assays are routinely used to gauge the effectiveness of cytotoxic drugs and also as an *in vitro* indicator of tumourigenic growth *in vivo*[347, 348]. Therefore, the effect of siRNA-mediated receptor knock-down on the ability of SW480 cells to undergo clonogenic survival was assessed. To assess whether receptor knock-down affected SW480 sensitivity to butyrate, parallel cultures were treated with 5mM butyrate for 24 or 48 hours prior to being returned to butyrate-free growth media.

Results from the clonogenic assays are presented in Figure 6.3 along with a representative Western blot indicating the level of receptor protein expression in the cells used in the assays. Transfection with control siRNA did result in small perturbations in both IGF1R and IR-A expression [Figure 6.3 A]. However, transfection with either a single 10nM dose, or sequential 10nM doses of control siRNA did not significantly alter the ability of SW480 cells to give rise to colonies compared to untransfected cells. This suggested the small effect that transfection with control siRNA had on IGF1R and IR-A receptor expression was not sufficient to alter the biological responses of the cells. Transfection with either IR or IGF1R siRNA resulted in significant decrease of the target receptors. Dual transfection resulted in comparable knock-down to that obtained when the receptors were targeted singly, indicating that dual transfection did not alter the efficacy of the IGF1R siRNA duplex. Doublet bands were consistently observed in IGF1R blots following SDS-PAGE [Figures 6.3 A, 6.4 A, 6.5 A, 6.6 A, 6.7 A, 6.8 A]. These were most likely due to the presence of both phosphorylated and non-phosphorylated IGF1R β-subunits.

Compared to untransfected and control transfected cells, IGF1R knock-down significantly decreased the ability of SW480 cells to proliferate and give rise to colonies when grown in 10% FCS [$p<0.001$, untreated, Figure 6.3 B]. Although knock-down of the IR-A decreased the ability of SW480 cells to undergo clonogenic survival in the presence of 10% FCS [untreated, Figure 6.3 C], this decrease was not as marked as that seen in the IGF1R transfected cells and was not statistically significant from the 10nM control transfected cells [$p>0.05$; 95%CI -65.16 to 78.44]. It did, however, differ significantly from untransfected cells [$p<0.001$]. Dual knock-down of both the
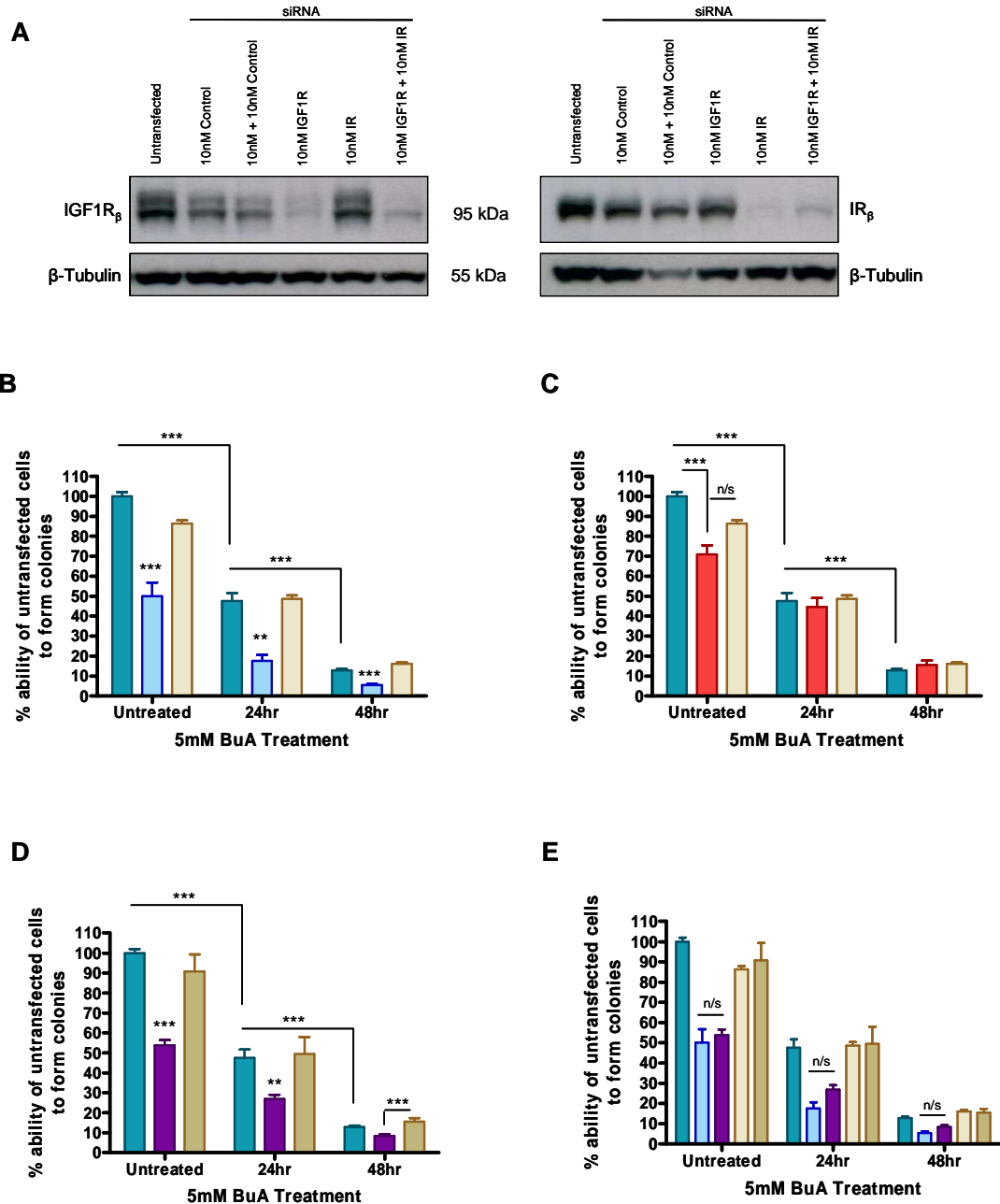
Figure 6.3 The effect of siRNA mediated receptor knock-down on SW480 clonogenic survival and sensitivity to butyrate

Clonogenic survival assays were used to assess the effect siRNA mediated receptor knock-down had on the ability of single cells to proliferate and give rise to colonies. Cells were grown in the presence of butyrate [5mM] for either 24 or 48 hours as described in section 2.2.1.2.6. A representative Western blot [A] from the three independent experiments conducted on separate occasions demonstrates the level of receptor protein knock-down in siRNA transfected cells used in the clonogenic assays [B – E]. Statistical significance was determined by ANOVA using Bonferroni's multiple comparison test and p values are represented as follows: * p<0.05, **p<0.01, *** p<0.001. Results are the mean from three individual experiments conducted on separate occasions plotted as the percentage ability of untransfected cells to form colonies, ± SEM. Coloured bars are representative of the following transfection conditions: untransfected [ ], 10nM control siRNA transfected [ ], 10nM control + 10nM control siRNA transfected [ ], 10nM IGF1R siRNA transfected [ ], 10nM IR siRNA transfected [ ], 10nM IGF1R siRNA + 10nM IR siRNA transfected [ ].

IGF1R and IR-A significantly decreased the ability of SW480 cells to proliferate and give rise to colonies compared to both untransfected and sequentially transfected control cells [p<0.001, Figure 6.3 D].

Treatment with 5mM butyrate had a dramatic effect on the ability of SW480 cells to undergo clonogenic survival. Twenty-four hour treatment with 5mM butyrate led to a 50% reduction in the ability of untransfected and control transfected cells to form colonies, while treatment for a total of 48 hours led to an approximately 85% reduction in colony formation. Knock-down of the IGF1R significantly increased SW480 sensitivity to 5mM butyrate at both 24 and 48 hour treatment time points [p<0.01 and p<0.001, respectively]. Interestingly, knock-down of the IR did not alter the sensitivity of SW480 cells to 5mM butyrate for either of the two treatment periods. Dual-targeting of the IGF1R and IR also resulted in increased sensitivity to 5mM butyrate at both 24 and 48 hour treatment lengths compared to untransfected and control transfected cells [p<0.01]. However, dual-targeting of the IGF1R and IR did not confer any additional decrease in clonogenic survival or increase sensitivity to butyrate compared to cells with targeted knock-down of the IGF1R alone [Figure 6.3 E].

6.2.3 The effect of knocking-down IGF1R expression on ligand stimulated cell survival from butyrate induced apoptosis

Cell viability assays were used to assess the effect of IGF1R receptor knock-down on the ability of IGFs and insulin to rescue SW480 cells from the effects of butyrate [Figure 6.4]. Western blot and densitometry analysis [Figure 6.4 A and B] of lysates from cells remaining after plating demonstrated an approximate 60% decrease in IGF1R expression following transfection with 10nM IGF1R siRNA [p < 0.05 c.f control; p < 0.01 c.f. untransfected]. Transfection with control siRNA did not significantly affect either IGF1R or IR-A expression. In addition, IGF1R siRNA did not significantly alter IR-A expression. Butyrate treatment [5mM] decreased SW480 cell viability by approximately 90% [Figure 6.4 C]. IGF-I, IGF-II, and insulin stimulated rescue from butyrate induced apoptosis and was consistent with the response seen previously in SW480 cells [Chapter 4, Figure 4.5 B]. IGF-I stimulated the greatest survival, followed by IGF-II, then insulin, reflecting a response characteristic of signalling via the IGF1R or hybrid receptors. Control transfected cells behaved similar to untransfected cells, indicating although transfection with control siRNA did

142
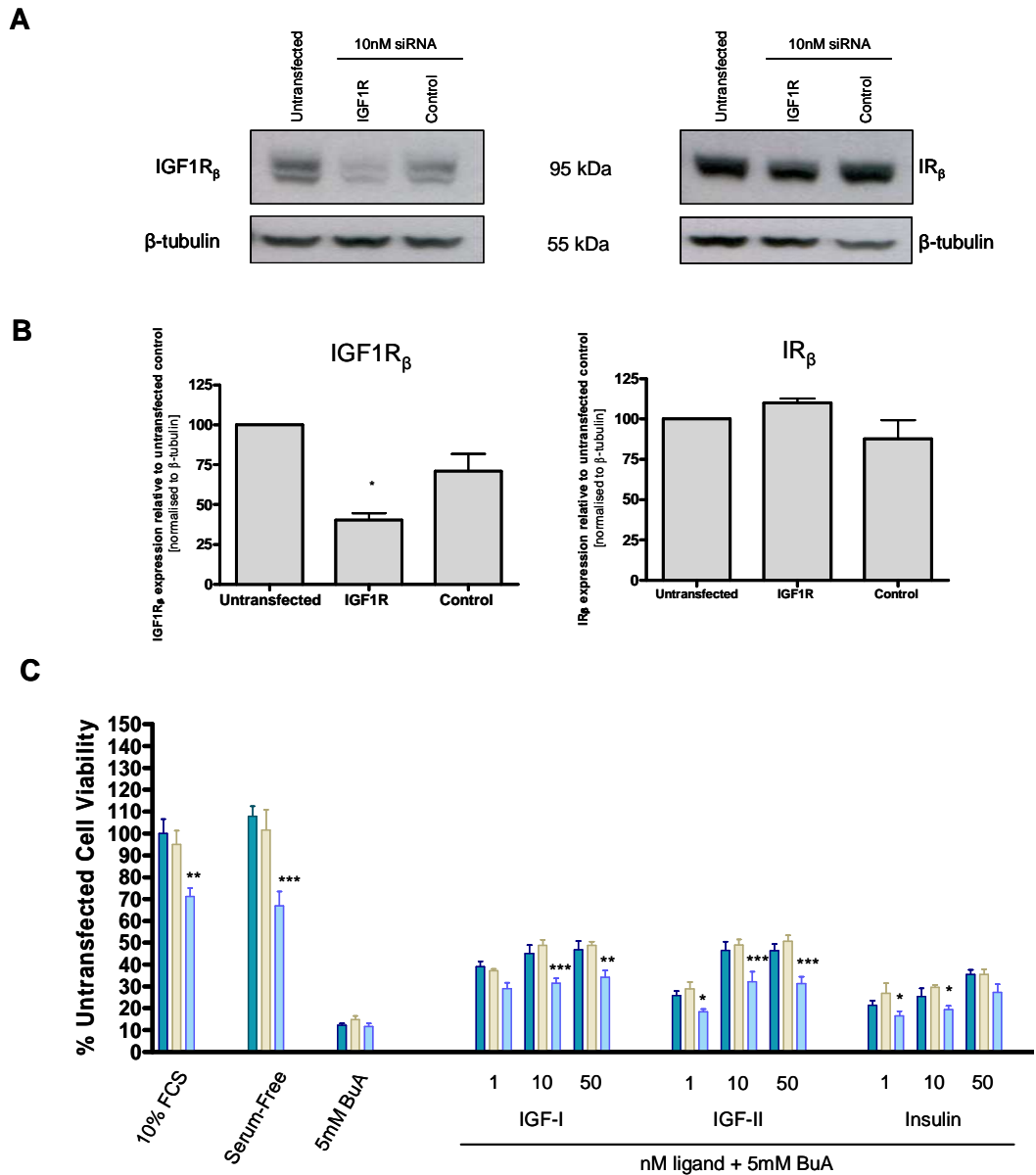
Figure 6.4 Knock-down of the IGF1R results in decreased ability of SW480 cells to respond to ligand stimulated cell survival from butyrate-induced apoptosis

*Butyrate-treated [5mM] cells were incubated in the presence or absence of increasing concentrations of IGF-I, IGF-II, and insulin as described in section 2.2.1.2.3. A representative Western blot [**A**], with accompanying densitometry data normalized to beta-tubulin expression [**B**] from the three independent experiments conducted on separate occasions are displayed above. [**C**] The effect of IGF1R knock-down on the ability of SW480 cells to respond to ligand stimulated cell survival. Statistical significance compared to untransfected cells was determined by ANOVA using Bonferroni's multiple comparison test and p values are represented as follows: * p<0.05, **p<0.01, *** p<0.001. Results are the mean from three individual experiments conducted on separate occasions plotted as the percentage cell viability of untransfected cells to 10% FCS, ± SEM. Coloured bars are representative of the following transfection conditions: untransfected [▬], 10nM control siRNA transfected [▭], and 10nM IGF1R siRNA transfected [▭].*

have some effect on receptor expression, these effects were insufficient to have a biological influence. Interestingly, although IGF1R knock-down significantly decreased SW480 cell viability in 10% FCS and serum-free media, it did not result in further sensitivity to 5mM butyrate, in this particular assay. IGF1R knock-down inhibited the ability of all three ligands to stimulate cell survival from butyrate. Only the response to IGF-II was significantly decreased across all concentrations. IGF1R knock-down significantly decreased the response to 10 and 50nM IGF-I [p < 0.001 and p < 0.01, respectively], and 1 and 10nM insulin [p < 0.05].

6.2.4 The effect of silencing the IR-A on ligand-stimulated cell survival from butyrate-induced apoptosis

Cell viability assays were used to assess the effects of IR-A knock-down on the ability of ligand to stimulate SW480 cell survival from butyrate [Figure 6.5]. Western blot and densitometric analysis [Figure 6.5 A and B] demonstrated transfection of SW480 cells with 10nM IR siRNA resulted in approximately 66% decrease in IR-A expression [p < 0.05]. Transfection with control siRNA did not significantly affect either IGF1R or IR-A expression. In addition, IR siRNA did not significantly alter IGF1R expression. Untransfected and control transfected cells responded to all three ligands as observed previously. Cell viability of IR siRNA transfected cells was significantly higher [p < 0.001] than untransfected cells when treated with butyrate, indicating these cells had decreased sensitivity to the effects of butyrate. Silencing the IR-A also resulted in increased ability of SW480 cells to respond to ligand stimulation. Increased cell viability was observed in response to all three ligands, however only IGF-I and IGF-II stimulated a significant increase in survival across all three concentrations. In response to insulin, significant increase in survival was only observed in 1 and 50nM treatments [p < 0.05]. Interestingly, the response seen in IR siRNA transfected cells was characteristic of IGF1R signalling, in that IGF-I elicited the greatest response, followed by IGF-II, then insulin. These data suggested silencing the IR-A augmented signalling outcomes of the IGF1R.
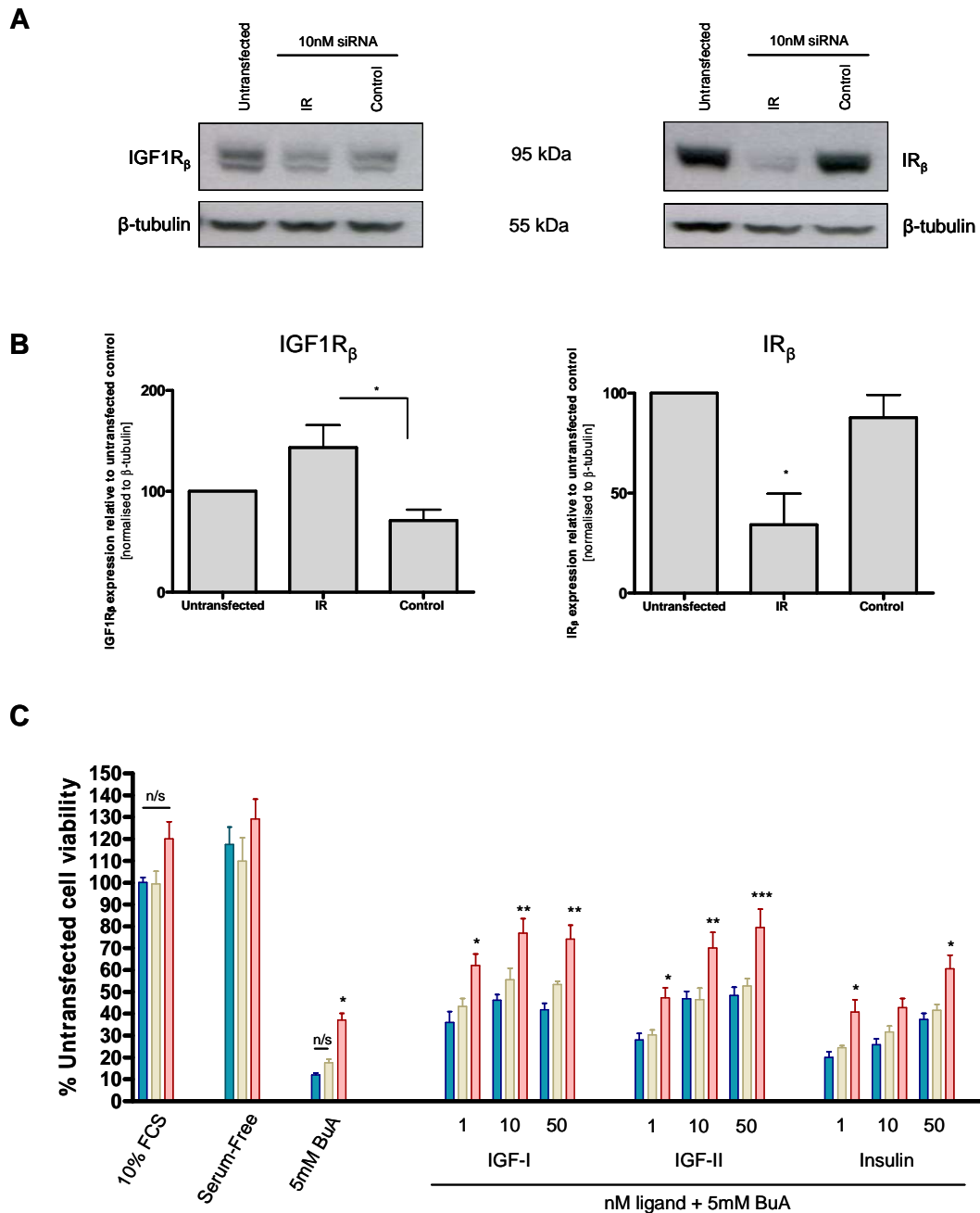
Figure 6.5 Knock-down of the IR-A results in increased ability of SW480 cells to respond to ligand stimulated cell survival from butyrate-induced apoptosis

*Butyrate-treated [5mM] cells were incubated in the presence or absence of increasing concentrations of IGF-I, IGF-II, and insulin as described in section 2.2.1.2.3. A representative western blot [A], with accompanying densitometry data normalized to beta-tubulin expression [B] from the three independent experiments conducted on separate occasions are displayed above. [C] The effect of IR-A knock-down on the ability of SW480 cells to respond to ligand stimulated cell survival. Statistical significance compared to untransfected cells was determined by ANOVA using Bonferroni's multiple comparison test and p values are represented as follows: * $p<0.05$, **$p<0.01$, *** $p<0.001$. Results are the mean from three individual experiments conducted on separate occasions plotted as the percentage cell viability of untransfected cells to 10% FCS, ± SEM. Coloured bars are representative of the following transfection conditions: untransfected [ ], 10nM control siRNA transfected [ ], and 10nM IR siRNA transfected [ ].*

A

	Untransfected	10nM siRNA	
		IGF1R + IR	Control + Control

IGF1R$_\beta$

β-tubulin

95 kDa

55 kDa

IR$_\beta$

β-tubulin

B

IGF1R$_\beta$

IR$_\beta$
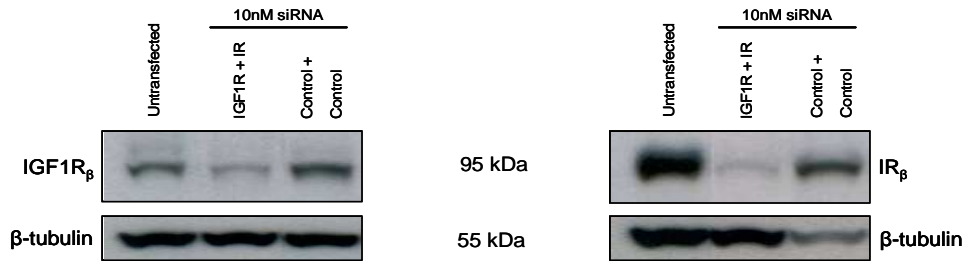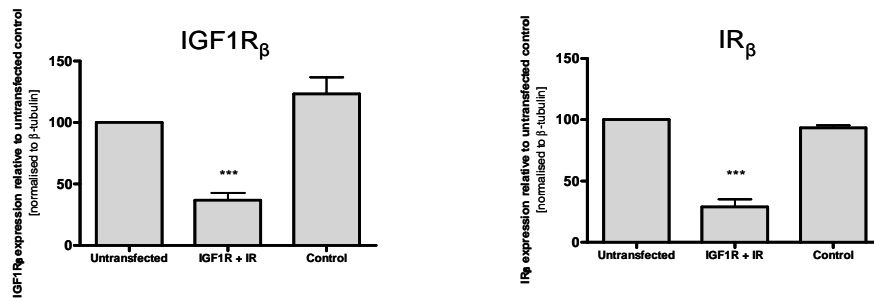
C

Figure 6.6 The effect of dual IGF1R and IR-A knock-down on ligand stimulated SW480 cell survival from butyrate-induced apoptosis

*Butyrate-treated [5mM] cells were incubated in the presence or absence of increasing concentrations of IGF-I, IGF-II, and insulin as described in section 2.2.1.2.3. A representative western blot [**A**], with accompanying densitometry data normalized to beta-tubulin expression [**B**] from the three independent experiments conducted on separate occasions are displayed above. The effect of dual IGF1R and IR-A knock-down on the ability of SW480 cells to respond to ligand stimulated cell survival is shown in [**C**]. Although there was a general trend of decreased ability of ligand to stimulate cell survival with dual knock-down, this was found to be statistically significant only upon treatment with either 50nM IGF-I [$p<0.001$], 50nM IGF-II [$p<0.01$], or 10nM insulin [$p<0.01$], denoted by hashes [#]. Although sequential transfection with 10nM control siRNA did not significantly alter receptor expression, it led to significantly increased cell viability compared to untransfected cells; p values denoted as follows: a = $p<0.05$, b = $p<0.01$, c = $p<0.001$. Statistical significance between control transfected cells and dual receptor knock-down cells are denoted by asterisks where * = $p<0.05$, ** = $p<0.01$, and *** = $p<0.001$. Statistical significance in all cases was determined by ANOVA using Bonferroni's multiple comparison test. Results are the mean from three individual experiments conducted on separate occasions plotted as the percentage maximal proliferation of untransfected cells to 10% FCS, ± SEM. Coloured bars are representative of the following transfection conditions: untransfected [▬], 10nM control + 10nM control siRNA transfected [▭], and 10nM IGF1R siRNA + 10nM IR siRNA transfected [▬].*

6.2.5 The effect of dual knock-down of IGF1R and IR-A on ligand stimulated cell survival from butyrate-induced apoptosis

Although SW480 cells transfected with IGF1R siRNA demonstrated decreased ability to respond to ligand, ligand still stimulated survival from the effects of butyrate. In order to assess the contribution of the IR-A in signalling this residual response, SW480 cells were sequentially transfected with 10nM IGF1R siRNA followed 24 hours later by transfection with 10nM IR siRNA. Furthermore, these studies enabled investigation of whether dual targeting of both receptors conferred any additional inhibition to ligand stimulated cell survival from butyrate.

Receptor expression post-transfection was assessed by Western blot [Figure 6.6 A]. Sequential transfection of 10nM non-silencing control siRNA did not have a significant effect on either IGF1R or IR-A expression compared to untransfected SW480 cells. Sequential transfection with 10nM IGF1R siRNA followed by 10nM IR siRNA significantly decreased both IGF1R [approximately 63% reduction, $p < 0.01$] and IR-A [approximately 71% reduction, $p<0.001$] expression [Figure 6.6 B]. Dual knock-down of the IGF1R and IR-A was as effective at knocking down each receptor as individual targeting alone, suggesting that dual transfection did not alter the efficacy of either of the two siRNA duplexes. Untransfected SW480 cells behaved similarly to previous experiments, with ligand stimulated cell survival following an IGF1R type response [Figure 6.6 C]. Sequential transfection with control siRNA resulted in increased cell viability [significance compared to untransfected cells is indicated by lower case letters]. This was of interest as transfection did not have any obvious effect on either IR-A or IGF1R expression when assessed by Western blot [Figure 6.6 A]. Dual IGF1R and IR-A knock-down decreased cell viability compared to control cells [significance is indicated by asterisks]. Dual IGF1R and IR-A knock-down did result in decreased responses to ligand stimulation compared to untransfected cells, however this was only statistically significant at 50nM concentrations of IGF-I and IGF-II, 10nM insulin, and 10% FCS treatments [indicated in the figure by hashes '#'].
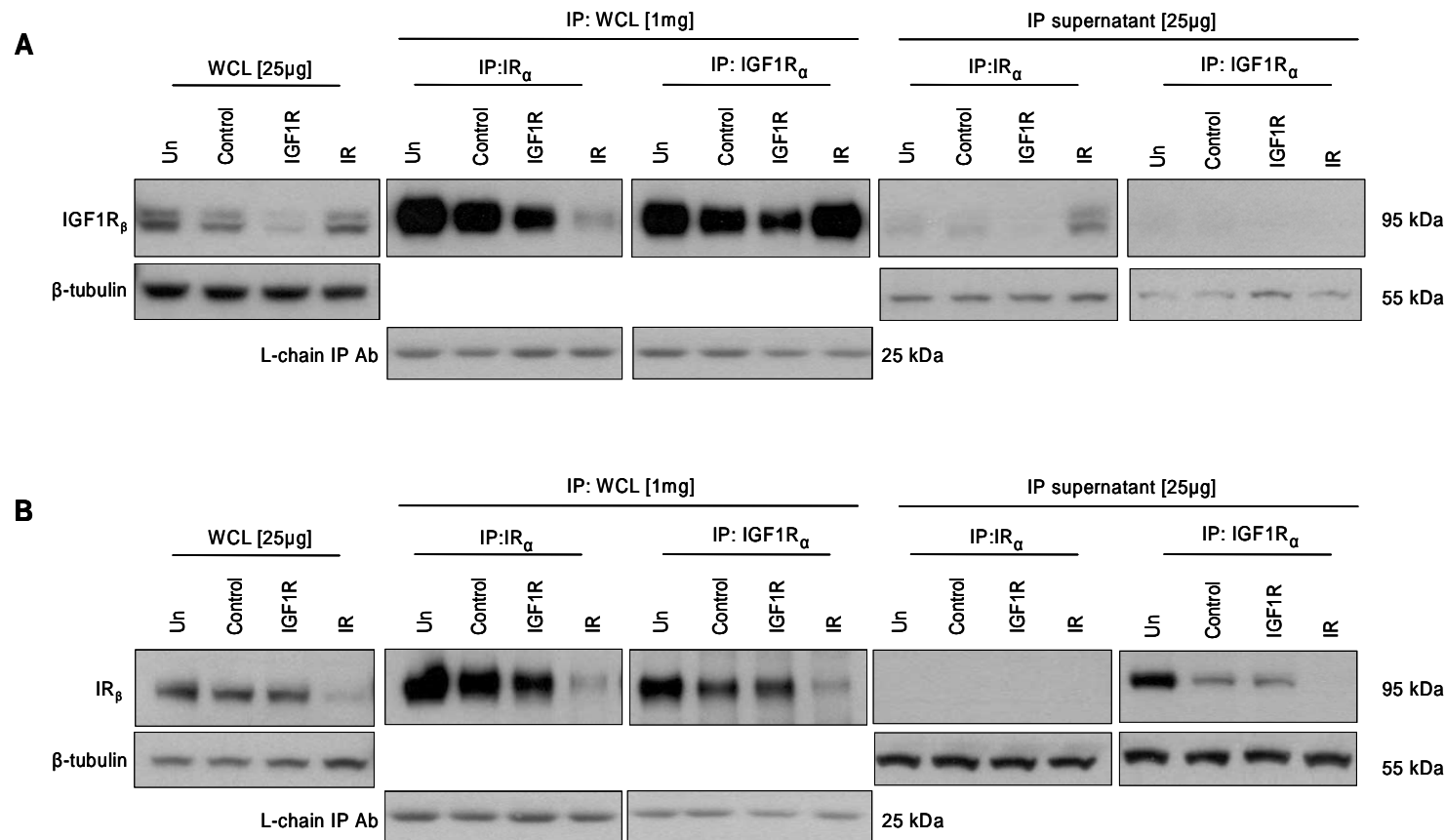
Figure 6.7 Down-regulation of either the IGF1R or IR-A leads to the disruption of the formation of hybrid receptors in SW480 cells

Forty eight hours post-transfection with 10nM siRNA [as indicated above the lanes] SW480 cell monolayers were lysed and pre-cleared prior to immunoprecipitation [IP] overnight with antibodies directed against either the IGF1Rα [24-60] or IRα [83-14]. Whole cell lysates [WCL] and immunoprecipitates [IP] were resolved by SDS-PAGE and IGF1R$_\beta$ [A] or IR-A$_\beta$ [B] were detected by immunoblotting with anti-IGF1R$_\beta$ [Cell Signaling] and anti-IR$_\beta$ [C-19] antibodies, respectively. Hybrid receptors were detected by immunoblotting for the opposite receptor targeted in the IP. Immunoblotting for the same receptor targeted in the IP would be indicative of both hybrid receptors and homodimers. L-chain, light chain of IP antibody, demonstrates equal amounts of antibody used in IP and acts as a load control in the immunoblots. Immunoblots of the IP supernatants indicate the level of immunodepletion achieved by the IP.
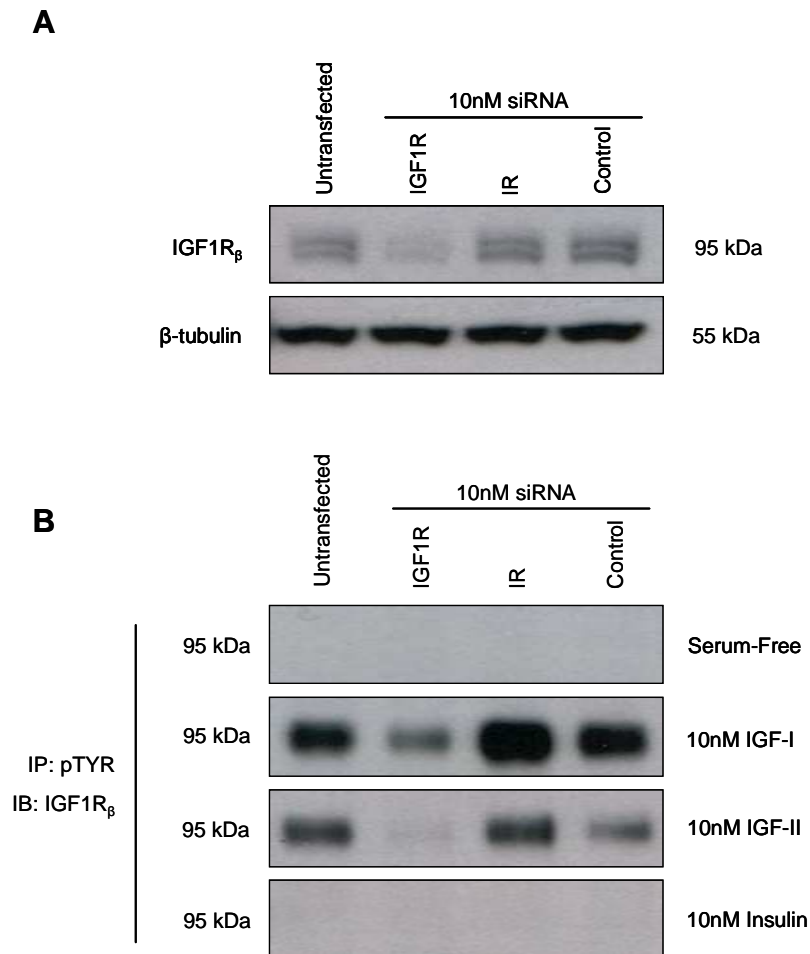
Figure 6.8 Effects of IGF1R and IR-A down-regulation on ligand stimulated IGF1Rβ phosphorylation

*Thirty two hours post-transfection, SW480 cells were serum-starved overnight prior to stimulation with 10nM ligand for 10 minutes. [**A**] Whole-cell lysates [25µg/lane] were prepared and subjected to SDS-PAGE and then immunoblotted and assayed for receptor knock-down. [**B**] Pre-cleared whole-cell lysates [1mg protein] were immunoprecipitated [IP] overnight with an anti-phosphotyrosine antibody [pTYR-100]. Immunoprecipitates were then resolved by SDS-PAGE and phosphorylated IGF1Rβ detected by immunoblotting [IB] with anti-IGF1Rβ antibody [Cell Signaling, see Table 2.7].*
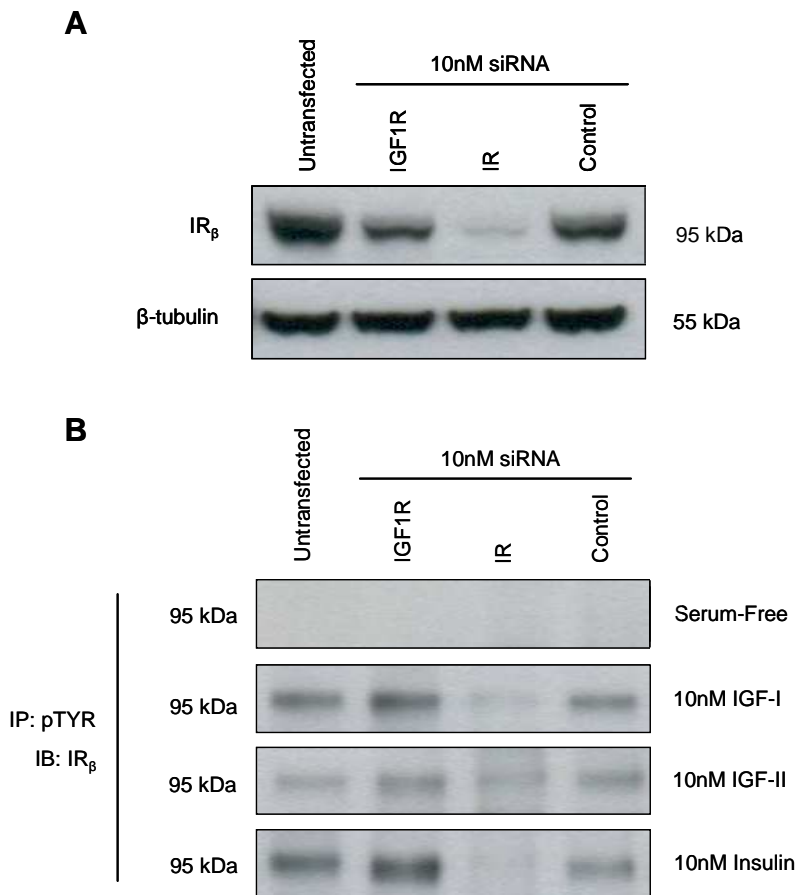
Figure 6.9 Effects of IGF1R and IR-A down-regulation on ligand stimulated IR-Aβ phosphorylation

*Thirty two hours post-transfection, SW480 cells were serum-starved overnight prior to stimulation with 10nM ligand for 10 minutes. [**A**] Whole-cell lysates [25μg/lane] were prepared and subjected to SDS-PAGE and then immunoblotted and assayed for receptor knock-down. [**B**] Pre-cleared whole-cell lysates [1mg protein] were immunoprecipitated [IP] overnight with an anti-phosphotyrosine antibody [pTYR-100]. Immunoprecipitates were then resolved by SDS-PAGE and phosphorylated IR-Aβ detected by immunoblotting [IB] with anti-IRβ antibody C-19 [see Table 2.7].*

6.2.6   The effect of IGF1R and IR-A knock-down on hybrid receptor formation

Since hybrid receptors form via random dimerisation as a function of the molar fractions of the IGF1R and IR[139-141], altering expression of either the IGF1R or IR-A would be expected to affect hybrid receptor expression. The effect of siRNA mediated knock-down of the IGF1R or IR-A on hybrid receptor expression was therefore assessed forty-eight hours after transfection by immunoprecipitation antibodies directed against the alpha-subunit of either the IGF1R or IR [24-60 and 83-14, respectively]. Hybrid receptors were immunodetected by blotting for the opposite receptor to that targeted in the co-immunoprecipitation.

Results demonstrating the effect of down-regulation of either the IGF1R or IR-A on hybrid receptor expression are presented in Figure 6.7. Transfection with 10nM IGF1R siRNA resulted in considerable IGF1R knock-down, while transfection with either control or IR siRNA did not significantly alter IGF1R expression. A similar level of hybrid receptor expression was observed in untransfected and control transfected SW480 cell lysates, while knock-down of either the IGF1R or IR-A resulted in decreased hybrid receptor expression compared to untransfected and control transfected SW480 cells. Silencing of the IR-A resulted in a more prominent decrease in hybrid receptor expression than silencing of the IGF1R. Silencing of the IR-A was accompanied by increased in IGF1R homodimer formation, as evidenced by increased detection of IGF1R in the supernatants of anti-IR$_\alpha$ immunoprecipitates.

6.2.7   The effect of siRNA-mediated receptor knock-down on ligand-stimulated receptor tyrosine phosphorylation

Figures 6.8 and 6.9 show the effect of siRNA-mediated receptor knock-down on ligand-stimulated IGF1R and IR-A tyrosine phosphorylation, respectively. Data demonstrating 10nM IGF-I, IGF-II, or insulin stimulation of IGF1R tyrosine phosphorylation in SW480 are shown in Figure 6.8. In untransfected SW480 cells, IGF-I stimulated IGF1R phosphorylation to a greater extent than IGF-II. Insulin stimulation did not cause any appreciable phosphorylation of the IGF1R beta-subunit. Transfection of SW480 cells with control siRNA did not appreciably alter the ability of IGF1R to be activated by ligand. Knocking-down the IGF1R by transfection with 10nM IGF1R siRNA, decreased

phosphorylation of the IGF1R by both IGF-I and IGF-II, consistent with diminished receptor expression. Knock-down of the IR-A resulted in increased activation of the IGF1R by IGF-I and possibly IGF-II [Figure 6.8, lane denoted 'IR'].

The effects of receptor knock-down on IR-A tyrosine phosphorylation by either 10nM IGF-I, IGF-II, or insulin are shown in Figure 6.9. In untransfected cells, insulin stimulated tyrosine phosphorylation of the IR-A to a greater extent than IGF-I. IGF-II had lesser effects on IR-A tyrosine phosphorylation. This observation was unusual as it does not fit the conventional phosphorylation pattern for IGF activation of the IR-A, where the rank order of IR-A activation is observed to be insulin > IGF-II > IGF-I[304]. Transfection with control siRNA did not affect the ability of the ligands to activate the IR. Knock-down of the IR-A by transfection with IR siRNA resulted in decreased phosphorylation of the IR-A by all three ligands, an observation consistent with diminished receptor expression. Transfection with IGF1R siRNA did not affect IGF-I or IGF-II phosphorylation of the IR-A, but did result in increased phosphorylation of the IR-A by insulin [Figure 6.9, lane denoted 'IGF1R'].

6.3   Discussion

The overall goal of this study was to examine whether signaling via the IR-A could compensate for the targeted loss of the IGF1R. Inhibition of the IGF1R is gaining attention as a potential anti-cancer therapeutic strategy[239, 241, 244-246]. An important determinant in the likely success of these therapeutic strategies is the identification and circumnavigation of potential mechanisms by which IGF1R signaling could be rendered ineffective, such as compensatory signaling via other receptor tyrosine kinases, like the IR-A. There is already some evidence in the literature to suggest that this may be possible. Down-regulation of the IGF1R was demonstrated to increase the sensitivity of breast cancer cells to insulin[151]. However, dual targeting was not examined. Vella *et al* 2002 demonstrated that inhibitory antibodies towards both the IR and IGF1R were more effective together than either antibody alone at inhibiting IGF-II stimulated cell growth in B-CPAP thyroid cancer cells[123]. In addition, a dual IGF1R and IR tyrosine kinase inhibitor was shown to inhibit xenograft tumour growth in vivo[269]. The present study builds on these findings. By using an siRNA

Figure 6.10 Schematic representation of how siRNA mediated silencing of either the IGF1R or IR-A affects both homodimer and hybrid receptor expression

*Hybrid receptors form randomly between one αβ monomer of the IGF1R [blue] and one αβ monomer of the IR-A [red] at the endoplasmic reticulum in a fashion that reflects the molar ratios of the two receptors19-21. Untransfected SW480 cells [**A**], IGF1R is expressed to a slightly greater extent than the IR-A. Therefore, more IR-A is incorporated into hybrids than IR-A homodimers. The overall biological response to ligand stimulation in these cells is observed to be characteristic of IGF1R signalling.*

*In the IGF1R siRNA transfected SW480 cells [**B**], there is an overall decrease in IGF1R expression, the majority of any remaining IGF1R will therefore be incorporated into hybrids. The expression of IR-A is unaffected, but, there is less IGF1R to form hybrids with, and therefore there are increased levels of IR-A homodimers expressed. This results in decreased IGF1R signalling potential, and increased IR-A signalling potential. The overall biological response to ligand stimulation is decreased in cells displaying this receptor expression profile.*

*In the IR siRNA transfected SW480 cells [**C**], where there is an overall decrease in IR-A expression, the majority of any remaining IR-A will be incorporated into hybrids. The expression of IGF1R is unaffected, but, there is less IR-A to form hybrids with, therefore there is increased levels of IGF1R homodimers. This results in decreased IR-A signalling potential and increased IGF1R signalling potential. The overall biological response to ligand stimulation in these cells is increased compared to that of untransfected SW480 cells and was observed to be characteristic of IGF1R signalling.*

*In the dual IGF1R and IR siRNA transfected SW480 cells [**D**], there is an overall decrease in both IGF1R and IR-A expression levels compared to untransfected cells. However, IR-A knock-down was more efficient than IGF1R knock-down, and therefore dual transfected cells display a receptor expression profile where although overall levels of both receptors are decreased, the IGF1R is still expressed to a greater extent than the IR-A. While biological responses in these cells are decreased compared to untransfected cells, there was no additional inhibition of cell growth or survival compared to cells where the IGF1R was targeted singly. Because targeting the IR-A is more effective than targeting the IGF1R, the balance of remaining receptors expressed is pushed towards the formation of IGF1R homodimers.*

A: In 'normal' untransfected SW480 cells

IGF1R homodimer   :   IGF1R/IR-A hybrid receptors   :   IR-A homodimer

Extracellular
Cell Membrane
Intracellular

Biological response to ligand is characteristic of IGF1R type response

[IGF-I > IGF-II > Insulin]

B: in SW480 cells transfected with siRNA targeting the IGF1R

IGF1R homodimer   :   IGF1R/IR-A hybrid receptors   :   IR-A homodimer

Extracellular
Cell Membrane
Intracellular

Decreased biological response

C: in SW480 cells transfected with siRNA targeting the IR

IGF1R homodimer   :   IGF1R/IR-A hybrid receptors   :   IR-A homodimer

Extracellular
Cell Membrane
Intracellular

Increased biological response

D: in SW480 cells transfected with siRNA targeting the IGF1R and IR

IGF1R homodimer   :   IGF1R/IR-A hybrid receptors   :   IR-A homodimer

Extracellular
Cell Membrane
Intracellular

Biological response is decreased but not to the extent seen when IGF1R targeted singly

based approach, unlike antibody or small molecule approaches, either the IGF1R or IR-A could be targeted individually without directly affecting the other. This approach enabled the manipulation of the expression of IGF1R, IR-A, and IGF1R/IR-A hybrids, effectively producing four different receptor profile models in an SW480 cell background [Figure 6.10]. These cells were then used to examine receptor activation by ligand, and biological outcomes to signaling. Therefore, not only did this approach enable the possibility of compensatory IR-A signaling to be investigated, it also enabled the interactions between the IR-A and IGF1R to be examined.

The importance of signaling via the IGF1R is already well established in terms of determining its role in signaling growth, survival from apoptosis, and migratory outcomes[22, 58, 344, 349]. In the present study, single knock-down of the IGF1R in SW480 cells served as a benchmark for subsequent experiments, by illustrating the potential for the IGF1R to signal proliferative and survival outcomes in the SW480 cells. Knock-down of the IGF1R significantly inhibited the ability of SW480 cells to undergo clonogenic survival [untreated, Figure 6.3 B]. Furthermore, silencing of the IGF1R resulted in significantly increased sensitivity to 5mM butyrate [Figure 6.3 B], correlating with literature demonstrating that signaling via the IGF1R can protect cells from induction of apoptosis from a range of cytotoxic drugs[67, 72-74]. In addition, knock-down of the IGF1R inhibited the ability of insulin, IGF-I, and IGF-II to stimulate SW480 cell survival from butyrate-induced apoptosis [Figure 6.4 C]. While silencing the IGF1R resulted in significant effects on the ability of SW480 cells to respond to biological stimuli, it did not completely ablate the response of these cells, suggesting that the IR-A may compensate for loss of the IGF1R. A caveat of this interpretation is that IGF1R knock-down was not total. IGF1R siRNA transfection resulted in only approximately 60% decrease in IGF1R expression. These responses seen in the knock-down cells were therefore due, in part, to residual IGF1R expression, not just the IR-A.

Knock-down of the IGF1R resulted in increased activation of the IR-A by insulin, as indicated by increased phosphorylation of the IR-A beta-subunit in IGF1R siRNA transfected cells [Figure 6.9 B]. These results correlate with those published recently by Zhang *et al* 2007, where IGF1R down-regulation was observed to increase sensitivity of LCC6 breast cancer cells to insulin[151]. Increased activation of the IR in LCC6 cells [where the IGF1R had been specifically targeted utilizing siRNA] was interpreted to be due to the disruption of hybrid receptor formation, by the decrease in IGF1R expression, and therefore the movement of receptor formation to favor IR homodimerisation[151].
156

Similar results were observed in the present study, where IGF1R targeting by siRNA was observed to result in decreased hybrid receptor formation [Figure 6.7]. However no discernable increase in IR-A homodimers was observed [Figure 6.7]. This could be due to the non-specific impact that transfection had on IR-A expression in the SW480 cell line [Figures 6.1 and 6.2], such that when the IGF1R was specifically targeted, the difference in expression of the two receptor types was not sufficient for the effect on IR-A homodimerisation to be observed in the supernatants of anti-IGF1R$_\alpha$ antibody immunoprecipitates [Figure 6.7]. This increased activation of the IR-A through increased IR-A homodimer formation, as a result of IGF1R down-regulation and decreased hybrid receptor formation, may be one way the IR-A could compensate for the targeted loss of the IGF1R.

By targeting the IR-A individually, the relative contribution of signaling via the IR-A on SW480 cell proliferation and survival was examined. These experiments also demonstrated how IR-A expression could influence IGF1R signaling. Silencing the IR-A by transient transfection with siRNA was efficient and resulted in between 60 - 90% decrease in IR-A receptor expression [Figures 6.1 – 6.3 and 6.5]. Although silencing of the IR-A did result in decreased ability of SW480 cells to undergo clonogenic survival when grown in 10% FCS [untreated, Figure 6.3 D], this was only statistically significant when compared to untransfected cells and not control duplex transfected cells. Thus it was not surprising that knock-down of the IR-A did not affect SW480 sensitivity to treatment with 5mM butyrate at either 24 or 48 hour treatment periods [Figure 6.3 D]. However, in the cell viability assays, knock-down of the IR-A decreased SW480 sensitivity to 5mM butyrate [Figure 6.5 C]. The difference in these two observations could be due to the sensitivity of the two different techniques utilised. Indeed, silencing of the IR-A led to significantly increased ability of SW480 cells to respond to ligand stimulated cell survival from butyrate-induced apoptosis compared to both untransfected and control duplex transfected cells [Figure 6.5 C]. This augmented response to ligand followed an IGF1R type response, where IGF-I stimulated the greatest response, followed by IGF-II, then insulin, suggesting that not only did the IGF1R compensate for the loss of the IR-A, but the IR-A in someway attenuated signaling via the IGF1R.

This attenuation of IGF1R signaling could possibly be accounted for by the formation of hybrid receptors. In cells co-expressing the IR and IGF1R, hybrid receptors form randomly in a fashion that reflects the molar ratios of the two receptors[139-141]. Therefore, if expression of one receptor is

reduced [in this case, the IR-A through siRNA mediated silencing] there would be an overall decrease in hybrid receptor expression and an increase in the reciprocal receptor homodimer expression [in this case, IGF1R homodimers]. This was observed to be the case [Figure 6.7]. Decreased expression of the IR-A led to increased expression of classical IGF1R homodimers as evidenced by elevated levels of IGF1R beta-subunit detected in the supernatants of anti-IR$_\alpha$ immunoprecipitates, and indirectly demonstrated by increased detection of the IGF1R in anti-IGF1R$_\alpha$ immunoprecipitates [Figure 6.7]. Therefore, in IR siRNA transfected cells, there was a movement away from hybrid receptor expression towards increased IGF1R homodimer expression. This was matched by an increased biological response to ligand that reflected increased activation of the IGF1R. When ligand stimulated activation of the IGF1R was assessed, silencing of the IR-A led to hyper-phosphorylation of IGF1R beta-subunits in response to IGF-I and possibly IGF-II [Figure 6.8]. Despite the increased ability to respond to insulin in the cell survival assays [Figure 6.5], 10 minute stimulation with 10nM insulin did not result in appreciable phosphorylation of the IGF1R beta subunit. However, it is possible that this was due to either poor signal in response to insulin compared to IGF-I and IGF-II phosphorylation, or the 10 minute time point was insufficient to observe delayed activation of the IGF1R.

The data presented here suggest that signaling via hybrid receptors may not be as potent as signaling via IGF1R homodimers. This raises interesting questions about how cells interpret incoming signals from the IGF receptor family and how incoming signals from homodimers can be interpreted differentially to heterodimers, suggesting there must be some context-specific downstream mediator/s of signaling. Particularly when it is considered activation of hybrid receptors would lead to initiation of both IR and IGF1R downstream signaling cascades due to trans-autophosphorylation of both beta-subunits upon ligand binding[144-146, 149]. Very little is known about hybrid receptors due to the inability to study hybrid receptors without interference from either IR or IGF1R homodimers. Specific activation of hybrid receptors by ligands has only recently been able to be studied due to the use of BRET techniques[110, 149]. As yet, it is unknown whether there is a distinct physiological role for hybrid receptors. Furthermore, it still remains unclear whether hybrid receptors are able to potentiate signals that result in biological outcomes. It is assumed that signals originating from hybrid receptors are biologically relevant since inhibitory antibodies [47-9] towards hybrid receptors inhibit IGF-I stimulated growth of breast cancer cells[143]. However, that antibody was originally derived against the IR[350], also binds and inhibits the actions of ligand-stimulated cell

growth via the IR. Although 47-9 can inhibit IGF-I binding to hybrid receptors, its affinity is reported to be lower for hybrids than for IR homodimers[350]. In Chapter 3 it was demonstrated that IGF-I can stimulate biological responses via the IR. Therefore, experiments utilizing 47-9 may also be indicative of the inhibition of IGF-I signaling via the IR-A. Retrospective analysis of antibody cross-reactivity has also cast doubt on other hybrid receptor studies. Pandini et al 1999[143] utilised an anti-IR antibody [MA-20] as a specific IR homodimer capture antibody and immunoprecipitating antibody. However, this antibody has since been reported to also recognize hybrid receptors[151]. Therefore experiments utilizing MA-20 may be indicative of IR homodimers and hybrid receptors.

The results presented here are contrary to other published data where the IR-A was targeted in cells co-expressing the IGF1R[123, 125]. In those studies, inhibition of the IR-A led to decreased cell growth and proliferation[123, 125]. However there are several key differences between these studies that may help explain the differences in these observations. Firstly, the previous published studies utilised inhibitory antibodies directed towards the IR to inhibit ligand stimulated cell proliferation through the IR-A[123, 125]. Sachdev et al 2006, recently demonstrated that inhibitory antibodies directed against the IGF1R also down-regulated the IR, due to endocytosis of hybrid receptors. These antibodies also affected IR homodimers in close physical proximity to IGF1Rs in lipid rafts[257]. It is thus conceivable that antibodies directed towards the IR may similarly affect IGF1Rs. If the inhibitory antibodies against the IR also affected IGF1R signaling, there would be not only be decreased IR-A signaling but also decreased IGF1R and hybrid signaling which could contribute to the decreased cell growth and proliferation observed in those studies. Secondly, the present study utilised siRNA mediated down-regulation of the IR-A. This resulted in decreased IR-A protein expression that in turn, affected hybrid receptor formation, and also consequently increased IGF1R homodimer formation. Thus the present study demonstrated how IR-A expression itself can modulate and affect signaling via the IGF1R, whereas the studies utilising inhibitory antibodies demonstrate the effect of inhibiting ligand binding to and activating receptors that are already present. Thirdly, in the antibody inhibition studies, one study did not report on the expression levels of IR-A vs. IGF1R[123], whilst the other reported the IR-A was expressed to a 5-fold greater extent than the IGF1R[125]. If the IR-A was expressed to a far greater extent than the IGF1R, it is possible that inhibiting the IR-A would have a greater effect, as the cell would be losing its major source of incoming signal in response to IGF stimulation. Lastly, the antibody inhibition studies were

conducted in thyroid cancer cells, and it is entirely possible that the IR-A may play a more prominent role in thyroid cancer cells than in colorectal cancer cells.

Together, these results suggest signaling via the IGF1R is dominant to the IR-A, and that the IR-A may attenuate the IGF1R by sequestering it in hybrid receptors, since decreasing the IR-A, and consequently hybrid receptors, led to augmented signaling via the IGF1R. What does pose an interesting question, if signaling via the IR-A is interpreted to be secondary to signaling via the IGF1R, what happens in current anti-cancer therapeutic strategies that inhibit the IGF1R? Do they result in signaling arising predominantly from IR-A homodimers, thus mimicking the cells used in previous published studies that only express the IR-A? Is the IR-A able to compensate for the loss of the IGF1R, and provide a means for cancer cells to circumvent the effects of therapeutic targeting of the IGF1R? The present data suggests targeting the IGF1R alone did not completely abolish SW480 cellular responses to ligand. Although IGF1R silencing was not complete, the resultant response was indicative of both IR-A and residual IGF1R signaling. Dual silencing of the IGF1R and IR-A was therefore examined to assess what proportion of this residual response was due to the IR-A.

Dual silencing of the IGF1R and IR-A resulted in inhibition of clonogenic survival, and increased sensitivity to 5mM butyrate. However, dual silencing was no more effective than silencing of the IGF1R alone [Figure 6.3 E]. This suggests that the residual biological response observed in the single IGF1R siRNA transfected cells was due to the remnant IGF1R and not compensation by the IR-A, since the additional silencing of the IR-A did not confer any further inhibition. Unfortunately, the results of dual receptor knock-down on ligand-stimulated cell survival from butyrate-induced apoptosis were not as clear cut, due to the large effect observed with sequential control siRNA transfection [Figure 6.6 C]. Sequential transfection of 10nM non-silencing control siRNA resulted in increased SW480 cell viability compared to untransfected SW480 cells. A possible explanation for these observations can be found in the results from cell surface analysis of receptor expression in these dual transfected cells [Figures 6.1 and 6.2]. Transfection with control siRNA affected cell surface expression of both receptors, presumably due to the action of the transfection reagent. This effect was more apparent for the IR-A than the IGF1R, resulting in cells that were more disparate in their relative expression of IR-A and IGF1R, with IGF1R expressed in significant excess [Figure 6.1 C]. These cells [following the random dimerisation model of hybrid receptor formation] would be

predicted to have increased levels of hybrid receptors and IGF1R homodimers due to the IR-A being expressed at a lower level. Indeed, the response of the dual control transfected cells followed an IGF1R type response. IGF-I stimulated the greatest response, followed by IGF-II, and the response to insulin was not appreciably different in these cells compared to untransfected SW480 cells. These results, along with those from cells transfected singly with control siRNA, suggests that while relatively small changes in the cell surface expression of the two receptors can be tolerated before affecting cellular biological responses, small permutations in addition to this can result in quite large effects. Furthermore, they suggest that relative receptor ratios are more important in signaling biological responses than absolute receptor numbers.

Interestingly, dual silencing of the IR and IGF1R did not appreciably decrease the response of SW480 cells to ligand-stimulated cell survival from butyrate-induced apoptosis in comparison to untransfected SW480 cells [Figure 6.6 C]. This observation supports the concept mentioned above, that expression of relative receptor ratios are a more important determinant than absolute receptor numbers expressed at the cell surface. While the dual transfected SW480 cells had decreased levels of both IR-A and IGF1R compared to untransfected cells, the more efficient silencing of the IR-A than IGF1R, resulted in the IGF1R being expressed to a greater extent than the IR-A. Since IR-A levels were so low compared to the IGF1R in the dual transfected cells, this could shift the balance of the system towards signaling through IGF1R homodimers. This balance shift could also explain why dual silencing of the IGF1R and IR did not confer any additional advantage over single targeting of the IGF1R alone. If one compares this expression ratio to that of the single IGF1R knock-down alone, the levels of receptor knock-down are similar for the IGF1R. However, in the dual knock-down cells, there is also a decreased level of the IR-A. Therefore, the IR-A cannot sequester the IGF1R into hybrids to the same extent, and in comparison to the single IGF1R knock-down cells, there would be more IGF1R homodimers expressed in the dual knock-down cells [Figure 6.10 D]. This suggests that greater silencing of the IGF1R may be needed in order to discern whether the IR-A can compensate for targeted loss of the IGF1R.

Since dual knock-down of the IR-A and IGF1R did not confer additional inhibition of cell proliferation or survival compared to single targeting of the IGF1R, one must question whether the IR-A is functional in this cell line. The IR-A is functional in SW480 cells with respect to its phosphorylation and activation by insulin and IGFs. However, downstream effects, such as glucose

uptake, should be considered as an indicator of IR-A functionality in these cells. If the IR-A is fully functional in this cell line, what is the biological role of this receptor in cancer? Does up-regulation of the IR-A provide a growth and migratory advantage to cancer cells by increasing the IGF-II binding sites at the cell surface either by IR-A homodimers or by forming hybrid receptors with the IGF1R and also thereby providing increased binding sites for IGF-I? Or does the up-regulation of the IR-A help balance out the up-regulation of the IGF1R? The role of the IR-A in the potentiation and progression of cancer may be multifaceted. There are two general views expressed in the literature regarding the role of the IR-A in cancer. One view is that the IR-A is directly involved, by mediating the effects of IGF-II over-expressed by the tumour via either IR-A homodimers or hybrid receptors. The other view is a less direct role for the IR-A, via modulation of the IGF system as evidenced by the correlation between metabolic disease states and increased cancer risk[101, 129]. The present study suggests that signaling via the IGF1R is dominant to IR-A signaling in SW480 cells co-expressing both receptors in approximately equal amounts. Most published literature addressing the ability of IR-A to signal proliferative, migratory, and survival outcomes has been conducted in cells only expressing the IR-A, not in cells co-expressing the IGF1R as well[7, 12, 127, 135, 136, 305]. Of those studies that have expressed both receptors, the IR-A vs. IGF1R content was either not reported[123], or the IR-A was expressed in vast excess to the IGF1R[125]. Indeed, data presented in this thesis in Chapter 3, demonstrates that the IR-A is able to signal potent proliferative, survival, and migratory outcomes in response to ligand stimulation in R⁻ cells transfected to express the IR-A. However, in cells co-expressing the IGF1R and IR [SW480 cells] signaling via the IR-A appears to be ancillary to that of the IGF1R. This, in part, suggests the role of up-regulation of the IR-A in colorectal cancer may not be as direct. The observation that expression of the IR-A may modulate and affect signaling via the IGF1R, is an important one and provides a potential explanation for the correlation found in patients with early stage breast cancer, where high levels of IR expression in tumours is independently and significantly associated with improved prognosis and overall survival[119]. The observed correlation between IR expression and improved prognosis in breast cancer patients has been largely ignored in the recent literature possibly because it does not fit with the current thoughts on how the IR-A is involved in cancer biology. In a system with multiple levels of regulation, cross-interaction and interplay between its components it is possible that individual components of the IGF system may have multiple roles in the potentiation and progression of cancer that can be both beneficiary as well as detrimental to the patient. This may especially be the

case when one considers cancer is a disease state which arises from the permutation of multiple normal cellular processes in which the IGF system is far from being fully understood.

6.4   Conclusions

The results presented here demonstrate that signaling via the IGF1R is dominant to the IR-A, and suggests co-expression of the IR-A may influence signaling via the IGF1R. These observations may help explain the published results from other groups linking higher IR expression with better prognosis in breast cancer patients[119]. These data presented here do not suggest that the IR-A is not important in cancer biology, and indeed there is abundant evidence to suggest otherwise[7, 101, 123, 125]. However, the data presented here highlight the importance and dominance of signaling via the IGF1R. The results suggest the IR-A cannot compensate for the loss of the IGF1R. However, observation of these results in cells with increased knock-down of the IGF1R would add strength to this conclusion. It is suggested here, that relative receptor expression ratios may be a more important determinant than absolute receptor numbers. Thus, if considered beneficial, dual IGF1R/IR-A therapy would need to target both receptors equally or risk a potentially detrimental phenotype.

Chapter 7

Final Discussion

7.1   Scope and Aims of Thesis

Recent interest has focused on the potential role of the IR-A in mediating proliferative, migratory, and survival responses to IGF-II in the development of cancer[12, 125, 127, 135, 136]. However, one shortcoming of the published research examining the IR-A, is that the majority of studies were conducted in cells devoid of the IGF1R[12, 125, 127, 135, 136, 305]. As a result of this, it is not known how the IR-A interacts and functions in conjunction with the IGF1R to signal biologically relevant outcomes.   Determining how the IR-A functions in cells co-expressing the IGF1R is of particular relevance when considering the range of novel anti-cancer therapeutics currently under development that target the IGF1R. Compensatory signaling from the IR-A is one possible mechanism by which IGF1R targeting could be rendered ineffective. Therefore, the major aim of this thesis was to determine whether signaling via the IR-A could compensate for the targeted loss of the IGF1R. In the broader context of investigating the biological role of the IR, a secondary, but related aim of this thesis was to investigate the ability of a range of IGF chimeras to signal biological responses through the IR-A and IR-B.

7.2   Summary of Findings

Despite the previously mentioned limitations of investigating outcomes of IR-A signaling in cells devoid of the IGF1R, these approaches do have merit in that they enable the IR to be investigated without interference from either the IGF1R or IGF1R/IR hybrid receptors. The binding and signaling response through the IR-A and IR-B of a range of IGF chimeras was investigated in Chapter 3. Binding studies revealed exchange of both the IGF C and D domains are required for a near total conversion of the two IGFs binding specificities for the IR-A and IR-B. However, analysis of signaling downstream of receptor binding demonstrated that exchange of the IGF C domain alone accounts for the differential ability of IGF-I and IGF-II to activate and signal biological responses via the two IR isoforms. Together these results suggest a discrepancy between the requirements for

ligand binding and receptor activation. These studies not only provide insights into the biological response elicited by IGF ligand-receptor interactions, but also identify a novel pathway for IGF activation via the IR. IGF-I was demonstrated to act through both isoforms of the IR to preferentially activate IRS-2, resulting in downstream biological outcomes relevant to cancer biology, namely cell survival and migration. In addition, through these studies, insulin was demonstrated to stimulate chemotaxis directly via the IR-A, an event previously thought to occur due to activation of the IGF1R[148]. Moreover, it was demonstrated that IGF and insulin signaling via both IR isoforms can protect cells from butyrate-induced apoptosis.

The major aim of this thesis was to determine whether the IR-A can compensate for targeted loss of the IGF1R, thereby providing cancer cells a pathway by which they can evade anti-cancer therapeutics aimed at targeting the IGF1R. Before this could be investigated, an appropriate cell line model needed to be identified. Chapter 4 details various experiments that identify SW480 cells are an appropriate cell line model for use in investigating how the IR-A functions in conjunction with the IGF1R to signal biologically relevant outcomes. SW480 cells expressed similar levels of IGF1R and IR-A, but did not express the IR-B, and could be used in a range of biological endpoint assays representative of cellular processes relevant to cancer pathology. Interestingly, IGFs and insulin, at physiologically relevant concentrations rescued four different colorectal adenocarcinoma cell lines from the effects of butyrate. These results suggest IGF and insulin stimulation of the IGF receptors may provide a mechanism by which cancer cells could evade the anti-tumourigenic effects of butyrate in the colonic lumen. Furthermore, for the first time it was demonstrated that insulin can have direct effects on colorectal cancer cells resulting in physiologically relevant outcomes to cancer biology.

An siRNA based approach was chosen to investigate the biological role of the IR-A in cells co-expressing the IGF1R. Chapter 5 describes the multiple optimisation steps that led to an siRNA transfection protocol that resulted in effective, specific, and reliable knock-down of the IR-A and IGF1R in SW480 cells. This strategy was then successfully utilised to address the main aim of this thesis, showing the IR-A could not compensate for the targeted loss of the IGF1R in SW480 cells [Chapter 6]. Furthermore, dual silencing of the IR-A and IGF1R did not confer any additional inhibition of SW480 cell survival and proliferation than IGF1R silencing alone. Interestingly, silencing of the IR-A increased the ligand response of SW480 cells, and increased phosphorylation

of the IGF1R by IGFs. Together, these results suggest the IR-A may attenuate signaling via the IGF1R, perhaps by sequestering it into hybrid receptors. Moreover, these results imply signaling via IGF1R/IR-A hybrid receptors may not be as potent as signals arising from IGF1R homodimers, thereby providing some insight into the functionality of hybrid receptors.

7.3   *Discussion*

Results presented in this thesis complement those recently published by Zhang *et al* 2007[151] and Reidermann *et al* 2007[297]. Zhang *et al* 2007, demonstrated that siRNA-mediated silencing of the IGF1R resulted in increased sensitivity of LCC6 breast cancer cells to insulin[151]. This occurred by increased activation of the IR, which was interpreted to be due to decreased IGF1R expression disrupting hybrid receptor formation thereby resulting in the movement of receptor formation to favor IR homodimers[151]. Similar results were found in the studies outlined in this thesis. The present study built on these findings by addressing the effect of IR-A down-regulation of IGF1R signaling outcomes. Down-regulation of the IR-A led to increased signaling via the IGF1R, and increased biological response to ligand. It was demonstrated that decreased IR-A expression disrupted hybrid receptor expression, resulting in the movement of receptor formation to favor IGF1R homodimers. The increased biological response to ligand in IR-A knock-down cells suggested that IR-A expression attenuates the IGF1R, possibly by sequestering the IGF1R into hybrid receptors, that appear less active than IGF1R homodimers. This, together with the observation that dual silencing of the IR-A and IGF1R did not confer any additional inhibition of SW480 clonogenic survival or increase SW480 sensitivity to butyrate compared to IGF1R knock-down alone, suggested signaling via the IGF1R was dominant to the IR-A in SW480 cells. This observation complements those of Reidermann *et al* 2007, where dual silencing of the EGFR and IGF1R suggested dominance of IGF1R signaling over that of the EGFR[297]. The present study and that of Reidermann *et al* 2007 suggest that neither the IR-A nor EGFR can compensate for the targeted loss of the IGF1R[297]. Together, these results provide encouragement for the potential efficacy of anti-cancer therapeutics aimed at targeting the IGF1R.

Disruption of hybrid receptors by down-regulation of the IR-A led to increased signaling via IGF1R homodimers and increased biological outcome to ligand stimulation [Chapter 6]. This suggests that hybrid receptors may attenuate signaling via IGF1R homodimers. This raises interesting questions about how cells interpret incoming signals arising from the various receptors of the IGF family. If signals incoming from homodimers are interpreted differently to those incoming from heterodimers, it would suggest there must be some context specific mediator/s of signaling. This is especially interesting considering it is generally thought that activation of hybrid receptors would result in activation of both IGF1R and IR downstream signaling cascades due to *trans*-phosphorylation of both beta-subunits[144-146, 149]. It is unknown whether there is a distinct physiological role for hybrid receptors. Moreover, it remains unclear as to what extent hybrid receptors are functional in terms of being able to initiate signals that result in biological outcomes. It is thought that signals originating from hybrid receptors are biologically relevant since an inhibitory antibody towards hybrid receptors [47-9] was shown to inhibit IGF-I stimulated growth of breast cancer cells[143]. However, 47-9 was originally derived against the IR[350], and would also bind and inhibit the actions of ligand stimulated growth of the IR. Moreover, although 47-9 can inhibit IGF-I binding to hybrid receptors, its affinity for hybrid receptors is reported to be lower than for IR homodimers[350]. Furthermore, at the time of the Pandini *et al* 1999[143] study it was not known that IGF-I could stimulate physiologically relevant outcomes via the IR [Chapter 3 and [305]]. Therefore, in light of the results presented in this thesis, an updated interpretation of the results in the Pandini *et al* 1999[143] study suggests the decrease in IGF-I stimulated growth of breast cancer cells by inhibitory antibody 47-9 may reflect the inhibition of IGF-I signaling though the IR.

The observation that expression of the IR-A may modulate and affect signaling via the IGF1R [Chapter 6], is significant. Attenuation of the IGF1R by the IR-A via the formation of hybrid receptors may be one explanation for the correlation found in patients with early stage breast cancer, where high levels of IR expression in tumours is independently and significantly associated with improved prognosis and overall survival[119]. The observed correlation between IR expression and increased prognosis in breast cancer patients has been largely ignored in the recent literature, possibly because it does not fit with the current thoughts on how the IR-A is involved in cancer biology. In a system with multiple levels of regulation, cross-interaction, and interplay between its components, it is possible that individual components of the IGF system may have multiple roles in the potentiation and progression of cancer that can be both beneficial as well as detrimental to the

patient. This possibility is especially important when one considers cancer is a manifestation arising from the permutation and corruption of multiple normal cellular processes, and that the IGF system is far from being fully understood. It is therefore possible that outcomes of ligand stimulation may be context specific. Indeed, data presented in Chapter 3 demonstrated that, in cells devoid of the IGF1R, the IR-A was able to signal potent proliferative, survival, and migratory outcomes in response to ligand stimulation. These results correlated well with those of previously published studies where biological outcomes of IR-A signaling was assessed in cells devoid of the IGF1R[12, 127, 135, 136, 305]. However, in cells co-expressing the IR-A and IGF1R in similar levels [SW480 cells], signaling via the IR-A appeared to be ancillary to that of the IGF1R. Together, the data presented in Chapters 3 and 6 demonstrated how IGF receptor context can affect biological outcome to ligand stimulation. These studies, like essentially all other studies of IGF and insulin action at the molecular level, were conducted in serum-starved cells treated with each ligand in isolation, an artificial situation that does not occur in vivo. Therefore, perhaps one of the greatest contextual related questions facing the IGF field to date is how do cells respond to simultaneous exposure to the ligands of the IGF system? Indeed, results presented in this thesis demonstrated, despite low affinity and poor phosphorylation of the IR, IGF-I at physiologically relevant concentrations could preferentially activate IRS-2 resulting in biological outcomes. It is not known how such activation of the IR by IGF-I would be interpreted by cells also exposed to insulin and IGF-II, let alone, how simultaneous ligand stimulation would be interpreted by cells co-expressing the IGF1R and IR.

Three other observations relevant to colorectal cancer biology were made through addressing the main aims of this thesis. Firstly, insulin was demonstrated to stimulate chemotaxis directly via the IR-A [Chapter 3]. This was a particularly relevant observation, as previous studies have suggested that insulin-stimulated cell migration was due to 'spill-over' activation of the IGF1R[148]. Secondly, insulin was demonstrated to have direct effects on colorectal cancer cell survival from the effects of butyrate. It has previously been speculated that several direct and indirect mechanisms may underlie the association between circulating insulin levels and colorectal cancer risk[189, 195]. Results presented here provide some evidence for a direct effect of insulin on colorectal cancer cells thereby promoting their survival from the effects of butyrate. Thirdly, IGF and insulin signaling via both isoforms of the IR [Chapter 3 and Chapter 4] and IGF1R [Chapter 4] may provide a mechanism by which cancer cells could evade the potent anti-tumourigenic effects of butyrate in the colonic lumen. These results not only complement those of Leng et al 2001[233], but build on their

findings by identifying multiple ligands and receptors of the IGF system that can protect cells from the effects of butyrate. Butyrate is present in the colonic lumen at concentrations that are sufficient to result in the death of almost all cells treated *in vitro*[233], but colorectal cancers still develop *in vivo*. Along with other mechanisms of butyrate-resistance, the finding that IGFs are overexpressed in colon cancer tissues[210, 213], along with the overexpression of the IR[7, 228] and IGF1R[24, 65, 223, 227], may account for the modest anti-tumourigenic effects of butyrate in *in vivo* studies[326, 327].

7.4   *Future Directions*

One shortcoming of the siRNA mediated silencing studies presented in this thesis, was IGF1R siRNA transfection only resulted in approximately 60% receptor knock-down. It is possible that dominant IGF1R signaling from residual IGF1R expression overshadowed any compensatory signaling from the IR-A. Therefore, these studies would benefit from being repeated with an siRNA that results in more substantial IGF1R knock-down. If siRNAs that result in greater IGF1R receptor knock-down gave similar results to those presented in this thesis, they would greatly strengthen the conclusions presented here. Further, repeating these experiments in another cell line would also strengthen the current study as it would address any concerns of cell line specific artifacts.

The work described within this thesis has raised an important question about the interactions between the IGF1R and IR for future investigation: *How do cells interpret incoming signals from homodimers vs. heterodimers?* Results from Chapter 6 suggest that signals arising from IGF1R homodimers may be more potent than those arising from IGF1R/IR-A hybrid receptors. This suggests signals from homodimers and heterodimers may be context specific. This is an interesting concept considering stimulation of hybrid receptors is thought to result in activation of both IR and IGF1R signaling pathways due to *trans*-phosphorylation of the beta-subunits[81, 146]. The siRNA based approach utilised in this thesis could be used in conjunction with Western blotting and proteomic based techniques to investigate the pathways and signaling molecules activated by these two receptor types. Time-course studies, along with examining the global phosphorylation profile, would enable the possibility of temporal and/or context-specific downstream mediators of signaling to be investigated.

An additional observation warranting investigation is the apparent disparity between siRNA mediated dual silencing of the IGF1R and IR-A and antibody-mediated co-targeting of both receptors. Results presented in this thesis showed siRNA mediated dual silencing of the IGF1R and IR-A conferred no additional inhibition of SW480 cell growth than targeting the IGF1R alone. These results contrast those obtained by Vella *et al* 2002, where antibody-mediated co-targeting of the IGF1R and IR-A was more effective at inhibiting IGF-II stimulated growth of B-CPAP cells than either antibody alone[123]. Similar results have been observed in co-targeting of the EGFR and IGF1R. Dual silencing of the EGFR and IGF1R by siRNA induced no greater inhibition of MDA-MB-468 breast cancer cell clonogenic survival than IGF1R knockdown alone[297]. This contrasts the synergistic anti-tumour effect of antibody-mediated co-targeting of the IGF1R and EGFR observed in an A549 xenograft model[250]. Together, these results suggest there may be a difference in cellular outcome between inhibiting receptors that are already expressed [antibody inhibition] and inhibiting receptor expression [siRNA]. This conclusion is currently difficult to draw as the studies outlined above were all conducted by different groups and in different cell lines. By performing a study in one [or two] model cell lines to address this possibility may provide insights into the different mechanisms of action of these two inhibition techniques, and perhaps more importantly, provide some insight as to how cells interpret their environment.

The need to investigate how cells respond to simultaneous exposure to ligands is an important contextual related question facing the IGF field. The effects of simultaneous exposure to various concentrations of IGF-I, IGF-II, and insulin on receptor activation and biological outcomes could easily be addressed utilising the techniques and cell lines used throughout this thesis. Further, there is the additional complexity of cross-talk between the IGF1R, IR and other growth factor, cytokine, and chemokine receptor families. Interactions between the EGFR and IGF1R have recently been described[297, 298]. Studies in oligodendrocytes have revealed synergistic induction of cyclin D1 by IGF-I and FGF-2 suggesting cross-talk between the IGF1R and FGFR[351]. Some of these interactions and mechanisms of cross-talk may be revealed to be cell type specific. Nevertheless deciphering how cells interpret and respond to their external environment will only occur through such studies.

7.5   Conclusions

The main aim of this thesis was to examine whether signaling via the IR-A could compensate for the targeted loss of the IGF1R. An siRNA-based approach was successfully utilised to address this possibility and results show the IR-A does not compensate for IGF1R downregulation in SW480 cells. Furthermore, dual silencing of the IR-A and IGF1R induced no greater inhibition of clonogenic survival than IGF1R silencing alone, therefore suggesting the implications of IR-A expression on the efficacy of anti-cancer therapeutics aimed at targeting the IGF1R may not be as considerable as first anticipated. Moreover, the results inferred signaling via IGF1R/IR-A hybrid receptors may not be as potent as signals arising from IGF1R homodimers, thereby providing insight into the functionality of hybrid receptors. A secondary aim of this thesis was to investigate the ability of a range of IGF chimeras to signal biological responses through the IR-A and IR-B. These studies, conducted in cells devoid of the IGF1R, provided insights into the biological response elicited by IGF ligand-receptor interactions, and identified a novel pathway for IGF activation through the IR. Together, these studies contribute to a better understanding of the biological outcomes of cross-talk between multiple components of the IGF system.

References

1.	Sato A, Nishimura S, Ohkubo T, Kyogoku Y, Koyama S, Kobayashi M, Yasuda T, Kobayashi Y. Three-dimensional structure of human insulin-like growth factor-I (IGF-I) determined by 1H-NMR and distance geometry. International Journal of Peptide and Protein Research 1993;41:433-40.
2.	Torres AM, Forbes BE, Aplin SE, Wallace JC, Francis GL, Norton RS. Solution structure of human insulin-like growth factor II. Relationship to receptor and binding protein interactions. Journal of Molecular Biology 1995;248:385-401.
3.	Cooke RM, Harvey TS, Campbell ID. Solution structure of human insulin-like growth factor 1: a nuclear magnetic resonance and restrained molecular dynamics study. Biochemistry 1991;30:5484-91.
4.	Brissenden JE, Ullrich A, Francke U. Human chromosomal mapping of genes for insulin-like growth factors I and II and epidermal growth factor. Nature 1984;310:781-4.
5.	Sara VR, Hall K. Insulin-like growth factors and their binding proteins. Physiol Rev 1990;70:591-614.
6.	Rinderknecht E, Humbel RE. The amino acid sequence of human insulin-like growth factor I and its structural homology with proinsulin. J Biol Chem 1978;253:2769-76.
7.	Frasca F, Pandini G, Scalia P, Sciacca L, Mineo R, Costantino A, Goldfine ID, Belfiore A, Vigneri R. Insulin receptor isoform A, a newly recognized, high-affinity insulin-like growth factor II receptor in fetal and cancer cells. Molecular and Cellular Biology 1999;19:3278-88.
8.	McClain DA. Different ligand affinities of the two human insulin receptor splice variants are reflected in parallel changes in sensitivity for insulin action. Molecular Endocrinology 1991;5:734-9.
9.	Mosthaf L, Grako K, Dull TJ, Coussens L, Ullrich A, McClain DA. Functionally distinct insulin receptors generated by tissue-specific alternative splicing. The Embo Journal 1990;9:2409-13.
10.	Yamaguchi Y, Flier JS, Benecke H, Ransil BJ, Moller DE. Ligand-binding properties of the two isoforms of the human insulin receptor. Endocrinology 1993;132:1132-8.
11.	Yamaguchi Y, Flier JS, Yokota A, Benecke H, Backer JM, Moller DE. Functional properties of two naturally occurring isoforms of the human insulin receptor in Chinese hamster ovary cells. Endocrinology 1991;129:2058-66.
12.	Denley A, Brierley GV, Carroll JM, Lindenberg A, Booker GW, Cosgrove LJ, Wallace JC, Forbes BE, Roberts CT, Jr. Differential activation of insulin receptor isoforms by insulin-like growth factors is determined by the C domain. Endocrinology 2006;147:1029-36.
13.	Denley A, Bonython ER, Booker GW, Cosgrove LJ, Forbes BE, Ward CW, Wallace JC. Structural determinants for high affinity binding of IGF-II to IR-A, the exon 11 minus isoform of the insulin receptor. Mol Endocrinol 2004.
14.	Mathews LS, Norstedt G, Palmiter RD. Regulation of insulin-like growth factor I gene expression by growth hormone. Proc Natl Acad Sci U S A 1986;83:9343-7.
15.	Jones JI, Clemmons DR. Insulin-like growth factors and their binding proteins: biological actions. Endocrine Reviews 1995;16:3-34.
16.	Giannoukakis N, Deal C, Paquette J, Goodyer CG, Polychronakos C. Parental genomic imprinting of the human IGF2 gene. Nat Genet 1993;4:98-101.
17.	Daughaday WH, Rotwein P. Insulin-like growth factors I and II. Peptide, messenger ribonucleic acid and gene structures, serum, and tissue concentrations. Endocr Rev 1989;10:68-91.
18.	Han VK, Lund PK, Lee DC, D'Ercole AJ. Expression of somatomedin/insulin-like growth factor messenger ribonucleic acids in the human fetus: identification, characterization, and tissue distribution. J Clin Endocrinol Metab 1988;66:422-9.
19.	Liu JP, Baker J, Perkins AS, Robertson EJ, Efstratiadis A. Mice carrying null mutations of the genes encoding insulin-like growth factor I (Igf-1) and type 1 IGF receptor (Igf1r). Cell 1993;75:59-72.
20.	Walenkamp MJ, Karperien M, Pereira AM, Hilhorst-Hofstee Y, van Doorn J, Chen JW, Mohan S, Denley A, Forbes B, van Duyvenvoorde HA, van Thiel SW, Sluimers CA, Bax JJ, de Laat JA, Breuning MB, Romijn JA, Wit JM. Homozygous and heterozygous expression of a novel insulin-like growth factor-I mutation. J Clin Endocrinol Metab 2005;90:2855-64.
21.	Woods KA, Camacho-Hubner C, Barter D, Clark AJ, Savage MO. Insulin-like growth factor I gene deletion causing intrauterine growth retardation and severe short stature. Acta Paediatr Suppl 1997;423:39-45.

22. Khandwala HM, McCutcheon IE, Flyvbjerg A, Friend KE. The effects of insulin-like growth factors on tumorigenesis and neoplastic growth. Endocrine Reviews 2000;21:215-44.

23. Vincent AM, Feldman EL. Control of cell survival by IGF signaling pathways. Growth Hormone & IGF Research 2002;12:193-7.

24. Yu H, Rohan T. Role of the insulin-like growth factor family in cancer development and progression. Journal of the National Cancer Institute 2000;92:1472-89.

25. Mohan S, Baylink DJ. IGF-binding proteins are multifunctional and act via IGF-dependent and -independent mechanisms. The Journal of Endocrinology 2002;175:19-31.

26. Kornfeld S. Structure and function of the mannose 6-phosphate/insulinlike growth factor II receptors. Annu Rev Biochem 1992;61:307-30.

27. Scott CD, Firth SM. The role of the M6P/IGF-II receptor in cancer: tumor suppression or garbage disposal? Horm Metab Res 2004;36:261-71.

28. Ewton DZ, Falen SL, Florini JR. The type II insulin-like growth factor (IGF) receptor has low affinity for IGF-I analogs: pleiotypic actions of IGFs on myoblasts are apparently mediated by the type I receptor. Endocrinology 1987;120:115-23.

29. Lee PD, Hodges D, Hintz RL, Wyche JH, Rosenfeld RG. Identification of receptors for insulin-like growth factor II in two insulin-like growth factor II producing cell lines. Biochem Biophys Res Commun 1986;134:595-600.

30. Tong PY, Tollefsen SE, Kornfeld S. The cation-independent mannose 6-phosphate receptor binds insulin-like growth factor II. J Biol Chem 1988;263:2585-8.

31. Lau MM, Stewart CE, Liu Z, Bhatt H, Rotwein P, Stewart CL. Loss of the imprinted IGF2/cation-independent mannose 6-phosphate receptor results in fetal overgrowth and perinatal lethality. Genes Dev 1994;8:2953-63.

32. Ludwig T, Eggenschwiler J, Fisher P, D'Ercole AJ, Davenport ML, Efstratiadis A. Mouse mutants lacking the type 2 IGF receptor (IGF2R) are rescued from perinatal lethality in Igf2 and Igf1r null backgrounds. Dev Biol 1996;177:517-35.

33. Oka Y, Rozek LM, Czech MP. Direct demonstration of rapid insulin-like growth factor II Receptor internalization and recycling in rat adipocytes. Insulin stimulates 125I-insulin-like growth factor II degradation by modulating the IGF-II receptor recycling process. J Biol Chem 1985;260:9435-42.

34. Ellis MJ, Leav BA, Yang Z, Rasmussen A, Pearce A, Zweibel JA, Lippman ME, Cullen KJ. Affinity for the insulin-like growth factor-II (IGF-II) receptor inhibits autocrine IGF-II activity in MCF-7 breast cancer cells. Mol Endocrinol 1996;10:286-97.

35. Costello M, Baxter RC, Scott CD. Regulation of soluble insulin-like growth factor II/mannose 6-phosphate receptor in human serum: measurement by enzyme-linked immunosorbent assay. J Clin Endocrinol Metab 1999;84:611-7.

36. MacDonald RG, Tepper MA, Clairmont KB, Perregaux SB, Czech MP. Serum form of the rat insulin-like growth factor II/mannose 6-phosphate receptor is truncated in the carboxyl-terminal domain. J Biol Chem 1989;264:3256-61.

37. Zaina S, Squire S. The soluble type 2 insulin-like growth factor (IGF-II) receptor reduces organ size by IGF-II-mediated and IGF-II-independent mechanisms. J Biol Chem 1998;273:28610-6.

38. Oates A, Schumaker L, Jenkins S, Pearce A, DaCosta S, Arun B. The mannose 6-phosphate/insulin-like growth factor 2 receptor (M6P/IGF2R), a putative breast tumor suppressor gene. Breast Cancer Res Treat 1998;47:235-53.

39. De Souza AT, Hankins GR, Washington MK, Orton TC, Jirtle RL. M6P/IGF2R gene is mutated in human hepatocellular carcinomas with loss of heterozygosity. Nat Genet 1995;11:447-9.

40. Jamieson TA, Brizel DM, Killian JK, Oka Y, Jang HS, Fu X, Clough RW, Vollmer RT, Anscher MS, Jirtle RL. M6P/IGF2R loss of heterozygosity in head and neck cancer associated with poor patient prognosis. BMC Cancer 2003;3:4.

41. Oka Y, Waterland RA, Killian JK, Nolan CM, Jang HS, Tohara K, Sakaguchi S, Yao T, Iwashita A, Yata Y, Takahara T, Sato S, Suzuki K, Masuda T, Jirtle RL. M6P/IGF2R tumor suppressor gene mutated in hepatocellular carcinomas in Japan. Hepatology 2002;35:1153-63.

42. Adams TE, Epa VC, Garrett TP, Ward CW. Structure and function of the type 1 insulin-like growth factor receptor. Cellular and Molecular Life Sciences : Cmls 2000;57:1050-93.

43. Ullrich A, Gray A, Tam AW, Yang-Feng T, Tsubokawa M, Collins C, Henzel W, Le Bon T, Kathuria S, Chen E, et al. Insulin-like growth factor I receptor primary structure: comparison with insulin receptor suggests structural determinants that define functional specificity. Embo J 1986;5:2503-12.

44. Forbes BE, Hartfield P, McNeil K, Surinya KH, Milner S, Cosgrove L, Wallace JC. Characterisation of binding of insulin-like growth factor (IGF)-I and IGF-II analogues to the

type I IGF receptor determined by BIAcore analysis. European Journal of Biochemistry 2002;269:787-92.

45. Rubin JB, Shia MA, Pilch PF. Stimulation of tyrosine-specific phosphorylation in vitro by insulin-like growth factor I. Nature 1983;305:438-40.

46. Gray SG, Stenfeldt Mathiasen I, De Meyts P. The insulin-like growth factors and insulin-signalling systems: an appealing target for breast cancer therapy? Horm Metab Res 2003;35:857-71.

47. O'Connor R. Regulation of IGF-I receptor signaling in tumor cells. Horm Metab Res 2003;35:771-7.

48. Sachdev D, Yee D. Disrupting insulin-like growth factor signaling as a potential cancer therapy. Mol Cancer Ther 2007;6:1-12.

49. Chang L, Karin M. Mammalian MAP kinase signalling cascades. Nature 2001;410:37-40.

50. Cantrell DA. Phosphoinositide 3-kinase signalling pathways. J Cell Sci 2001;114:1439-45.

51. Peruzzi F, Prisco M, Dews M, Salomoni P, Grassilli E, Romano G, Calabretta B, Baserga R. Multiple signaling pathways of the insulin-like growth factor 1 receptor in protection from apoptosis. Mol Cell Biol 1999;19:7203-15.

52. Valentinis B, Morrione A, Peruzzi F, Prisco M, Reiss K, Baserga R. Anti-apoptotic signaling of the IGF-I receptor in fibroblasts following loss of matrix adhesion. Oncogene 1999;18:1827-36.

53. Valentinis B, Romano G, Peruzzi F, Morrione A, Prisco M, Soddu S, Cristofanelli B, Sacchi A, Baserga R. Growth and differentiation signals by the insulin-like growth factor 1 receptor in hemopoietic cells are mediated through different pathways. J Biol Chem 1999;274:12423-30.

54. Brodt P, Samani A, Navab R. Inhibition of the type I insulin-like growth factor receptor expression and signaling: novel strategies for antimetastatic therapy. Biochemical Pharmacology 2000;60:1101-7.

55. Kaleko M, Rutter WJ, Miller AD. Overexpression of the human insulinlike growth factor I receptor promotes ligand-dependent neoplastic transformation. Mol Cell Biol 1990;10:464-73.

56. Pietrzkowski Z, Lammers R, Carpenter G, Soderquist AM, Limardo M, Phillips PD, Ullrich A, Baserga R. Constitutive expression of insulin-like growth factor 1 and insulin-like growth factor 1 receptor abrogates all requirements for exogenous growth factors. Cell Growth Differ 1992;3:199-205.

57. Sell C, Dumenil G, Deveaud C, Miura M, Coppola D, DeAngelis T, Rubin R, Efstratiadis A, Baserga R. Effect of a null mutation of the insulin-like growth factor I receptor gene on growth and transformation of mouse embryo fibroblasts. Mol Cell Biol 1994;14:3604-12.

58. Baserga R, Hongo A, Rubini M, Prisco M, Valentinis B. The IGF-I receptor in cell growth, transformation and apoptosis. Biochim Biophys Acta 1997;1332:F105-26.

59. Coppola D, Ferber A, Miura M, Sell C, D'Ambrosio C, Rubin R, Baserga R. A functional insulin-like growth factor I receptor is required for the mitogenic and transforming activities of the epidermal growth factor receptor. Mol Cell Biol 1994;14:4588-95.

60. Sell C, Rubini M, Rubin R, Liu JP, Efstratiadis A, Baserga R. Simian virus 40 large tumor antigen is unable to transform mouse embryonic fibroblasts lacking type 1 insulin-like growth factor receptor. Proc Natl Acad Sci USA 1993;90:11217-21.

61. Resnik JL, Reichart DB, Huey K, Webster NJ, Seely BL. Elevated insulin-like growth factor I receptor autophosphorylation and kinase activity in human breast cancer. Cancer Res 1998;58:1159-64.

62. Bergmann U, Funatomi H, Yokoyama M, Beger HG, Korc M. Insulin-like growth factor I overexpression in human pancreatic cancer: evidence for autocrine and paracrine roles. Cancer Res 1995;55:2007-11.

63. Sekyi-Otu A, Bell RS, Ohashi C, Pollak M, Andrulis IL. Insulin-like growth factor 1 (IGF-1) receptors, IGF-1, and IGF-2 are expressed in primary human sarcomas. Cancer Res 1995;55:129-34.

64. Kanter-Lewensohn L, Dricu A, Wang M, Wejde J, Kiessling R, Larsson O. Expression of the insulin-like growth factor-1 receptor and its anti-apoptotic effect in malignant melanoma: a potential therapeutic target. Melanoma Res 1998;8:389-97.

65. Hakam A, Yeatman TJ, Lu L, Mora L, Marcet G, Nicosia SV, Karl RC, Coppola D. Expression of insulin-like growth factor-1 receptor in human colorectal cancer. Hum Pathol 1999;30:1128-33.

66. Treins C, Giorgetti-Peraldi S, Murdaca J, Monthouel-Kartmann MN, Van Obberghen E. Regulation of hypoxia-inducible factor (HIF)-1 activity and expression of HIF hydroxylases in response to insulin-like growth factor I. Mol Endocrinol 2005;19:1304-17.

67. Peretz S, Kim C, Rockwell S, Baserga R, Glazer PM. IGF1 receptor expression protects against microenvironmental stress found in the solid tumor. Radiat Res 2002;158:174-80.

68. Zhang D, Brodt P. Type 1 insulin-like growth factor regulates MT1-MMP synthesis and tumor invasion via PI 3-kinase/Akt signaling. Oncogene 2003;22:974-82.

69. Hazan RB, Qiao R, Keren R, Badano I, Suyama K. Cadherin switch in tumor progression. Ann N Y Acad Sci 2004;1014:155-63.

70. Playford MP, Bicknell D, Bodmer WF, Macaulay VM. Insulin-like growth factor 1 regulates the location, stability, and transcriptional activity of beta-catenin. Proc Natl Acad Sci U S A 2000;97:12103-8.

71. Shen MR, Hsu YM, Hsu KF, Chen YF, Tang MJ, Chou CY. Insulin-like growth factor 1 is a potent stimulator of cervical cancer cell invasiveness and proliferation that is modulated by alphavbeta3 integrin signaling. Carcinogenesis 2006;27:962-71.

72. Dunn SE, Hardman RA, Kari FW, Barrett JC. Insulin-like growth factor 1 (IGF-1) alters drug sensitivity of HBL100 human breast cancer cells by inhibition of apoptosis induced by diverse anticancer drugs. Cancer Res 1997;57:2687-93.

73. Resnicoff M, Abraham D, Yutanawiboonchai W, Rotman HL, Kajstura J, Rubin R, Zoltick P, Baserga R. The insulin-like growth factor I receptor protects tumor cells from apoptosis in vivo. Cancer Res 1995;55:2463-9.

74. Resnicoff M, Burgaud JL, Rotman HL, Abraham D, Baserga R. Correlation between apoptosis, tumorigenesis, and levels of insulin-like growth factor I receptors. Cancer Res 1995;55:3739-41.

75. Olefsky JM. The insulin receptor. A multifunctional protein. Diabetes 1990;39:1009-16.

76. Czech MP. Structural and functional homologies in the receptors for insulin and the insulin-like growth factors. Cell 1982;31:8-10.

77. Ullrich A, Bell JR, Chen EY, Herrera R, Petruzzelli LM, Dull TJ, Gray A, Coussens L, Liao YC, Tsubokawa M. Human insulin receptor and its relationship to the tyrosine kinase family of oncogenes. Nature;313:756-61.

78. Yip CC, Jack E. Insulin receptors are bivalent as demonstrated by photoaffinity labeling. J Biol Chem 1992;267:13131-4.

79. De Meyts P, Whittaker J. Structural biology of insulin and IGF1 receptors: implications for drug design. Nat Rev Drug Discov 2002;1:769-83.

80. McKern NM, Lawrence MC, Streltsov VA, Lou MZ, Adams TE, Lovrecz GO, Elleman TC, Richards KM, Bentley JD, Pilling PA, Hoyne PA, Cartledge KA, Pham TM, Lewis JL, Sankovich SE, Stoichevska V, Da Silva E, Robinson CP, Frenkel MJ, Sparrow LG, Fernley RT, Epa VC, Ward CW. Structure of the insulin receptor ectodomain reveals a folded-over conformation. Nature 2006;443:218-21.

81. Frattali AL, Treadway JL, Pessin JE. Transmembrane signaling by the human insulin receptor kinase. Relationship between intramolecular beta subunit trans- and cis-autophosphorylation and substrate kinase activation. J Biol Chem 1992;267:19521-8.

82. Hubbard SR. Crystal structure of the activated insulin receptor tyrosine kinase in complex with peptide substrate and ATP analog. Embo J 1997;16:5572-81.

83. Siddle K, Urso B, Niesler CA, Cope DL, Molina L, Surinya KH, Soos MA. Specificity in ligand binding and intracellular signalling by insulin and insulin-like growth factor receptors. Biochemical Society Transactions 2001;29:513-25.

84. Shepherd PR, Withers DJ, Siddle K. Phosphoinositide 3-kinase: the key switch mechanism in insulin signalling. Biochem J 1998;333 (Pt 3):471-90.

85. Denton RM, Tavare JM. Does mitogen-activated-protein kinase have a role in insulin action? The cases for and against. Eur J Biochem 1995;227:597-611.

86. Blakesley VA, Scrimgeour A, Esposito D, Le Roith D. Signalling via the insulin-like growth factor-I receptor: does it differ from insulin receptor signalling? Cytokine Growth Factor Rev 1996;7:153-9.

87. Dupont J, LeRoith D. Insulin and insulin-like growth factor I receptors: similarities and differences in signal transduction. Horm Res 2001;55 Suppl 2:22-6.

88. Kim JJ, Accili D. Signalling through IGF-I and insulin receptors: where is the specificity? Growth Horm IGF Res 2002;12:84-90.

89. Nakae J, Kido Y, Accili D. Distinct and overlapping functions of insulin and IGF-I receptors. Endocrine Reviews 2001;22:818-35.

90. Louvi A, Accili D, Efstratiadis A. Growth-promoting interaction of IGF-II with the insulin receptor during mouse embryonic development. Developmental Biology 1997;189:33-48.

91. Accili D, Drago J, Lee EJ, Johnson MD, Cool MH, Salvatore P, Asico LD, Jose PA, Taylor SI, Westphal H. Early neonatal death in mice homozygous for a null allele of the insulin receptor gene. Nat Genet 1996;12:106-9.

92. Joshi RL, Lamothe B, Cordonnier N, Mesbah K, Monthioux E, Jami J, Bucchini D. Targeted disruption of the insulin receptor gene in the mouse results in neonatal lethality. Embo J 1996;15:1542-7.
93. Fisher SJ, Kahn CR. Insulin signaling is required for insulin's direct and indirect action on hepatic glucose production. J Clin Invest 2003;111:463-8.
94. Lauro D, Kido Y, Castle AL, Zarnowski MJ, Hayashi H, Ebina Y, Accili D. Impaired glucose tolerance in mice with a targeted impairment of insulin action in muscle and adipose tissue. Nat Genet 1998;20:294-8.
95. Kulkarni RN, Bruning JC, Winnay JN, Postic C, Magnuson MA, Kahn CR. Tissue-specific knockout of the insulin receptor in pancreatic beta cells creates an insulin secretory defect similar to that in type 2 diabetes. Cell 1999;96:329-39.
96. Entingh AJ, Taniguchi CM, Kahn CR. Bi-directional regulation of brown fat adipogenesis by the insulin receptor. J Biol Chem 2003;278:33377-83.
97. Kondo T, Vicent D, Suzuma K, Yanagisawa M, King GL, Holzenberger M, Kahn CR. Knockout of insulin and IGF-1 receptors on vascular endothelial cells protects against retinal neovascularization. J Clin Invest 2003;111:1835-42.
98. Ebina Y, Ellis L, Jarnagin K, Edery M, Graf L, Clauser E, Ou JH, Masiarz F, Kan YW, Goldfine ID. The human insulin receptor cDNA: the structural basis for hormone-activated transmembrane signalling. Cell 1985;40:747-58.
99. Seino S, Bell GI. Alternative splicing of human insulin receptor messenger RNA. Biochemical and Biophysical Research Communications 1989;159:312-6.
100. Kosaki A, Nelson J, Webster NJ. Identification of intron and exon sequences involved in alternative splicing of insulin receptor pre-mRNA. The Journal of Biological Chemistry 1998;273:10331-7.
101. Denley A, Wallace JC, Cosgrove LJ, Forbes BE. The insulin receptor isoform Exon 11-(IR-A) in cancer and other diseases: A review. Hormone and Metabolic Research 2003;35:778-85.
102. Ladd AN, Nguyen NH, Malhotra K, Cooper TA. CELF6, a member of the CELF family of RNA-binding proteins, regulates muscle-specific splicing enhancer-dependent alternative splicing. J Biol Chem 2004;279:17756-64.
103. Ho TH, Charlet BN, Poulos MG, Singh G, Swanson MS, Cooper TA. Muscleblind proteins regulate alternative splicing. Embo J 2004;23:3103-12.
104. Savkur RS, Philips AV, Cooper TA. Aberrant regulation of insulin receptor alternative splicing is associated with insulin resistance in myotonic dystrophy. Nature Genetics 2001;29:40-7.
105. Kellerer M, Lammers R, Ermel B, Tippmer S, Vogt B, Obermaier_Kusser B, Ullrich A, Haring HU. Distinct alpha-subunit structures of human insulin receptor A and B variants determine differences in tyrosine kinase activities. Biochemistry 1992;31:4588-96.
106. Vogt B, Carrascosa JM, Ermel B, Ullrich A, Haring HU. The two isotypes of the human insulin receptor (HIR-A and HIR-B) follow different internalization kinetics. Biochemical and Biophysical Research Communications 1991;177:1013-8.
107. Leibiger B, Leibiger IB, Moede T, Kemper S, Kulkarni RN, Kahn CR, de_Vargas LM, Berggren PO. Selective insulin signaling through A and B insulin receptors regulates transcription of insulin and glucokinase genes in pancreatic beta cells. Molecular Cell 2001;7:559-70.
108. Uhles S, Moede T, Leibiger B, Berggren PO, Leibiger IB. Isoform-specific insulin receptor signaling involves different plasma membrane domains. J Cell Biol 2003;163:1327-37.
109. Olson TS, Bamberger MJ, Lane MD. Post-translational changes in tertiary and quaternary structure of the insulin proreceptor. Correlation with acquisition of function. J Biol Chem 1988;263:7342-51.
110. Benyoucef S, Surinya KH, Hadaschik D, Siddle K. Characterization of insulin/IGF hybrid receptors: contributions of the insulin receptor L2 and Fn1 domains and the alternatively spliced exon 11 sequence to ligand binding and receptor activation. Biochem J 2007;403:603-13.
111. Hribal ML, Perego L, Lovari S, Andreozzi F, Menghini R, Perego C, Finzi G, Usellini L, Placidi C, Capella C, Guzzi V, Lauro D, Bertuzzi F, Davalli A, Pozza G, Pontiroli A, Federici M, Lauro R, Brunetti A, Folli F, Sesti G. Chronic hyperglycemia impairs insulin secretion by affecting insulin receptor expression, splicing, and signaling in RIN beta cell line and human islets of Langerhans. The Faseb Journal 2003;17:1340-2.
112. Kosaki A, Webster NJ. Effect of dexamethasone on the alternative splicing of the insulin receptor mRNA and insulin action in HepG2 hepatoma cells. The Journal of Biological Chemistry 1993;268:21990-6.

113. Norgren S, Li LS, Luthman H. Regulation of human insulin receptor RNA splicing in HepG2 cells: effects of glucocorticoid and low glucose concentration. Biochemical and Biophysical Research Communications 1994;199:277-84.

114. Sell SM, Reese D, Ossowski VM. Insulin-inducible changes in insulin receptor mRNA splice variants. J Biol Chem 1994;269:30769-72.

115. Heuson JC, Legros N, Heimann R. Influence of insulin administration on growth of the 7,12-dimethylbenz(a)anthracene-induced mammary carcinoma in intact, oophorectomized, and hypophysectomized rats. Cancer Res 1972;32:233-8.

116. Nandi S, Guzman RC, Yang J. Hormones and mammary carcinogenesis in mice, rats, and humans: a unifying hypothesis. Proc Natl Acad Sci USA 1995;92:3650-7.

117. Papa V, Pezzino V, Costantino A, Belfiore A, Giuffrida D, Frittitta L, Vannelli GB, Brand R, Goldfine ID, Vigneri R. Elevated insulin receptor content in human breast cancer. J Clin Invest 1990;86:1503-10.

118. Mathieu MC, Clark GM, Allred DC, Goldfine ID, Vigneri R. Insulin receptor expression and clinical outcome in node-negative breast cancer. Proc Assoc Am Physicians 1997;109:565-71.

119. Mulligan AM, O'Malley F P, Ennis M, Fantus IG, Goodwin PJ. Insulin receptor is an independent predictor of a favorable outcome in early stage breast cancer. Breast Cancer Res Treat 2007;106:39-47.

120. Frittitta L, Sciacca L, Catalfamo R, Ippolito A, Gangemi P, Pezzino V, Filetti S, Vigneri R. Functional insulin receptors are overexpressed in thyroid tumors: is this an early event in thyroid tumorigenesis? Cancer 1999;85:492-8.

121. Papa V, Belfiore A. Insulin receptors in breast cancer: biological and clinical role. J Endocrinol Invest 1996;19:324-33.

122. Papa V, Milazzo G, Goldfine ID, Waldman FM, Vigneri R. Sporadic amplification of the insulin receptor gene in human breast cancer. J Endocrinol Invest 1997;20:531-6.

123. Vella V, Pandini G, Sciacca L, Mineo R, Vigneri R, Pezzino V, Belfiore A. A novel autocrine loop involving IGF-II and the insulin receptor isoform-A stimulates growth of thyroid cancer. The Journal of Clinical Endocrinology and Metabolism 2002;87:245-54.

124. Vella V, Sciacca L, Pandini G, Mineo R, Squatrito S, Vigneri R, Belfiore A. The IGF system in thyroid cancer: new concepts. Mol Pathol 2001;54:121-4.

125. Sciacca L, Costantino A, Pandini G, Mineo R, Frasca F, Scalia P, Sbraccia P, Goldfine ID, Vigneri R, Belfiore A. Insulin receptor activation by IGF-II in breast cancers: evidence for a new autocrine/paracrine mechanism. Oncogene 1999;18:2471-9.

126. Kalli KR, Falowo OI, Bale LK, Zschunke MA, Roche PC, Conover CA. Functional insulin receptors on human epithelial ovarian carcinoma cells: implications for IGF-II mitogenic signaling. Endocrinology 2002;143:3259-67.

127. Sciacca L, Mineo R, Pandini G, Murabito A, Vigneri R, Belfiore A. In IGF-I receptor-deficient leiomyosarcoma cells autocrine IGF-II induces cell invasion and protection from apoptosis via the insulin receptor isoform A. Oncogene 2002;21:8240-50.

128. Frittitta L, Cerrato A, Sacco MG, Weidner N, Goldfine ID, Vigneri R. The insulin receptor content is increased in breast cancers initiated by three different oncogenes in transgenic mice. Breast Cancer Res Treat 1997;45:141-7.

129. Belfiore A. The role of insulin receptor isoforms and hybrid insulin/IGF-I receptors in human cancer. Curr Pharm Des 2007;13:671-86.

130. Smith ML, Fornace AJ, Jr. Genomic instability and the role of p53 mutations in cancer cells. Curr Opin Oncol 1995;7:69-75.

131. Ohlsson C, Kley N, Werner H, LeRoith D. p53 regulates insulin-like growth factor-I (IGF-I) receptor expression and IGF-I-induced tyrosine phosphorylation in an osteosarcoma cell line: interaction between p53 and Sp1. Endocrinology 1998;139:1101-7.

132. Foti D, Iuliano R, Chiefari E, Brunetti A. A nucleoprotein complex containing Sp1, C/EBP beta, and HMGI-Y controls human insulin receptor gene transcription. Mol Cell Biol 2003;23:2720-32.

133. Reeves R. Molecular biology of HMGA proteins: hubs of nuclear function. Gene 2001;277:63-81.

134. Sgarra R, Rustighi A, Tessari MA, Di Bernardo J, Altamura S, Fusco A, Manfioletti G, Giancotti V. Nuclear phosphoproteins HMGA and their relationship with chromatin structure and cancer. FEBS Lett 2004;574:1-8.

135. Morrione A, Valentinis B, Xu SQ, Yumet G, Louvi A, Efstratiadis A, Baserga R. Insulin-like growth factor II stimulates cell proliferation through the insulin receptor. Proceedings of the National Academy of Sciences USA 1997;94:3777-82.

136. Jones HE, Gee JM, Barrow D, Tonge D, Holloway B, Nicholson RI. Inhibition of insulin receptor isoform-A signalling restores sensitivity to gefitinib in previously de novo resistant colon cancer cells. Br J Cancer 2006;95:172-80.

137. Soos MA, Field CE, Siddle K. Purified hybrid insulin/insulin-like growth factor-I receptors bind insulin-like growth factor-I, but not insulin, with high affinity. The Biochemical Journal 1993;290 (Pt 2):419-26.

138. Soos MA, Whittaker J, Lammers R, Ullrich A, Siddle K. Receptors for insulin and insulin-like growth factor-I can form hybrid dimers. Characterisation of hybrid receptors in transfected cells. The Biochemical Journal 1990;270:383-90.

139. Treadway JL, Morrison BD, Goldfine ID, Pessin JE. Assembly of insulin/insulin-like growth factor-1 hybrid receptors in vitro. J Biol Chem 1989;264:21450-3.

140. Bailyes EM, Nave BT, Soos MA, Orr SR, Hayward AC, Siddle K. Insulin receptor/IGF-I receptor hybrids are widely distributed in mammalian tissues: quantification of individual receptor species by selective immunoprecipitation and immunoblotting. The Biochemical Journal 1997;327 (Pt 1):209-15.

141. Federici M, Porzio O, Zucaro L, Fusco A, Borboni P, Lauro D, Sesti G. Distribution of insulin/insulin-like growth factor-I hybrid receptors in human tissues. Molecular and Cellular Endocrinology 1997;129:121-6.

142. Belfiore A, Pandini G, Vella V, Squatrito S, Vigneri R. Insulin/IGF-I hybrid receptors play a major role in IGF-I signaling in thyroid cancer. Biochimie 1999;81:403-7.

143. Pandini G, Vigneri R, Costantino A, Frasca F, Ippolito A, Fujita_Yamaguchi Y, Siddle K, Goldfine ID, Belfiore A. Insulin and insulin-like growth factor-I (IGF-I) receptor overexpression in breast cancers leads to insulin/IGF-I hybrid receptor overexpression: evidence for a second mechanism of IGF-I signaling. Clinical Cancer Research 1999;5:1935-44.

144. Frattali AL, Pessin JE. Relationship between alpha subunit ligand occupancy and beta subunit autophosphorylation in insulin/insulin-like growth factor-1 hybrid receptors. The Journal of Biological Chemistry 1993;268:7393-400.

145. Langlois WJ, Sasaoka T, Yip CC, Olefsky JM. Functional characterization of hybrid receptors composed of a truncated insulin receptor and wild type insulin-like growth factor 1 or insulin receptors. Endocrinology 1995;136:1978-86.

146. Seely BL, Reichart DR, Takata Y, Yip C, Olefsky JM. A functional assessment of insulin/insulin-like growth factor-I hybrid receptors. Endocrinology 1995;136:1635-41.

147. Slaaby R, Schaffer L, Lautrup-Larsen I, Andersen AS, Shaw AC, Mathiasen IS, Brandt J. Hybrid receptors formed by insulin receptor (IR) and insulin-like growth factor I receptor (IGF-IR) have low insulin and high IGF-1 affinity irrespective of the IR splice variant. J Biol Chem 2006;281:25869-74.

148. Pandini G, Frasca F, Mineo R, Sciacca L, Vigneri R, Belfiore A. Insulin/insulin-like growth factor I hybrid receptors have different biological characteristics depending on the insulin receptor isoform involved. The Journal of Biological Chemistry 2002;277:39684-95.

149. Blanquart C, Gonzalez-Yanes C, Issad T. Monitoring the activation state of insulin/insulin-like growth factor-1 hybrid receptors using bioluminescence resonance energy transfer. Mol Pharmacol 2006;70:1802-11.

150. Lawrence MC, McKern NM, Ward CW. Insulin receptor structure and its implications for the IGF-1 receptor. Curr Opin Struct Biol 2007;17:699-705.

151. Zhang H, Pelzer AM, Kiang DT, Yee D. Down-regulation of type I insulin-like growth factor receptor increases sensitivity of breast cancer cells to insulin. Cancer Res 2007;67:391-7.

152. Parkin. Estimates of world wide incidence of major cancers in 1990. International Journal of Cancer 1999;80:827-41.

153. Lynch HT, de_la_Chapelle A. Hereditary colorectal cancer. The New England Journal of Medicine 2003;348:919-32.

154. Robbins DH, Itzkowitz SH. The molecular and genetic basis of colon cancer. The Medical Clinics of North America 2002;86:1467-95.

155. Michor F, Iwasa Y, Lengauer C, Nowak MA. Dynamics of colorectal cancer. Semin Cancer Biol 2005;15:484-93.

156. Weitz J, Koch M, Debus J, Hohler T, Galle PR, Buchler MW. Colorectal cancer. Lancet 2005;365:153-65.

157. Norat T, Bingham S, Ferrari P, Slimani N, Jenab M, Mazuir M, Overvad K, Olsen A, Tjonneland A, Clavel F, Boutron-Ruault MC, Kesse E, Boeing H, Bergmann MM, Nieters A, Linseisen J, Trichopoulou A, Trichopoulos D, Tountas Y, Berrino F, Palli D, Panico S, Tumino R, Vineis P, Bueno-de-Mesquita HB, Peeters PH, Engeset D, Lund E, Skeie G, Ardanaz E, Gonzalez C, Navarro C, Quiros JR, Sanchez MJ, Berglund G, Mattisson I, Hallmans G, Palmqvist R, Day NE, Khaw KT, Key TJ, San Joaquin M, Hemon B, Saracci

R, Kaaks R, Riboli E. Meat, fish, and colorectal cancer risk: the European Prospective Investigation into cancer and nutrition. J Natl Cancer Inst 2005;97:906-16.

158. Vogelstein B, Kinzler KW. The multistep nature of cancer. Trends Genet 1993;9:138-41.
159. Kinzler KW, Vogelstein B. Lessons from hereditary colorectal cancer. Cell 1996;87:159-70.
160. Bingham SA. High-meat diets and cancer risk. Proc Nutr Soc 1999;58:243-8.
161. Caderni G, Lancioni L, Luceri C, Giannini A, Lodovici M, Biggeri A, Dolara P. Dietary sucrose and starch affect dysplastic characteristics in carcinogen-induced aberrant crypt foci in rat colon. Cancer Letters 1997;114:39-41.
162. Koohestani N, Chia MC, Pham NA, Tran TT, Minkin S, Wolever TM, Bruce WR. Aberrant crypt focus promotion and glucose intolerance: correlation in the rat across diets differing in fat, n-3 fatty acids and energy. Carcinogenesis 1998;19:1679-84.
163. Zhang W, Thornton WH, MacDonald RS. Insulin-like growth factor-I and II receptor expression in rat colon mucosa are affected by dietary lipid intake. The Journal of Nutrition 1998;128:158-65.
164. Thornton WH, MacDonald RS. Dietary fat quantity and composition alter colon cell kinetics in growing rats. Ann nutr metab 1994;38:270-280.
165. Bingham SA, Day NE, Luben R, Ferrari P, Slimani N, Norat T, Clavel-Chapelon F, Kesse E, Nieters A, Boeing H, Tjonneland A, Overvad K, Martinez C, Dorronsoro M, Gonzalez CA, Key TJ, Trichopoulou A, Naska A, Vineis P, Tumino R, Krogh V, Bueno-de-Mesquita HB, Peeters PH, Berglund G, Hallmans G, Lund E, Skeie G, Kaaks R, Riboli E. Dietary fibre in food and protection against colorectal cancer in the European Prospective Investigation into Cancer and Nutrition (EPIC): an observational study. Lancet 2003;361:1496-501.
166. Duncan SH, Holtrop G, Lobley GE, Calder AG, Stewart CS, Flint HJ. Contribution of acetate to butyrate formation by human faecal bacteria. Br J Nutr 2004;91:915-23.
167. Bowling TE, Raimundo AH, Grimble GK, Silk DB. Reversal by short-chain fatty acids of colonic fluid secretion induced by enteral feeding. Lancet 1993;342:1266-8.
168. Narcy A, Robert L, Mazur A, Demigne C, Remesy C. Effect of potato on acid-base and mineral homeostasis in rats fed a high-sodium chloride diet. Br J Nutr 2006;95:925-32.
169. Jacobasch G, Dongowski G, Schmiedl D, Muller-Schmehl K. Hydrothermal treatment of Novelose 330 results in high yield of resistant starch type 3 with beneficial prebiotic properties and decreased secondary bile acid formation in rats. Br J Nutr 2006;95:1063-74.
170. Remesy C, Deningne C, Morand C. Metabolism of short-chain fatty acids in the liver. In Physiological and clinical aspects of short-chain fatty acids 1995:171 - 190.
171. Ahmad MS, Krishnan S, Ramakrishna BS, Mathan M, Pulimood AB, Murthy SN. Butyrate and glucose metabolism by colonocytes in experimental colitis in mice. Gut 2000;46:493-9.
172. Blottiere HM, Buecher B, Galmiche JP, Cherbut C. Molecular analysis of the effect of short-chain fatty acids on intestinal cell proliferation. Proc Nutr Soc 2003;62:101-6.
173. van Nuenen MH, de Ligt RA, Doornbos RP, van der Woude JC, Kuipers EJ, Venema K. The influence of microbial metabolites on human intestinal epithelial cells and macrophages in vitro. FEMS Immunol Med Microbiol 2005;45:183-9.
174. Andoh A, Tsujikawa T, Fujiyama Y. Role of dietary fiber and short-chain fatty acids in the colon. Curr Pharm Des 2003;9:347-58.
175. Levy P, Robin H, Bertrand F, Kornprobst M, Capeau J. Butyrate-treated colonic Caco-2 cells exhibit defective integrin-mediated signaling together with increased apoptosis and differentiation. J Cell Physiol 2003;197:336-47.
176. Miller SJ. Cellular and physiological effects of short-chain fatty acids. Mini Rev Med Chem 2004;4:839-45.
177. Soergel KH. Colonic fermentation: metabolic and clinical implications. Clin Investig 1994;72:742-8.
178. Myzak MC, Ho E, Dashwood RH. Dietary agents as histone deacetylase inhibitors. Mol Carcinog 2006;45:443-6.
179. Nishimura A, Fujimoto M, Oguchi S, Fusunyan RD, MacDermott RP, Sanderson IR. Short-chain fatty acids regulate IGF-binding protein secretion by intestinal epithelial cells. Am J Physiol 1998;275:E55-63.
180. Le_Marchand L, Wilkens LR, Kolonel LN, Hankin JH, Lyu LC. Associations of sedentary lifestyle, obesity, smoking, alcohol use, and diabetes with the risk of colorectal cancer. Cancer Research 1997;57:4787-94.
181. Slattery. Physical acts and colorectal cancer. Epidemiology 1990;1:481-485.
182. Nilsen TI, Vatten LJ. Prospective study of colorectal cancer risk and physical activity, diabetes, blood glucose and BMI: exploring the hyperinsulinaemia hypothesis. British Journal of Cancer 2001;84:417-22.

183. Ma J, Pollak MN, Giovannucci E, Chan JM, Tao Y, Hennekens CH, Stampfer MJ. Prospective study of colorectal cancer risk in men and plasma levels of insulin-like growth factor (IGF)-I and IGF-binding protein-3. Journal of the National Cancer Institute 1999;91:620-5.

184. Giovannucci E. Nutrition, insulin, insulin-like growth factors and cancer. Horm Metab Res 2003;35:694-704.

185. Murphy TK, Calle EE, Rodriguez C, Kahn HS, Thun MJ. Body mass index and colon cancer mortality in a large prospective study. American Journal of Epidemiology 2000;152:847-54.

186. Pischon T, Lahmann PH, Boeing H, Tjonneland A, Halkjaer J, Overvad K, Klipstein-Grobusch K, Linseisen J, Becker N, Trichopoulou A, Benetou V, Trichopoulos D, Sieri S, Palli D, Tumino R, Vineis P, Panico S, Monninkhof E, Peeters PH, Bueno-de-Mesquita HB, Buchner FL, Ljungberg B, Hallmans G, Berglund G, Gonzalez CA, Dorronsoro M, Gurrea AB, Navarro C, Martinez C, Quiros JR, Roddam A, Allen N, Bingham S, Khaw KT, Kaaks R, Norat T, Slimani N, Riboli E. Body size and risk of renal cell carcinoma in the European Prospective Investigation into Cancer and Nutrition (EPIC). Int J Cancer 2006;118:728-38.

187. Terry P, Giovannucci E, Bergkvist L, Holmberg L, Wolk A. Body weight and colorectal cancer risk in a cohort of Swedish women: relation varies by age and cancer site. British Journal of Cancer 2001;85:346-9.

188. Terry PD, Miller AB, Rohan TE. Obesity and colorectal cancer risk in women. Gut 2002;51:191-4.

189. Giovannucci E, Michaud D. The role of obesity and related metabolic disturbances in cancers of the colon, prostate, and pancreas. Gastroenterology 2007;132:2208-25.

190. Bostick RM, Potter JD, Kushi LH, Sellers TA, Steinmetz KA, McKenzie DR, Gapstur SM, Folsom AR. Sugar, meat, and fat intake, and non-dietary risk factors for colon cancer incidence in Iowa women (United States). Cancer Causes Control 1994;5:38-52.

191. Giovannucci E, Colditz GA, Stampfer MJ, Willett WC. Physical activity, obesity, and risk of colorectal adenoma in women (United States). Cancer Causes Control 1996;7:253-63.

192. Russo A, Franceschi S, La Vecchia C, Dal Maso L, Montella M, Conti E, Giacosa A, Falcini F, Negri E. Body size and colorectal-cancer risk. Int J Cancer 1998;78:161-5.

193. Kahn BB, Flier JS. Obesity and insulin resistance. The Journal of Clinical Investigation 2000;106:473-81.

194. Komninou D, Ayonote A, Richie JP, Rigas B. Insulin resistance and its contribution to colon carcinogenesis. 2003;228:396-405.

195. Sandhu MS, Dunger DB, Giovannucci EL. Insulin, insulin-like growth factor-I (IGF-I), IGF binding proteins, their biologic interactions, and colorectal cancer. Journal of the National Cancer Institute 2002;94:972-80.

196. Giovannucci E. Insulin, insulin-like growth factors and colon cancer: a review of the evidence. The Journal of Nutrition 2001;131:3109S-20S.

197. Schoen RE, Tangen CM, Kuller LH, Burke GL, Cushman M, Tracy RP, Dobs A, Savage PJ. Increased blood glucose and insulin, body size, and incident colorectal cancer. Journal of the National Cancer Institute 1999;91:1147-54.

198. Colangelo LA, Gapstur SM, Gann PH, Dyer AR, Liu K. Colorectal cancer mortality and factors related to the insulin resistance syndrome. Cancer Epidemiology, Biomarkers & Prevention 2002;11:385-91.

199. Hu FB, Manson JE, Liu S, Hunter D, Colditz GA, Michels KB, Speizer FE, Giovannucci E. Prospective study of adult onset diabetes mellitus (type 2) and risk of colorectal cancer in women. Journal of the National Cancer Institute 1999;91:542-7.

200. Will JC, Galuska DA, Vinicor F, Calle EE. Colorectal cancer: another complication of diabetes mellitus? American Journal of Epidemiology 1998;147:816-25.

201. Argente J, Caballo N, Barrios V, Munoz MT, Pozo J, Chowen JA, Hernandez M. Disturbances in the growth hormone-insulin-like growth factor axis in children and adolescents with different eating disorders. Horm Res 1997;48 Suppl 4:16-8.

202. Jenkins PJ, Fairclough PD, Richards T, Lowe DG, Monson J, Grossman A, Wass JA, Besser M. Acromegaly, colonic polyps and carcinoma. 1997;47:17-22.

203. Baris D, Gridley G, Ron E, Weiderpass E, Mellemkjaer L, Ekbom A, Olsen JH, Baron JA, Fraumeni JF, Jr. Acromegaly and cancer risk: a cohort study in Sweden and Denmark. Cancer Causes Control 2002;13:395-400.

204. Orme SM, McNally RJ, Cartwright RA, Belchetz PE. Mortality and cancer incidence in acromegaly: a retrospective cohort study. United Kingdom Acromegaly Study Group. The Journal of Clinical Endocrinology and Metabolism 1998;83:2730-4.

205. Wu Y, Yakar S, Zhao L, Hennighausen L, LeRoith D. Circulating insulin-like growth factor-I levels regulate colon cancer growth and metastasis. Cancer Research 2002;62:1030-5.

206. Renehan AG, Zwahlen M, Minder C, O'Dwyer ST, Shalet SM, Egger M. Insulin-like growth factor (IGF)-I, IGF binding protein-3, and cancer risk: systematic review and meta-regression analysis. Lancet 2004;363:1346-53.

207. Cats A, Dullaart RP, Kleibeuker JH, Kuipers F, Sluiter WJ, Hardonk MJ, de_Vries EG. Increased epithelial cell proliferation in the colon of patients with acromegaly. Cancer Research 1996;56:523-6.

208. Durai R, Yang W, Gupta S, Seifalian AM, Winslet MC. The role of the insulin-like growth factor system in colorectal cancer: review of current knowledge. Int J Colorectal Dis 2005;20:203-20.

209. Hassan AB, Macaulay VM. The insulin-like growth factor system as a therapeutic target in colorectal cancer. Ann Oncol 2002;13:349-56.

210. Tricoli JV, Rall LB, Karakousis CP, Herrera L, Petrelli NJ, Bell GI, Shows TB. Enhanced levels of insulin-like growth factor messenger RNA in human colon carcinomas and liposarcomas. Cancer Res 1986;46:6169-73.

211. Zhang L, Zhou W, Velculescu VE, Kern SE, Hruban RH, Hamilton SR, Vogelstein B, Kinzler KW. Gene expression profiles in normal and cancer cells. Science 1997;276:1268-72.

212. Notterman DA, Alon U, Sierk AJ, Levine AJ. Transcriptional gene expression profiles of colorectal adenoma, adenocarcinoma, and normal tissue examined by oligonucleotide arrays. Cancer Res 2001;61:3124-30.

213. Kawamoto K, Onodera H, Kondo S, Kan S, Ikeuchi D, Maetani S, Imamura M. Expression of insulin-like growth factor-2 can predict the prognosis of human colorectal cancer patients: correlation with tumor progression, proliferative activity and survival. Oncology 1998;55:242-8.

214. Cui H, Cruz-Correa M, Giardiello FM, Hutcheon DF, Kafonek DR, Brandenburg S, Wu Y, He X, Powe NR, Feinberg AP. Loss of IGF2 imprinting: a potential marker of colorectal cancer risk. Science 2003;299:1753-5.

215. Hodzic D, Delacroix L, Willemsen P, Bensbaho K, Collette J, Broux R, Lefebvre P, Legros JJ, Grooteclaes M, Winkler R. Characterization of the IGF system and analysis of the possible molecular mechanisms leading to IGF-II overexpression in a mesothelioma. Horm Metab Res 1997;29:549-55.

216. Hodzic D, Frey B, Marechal D, Scarcez T, Grooteclaes M, Winkler R. Cloning of breakpoints in and downstream the IGF2 gene that are associated with overexpression of IGF2 transcripts in colorectal tumours. Oncogene 1999;18:4710-7.

217. Hassan AB, Howell JA. Insulin-like growth factor II supply modifies growth of intestinal adenoma in Apc(Min/+) mice. Cancer Res 2000;60:1070-6.

218. Peters G, Gongoll S, Langner C, Mengel M, Piso P, Klempnauer J, Ruschoff J, Kreipe H, von_Wasielewski R. IGF-1R, IGF-1 and IGF-2 expression as potential prognostic and predictive markers in colorectal-cancer. Virchows Archiv : An International Journal of Pathology 2003;443:139-45.

219. Reinmuth N, Fan F, Liu W, Parikh AA, Stoeltzing O, Jung YD, Bucana CD, Radinsky R, Gallick GE, Ellis LM. Impact of insulin-like growth factor receptor-I function on angiogenesis, growth, and metastasis of colon cancer. Lab Invest 2002;82:1377-89.

220. Kawamoto K, Onodera H, Kan S, Kondo S, Imamura M. Possible paracrine mechanism of insulin-like growth factor-2 in the development of liver metastases from colorectal carcinoma. Cancer 1999;85:18-25.

221. Ma J, Pollak MN, Giovannucci E, Chan JM, Tao Y, Hennekens CH, Stampfer MJ. Prospective study of colorectal cancer risk in men and plasma levels of insulin-like growth factor (IGF)-I and IGF-binding protein-3. J Natl Cancer Inst 1999;91:620-5.

222. Renehan AG, Painter JE, Atkin WS, Potten CS, Shalet SM, O'Dwyer ST. High-risk colorectal adenomas and serum insulin-like growth factors. Br J Surg 2001;88:107-13.

223. Michell NP, Langman MJ, Eggo MC. Insulin-like growth factors and their binding proteins in human colonocytes: preferential degradation of insulin-like growth factor binding protein 2 in colonic cancers. Br J Cancer 1997;76:60-6.

224. Guo YS, Jin GF, Townsend CM, Zhang T, Sheng HM, Beauchamp RD, Thompson JC. Insulin-like growth factor-II expression in carcinoma in colon cell lines: implications for autocrine actions. Journal of the American College of Surgeons 1995;181:145-54.

225. Zarrilli R, Pignata S, Romano M, Gravina A, Casola S, Bruni CB, Acquaviva AM. Expression of insulin-like growth factor (IGF)-II and IGF-I receptor during proliferation and differentiation of CaCo-2 human colon carcinoma cells. Cell Growth Differ 1994;5:1085-91.

226. Howarth GS. Insulin-like growth factor-I and the gastrointestinal system: therapeutic indications and safety implications. J Nutr 2003;133:2109-12.

227. Ouban A, Muraca P, Yeatman T, Coppola D. Expression and distribution of insulin-like growth factor-1 receptor in human carcinomas. Hum Pathol 2003;34:803-8.

228. Kiunga GA, Raju J, Sabljic N, Bajaj G, Good CK, Bird RP. Elevated insulin receptor protein expression in experimentally induced colonic tumors. Cancer Lett 2004;211:145-53.

229. Weber MM, Fottner C, Liu SB, Jung MC, Engelhardt D, Baretton GB. Overexpression of the insulin-like growth factor I receptor in human colon carcinomas. Cancer 2002;95:2086-95.

230. Adachi Y, Lee CT, Coffee K, Yamagata N, Ohm JE, Park KH, Dikov MM, Nadaf SR, Arteaga CL, Carbone DP. Effects of genetic blockade of the insulin-like growth factor receptor in human colon cancer cell lines. Gastroenterology 2002;123:1191-204.

231. Shi B, Sepp-Lorenzino L, Prisco M, Linsley P, deAngelis T, Baserga R. Micro RNA 145 targets the insulin receptor substrate-1 and inhibits the growth of colon cancer cells. J Biol Chem 2007;282:32582-90.

232. Cummins JM, He Y, Leary RJ, Pagliarini R, Diaz LA, Jr., Sjoblom T, Barad O, Bentwich Z, Szafranska AE, Labourier E, Raymond CK, Roberts BS, Juhl H, Kinzler KW, Vogelstein B, Velculescu VE. The colorectal microRNAome. Proc Natl Acad Sci U S A 2006;103:3687-92.

233. Leng SL, Leeding KS, Gibson PR, Bach LA. Insulin-like growth factor-II renders LIM 2405 human colon cancer cells resistant to butyrate-induced apoptosis: a potential mechanism for colon cancer cell survival in vivo. Carcinogenesis 2001;22:1625-31.

234. Di Popolo A, Memoli A, Apicella A, Tuccillo C, di Palma A, Ricchi P, Acquaviva AM, Zarrilli R. IGF-II/IGF-I receptor pathway up-regulates COX-2 mRNA expression and PGE2 synthesis in Caco-2 human colon carcinoma cells. Oncogene 2000;19:5517-24.

235. Nosho K, Yamamoto H, Taniguchi H, Adachi Y, Yoshida Y, Arimura Y, Endo T, Hinoda Y, Imai K. Interplay of insulin-like growth factor-II, insulin-like growth factor-I, insulin-like growth factor-I receptor, COX-2, and matrix metalloproteinase-7, play key roles in the early stage of colorectal carcinogenesis. Clin Cancer Res 2004;10:7950-7.

236. Prescott SM, Fitzpatrick FA. Cyclooxygenase-2 and carcinogenesis. Biochim Biophys Acta 2000;1470:M69-78.

237. Williams CS, Smalley W, DuBois RN. Aspirin use and potential mechanisms for colorectal cancer prevention. J Clin Invest 1997;100:1325-9.

238. Oshima M, Dinchuk JE, Kargman SL, Oshima H, Hancock B, Kwong E, Trzaskos JM, Evans JF, Taketo MM. Suppression of intestinal polyposis in Apc delta716 knockout mice by inhibition of cyclooxygenase 2 (COX-2). Cell 1996;87:803-9.

239. Bohula EA, Playford MP, Macaulay VM. Targeting the type 1 insulin-like growth factor receptor as anti-cancer treatment. Anticancer Drugs 2003;14:669-82.

240. Letsch M, Schally AV, Busto R, Bajo AM, Varga JL. Growth hormone-releasing hormone (GHRH) antagonists inhibit the proliferation of androgen-dependent and -independent prostate cancers. Proc Natl Acad Sci USA 2003;100:1250-5.

241. Yee D. Targeting insulin-like growth factor pathways. Br J Cancer 2006;94:465-8.

242. Van den Berg CL, Cox GN, Stroh CA, Hilsenbeck SG, Weng CN, McDermott MJ, Pratt D, Osborne CK, Coronado-Heinsohn EB, Yee D. Polyethylene glycol conjugated insulin-like growth factor binding protein-1 (IGFBP-1) inhibits growth of breast cancer in athymic mice. Eur J Cancer 1997;33:1108-13.

243. Miyamoto S, Nakamura M, Shitara K, Nakamura K, Ohki Y, Ishii G, Goya M, Kodama K, Sangai T, Maeda H, Shi-Chuang Z, Chiba T, Ochiai A. Blockade of paracrine supply of insulin-like growth factors using neutralizing antibodies suppresses the liver metastasis of human colorectal cancers. Clin Cancer Res 2005;11:3494-502.

244. Riedemann J, Macaulay VM. IGF1R signalling and its inhibition. Endocr Relat Cancer 2006;13 Suppl 1:S33-43.

245. Garber K. IGF-1: old growth factor shines as new drug target. J Natl Cancer Inst 2005;97:790-2.

246. Surmacz E. Growth factor receptors as therapeutic targets: strategies to inhibit the insulin-like growth factor I receptor. Oncogene 2003;22:6589-97.

247. Arteaga CL, Osborne CK. Growth inhibition of human breast cancer cells in vitro with an antibody against the type I somatomedin receptor. Cancer Research 1989;49:6237-41.

248. Burtrum D, Zhu Z, Lu D, Anderson DM, Prewett M, Pereira DS, Bassi R, Abdullah R, Hooper AT, Koo H, Jimenez X, Johnson D, Apblett R, Kussie P, Bohlen P, Witte L, Hicklin DJ, Ludwig DL. A fully human monoclonal antibody to the insulin-like growth factor I receptor blocks ligand-dependent signaling and inhibits human tumor growth in vivo. Cancer Res 2003;63:8912-21.

249. Furlanetto RW, Harwell SE, Baggs RB. Effects of insulin-like growth factor receptor inhibition on human melanomas in culture and in athymic mice. Cancer Res 1993;53:2522-6.

250. Goetsch L, Gonzalez A, Leger O, Beck A, Pauwels PJ, Haeuw JF, Corvaia N. A recombinant humanized anti-insulin-like growth factor receptor type I antibody (h7C10) enhances the antitumor activity of vinorelbine and anti-epidermal growth factor receptor therapy against human cancer xenografts. Int J Cancer 2005;113:316-28.

251. Li SL, Liang SJ, Guo N, Wu AM, Fujita-Yamaguchi Y. Single-chain antibodies against human insulin-like growth factor I receptor: expression, purification, and effect on tumor growth. Cancer Immunol Immunother 2000;49:243-52.

252. Maloney EK, McLaughlin JL, Dagdigian NE, Garrett LM, Connors KM, Zhou XM, Blattler WA, Chittenden T, Singh R. An anti-insulin-like growth factor I receptor antibody that is a potent inhibitor of cancer cell proliferation. Cancer Research 2003;63:5073-83.

253. Wang Y, Hailey J, Williams D, Lipari P, Malkowski M, Wang X, Xie L, Li G, Saha D, Ling WL, Cannon-Carlson S, Greenberg R, Ramos RA, Shields R, Presta L, Brams P, Bishop WR, Pachter JA. Inhibition of insulin-like growth factor-I receptor (IGF-IR) signaling and tumor cell growth by a fully human neutralizing anti-IGF-IR antibody. Mol Cancer Ther 2005;4:1214-21.

254. Cohen BD, Baker DA, Soderstrom C, Tkalcevic G, Rossi AM, Miller PE, Tengowski MW, Wang F, Gualberto A, Beebe JS, Moyer JD. Combination therapy enhances the inhibition of tumor growth with the fully human anti-type 1 insulin-like growth factor receptor monoclonal antibody CP-751,871. Clin Cancer Res 2005;11:2063-73.

255. Wu JD, Odman A, Higgins LM, Haugk K, Vessella R, Ludwig DL, Plymate SR. In vivo effects of the human type I insulin-like growth factor receptor antibody A12 on androgen-dependent and androgen-independent xenograft human prostate tumors. Clin Cancer Res 2005;11:3065-74.

256. Sachdev D, Li SL, Hartell JS, Fujita-Yamaguchi Y, Miller JS, Yee D. A chimeric humanized single-chain antibody against the type I insulin-like growth factor (IGF) receptor renders breast cancer cells refractory to the mitogenic effects of IGF-I. Cancer Res 2003;63:627-35.

257. Sachdev D, Singh R, Fujita-Yamaguchi Y, Yee D. Down-regulation of insulin receptor by antibodies against the type I insulin-like growth factor receptor: implications for anti-insulin-like growth factor therapy in breast cancer. Cancer Res 2006;66:2391-402.

258. Russell SJ, Llewelyn MB, Hawkins RE. Principles of antibody therapy. Bmj 1992;305:1424-9.

259. Hudson PJ. Recombinant antibody fragments. Curr Opin Biotechnol 1998;9:395-402.

260. Prager D, Yamasaki H, Weber MM, Gebremedhin S, Melmed S. Human insulin-like growth factor I receptor function in pituitary cells is suppressed by a dominant negative mutant. J Clin Invest 1992;90:2117-22.

261. D'Ambrosio C, Ferber A, Resnicoff M, Baserga R. A soluble insulin-like growth factor I receptor that induces apoptosis of tumor cells in vivo and inhibits tumorigenesis. Cancer Res 1996;56:4013-20.

262. Dunn SE, Ehrlich M, Sharp NJ, Reiss K, Solomon G, Hawkins R, Baserga R, Barrett JC. A dominant negative mutant of the insulin-like growth factor-I receptor inhibits the adhesion, invasion, and metastasis of breast cancer. Cancer Res 1998;58:3353-61.

263. Lee CT, Park KH, Adachi Y, Seol JY, Yoo CG, Kim YW, Han SK, Shim YS, Coffee K, Dikov MM, Carbone DP. Recombinant adenoviruses expressing dominant negative insulin-like growth factor-I receptor demonstrate antitumor effects on lung cancer. Cancer Gene Ther 2003;10:57-63.

264. Min Y, Adachi Y, Yamamoto H, Imsumran A, Arimura Y, Endo T, Hinoda Y, Lee CT, Nadaf S, Carbone DP, Imai K. Insulin-like growth factor I receptor blockade enhances chemotherapy and radiation responses and inhibits tumour growth in human gastric cancer xenografts. Gut 2005;54:591-600.

265. Romano G, Reiss K, Tu X, Peruzzi F, Belletti B, Wang JY, Zanocco-Marani T, Baserga R. Efficient in vitro and in vivo gene regulation of a retrovirally delivered pro-apoptotic factor under the control of the Drosophila HSP70 promoter. Gene Ther 2001;8:600-7.

266. Hartog H, Wesseling J, Boezen HM, van der Graaf WT. The insulin-like growth factor 1 receptor in cancer: old focus, new future. Eur J Cancer 2007;43:1895-904.

267. Girnita A, Girnita L, del Prete F, Bartolazzi A, Larsson O, Axelson M. Cyclolignans as inhibitors of the insulin-like growth factor-1 receptor and malignant cell growth. Cancer Res 2004;64:236-42.

268. Youngren JF, Gable K, Penaranda C, Maddux BA, Zavodovskaya M, Lobo M, Campbell M, Kerner J, Goldfine ID. Nordihydroguaiaretic acid (NDGA) inhibits the IGF-1 and c-

erbB2/HER2/neu receptors and suppresses growth in breast cancer cells. Breast Cancer Res Treat 2005;94:37-46.

269. Haluska P, Carboni JM, Loegering DA, Lee FY, Wittman M, Saulnier MG, Frennesson DB, Kalli KR, Conover CA, Attar RM, Kaufmann SH, Gottardis M, Erlichman C. In vitro and in vivo antitumor effects of the dual insulin-like growth factor-I/insulin receptor inhibitor, BMS-554417. Cancer Res 2006;66:362-71.

270. Withers DJ, Burks DJ, Towery HH, Altamuro SL, Flint CL, White MF. Irs-2 coordinates Igf-1 receptor-mediated beta-cell development and peripheral insulin signalling. Nat Genet 1999;23:32-40.

271. Crooke ST. Molecular mechanisms of action of antisense drugs. Biochim Biophys Acta 1999;1489:31-44.

272. Stein CA, Cohen JS. Oligodeoxynucleotides as inhibitors of gene expression: a review. Cancer Res 1988;48:2659-68.

273. Sohail M, Southern EM. Selecting optimal antisense reagents. Adv Drug Deliv Rev 2000;44:23-34.

274. Coppola D, Saunders B, Fu L, Mao W, Nicosia SV. The insulin-like growth factor 1 receptor induces transformation and tumorigenicity of ovarian mesothelial cells and down-regulates their Fas-receptor expression. Cancer Res 1999;59:3264-70.

275. Macaulay VM, Salisbury AJ, Bohula EA, Playford MP, Smorodinsky NI, Shiloh Y. Downregulation of the type 1 insulin-like growth factor receptor in mouse melanoma cells is associated with enhanced radiosensitivity and impaired activation of Atm kinase. Oncogene 2001;20:4029-40.

276. Muller M, Dietel M, Turzynski A, Wiechen K. Antisense phosphorothioate oligodeoxynucleotide down-regulation of the insulin-like growth factor I receptor in ovarian cancer cells. Int J Cancer 1998;77:567-71.

277. Pavelic J, Pavelic L, Karadza J, Krizanac S, Unesic J, Spaventi S, Pavelic K. Insulin-like growth factor family and combined antisense approach in therapy of lung carcinoma. Mol Med 2002;8:149-57.

278. Pietrzkowski Z, Mulholland G, Gomella L, Jameson BA, Wernicke D, Baserga R. Inhibition of growth of prostatic cancer cell lines by peptide analogues of insulin-like growth factor 1. Cancer Res 1993;53:1102-6.

279. Resnicoff M, Sell C, Rubini M, Coppola D, Ambrose D, Baserga R, Rubin R. Rat glioblastoma cells expressing an antisense RNA to the insulin-like growth factor-1 (IGF-1) receptor are nontumorigenic and induce regression of wild-type tumors. Cancer Res 1994;54:2218-22.

280. Chernicky CL, Yi L, Tan H, Gan SU, Ilan J. Treatment of human breast cancer cells with antisense RNA to the type I insulin-like growth factor receptor inhibits cell growth, suppresses tumorigenesis, alters the metastatic potential, and prolongs survival in vivo. Cancer Gene Ther 2000;7:384-95.

281. Scotlandi K, Maini C, Manara MC, Benini S, Serra M, Cerisano V, Strammiello R, Baldini N, Lollini PL, Nanni P, Nicoletti G, Picci P. Effectiveness of insulin-like growth factor I receptor antisense strategy against Ewing's sarcoma cells. Cancer Gene Ther 2002;9:296-307.

282. Wang H, Wang S, Nan L, Yu D, Agrawal S, Zhang R. Antisense anti-MDM2 mixed-backbone oligonucleotides enhance therapeutic efficacy of topoisomerase I inhibitor irinotecan in nude mice bearing human cancer xenografts: In vivo activity and mechanisms. Int J Oncol 2002;20:745-52.

283. Krieg AM, Stein CA. Phosphorothioate oligodeoxynucleotides: antisense or anti-protein? Antisense Res Dev 1995;5:241.

284. Andrews DW, Resnicoff M, Flanders AE, Kenyon L, Curtis M, Merli G, Baserga R, Iliakis G, Aiken RD. Results of a pilot study involving the use of an antisense oligodeoxynucleotide directed against the insulin-like growth factor type I receptor in malignant astrocytomas. J Clin Oncol 2001;19:2189-200.

285. Fire A, Xu S, Montgomery MK, Kostas SA, Driver SE, Mello CC. Potent and specific genetic interference by double-stranded RNA in Caenorhabditis elegans. Nature 1998;391:806-11.

286. Guo S, Kemphues KJ. par-1, a gene required for establishing polarity in C. elegans embryos, encodes a putative Ser/Thr kinase that is asymmetrically distributed. Cell 1995;81:611-20.

287. Gil J, Esteban M. Induction of apoptosis by the dsRNA-dependent protein kinase (PKR): mechanism of action. Apoptosis 2000;5:107-14.

288. Kumar M, Carmichael GG. Antisense RNA: function and fate of duplex RNA in cells of higher eukaryotes. Microbiol Mol Biol Rev 1998;62:1415-34.

289. Elbashir SM, Harborth J, Lendeckel W, Yalcin A, Weber K, Tuschl T. Duplexes of 21-nucleotide RNAs mediate RNA interference in cultured mammalian cells. Nature 2001;411:494-8.

290. Bohula EA, Salisbury AJ, Sohail M, Playford MP, Riedemann J, Southern EM, Macaulay VM. The efficacy of small interfering RNAs targeted to the type 1 insulin-like growth factor receptor (IGF1R) is influenced by secondary structure in the IGF1R transcript. J Biol Chem 2003;278:15991-7.

291. Rochester MA, Riedemann J, Hellawell GO, Brewster SF, Macaulay VM. Silencing of the IGF1R gene enhances sensitivity to DNA-damaging agents in both PTEN wild-type and mutant human prostate cancer. Cancer Gene Ther 2005;12:90-100.

292. Yeh AH, Bohula EA, Macaulay VM. Human melanoma cells expressing V600E B-RAF are susceptible to IGF1R targeting by small interfering RNAs. Oncogene 2006;25:6574-81.

293. McMenamin ME, Soung P, Perera S, Kaplan I, Loda M, Sellers WR. Loss of PTEN expression in paraffin-embedded primary prostate cancer correlates with high Gleason score and advanced stage. Cancer Res 1999;59:4291-6.

294. Baserga R. The IGF-I receptor in cancer research. Exp Cell Res 1999;253:1-6.

295. Davies MA, Koul D, Dhesi H, Berman R, McDonnell TJ, McConkey D, Yung WK, Steck PA. Regulation of Akt/PKB activity, cellular growth, and apoptosis in prostate carcinoma cells by MMAC/PTEN. Cancer Res 1999;59:2551-6.

296. Chakravarti A, Loeffler JS, Dyson NJ. Insulin-like growth factor receptor I mediates resistance to anti-epidermal growth factor receptor therapy in primary human glioblastoma cells through continued activation of phosphoinositide 3-kinase signaling. Cancer Res 2002;62:200-7.

297. Riedemann J, Sohail M, Macaulay VM. Dual silencing of the EGF and type 1 IGF receptors suggests dominance of IGF signaling in human breast cancer cells. Biochem Biophys Res Commun 2007;355:700-6.

298. Riedemann J, Takiguchi M, Sohail M, Macaulay VM. The EGF receptor interacts with the type 1 IGF receptor and regulates its stability. Biochem Biophys Res Commun 2007;355:707-14.

299. Mazor O, Hillairet de Boisferon M, Lombet A, Gruaz-Guyon A, Gayer B, Skrzydelsky D, Kohen F, Forgez P, Scherz A, Rostene W, Salomon Y. Europium-labeled epidermal growth factor and neurotensin: novel probes for receptor-binding studies. Anal Biochem 2002;301:75-81.

300. Li G, Barrett EJ, Wang H, Chai W, Liu Z. Insulin at physiological concentrations selectively activates insulin but not insulin-like growth factor I (IGF-I) or insulin/IGF-I hybrid receptors in endothelial cells. Endocrinology 2005;146:4690-6.

301. Andersen AS, Kjeldsen T, Wiberg FC, Vissing H, Schaffer L, Rasmussen JS, De Meyts P, Moller NP. Identification of determinants that confer ligand specificity on the insulin receptor. J Biol Chem 1992;267:13681-6.

302. Schaffer L. A model for insulin binding to the insulin receptor. Eur J Biochem 1994;221:1127-32.

303. Moxham CP, Duronio V, Jacobs S. Insulin-like growth factor I receptor beta-subunit heterogeneity. Evidence for hybrid tetramers composed of insulin-like growth factor I and insulin receptor heterodimers. J Biol Chem 1989;264:13238-44.

304. Denley A, Brierley GV, Carroll JM, Lindenberg A, Booker GW, Cosgrove LJ, Wallace JC, Forbes BE, Roberts CT, Jr. Differential Activation of Insulin Receptor Isoforms by Insulin-Like Growth Factors Is Determined by the C Domain. Endocrinology 2005.

305. Denley A, Carroll JM, Brierley GV, Cosgrove L, Wallace J, Forbes B, Roberts CT, Jr. Differential activation of insulin receptor substrates 1 and 2 by insulin-like growth factor-activated insulin receptors. Mol Cell Biol 2007;27:3569-77.

306. Denley A. Investigation into the molecular specificity of the IGFs: A chimeric approach. PhD thesis University of Adelaide 2004.

307. Kosaki A, Pillay TS, Xu L, Webster NJ. The B isoform of the insulin receptor signals more efficiently than the A isoform in HepG2 cells. The Journal of Biological Chemistry 1995;270:20816-23.

308. Le MN, Kohanski RA, Wang LH, Sadowski HB. Dual mechanism of signal transducer and activator of transcription 5 activation by the insulin receptor. Mol Endocrinol 2002;16:2764-79.

309. Sawka-Verhelle D, Tartare-Deckert S, White MF, Van Obberghen E. Insulin receptor substrate-2 binds to the insulin receptor through its phosphotyrosine-binding domain and through a newly identified domain comprising amino acids 591-786. J Biol Chem 1996;271:5980-3.

310. Hara K, Yonezawa K, Sakaue H, Ando A, Kotani K, Kitamura T, Kitamura Y, Ueda H, Stephens L, Jackson TR, et al. 1-Phosphatidylinositol 3-kinase activity is required for insulin-stimulated glucose transport but not for RAS activation in CHO cells. Proc Natl Acad Sci U S A 1994;91:7415-9.
311. Bevan P. Insulin signalling. J Cell Sci 2001;114:1429-30.
312. Brazil DP, Yang ZZ, Hemmings BA. Advances in protein kinase B signalling: AKTion on multiple fronts. Trends Biochem Sci 2004;29:233-42.
313. Roux PP, Blenis J. ERK and p38 MAPK-activated protein kinases: a family of protein kinases with diverse biological functions. Microbiol Mol Biol Rev 2004;68:320-44.
314. Sun XJ, Wang LM, Zhang Y, Yenush L, Myers MG, Jr., Glasheen E, Lane WS, Pierce JH, White MF. Role of IRS-2 in insulin and cytokine signalling. Nature 1995;377:173-7.
315. Chaika OV, Chaika N, Volle DJ, Hayashi H, Ebina Y, Wang LM, Pierce JH, Lewis RE. Mutation of tyrosine 960 within the insulin receptor juxtamembrane domain impairs glucose transport but does not inhibit ligand-mediated phosphorylation of insulin receptor substrate-2 in 3T3-L1 adipocytes. J Biol Chem 1999;274:12075-80.
316. Shao Y, Gao Z, Marks PA, Jiang X. Apoptotic and autophagic cell death induced by histone deacetylase inhibitors. Proc Natl Acad Sci U S A 2004;101:18030-5.
317. Zhang XD, Gillespie SK, Hersey P. Staurosporine induces apoptosis of melanoma by both caspase-dependent and -independent apoptotic pathways. Mol Cancer Ther 2004;3:187-97.
318. Cui X, Kim HJ, Kuiatse I, Kim H, Brown PH, Lee AV. Epidermal growth factor induces insulin receptor substrate-2 in breast cancer cells via c-Jun NH(2)-terminal kinase/activator protein-1 signaling to regulate cell migration. Cancer Res 2006;66:5304-13.
319. Lingohr MK, Dickson LM, Wrede CE, Briaud I, McCuaig JF, Myers MG, Jr., Rhodes CJ. Decreasing IRS-2 expression in pancreatic beta-cells (INS-1) promotes apoptosis, which can be compensated for by introduction of IRS-4 expression. Mol Cell Endocrinol 2003;209:17-31.
320. Tseng YH, Ueki K, Kriauciunas KM, Kahn CR. Differential roles of insulin receptor substrates in the anti-apoptotic function of insulin-like growth factor-1 and insulin. J Biol Chem 2002;277:31601-11.
321. Valverde AM, Fabregat I, Burks DJ, White MF, Benito M. IRS-2 mediates the antiapoptotic effect of insulin in neonatal hepatocytes. Hepatology 2004;40:1285-94.
322. Ranke MB. Insulin-like growth factor-I treatment of growth disorders, diabetes mellitus and insulin resistance. Trends Endocrinol Metab 2005;16:190-7.
323. Simpson HL, Jackson NC, Shojaee-Moradie F, Jones RH, Russell-Jones DL, Sonksen PH, Dunger DB, Umpleby AM. Insulin-like growth factor I has a direct effect on glucose and protein metabolism, but no effect on lipid metabolism in type 1 diabetes. J Clin Endocrinol Metab 2004;89:425-32.
324. Jones HE, Gee JM, Hutcheson IR, Knowlden JM, Barrow D, Nicholson RI. Growth factor receptor interplay and resistance in cancer. Endocr Relat Cancer 2006;13 Suppl 1:S45-51.
325. Shimizu M, Deguchi A, Hara Y, Moriwaki H, Weinstein IB. EGCG inhibits activation of the insulin-like growth factor-1 receptor in human colon cancer cells. Biochem Biophys Res Commun 2005;334:947-53.
326. Sengupta S, Muir JG, Gibson PR. Does butyrate protect from colorectal cancer? J Gastroenterol Hepatol 2006;21:209-18.
327. Zoran DL, Turner ND, Taddeo SS, Chapkin RS, Lupton JR. Wheat bran diet reduces tumor incidence in a rat model of colon cancer independent of effects on distal luminal butyrate concentrations. J Nutr 1997;127:2217-25.
328. Jayasena SD. Designer siRNAs to overcome the challenges from the RNAi pathway. Journal of RNAi and Gene Silencing 2006;2:109-117.
329. Ambion. Product Catalogue. http://www.ambion.com/catalog/: Ambion, 2008.
330. Jagla B, Aulner N, Kelly PD, Song D, Volchuk A, Zatorski A, Shum D, Mayer T, De Angelis DA, Ouerfelli O, Rutishauser U, Rothman JE. Sequence characteristics of functional siRNAs. RNA 2005;11:864-72.
331. Reynolds A, Leake D, Boese Q, Scaringe S, Marshall WS, Khvorova A. Rational siRNA design for RNA interference. Nat Biotechnol 2004;22:326-30.
332. Spagnou S, Miller AD, Keller M. Lipidic carriers of siRNA: differences in the formulation, cellular uptake, and delivery with plasmid DNA. Biochemistry 2004;43:13348-56.
333. Zhang S, Xu Y, Wang B, Qiao W, Liu D, Li Z. Cationic compounds used in lipoplexes and polyplexes for gene delivery. J Control Release 2004;100:165-80.
334. Chesnoy S, Huang L. Structure and function of lipid-DNA complexes for gene delivery. Annu Rev Biophys Biomol Struct 2000;29:27-47.

335.	Lv H, Zhang S, Wang B, Cui S, Yan J. Toxicity of cationic lipids and cationic polymers in gene delivery. J Control Release 2006;114:100-9.

336.	Aberle AM, Tablin F, Zhu J, Walker NJ, Gruenert DC, Nantz MH. A novel tetraester construct that reduces cationic lipid-associated cytotoxicity. Implications for the onset of cytotoxicity. Biochemistry 1998;37:6533-40.

337.	Lappalainen K, Jaaskelainen I, Syrjanen K, Urtti A, Syrjanen S. Comparison of cell proliferation and toxicity assays using two cationic liposomes. Pharm Res 1994;11:1127-31.

338.	Ambion. RNA Interference Research Guide. www.ambion.com/RNAi 2006.

339.	Qiagen. HiPerFect Transfection Reagent Handbook. www.qiagen.com 2006;Second Edition, February 2006.

340.	Jackson AL, Bartz SR, Schelter J, Kobayashi SV, Burchard J, Mao M, Li B, Cavet G, Linsley PS. Expression profiling reveals off-target gene regulation by RNAi. Nat Biotechnol 2003;21:635-7.

341.	Semizarov D, Frost L, Sarthy A, Kroeger P, Halbert DN, Fesik SW. Specificity of short interfering RNA determined through gene expression signatures. Proc Natl Acad Sci U S A 2003;100:6347-52.

342.	Hong J, Qian Z, Shen S, Min T, Tan C, Xu J, Zhao Y, Huang W. High doses of siRNAs induce eri-1 and adar-1 gene expression and reduce the efficiency of RNA interference in the mouse. Biochem J 2005;390:675-9.

343.	Toretsky JA, Helman LJ. Involvement of IGF-II in human cancer. The Journal of Endocrinology 1996;149:367-72.

344.	Moschos SJ, Mantzoros CS. The role of the IGF system in cancer: from basic to clinical studies and clinical applications. Oncology 2002;63:317-32.

345.	Wang S, Souza RF, Kong D, Yin J, Smolinski KN, Zou TT, Frank T, Young J, Flanders KC, Sugimura H, Abraham JM, Meltzer SJ. Deficient transforming growth factor-beta1 activation and excessive insulin-like growth factor II (IGFII) expression in IGFII receptor-mutant tumors. Cancer Research 1997;57:2543-6.

346.	Freier S, Weiss O, Eran M, Flyvbjerg A, Dahan R, Nephesh I, Safra T, Shiloni E, Raz I. Expression of the insulin-like growth factors and their receptors in adenocarcinoma of the colon. Gut 1999;44:704-8.

347.	Franken NA, Rodermond HM, Stap J, Haveman J, van Bree C. Clonogenic assay of cells in vitro. Nat Protoc 2006;1:2315-9.

348.	Fiebig HH, Maier A, Burger AM. Clonogenic assay with established human tumour xenografts: correlation of in vitro to in vivo activity as a basis for anticancer drug discovery. Eur J Cancer 2004;40:802-20.

349.	Pollak MN, Schernhammer ES, Hankinson SE. Insulin-like growth factors and neoplasia. Nat Rev Cancer 2004;4:505-18.

350.	Soos MA, Siddle K, Baron MD, Heward JM, Luzio JP, Bellatin J, Lennox ES. Monoclonal antibodies reacting with multiple epitopes on the human insulin receptor. The Biochemical Journal 1986;235:199-208.

351.	Frederick TJ, Min J, Altieri SC, Mitchell NE, Wood TL. Synergistic induction of cyclin D1 in oligodendrocyte progenitor cells by IGF-I and FGF-2 requires differential stimulation of multiple signaling pathways. Glia 2007;55:1011-22.

Appendix

Publications arising from this thesis